Protein homeostasis dysfunction in chronic brain disorders

Inaugural dissertation

for the attainment of the title of doctor
in the Faculty of Mathematics and Natural Sciences
at the Heinrich Heine University Düsseldorf

presented by

Rita M. Gomes Marreiros
from Lisbon, Portugal

Düsseldorf, July 2019

from the Institute of Neuropathology
the Heinrich Heine University Düsseldorf

Published by permission of the
Faculty of Mathematics and Natural Sciences at
Heinrich Heine University Düsseldorf

Supervisor: Prof. Dr. Carsten Korth
Co-supervisor: Prof. Dr. Sascha Weggen

Date of the oral examination:

Concerning the submitted dissertation:

Protein homeostasis dysfunction in chronic brain disorders

I declare under oath that I have compiled my dissertation independently and without any undue assistance by third parties under consideration of the 'Principles for the Safeguarding of Good Scientific Practice at Heinrich Heine University Düsseldorf

Furthermore, I declare that this dissertation has not been submitted to any other university or faculty before and that I have not made any other doctoral studies so far.

Düsseldorf,18 July 2019

_____

(Rita M. Gomes Marreiros)

Table of Contents

Abbreviations

3D = Three-dimensional

α-syn = α-synuclein

Aβ = Amyloid-beta

AD = Alzheimer's disease

ALS = Amyotrophic lateral sclerosis

BD = Bipolar disorder

CHIP = Carboxyl terminus of the Hsc70-interacting

CMA = Chaperone mediated autophagy

CMIs = Chronic mental illnesses

DISC1 = Disrupted in Schizophrenia 1

DLB = Dementia with Lew bodies

FTLD = Frontotemporal lobar degeneration

FUS = Fused in sarcoma

GAD2 = Glutamate decarboxylase 2

HD = Huntington's disease

Hsc70 = Heat shock cognate 70 kDa

HSPs = Heat shock proteins

HOP = HSP70–HSP90 organizing protein

Hsf1 = Heat shock transcription factor 1

JUNQ = Juxtanuclear quality control compartment

LAIV = Intranasal live attenuated influenza vaccine

Lys = Lysins

MDD = Major depression

MTOC = Microtubule-organizing center

MVBs = Multivesicular bodies

mHtt = mutant huntingtin

NDs = Neurodegenerative disorders

PD = Parkinson's disease

PN = Proteostasis network

PrP = Prion protein

PrP^{C} = Native prion protein

PrP^{Sc} = Cellular prion protein

SCZ = Schizophrenia

SOD1 = Superoxide dismutase 1

TDP-43 = TAR DNA-binding protein 43

TIV = Trivalent inactivated influenza vaccine

TNTs= Tunneling nanotubes

tRNAs = transfer RNAs

UPS = Ubiquitin–proteasome system

Dissertation scope

Disturbances in protein homeostasis, leading to the accumulation of misfolded toxic species, has been associated with protein conformational disorders. However, the precise cause-effect relationship of protein aggregation to disease progression is not yet characterized to molecular detail. Problems are the heterogeneity of the disorders and to the dynamic nature of protein aggregation. Understanding the mechanisms behind the protein homeostasis disruption is crucial to better define the relevant factors in the progression of protein aggregation disorders, such as neurodegenerative diseases (NDs) and chronic mental illnesses (CMIs). The factors that might trigger the formation of the first critical mass that later accumulates as protein inclusions in protein conformational disorders remain unknown. A strong gene-disease association has been described, however, in the majority of the cases, it is the sporadic form of the disease is most prevalent. For example, it has been hypothesized that environmental factors, such as microbes, air pollutants, or heavy metals, might have an enhanced seeding effect for protein aggregation.

In this cumulative dissertation, built around three major manuscripts, we addressed the protein homeostasis disruption from several perspectives. We discussed the assembly of protein aggregates, and the effect of a pathogen such as a virus was investigated as a possible ‘seed' for protein misfolding disorders. We were also interested in identifying new biological markers for mental illnesses based in an aberrant proteostasis signature.

In chapter 1 (page 25), we discussed an alternative view in the assembly of protein aggregates since similarities between virus capsid assembly and the protein aggregation had been suggested. We review current literature in protein conformational disorders and current perspectives in the viral capsid assembly. The evidence that cellular host factors are used for catalyzing virus capsid assembly and protein aggregates is discussed, as well as which host factors this could be.

In chapter 2 (page 36), we raise the question whether viral infections could be a real threat in protein misfolding disorders. We investigated the relevance of acute influenza A infection in the homeostasis disruption of distinct proteins associated with Parkinson’s disease (PD), schizophrenia (SCZ), Alzheimer’s disease (AD), and amyotrophic lateral sclerosis (ALS) in an *in vitro* and *in vivo* context. In dopaminergic-like neurons, the acute viral infection seems to ‘seed’ α-synuclein (α-syn) and Disrupted in Schizophrenia 1 (DISC1) aggregates, but neither tau or TAR DNA-binding protein 43 (TDP-43). These findings were corroborated *in vivo* by an increase in α-syn and DISC1 expression in the influenza-infected brain areas.

Besides, oseltamivir phosphate - an anti-influenza drug, proved to prevent α-syn influenza-induced aggregation. Disturbances in a protein clearance pathway were the proposed mechanism for the accumulation of misfolded proteins upon viral infection. Accordingly, impairment in early- and late- autophagy that might promote the accumulation of α-syn in the cell was observed. Our data suggested that influenza A can be the initial trigger for seeding of α-syn and DISC1. We consider that viral infections might be taken into consideration as a future risk factor for synucleinopathies and DISC1opathies.

Aberrant protein homeostasis was also described to be associated with subsets of chronic psychiatry disorders. In chapter 3 (page 84), we described the identification of insoluble proteins exclusively present in CMIs patients *post mortem* brains. The main question was to address if, misfolded proteins could be a biological signature of CMIs patient subsets crossing clinical diagnostic boundaries. Using a proteomic approach, we found insoluble glutamate decarboxylase 2 (GAD2) in a subset of CMIs patients. These findings were confirmed by biochemical fractionation of individual brain samples from disease patients and corroborated in an *in vitro* model (neuroblastoma cells) where a high tendency of GAD2 to aggregate was observed.

The present studies highlight a mechanistic aspect of initial aggregate formation, an environmental insult that might be involved in the etiology and pathophysiology of misfolded disorders, and emphasize that aberrant protein homeostasis could be a biological signature for a subset of chronic mental illnesses.

Umfang Dissertation

Störungen in der Proteinhomöostase können zur Aggregation missgefalteter toxischer Proteinspezies führen und sind mit Proteinkonformationserkrankungen, wie den neurodegenerativen und chronisch mentalen Erkrankungen assoziiert, wobei der exakte Zusammenhang zwischen Proteinaggregation und Krankheitsverlauf bislang unklar ist. Dies ist nicht zuletzt in der phänotypischen Heterogenität der Krankheiten, sowie der dynamischen Natur der Proteinaggregation begründet. Ein Verständnis der zugrundeliegenden Mechanismen der Proteinhomöostase ist unumgänglich, um relevante Faktoren für das Entstehen von Proteinaggregationserkrankungen zu definieren. Es ist daher wichtig biologische Ereignisse zu identifizieren, welche die Formierung einer ersten kritischen Masse von aggregierten Proteinen induzieren und zur späteren Akkumulation dieser Proteine während der Erkrankung führen. Für einen kleinen Teil der Proteinkonformationserkrankungen ist bereits eine genetische Grundlage beschrieben, der Großteil der Fälle ist jedoch von sporadischer Natur. Für Letztere wurden Umweltfaktoren wie Mikroben, Luftverschmutzungen oder Schwermetalle als Ursache der Proteinaggregation vermutet.

Diese kumulative Dissertation bezieht sich auf drei Arbeiten, welche eine Störung der Proteinhomöostase aus verschiedenen Perspektiven beleuchten. Hierfür wurden sowohl die Proteinassemblierung an sich, als auch die Induktion von Aggregationskeimen durch Pathogene, wie Viren, untersucht (Abbildung 1). Des Weiteren wurden über eine veränderte Proteostasesignatur neue potentielle Biomarker für mentale Erkrankungen definiert.

In der ersten Arbeit wird eine alternative Sicht auf Proteinaggregation diskutiert. Hierbei wurde ein ähnlicher Mechanismus sowohl der Assemblierung viraler Kapsidproteine, als auch der krankhaften Aggregation von Proteinen zugrunde gelegt. Die aktuelle Literatur bezüglich der Proteinkonformationserkrankungen, sowie die verschiedenen Sichtweisen auf die virale Kapsidassemblierung wurden zusammengefasst. Die Evidenz, dass zelluläre Wirtsproteine von Viren für die Kapsidzusammensetzung rekrutiert werden wie auch die Möglichkeit diese Wirtsproteine als neuartiges therapeutischen Ziel zu definieren definieren wurden diskutiert.

In der zweiten Arbeit wurde die Frage bearbeitet, inwieweit virale Infektionen Proteinkonformationserkrankungen auslösen können. Der Einfluss einer akuten Influenza A Infektion auf die Störung der Homöostase spezifischer Proteine, die mit Morbus Parkinson (α-synuklein), Schizophrenie (DISC1), Morbus Alzheimer (Tau), sowie der Amyotrophen

Lateralsklerose (TDP-43) wurden *in vitro* und *in vivo* untersucht. In dopaminergen Neuronen scheint die akute virale Infektion einen Keim für die Bildung von α-synuklein- und DISC1-Aggregaten, jedoch nicht von tau oder TDP-43, zu begünstigen. Diese Befunde wurden durch Ergebnisse aus *in vivo* Studien in Mäusen gestützt, in denen ein Anstieg der α-synuklein- und DISC1-Expression in Influenza-infizierten Gehirnarealen beobachtet wurde. Darüber hinaus konnte der Anti-Influenza-Wirkstoff Oseltamivirphosphat die Influenza-induzierte Aggregation von α-synuklein verhindern. Als Ursache für die virusinduzierte Proteinaggregation wurden Störungen im gezielten Abbau fehlgefalteter Proteine vermutet und untersucht. Hierbei ergab sich, dass Störungen der frühen und späten Autophagie die Aggregation von α-synuklein in der Zelle fördern. Zusammengefasst deuten die Daten darauf hin, dass eine Influenza A Infektion die Proteostase von α-synuklein und DISC1 initial stören kann und somit als potentielle Risikofaktoren für synukleinopathien und DISC1opathien zu berücksichtigen sind.

Eine gestörte Proteostase wurde nicht nur bei neurodegenerativen Erkrankungen beschrieben, sondern auch mit chronischen mentalen Erkrankungen (CME) assoziiert, deren biologische Charakterisierung bislang jedoch eine große Herausforderung darstellt. In der dritten Arbeit wurden neue unlösliche und missgefaltete Proteine identifiziert, die exklusiv bei Patienten mit CME auftraten. Dies ermöglicht die Identifikation einer biologisch definierten Untergruppe von Patienten mit CME, jenseits der rein klinischen Diagnose. Mittels eines proteomischen Ansatzes wurde unlösliches Glutamatdecarboxylase 2 (GAD2) Protein in einer Untergruppe von Patienten mit CME mittels biochemischer Fraktionierung von Gehirnmaterial identifiziert. Die hohe Tendenz von GAD2 unlösliche Aggregate zu bilden wurde auch *in vitro* in Neuroblastomazellen beobachtet.

Die hier vorgelegten Studien beleuchten mechanistische Aspekte der initialen Proteinaggregation, sowie einen Umwelteinfluss viraler Natur, der in der Ätiologie und Pathophysiologie von Proteinkonformationserkrankungen beteiligt sein könnte. Darüber hinaus bekräftigen sie, dass veränderte Proteostase die Grundlage für die Definition einer biologischen Signatur von CME bilden kann.

Introduction

1. Protein homeostasis

In the cellular environment, synthesis and degradation of proteins are in a balanced equilibrium so-called protein homeostasis (or proteostasis). That refers to the proteome maintenance by the readjustment of the innate biology of a eukaryotic cell through the control of concentration, conformation, binding interaction, and location of proteins. The process by which this occurs, so-called proteostasis network (PN), is tightly regulated in all aspects from the synthesis, folding, trafficking, and clearance to ensure proteome stability (1). The PN is mainly regulated by different chaperones classes that according to the definition proposed by John Ellis are, any factor involved in the folding or assembly of a protein without being in its final structure (2). It has been suggested that PN comprises more than 2,000 factors (reviewed in Fig.1B (3))

In the next chapters, more detailed information will be given in the major processes involved in PN: protein synthesis (section 1.1); protein folding (section 1.2); protein stability maintenance and degradation (section 1.3).

1.1. Protein synthesis

Proteins are involved in a range of biological processes to ensure regular cell survival and function. In a very simplistic way, proteins are composed of a unique amino acid sequence that is specified by different codons, translated from a nucleotide sequence that forms the correspondent gene. The translation procedure takes place in ribosomes in the cell cytoplasm, to where the mRNA transcript travels from the nucleus. The protein chain is catalyzed by small RNA molecules known as transfer RNAs (tRNAs). This procedure occurs in a repeated cycle of tRNA binding, peptide bond formation, and ribosome translocation until the complete polypeptide is released. The process ends aided by two leading chaperone families, hsp70 and hsp60, for proteins acquire the correct three-dimensional (3D) structure. Cellular quality control mechanisms destroyed proteins that failed or acquired an incomplete folded structure (see section 1.3) (4).

The human proteome, defined by Marc Wilkin as the complete set of proteins expressed in a cell at a particular time (5) comprises in average more than 10,000 proteins per cell (6). Furthermore, depending on the acquired cellular function, the protein copy number could fluctuate in a range of nine orders of magnitude being histones, ribosomes, and cytoskeleton proteins the most abundant (7). Apart from proteins with an intrinsically disordered region that might only acquire a defined structure when interacted with other partners (8), most

proteins acquired a stable folded 3D structure (9, 10). Proteins destined to the nucleus and peroxisomes are transported from the cytosol already in a folded structure. For proteins intended to the endoplasmic reticulum and/or to the correspondent secretory pathways, and mitochondria, the chaperones are responsible for aiding the transport preventing the protein folding prior their reach the target organelle (11).

1.2. Protein folding

The amino acid order in a polypeptide chain is the determinant factor in a 3D structure or conformation acquired by a protein (12). The majority of polypeptide chains adopt distinct conformations with equally stability, giving prevalence to the thermodynamically favorable (native states) where free energy is minimized (13). During the folding process, there are competing reactions leading to folding intermediates states, that might risk proteins adopting a kinetically stable non-native state (14). The current purposed model comprises a free-energy landscape (Figure 1) towards the proteins formed intramolecular contacts to maintain the native state. However, they must cross kinetic energy barriers through folding intermediates states. In the crowded cellular environmental with several molecules folding at the same compartment, proteins could form intermolecular interactions between non-native states. That might be thermodynamically more stable than the native states, leading to protein aggregation (15). In the *in vivo* system, the folding process is aided by chaperones that support the maintenance of proteins towards the folding intermediates through the native state. They lower the free-energy barriers avoiding pathway reactions that lead to aggregated species (1).

According to their structural organization, proteins are defined in four levels. The primary structure refers to the amino acid sequence (16); the secondary structure refers to the α-helix and β-sheet regions (17); the tertiary structure is the 3D organization of the polypeptide chain; and the quaternary structure refers to a complex structure (18). Even being the protein conformation unique, two main folded patterns, α-helix and the β-sheet are shared by proteins. The α-helix was the first identified pattern, and it is generated when a polypeptide chain twists around itself to form a rigid cylinder. They can also form stable coiled-coil structures when two or more α-helix wrap around each other. That structure is the most common in proteins due to the high stability of α-helix, i.e., transmembrane proteins are characterized by the abundant presence of short α-helix regions. β-sheet was first identified in fibroin protein, and it is a very rigid structure. They can form two distinct structures, a parallel chain- with two polypeptide chains with the same orientation, or an antiparallel chain- with a twisted structure from each polypeptide chain, with the chains being in the opposite direction to each other (17) .

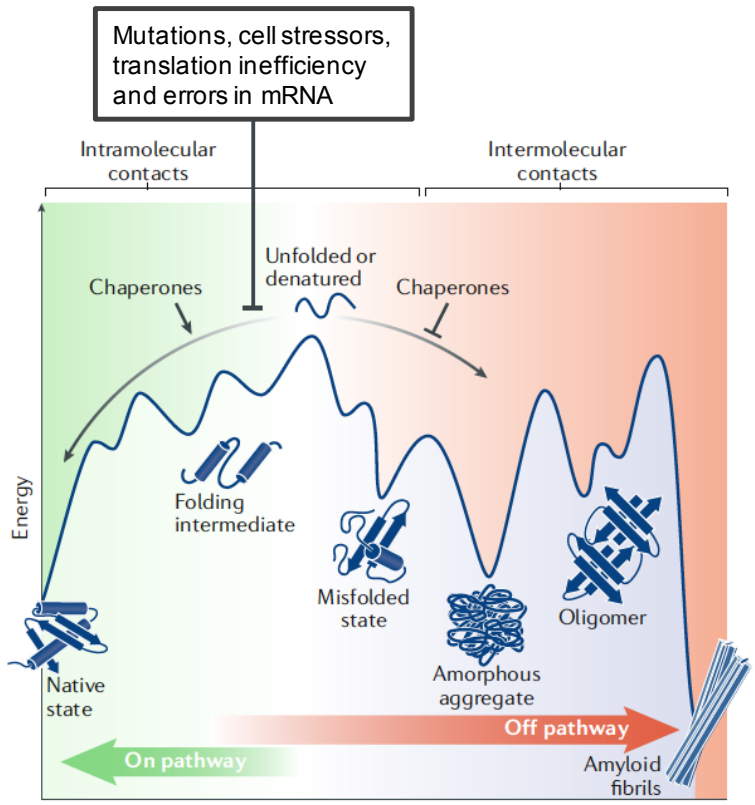

Figure 1. Conformations acquired by proteins during the folding process. Different energy stages that proteins can cross during the folding process. Folding intermediates stages are controlled by chaperone machinery, enhancing the 'on-pathway' reactions. That allows the progression of folding intermediates to the native thermodynamically stable state. Factors such as mutations, cell stressors, or translational errors favoring the passage of proteins to misfolded states and promote aggregate formation. Amyloid fibrils might occupy a more stable state that makes the refold process unlikely to happen. (Adapted from *Hipp et al. (11)*)

1.3. Protein stability maintenance and degradation

As mentioned in the section above, the native protein states are not in the majority of cases the most thermodynamically favorable as for i.e., it is the case of proteins with more than 100 amino acids (19). They are in high abundance in the cell and typically fold via intermediate states. That increases their aggregation propensity due to the vulnerability of the hydrophobic amino acid residues and unpaired β- strands, to the crowed cytosol (1). Multiple factors such as mutations, cell stressors, translation aberrations, or defects in mRNA, inhibits the 'on- pathway' reactions, favoring the 'of pathway' that results in protein aggregation (Figure 1). The cellular chaperone machinery responsible for the *de novo folding* and refolding processes in an ATP-dependent manner work in order to counteract the 'of-pathways' (20). The chaperone families mainly involved in this process are the heat-shock proteins (HSPs) 70 and 90 that are in general responsible for 15-20% of the newly synthesized proteins, and the chaperonins (Hsp60s) involved in 10% of protein folding (20). Heat shock factors, such as the heat shock factor 1, control their transcription. In a non-

stressed condition, heat shock factor 1 is in an inactive complex with the chaperones (21, 22). In many cases where proteins were unable to fold or being refolded properly, they are removed from the cell to avoid the accumulation of misfolded toxic species. Eukaryotic cells have two major proteolytic pathways responsible for this process that are mainly aided by molecular chaperones for the target recognition and maintenance of the degradation state (23). According to the nature of the disposable target, the cell clearance occurs in an ATP-dependent manner by the ubiquitin-proteasome system (UPS), or by the autophagy system.

1.3.1. Ubiquitin-proteasome system

Short-lived, misfolded, and defective proteins used the UPS as a clearance system in ~ 80-90% of the cases (24, 25). The unique feature of UPS is the selective degradation of target proteins by covalent binding to ubiquitin, a 76 KDa protein (25). The ubiquitination process involves three ubiquitin molecules in a sequential procedure, E1 (ubiquitin-activating enzyme), E2 (ubiquitin-transferring enzyme), and E3 (ubiquitin ligase). For the subsequent degradation by the proteasome, the ubiquitinated-target protein has to suffer a polyubiquitinated process. Different lysines (Lys) are involved in this process, with Lys 48 and Lys 11 mediating the degradation of short-lived proteins. Lys 48 and Lys 63 mediate the proteasomal and the autophagy degradation of misfolded proteins (26). 'Tagged' proteins are then ready to be cleared by the 26S proteasome. This structure is a large multicatalytic protease complex composed of two main components, the 20S catalytic core, and 19S regulatory complex (27). The Hsp70 and 90 chaperones families also play a role in UPS degradation through the interaction with the chaperone co-factor - carboxyl terminus of the Hsc70-interacting protein (CHIP) involved in protein ubiquitination (28). Due to the size constraints imposed by the proteasome, protein clearance by UPS is limited to monomeric and soluble proteins (29) .

1.3.2. Autophagy system

Autophagy occurs for ~ 10-20% of cellular proteolysis and is responsible for the degradation of insoluble and long-lived proteins (26). According to the mechanism used by the cell to deliver the cargo to the lysosomes, three main mechanisms have been characterized in mammals (30). 1) Macroautophagy is a multi-step process where the cytosolic cargo is engulfed by a double membrane vesicle called autophagosome. Autophagosomes are formed with the conjugation of the autophagy-related protein-LC3, with the lipid PE and a set of autophagy-related proteins, i.e., Atg5, Atg6, Atg12. This process initiates with the phosphorylation of the lipids present in the endoplasmic reticulum, in mitochondria or in the Golgi complex, triggered by a kinase complex regulated by Beclin-1. Different cargo types can be engulfed in the same autophagosome or selectively recruited according to the cargo

type and transported to lysosomes. The fusion of autophagosomes with lysosomes, forming a vesicle designated as autolysosome, allows the cargo to be degraded by the lysosome hydrolases (31, 32). The core machinery of macroautophagy could be used in a selective manner and depending on the selected cargo, different types were defined. In aggrephagy, aggregated proteins are sequestered by autophagosomes after recognition of the p62 receptor. Protein aggregates can also be degraded by the chaperone-assisted selective autophagy when the heat shock cognate 70 kDa (Hsc70) and Bag3 chaperones are involved in the process (33). Dysfunctional mitochondria use the macroautophagy machinery such as the receptors PTEN-induced putative kinase 1, Parkin, NIX, and BNIP, in a process called mitophagy (34). In the case of lipids and ribosomes they are degraded in a selective macroautophagy process called lipofagy and ribophagy, respectively (30); 2) Chaperone-mediated autophagy (CMA) where chaperones assisted the process of single cytosolic proteins selectively delivered to the lysosomes for degradation, is another clearance mechanism. Proteins containing the KFERQ-like motif are recognized by Hsc70 protein forming a complex that binds to the cytosolic part of lysosome-associated membrane protein type 2A. The chaperone-substrate complex is then uptaken to the lysosome to be degraded in the lysosomal matrix. On the other hand, the chaperone-substrate complex can also be primary unfolded aided by the chaperone complex containing Hsc70 and the co-chaperones BAG1, HIP, HSP70–HSP90 organizing protein (HOP) and HSP40/DNAJB1, and then be degraded in the lysosomal lumen (35, 36). 3) Degradation of cytosolic proteins and organelles, as well as small aggregates and oligomeric species, can occur in bulk by invagination of the lysosomal membrane in a process designated as microautophagy. An adaptation of microautophagy, endosomal microautophagy occurs when proteins containing the recognized motif KFERQ-like are selectively targeted by Hsc70 for endosomal degradation. Invaginations of the late endosome membrane form small vesicles for cargo uptake and later degraded in the endosomal lumen. Additionally, autophagy also plays a role in recycling essential cell components in order to maintain a proper brain function (37, 38).

2. Protein homeostasis disruption

Taking into consideration that around 5% of the proteins in human proteome are involved in synthesis and protein degradation, maintenance of stable protein homeostasis through life is a big challenge for the cell. As it was previously mentioned, a tight control from synthesis until protein degradation is crucial to avoid either the accumulation of proteins usually degraded, or an excessive protein degradation (3).

Throughout life, protein homeostasis gradually deteriorates, starting in early adulthood. A study conducted by Ben-Zvi et al in nematodes expressing temperature-sensitive folding sensor proteins in diverse tissues, demonstrated an aggregated and mislocalized pattern of proteins in early adulthood – day 2, 4 and 5 (39). In an independent study conducted by David et al also using nematodes, detergent-insoluble protein aggregates were collected at different time points during the lifespan. A proteomic-based approach analyzed the insoluble proteome, and an increase in aggregated proteins was detected from day 3 of adulthood up to aged animals (40). Both studies raise an essential point: proteostasis decline starts early in adulthood and is not an exclusive function of time, cell or tissue type. It is clear that age accelerates protein homeostasis disruption, however, it is still not known which are the main factors and the trigger for that (1, 41). It is being proposed on one hand, a direct disturbance in the components involved in the PN, such as a decline in the capacity of molecular chaperones, UPS or autophagy to deal with misfolded species, or an overloaded reaction of the PN components by an increase in misfolded species (3, 42). Many factors are associated with the folding failure of newly formed protein and a consequent protein homeostasis disruption. At the genetic level, i.e., some transcriptional errors, such as mutations or truncations, or lack of a binding partner, have been described (14, 43) as well as, environmental conditions, such as temperature, pH or reactive oxygen species (44, 45). Indeed, the concerning point is when the capacity of the PN drops below a threshold, and the aggregation-prone proteins can not long maintain a soluble state. That might result in a positive feedback loop with a reduction in proteostasis capacity that leads to an increase of misfolded species and a further PN collapse (11). To counteracts the PN disturbance, cells can take some adaptive response i.e., manipulation of stress genes and nutrient sensors. In a heat stress condition, the heat-shock transcription factor 1 (Hsf1) is activated and induces the transcription of some proteostasis components (46). Induction of the autophagy system by manipulation of the kinase target of rapamycin – TOR, was also observed with a dietary restriction (47). It was also described a reduction in the production of defective proteins by phosphorylation of the translation initiation factor 2α (48).

In the next chapters, the biological manifestation and cellular consequences of protein homeostasis disruption will be addressed.

2.1. Protein aggregation: Biological manifestation

The biological manifestation of protein homeostasis imbalance is the protein accumulation in aberrant conformational states well known as aggregated or misfolded proteins. According to their organizational structure, they can form amyloid fibrils, native-like, or amorphous deposits. In terms of biochemical characteristics, they are defined to be soluble either in a lipid- or in detergent-enriched solutions with aqueous insolubility (49). The aggregation

process starts when proteins acquire an aberrant conformation and turn insoluble. However, in this early aggregated stage, they are rather unstable and have weak intermolecular interactions being rather easy for the PN components to regenerate their solubility. If the PN 'checkpoint' fails, insoluble proteins organize in a more compact and stable species, rich in β-sheet structures called oligomers. By-self association with other oligomers, or by monomer addition, a high structured molecule rich in β-sheets is formed and vulgarly defined as amyloid fibrils (50-53). Alternatively, insoluble proteins without structured organization only maintained the initial oligomeric structure originates amorphous deposits of disordered proteins (54).

Amyloid-like aggregates have relatively short polypeptide chains length since they form an ordered structure with a core rich in β-sheets that must be thermodynamically stable (55). That contrasts with amorphous deposits that generally come from long-polypeptide chains. It is also interesting to mention that protein aggregation could be functional. The most known examples of that are the cytoskeletal proteins, actin, and tubulin, and the hemoglobin S. These proteins form functional, reversible ordered aggregates that not require a rearrangement of protein folding (56, 57). However, our attention will focus on non-functional insoluble deposits.

Amyloid-like aggregates

For a protein aggregate be considered amyloidogenic, three main features according to their biophysical characteristics might be observed: (1) Amyloid fibrils composed by 2-8 protofilaments with a central spine of β-strands, perpendicular to the fibril axis in a cross-β spine structure (58); (2) A fibril diameter that varies between 6-12 nm, that was observed in extracted fibrils from patients with amyloid pathology, and *in vitro* (58, 59); (3) A positive staining with dyes, i.e. Congo-Red or thioflavin-T (60). Most protein misfolding disorders, especially NDs (detailed information on page 18; Table 1) are hallmarked by amyloid aggregates (61). The overall pathway generally proposed to explain amyloid fibril formation is next briefly described. The formation of amyloid fibrils was defined as a sequential process starting with one-step nucleation. Monomeric species prone to acquire an aggregate conformation, assemble to form oligomeric structures. From then, in a thermodynamically unfavorable reaction, the initial nuclei are form, and the fibrils then grow by monomer addition. The rate-limiting step for this process, is the oligomeric conversion into the nuclei (62). This model has been used to described the aggregation kinetics of distinct misfolded proteins, i.e. Prion protein (PrP) (63), Amyloid-beta (Aβ) 42, Aβ40 (64) and α-syn (65). However, other models based on multi-step-nucleation were also proposed (66), making complicated find a consensual model to answer the question- how amyloid fibril formation initiate.

Amorphous aggregates

Macroscopic misfolded depositions characterized by the absence of a fibrillary amyloid structure are vulgarly defined as amorphous aggregates (67). Structurally they are globular proteins with a well-defined secondary and tertiary structure. *In vitro* they were observed after heat precipitation, or high protein concentration treatments, i.e,. in the presence of co-solvents (68). They have been defined by the maintenance of their initial oligomeric conformation without a nuclei polymerization. However, it has been suggested that amorphous-aggregates also acquired an ordered cross-β structure, but in a small range in comparison with amyloid fibrils. In a native-like state thermodynamically favorable, the repeated structures are exposed to the crowed solvent to be converted into amyloid-like aggregates (67). A representative example of that is the ataxin 3, and superoxide dismutase 1 (SOD1). These proteins were identified as macroscopically amorphous aggregates in brains of spinocerebellar ataxia type-3, and ALS patients, respectively (69).

Aggregate deposition compartments

In mammalian cells, misfolded proteins were found to be deposited in two major cytoplasmic compartments, depending on protein proprieties (70). Misfolded toxic species presenting a β-sheet-rich amyloid structure are normally sequestered to inclusion bodies localized next to the nuclear envelope at the microtubule-organizing center (MTOC), and so-called aggresomes (71). Morphologically they are characterized as spherical structures with 1-3 μm size, and they present a vimentin cage-like shell (72). Polyubiquitinated aggregates binds to the histone deacetylase 6 to be transported through the microtubules until the MTOC, and rapidly cleared by UPS. They are dynamic structures and only appearing in the cell associated with disease conditions (73). That is the case for misfolded DISC1 protein, which was observed to be deposited in aggresomes (74).

An immobile compartment was also found in cell cytoplasm linked with the sequestration of non-ubiquitinated misfolded or stress-damaged proteins (75). In the case that UPS is impaired, misfolded proteins can be stored in the juxtanuclear quality control compartment (JUNQ) for later clearance or refolding (70, 75). A representative example of JUNQ-like inclusions are SOD1, Fused in sarcoma (FUS), and TDP-43 proteins, found in misfolded forms in ALS (76, 77).

2.2. Protein aggregation: A pathological signature

PN disturbances are associated with many human diseases, including NDs (61), CMIs (78), metabolic diseases, cancer (79, 80) and aging (81). In the next chapters, we focus our attention on chronic brain disorders affecting the central nervous system, especially NDs and CMIs.

Mammalian brain serves as an integrator of a pre-established genetic print and the exposures to acute insults, such as trauma, infections, or toxins, that determine the brain resilience over the life course. The most dramatic consequence of brain equilibrium disturbance is chronic brain disorders, such as NDs and CMIs. NDs become the century health problem, with an alarming exponential increase in the number of diagnosed cases. Among them, AD is the most prevalent, followed by PD, ALS, and Frontotemporal lobar degeneration (FTLD) (Table 1). Huntington's disease, spinocerebellar ataxias, tauopathies (such as corticobasal degeneration, Pick's disease and, supranuclear palsy), dementia with Lewy bodies (DLB), and Transmissible spongiform encephalopathies or prion disorders, have the lowest prevalence.

In the past years, the world-health organization increased its concern regarding CMIs, such as SCZ or recurrent affective disorders. They are considered an epidemiological burden to the society, with a severe patient disability and socio-economic impact (82). While significant efforts have been taken in the research of these diseases over the last decades, they remain incurable.

One of the dominant challenges for chronic brain disorders is the fact that they are syndromic, which means that many different factors cause them. The genetic influence account only for 5 - 15% of the diagnosed cases. The majority of the new cases are sporadic manifestations, which might result from an interaction of environmental risk factors and predisposing genetic factors (83). In table 1, the main biological, cellular, and clinical characteristics, as well as the factors that might play a role in the etiology of NDs and CMIs are summarized. Even having differential clinical manifestations, chronic brain disorders seem to share many biological standard features. The chronic progressive nature, the cognitive decline, the neuronal dysfunction associated with specific brain regions and the synaptic network damage, indicates that they might have a similar pathological mechanism even with the involvement of distinct biological players. The main pathological feature in common to all of them is the deposition of extracellular or intracellular aggregates of specific proteins, resulting in cell toxicity. Notwithstanding the considerable effort that has been done to understand the progression of these disorders, there are still critical open questions. At which aggregation state these species are toxic, what are the factors that might trigger the aggregation cascade process, and how that spreads to other cells, are vital points still not well-understood (84).

2.2.1. The cellular aspect of misfolded disorders

The main effects of protein misfolded are neuronal death and cell dysfunction, due to i.e., the impairment in protein degradation mechanisms, oxidative stress, mitochondria dysfunction and disturbances in ion homeostasis (85). Aggregation process leads to changes in the

physiological function of proteins, generally classified into loss-of-function and gain-of-function effects. Proteins can lose their function due to the sequestration to inactive cellular inclusions, with similar effects for the cell as a genetic deletion. On the other side, misfolded proteins can acquire new functions, generally with more dramatic consequences for the cell then the loss of their original function (86). A new variant has been lately discussed that consists of a loss-of-function resulting in a gain of toxic function (87, 88).

An association with disease progression and dissemination of toxic inclusions through the brain is increasingly more apparent (89, 90). From the cellular perspective, these implicate the release of a misfolded conformer from a donor cell and the acceptance and propagation by a neighbor cell. The exact mechanism explaining how this is happening it is still not clear. However, some cellular pathways have been lately proposed (91). Small microvesicles denominated exosomes caring constituents from cytosolic and endocytic compartments are released from a donor cell when multivesicular bodies (MVBs) fuse with the membrane. Misfolded proteins might be packed in MVBs and incorporated in endosomes and then enter in a neighbor cell by a still unknown process (92-96). Another proposed mechanism is clathrin-dependent or - independent endocytosis. Here, misfolded species are secreted from the donor cell to the extracellular space and then internalized by the receptor cell in clathrin - depend or dynamin-dependent process (97-99). An alternative mechanism is a direct passage of misfolded proteins from the cytosol of a donor to the cytosol of an acceptance cell. That occurs through a membranous channel based in filamentous actin, and microtubules, called tunneling nanotubes (TNTs) (100). TNTs are a ‘transit' mechanism of cell connection responsible for transporting different cargos, i.e. organelles, such as the endosomes, lysosomes, mitochondria, Golgi and proteins, that includes in pathological cases, the misfolded ones (101-103).

Neurodegenerative disorders

				Risk factors		
Disease	**Aggregated protein**	**Cellular changes**	**Clinical phenotype**	**Familial (Genes)**	**Sporadic (External factors: environmental; pathogens, etc)**	**References**
AD	Aβ (extracellular plaques); Tau (Intracellular neurofibrillary tangles)	- Synaptic excitotoxicity; - Synaptic loss; - Microgliosis; - Astrogliosis; - UPS and autophagy dysfunction - Neurodegeneration	- Hippocampal and cortex shrinkage•; - Enlarged brain ventricles•; - Dementia•; - Cognitive decline•; - Spatial memory change•; - Personality change•; - Language impairment•; - Motor dysfunction•	*APP; PSEN1; PSEN2; TREM2; APOEε4; SORL1; BIN1*	HSV*; CMV*; HIV*; Chlamydia Pneumoniae*; *Helicobacter pylori**; Down Syndrome*; Head trauma*; MDD*; Atherosclerosis*; Stroke*; Hypertension*; Diabetes Mellitus*; Obesity*; Thyroid disorders*; Tabaco*; Aluminium toxicity*; Alcohol*	(104-109)
PD	α-Syn (Intracellular aggregates in Lewy bodies)	- Loss of DA neurons in SNpc; - Oxidative damage; - Mitochondrial dysfunction; - Microgliosis; - Astrogliosis; - Synapse loss; - Decrease and lost of synapse connectivity; - UPS and autophagy dysfunction - Neurodegeneration	- Pallor of the locus coeruleus•; - Motor impairments• - Resting tremor•, - Bradykinesia•, - Postural• instability•, - Rigidity •; - Slowness of movement•; - Dementia•; - Constipation•; - Psychiatry problems•; - Sleep disruption•;	*SNCA; PARKIN; LRRK2; PINK1; DJ-1;*	Influenza A virus *; HSV*; HCV* Pesticides*; Heavy-metals*; Melanoma*; Traumatic brain injury*;	(110-121)
ALS	TDP-43, FUS, SOD1 (cytoplasmic and nuclear aggregates);	- Mitochondrial dysfunction; - Astrogliosis; - Microgliosis; - Oxidative damage; - Defective axonal transport; - UPS and autophagy dysfunction - Neurodegeneration	- Motor cortex and spinal cord motor neuron degeneration •; - Fatal paralysis•; - Progressive muscle weakness•; - Atrophy•; - Dementia•;	*TARDBP; FUS; SOD1; CHMP2B; MAPT; VAPB; DCTN1; ANG; VEGF*	HSV*; Heavy-metals*; Pesticides*; Head trauma*; Diabetes Mellitus*;	(122-126)

FTLD	TDP-43; FUS; Ubiquitin (cytoplasmic and nuclear aggregates); Tau (Intracellular neurofibrillary tangles)	- Reduction in the axon terminals in glutamatergic neurons; - Neuroinflamation; - Microgliosis; - Neurodegeneration; - Astrocyte degeneration.	- Motor cortex and spinal cord motor neuron degeneration •; - Frontotemporal atrophy•; - Semantic dementia•; - Progressive non-fluent aphasia•; - Cognitive decline•; - Behavioral changes•;	*GRN; FUS; unknown gene ch9; VCP*	Head trauma*;	(127-131)

Chronic mental illnesses

				Risk factors		
Disease	**Aggregated protein**	**Cellular changes**	**Clinical phenotype**	**Familial (Genes)**	**Sporadic (External factors: environmental; pathogens, etc)**	**References**
SCZ	DISC1; CRMP1; Dysbindin-1; NPAS3; TRIOBP	- Dysfunction of dopaminergic neurotransmission (Increase in striatal DA); - Glutamatergic dysfunction (loss of GABA) - Reduced neuropil - Reduced dendritic spines	- Delusions•; - Hallucinations•; - Impaired motivation•; - Reduction in spontaneous speech•; - Social withdrawal•; - Cognitive decline• - Ventricular enlargement•; - Reductions in grey matter•; - Abnormalities of white matter•	*AKT1; COMT; DISC1; DRD3; DTNBP1; HTR2A; NRG; PRODH; RGS4; SLC6A4; ZDHHC8*	Influenza*; Rubella*;; Poliovirus*; Cannabis*; Prenatal environmental exposures (i.e. stress*, nutritional deficiency*, Toxoplasma gondii *; HSV-2*)	(132-137)

BD	DISC1; CRMP1; Dysbindin-1; TRIOBP	-Imbalance in monoaminergic neurotransmitter (mainly DA) - Dendritic spine loss - Mitochondrial dysfunction - Endoplasmic reticulum stress - Neuroinflammation - Apoptosis - Decrease of GABAergic interneurons - Imbalance of GABAergic system	- Episodes of elated mood•; - Episodes of depressive mood•; - Delusions•; - Hallucinations• - Sleep changes•;	*BDNF; CACNA1C, TENM4 NCAN; G72/DAOA; DISC1, NRG1; TPH2; HTT; DAT1; COMT*	Asthma*; Obesity*; Migraine*; Head injury* Influenza*; Rubella*; Poliovirus*; Cannabis*; prenatal environmental exposures (i.e. stress*, nutritional deficiency*, Toxoplasma gondii *; HSV-2*)	(138-141)
MDD	DISC1; CRMP1; Dysbindin-1; TRIOBP	- Impaired regulation of HPA axis -Activation of proinflammatory cytokines	- Increased amygdala, medial prefrontal cortex activity• - Dysphoria•; - Loss of interest in activities•; - Changes in sleep and appetite•; - Guilt and hopelessness•; - Fatigue•; - Restlessness•; - Concentration problems•; - Suicidal ideation•	*BDNF; NR3C1; MOAO; GSK-3; GRM3; SLC6A4; GRIK4; CRHR1; CRHBP*	Chronic diseases (anxiety disorder*; Angina*; Arthritis*; Asthma*; Diabetes*) prenatal environmental exposures (i.e. stress*, Alcohol*, Tabaco*)	(142-146)

Table 1. Features of chronic brain disorders characterized by aggregation and deposition of aberrant toxic species. The table summarized the biochemical, cellular and clinical characteristics, as well as, the risk factors that might be involved in the progression of the distinct neurodegenerative and psychiatric disorders associated with protein misfolding. Legend: * - Pathogens, such as virus or bacteria, that might act as disease triggers; * - Pathologic conditions that represents a risk factor; * - Environmental/ Toxins as a risk factor; •- Brain Anatomical changes; •- Behavioral symptoms. Abbreviations: HSV - Herpes simplex virus; CMV – Cytomegalovirus virus; MDD – Major depression; DA – Dopamine; SNpc - substantia nigra pars compacta; HCV - hepatitis C virus; FUS - Fused-In-Sarcoma; SOD1 - superoxide dismutase 1; GABA - Gamma-aminobutyric acid; HPA- hypothalamic-pituitary-adrenocortical

Neurodegenerative disorders

From the biochemical point of view, NDs are hallmarked by toxic inclusions with amyloid structure. A seeding-nucleation process occurs in the conformers of disease-associated proteins in order to form amyloid fibrils (as described in section 2.1). That mechanism has been hypothesized to occur as a prion-like mechanism (147).

Prion diseases are hallmarked by β-sheet-rich aggregates of cellular prion protein (PrP^{Sc}) that acts as a seed to initiate the conformation change of a native prion protein (PrP^{C}) (148, 149). During disease transmission, PrP^{Sc} propagates until achieve a toxicity threshold responsible for the cellular dysfunction and brain damage, characteristics of prion disorders (150). The concept of a misfolded protein be a 'prion' is dependent on several factors: 1) The non-native protein assemblies must be stable, with an irreversible aggregation process and resistance to the cell clearance machinery; 2) An efficient recruitment of non-native monomers to form aggregates; and 3) A cell-to-cell spreading capacity (148).

Despite that misfolded proteins implicated in NDs, seems to have a similar aggregation seeding process, and a cell to cell spreading, they lack the prion infectivity characteristic. Due that, it is being suggested the term 'prionoids' to defined them, instead of 'prion proteins' (151). Misfolded tau and Aβ, hallmark proteins of AD and tauopathies, aggregated α-syn, found in PD and cytoplasmic inclusions of TDP-43, related with ALS and FTLD, were proved to share prion-like proprieties. At the molecular level, the conversion into a misfolded protein state and consequent growth in a stable aggregate were described. At the cellular level, cell-to-cell transmission of misfolded protein was also observed, as well as, a progressive pathology spreading through the brain (109, 152-155). However, it is under discussion if infectivity should remain a requirement to define prion species (156, 157). It was demonstrated that oligomeric PrP^{Sc} species could exhibit cell toxicity, but not infectivity, be considered as 'bona fide' prions (158).

Interestingly to mention is the heterogeneity found in NDs among different patients, and within distinct clinical diagnosed disorders, even sharing the same hallmark misfolded protein (Table 1). One plausible explanation might be the existence of 'protein misfolded strains' that can characterize the disease progression and the distinct pathologies. That was previously described for prion protein, where different variants of PrP^{Sc} were found to be associated with the distinct clinical phenotypes of prion disorders (159, 160). A similar observation was seen *in vitro* and *in vivo* for tau protein, where strain-specific intracellular tau aggregates were found in different cell types and brain regions. Intracellular tau deposits isolated from brains of tauopathies patients showed an association of a differential strain phenotype with disease nature and progression (161-163). In a recent publication, Laferrière et al. also described a strain-phenotype of distinct misfolded TDP-43 conformations related to different

stages of FTLD (164). For several other proteins, i.e. α-syn (165-167), and Aβ (168, 169), similar evidence has been described.

On the other side, a cross-seeding phenomenon has been extensively observed in NDs. The intriguing question is if specific misfolded proteins can be considered as a hallmark of a disorder, or the misfolding of specific proteins are a shared feature of a clinical symptom found, overlapped in several NDs (170). For instance, in AD patients, intracellular tau neurofibrillary tangles and extracellular Aβ plaques are found simultaneously (171). Neuropathological studies also demonstrated α-syn deposition in Lewy bodies (172) and TDP-43 aggregation (173) nearly in half of AD cases. In PD patient brains, the presence of Aβ deposits, tau aggregates (174) and TDP-43 deposits (175) were also reported. Several studies have been lately conducted *in vitro* and *in vivo,* to understand if the disease is initiated by a single type of aggregate, that later triggers a cascade event that leads to the misfolding of other proteins (176-179, 180 , 181, 182); or if, there is no a 'main motor force' and the protein misfolding occurs at the same time to more than a single protein. It is also important to mention that the cross-seeding effect could be only a consequence of protein homeostasis disruption, which in a cascade-event manner enhances the neuronal vulnerability, i.e,. to external factors that might contribute to the disease progression (183).

Chronic mental illnesses

Unlike to NDs, in CMIs there is a lack of a biological hallmark. The absence of a biological signature associated with the mental illness conditions makes the clinical diagnosis still exclusively based on clinical interview between psychiatrist and patient. A singular feature of CMIs is the considerable overlap in symptomology and genetic background across SCZ, Bipolar (BD), and major depression (MDD) (184). It has been suggested they form a spectrum, which makes even more complicated the clinical diagnostic only based on the disease symptoms (185). In past years, strong evidence of an association of protein misfolding to mental illnesses conditions has been reported (186-190). In line with the research done for NDs which insoluble proteins found in sporadic forms of the diseases, were also found mutated in the familial cases of the same disorders (191), a risk factor gene for CMI was investigated. In 2018 Leliveld et al reported the first evidence on that direction for DISC1, previously genetic associated with SCZ and other recurrent affective disorders (192, 193). They found misfolded DISC1 as a hallmark of a subset of CMI patients. Aggregated DISC1 was described in ~ 20% of *pos-mortem* human brains, clinically diagnosed with SCZ, BD, and MDD but absent in healthy controls. Insoluble DISC1 conformers were then proved to lead to a loss-of-function phenotype by impairing the binding to a key DISC1 ligand, the nuclear distribution element 1 (186). Furthermore, *in vitro* and *in vivo* data gave new support to the hypothesis that aggregation of DISC1 protein has

consequences for regular cell function, that might be related to CMIs: 1) In an overexpressed cell model, DISC1 forms aggresomes that acquire a gain-of-toxic function by sequestration of the soluble protein - dysbindin; 2) DISC1 aggresomes showed cell-to-cell transmissibility (187), and a perinuclear vimentin cage (194) even without an amyloid structure; 3) A disease-associated polymorphism - S704C led to a high oligomerization of DISC1 (195, 196); 4) A transgenic rat, modeling the insoluble DISC1 found in CMI patients, demonstrated changes in dopamine homeostasis (194); 5) DISC1 also shows a co-aggregation phenotype with two proteins misfolded in NDs. In a transgenic mice model for Huntington's disease (HD), mutant huntingtin (mHtt) recruits DISC1 to the aggregates. A co-localization of mHtt was found in HD patient brains (197). In FTLD patient brains and in a transgenic model, a co-aggregation pattern of DISC1 and TDP43 was also reported (198). Altogether, these findings support the suggested classification of 'DISC1opathies' as a misfolded disorder (199).

Recent *in vivo* and *in vitro* data have been supporting the idea of aggregated proteins as a biological definition for CMIs patient subsets (78). Dysbindin-1 (200), CRMP1 (188), TRIOBP-1 (189, 201) and NPAS3 (202), are the best examples of candidate proteins that might be used as a biological marker. That gives new hope for a more accurate clinical diagnostic in mental illnesses and new insights to ameliorate pharmacotherapeutic strategies.

To summarize, an overlap in the clinical manifestation of CMIs and NDs is often reported not only restricted to the co-mobility of diseases but also the co-occurrence of them (for more detailed information, (78)). That lead us to think that protein homeostasis disruption is transversal to chronic brain disorders, and similar pathological mechanisms might be shared.

Research aims

The research aims of the present thesis were to understand the mechanisms behind the protein homeostasis disruption better, and in a translational approach find a biological signature for mental illnesses, based on misfolded proteins.

The following aims were addressed here:

1. Characterization of the molecular/cellular conditions of aberrant protein homeostasis induced by virus, in NDs and CMIs *(Chapter 1 & 2)*;

2. Identification of novel misfolded proteins in CMI *(Chapter 3)*.

Chapter 1

An alternative view in the aggregation process associated with protein misfolding disorders

Viral capsid assembly as a model for protein aggregation diseases: Active processes catalyzed by cellular assembly machines comprising novel drug targets

Rita Marreiros, Andreas Müller-Schiffmann, Verian Bader, Suganya Selvarajah, Debendranath Dey, Vishwanath R. Lingappa, Carsten Korth

Virus Research 207 (2015) 155–164

Author's contribution (80 %):

- Manuscript writing

The review presented here aimed to discuss a novel concept of how aggregated species, the hallmark of protein conformational disorders, are built. The proposed hypothesis is based on the assumption of a specific overlap with the cell assistance factors involved in the viral capsid assembly and the ones involved in the assembly/ disassembly of misfolded proteins.

It has been recently suggested that, assembly of viral components during viral replication is not a spontaneous process but is catalyzed by cellular host factors (203, 204) so-called assembly machines. For a more effective replication, the virus might recruit multiprotein complexes from the host cell in an energy-dependent manner, to accelerate the capsid assembly process. In a similar way to NDs or CMIs, the monomers and/or small oligomers of aggregated proteins are also substrates of these cellular multiprotein complexes. Disturbances in protein homeostasis by recruitment of cellular machinery for aberrant, non-homeostatic purposes, either during viral replication or in protein misfolding disorders lead to a specific cellular phenotype characterized by protein inclusions. It is hypothesized that cellular host factors involved in viral capsid assembly are also responsible for the impairment of specific proteostatic pathways. If it is correct, these cellular factors involved in the viral capsid assembly might be a valuable target for new therapeutics in NDs. To achieve the goal, antiviral compounds that interfere with the cellular assembly machines would have to be tested. In a cellular model showing oligomeric Aβ species, an overall reduction in multimers was seen upon antiviral compound treatment.

In this review, we suggested a shared pathway of virus and protein conformational disorders, involved in protein homeostasis disruption. Identification and validation of new assembly machines involved in the different protein conformational disorders might be a valuable approach to explore novel therapeutic routes.

Virus Research 207 (2015) 155–164

Contents lists available at ScienceDirect

Virus Research

journal homepage: www.elsevier.com/locate/virusres

Viral capsid assembly as a model for protein aggregation diseases: Active processes catalyzed by cellular assembly machines comprising novel drug targets

Rita Marreiros[a], Andreas Müller-Schiffmann[a], Verian Bader[a], Suganya Selvarajah[b], Debendranath Dey[b], Vishwanath R. Lingappa[b], Carsten Korth[a,*]

[a] Department Neuropathology, Heinrich Heine University Düsseldorf Medical School, Moorenstrasse 5, 40225 Düsseldorf, Germany
[b] Prosetta Biosciences, Inc, San Francisco, CA 94107, USA

ARTICLE INFO

Article history:
Received 30 June 2014
Received in revised form 9 September 2014
Accepted 1 October 2014
Available online 25 October 2014

Keywords:
Virus capsid
Protein assembly
Assembly machine
Host factor
Prions
Neurodegenerative diseases
Allosteric sites
Catalysis
Protein conformational disease
Protein aggregation
Alzheimer's disease
Disrupted-in-schizophrenia 1
Amyloid beta peptide

ABSTRACT

Viruses can be conceptualized as self-replicating multiprotein assemblies, containing coding nucleic acids. Viruses have evolved to exploit host cellular components including enzymes to ensure their replicative life cycle. New findings indicate that also viral capsid proteins recruit host factors to accelerate their assembly. These assembly machines are RNA-containing multiprotein complexes whose composition is governed by allosteric sites. In the event of viral infection, the assembly machines are recruited to support the virus over the host and are modified to achieve that goal. Stress granules and processing bodies may represent collections of such assembly machines, readily visible by microscopy but biochemically labile and difficult to isolate by fractionation.

We hypothesize that the assembly of protein multimers such as encountered in neurodegenerative or other protein conformational diseases, is also catalyzed by assembly machines. In the case of viral infection, the assembly machines have been modified by the virus to meet the virus' need for rapid capsid assembly rather than host homeostasis. In the case of the neurodegenerative diseases, it is the monomers and/or low n oligomers of the so-called aggregated proteins that are substrates of assembly machines. Examples for substrates are amyloid β peptide (Aβ) and tau in Alzheimer's disease, α-synuclein in Parkinson's disease, prions in the prion diseases, Disrupted-in-schizophrenia 1 (DISC1) in subsets of chronic mental illnesses, and others. A likely continuum between virus capsid assembly and cell-to-cell transmissibility of aggregated proteins is remarkable. Protein aggregation diseases may represent dysfunction and dysregulation of these assembly machines analogous to the aberrations induced by viral infection in which cellular homeostasis is pathologically reprogrammed. In this view, as for viral infection, reset of assembly machines to normal homeostasis should be the goal of protein aggregation therapeutics.

A key basis for the commonality between viral and neurodegenerative disease aggregation is a broader definition of *assembly* as more than just simple aggregation, particularly suited for the crowded cytoplasm. The assembly machines are collections of proteins that catalytically accelerate an assembly reaction that would occur spontaneously but too slowly to be relevant *in vivo*. Being an enzyme complex with a functional allosteric site, appropriated for a non-physiological purpose (e.g. viral infection or conformational disease), these assembly machines present a superior pharmacological target because inhibition of their active site will amplify an effect on their substrate reaction. Here, we present this hypothesis based on recent proof-of-principle studies against Aβ assembly relevant in Alzheimer's disease.

Proteins have evolved to execute multiple functions, amongst them the prominent function of catalysis, i.e. the acceleration of a chemical reaction without changing its final equilibrium. Biochemical reactions occur spontaneously if given enough time, but their kinetic facilitation by enzymes greatly accelerates evolvability of biological processes themselves which is why, ultimately, they were selected by evolution (Kirschner and Gerhart, 1998).

Proteins are generated in the cell through translating mRNA according to the genetic code on multiprotein assemblies containing RNAs, called ribosomes, followed by posttranslational

* Corresponding author. Tel.: +49 211 8116153; fax: +49 211 8117804.
E-mail address: ckorth@hhu.de (C. Korth).

http://dx.doi.org/10.1016/j.virusres.2014.10.003
0168-1702/

modifications by virtue of a remarkable diversity of more or less complex energy-requiring processes (Xue and Barna, 2012). Complementing Anfinsen's paradigm of sequence-encoded spontaneous (Anfinsen, 1973), and unassisted folding of a protein notwithstanding, two critical dimensions of this process require enzymic catalysis to be fully explained. The first is how these processes proceed on the timescale observed in living cells, and the second is how they can occur in the crowded environment within the cell, where interacting proteins cannot find themselves as readily as it would occur for purified proteins in isolation (Fulton, 1982; Alberts, 1998; Hartl et al., 2011).

Full functionality of a protein is achieved after a series of posttranslational modifications that occur simultaneously with or after protein biogenesis. These can include covalent modifications like glycosylation, sumoylation and others, but also folding into different conformers or multimerization. For posttranslational modifications such as glycosylation, the host glycosyl transferases that catalyze the addition of carbohydrate moieties to defined amino acids within a recognition motif (Dennis et al., 1999) are known. However, host factors regulating the folding of a protein into different conformations (Lingappa et al., 2002) or multimers (Fink, 1999) are less well understood. One reason for this could be that the enzymatic activity for protein multimerization is not performed by a single protein molecule as for glycosylation but by a transient and labile complex of proteins that are difficult to detect as such. Put another way, if the ribosome, itself a multiprotein complex RNA-containing covalent assembly machine, were as unstable as hypothesized here for non-covalent assembly machines, we might still not understand how proteins are made.

In the course of our studies we have noted a striking similarity between new findings in virus capsid assembly (Gay and Neuman, 2013; Lingappa et al., 2013a,b) and endogenous protein aggregation. This leads us to speculate that much of what has been conventionally viewed as spontaneous protein *aggregation* may in fact be catalyzed protein *assembly*. By analogy to viral capsid formation, long viewed as self-assembly, and only more recently recognized as the result of host catalysis through the action of labile multiprotein complexes, perhaps diseases of protein aggregation are initiated by action of aberrant assembly machines and their disordered or dysregulated assembly intermediate products. The novel notion that viral capsid assembly is an active process executed by host factors that may be similar, overlapping or completely different from host factors promoting assembly of other endogenous host proteins, including those involved key events in neurodegenerative diseases, has consequences for drug discovery strategies – it may greatly accelerate drug discovery by directing research in a completely new direction from the current dominant focus. What we should be asking then, is what are the catalysts that bring this about, how are their functions different from the catalysis that occurs under physiological, homeostatic conditions, and how can that dysfunctional non-homeostatsis catalysis be normalized.

1. Virus capsid assembly

Viruses can be considered as dynamic molecular assemblies, containing a nucleic acid genome that is enclosed in a protein capsid shell. In many cases a lipid envelope is also observed. Typically, the envelope also contains the protein(s) that bind to cell surface receptors to target the virus. Some viral families (e.g. the *Picornaviridae* and *Enteroviridae*) have no envelope: for them, the capsid *is* the virus.

Through evolutionary selection pressure favoring the fastest generation cycles, virus components have evolved to manipulate host cellular machinery for rapid and optimal replication (Dimmock et al., 2007; Prasad and Schmid, 2012). By virtue of their fast replication cycles they have, in effect, discovered all cellular "niches" that can be exploited to their advantages. That diverse viral families appear to have chosen distinctive pathways of host-catalyzed capsid assembly is remarkable (Lingappa et al., 2013b): it suggests that such reprogramming of assembly machines is highly profitable for viruses and therefore may be an inherent weakness of metazoan biology–the price we pay for such complex organ systems such as the central nervous system (CNS) in constant need of repair and attention, and therefore at constant risk of subversion. And since protein machines are likely themselves built by protein machines, the potential for "prion-like" epigenetic propagation of dysfunctional assembly may exist.

Viral replication and propagation is a process of alternating cycles with viral invasion of suitable cells, release of virus genome into the cytosol where encoded viral components are replicated and, finally, assembly of new infectious particles before their release from the host cell, subsequently possibly infecting other host cells and re-initiating the replication cycle (Mateu, 2013b). The viral capsid consists of a protein shell that serves as a protection of the virus genome and encodes invasion and release signals.

Several different stages in virus morphogenesis can be distinguished such as capsid assembly, nucleic acid packaging, and virus particle maturation. Here, the focus will be on capsid assembly. The size and shape of capsid structure is in general regular like symmetric oligomers made by assembling of capsid protein subunits (Klug, 1999; Prasad and Schmid, 2012). The individual protein subunits are asymmetrical, but they are assembled to form symmetrical structures. Different viruses can build their capsids with a different number of capsid protein subunits. The most abundant type of capsids throughout virus families are helical and icosahedral capsids. Theoretically, the structure of helical capsid is extremely simple, since the number of capsid protein subunits required is extendable, depending only the length of nucleic acid genome that needs to be encapsulated. On the other hand, the small icosahedral capsids are made exactly with 60 capsid protein subunits that limit the size of nucleic acid genome that can be enclosed. The larger icosahedral capsids can be made using 60 multiples of subunits of a capsid protein (Amos and Finch, 2004; Carter and Saunders, 2007). The intracellular compartments where this process occurs are denominated "viral factories" (Novoa et al., 2005) (see below).

So far, capsid assembly has mainly been viewed as a spontaneously occurring process of self-assembly (Zlotnick, 2005), dependent only on the presence of capsid protein subunits themselves (Johnson et al., 2005; Mateu, 2013a; Prevelige, 1998). Thermodynamically, viral capsid assembly is described in two states, the dissociated state where monomers of the capsid protein are found, and the associated state where the capsid is formed (Fig. 1a). Energetically, this assembly process follows a sigmoidal curve with a lag phase where the concentration of the proteins that compose the capsid determines the speed of the reaction rate. Off-pathway reactions can occur leading to aberrant capsid formation where the quaternary structure is not native (Endres and Zlotnick, 2002; Zlotnick, 2003). In the self-assembly of complex icosahedral capsids, different thermodynamic kinetic models have been proposed consisting of a lag phase, an equilibrium phase, and an elongation phase with the formation of new virus capsid nuclei, that initiate viral capsid assembly (Endres and Zlotnick, 2002; Zlotnick, 2005). *In vitro* experiments are useful to understand the self-assembly of capsids, but do not take into account the interaction with scaffolding proteins or viral nucleic acids that are present *in vivo*. More specifically, because something can happen spontaneously does not mean that *in vivo* it is not accelerated by catalysis.

Recently, findings comprising various viral families (Klein et al., 2004, 2011; Lingappa et al., 2006, 2013a,b; Zimmerman et al., 2002) suggest that the cellular pathway to capsid assembly may be

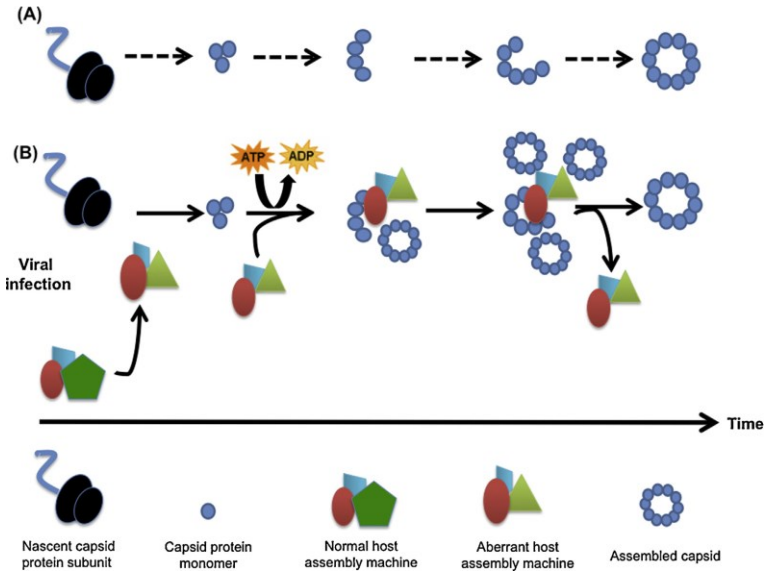

Fig. 1. Representative scheme of the strategies for the assembly of virus capsids. (A) Unassisted capsid self-assembly. Note that the lines are dashed because capsids would form by a progressive accretion of monomers rather than via discrete assembly intermediates. (B) Capsid assembly is catalyzed by host proteins serving as aberrant assembly machines modified from their normal homeostatic assembly-related functions, and is an energy-dependent process occurring via discrete assembly intermediates, perhaps with the participation of different assembly machines for distinct steps.

substantially different from the foundational self-assembly models that conform to the minimum requirements of thermodynamics. Indeed, without such catalytic "add ons" viral propagation might not be possible, given the obstacles not only of cytoplasmic crowding but also of innate immune mechanisms. Specifically, it has been suggested that capsid assembly is accelerated by transient formation of virus-recruited multiprotein complexes with enzymatic activity that serve as "assembly machines" to accelerate capsid formation (Lingappa et al., 2013a,b). This catalyzed viral capsid assembly was demonstrated to be an energy-dependent process, and host protein factors seem to play a major role (Lingappa et al., 2013a,b). These novel assembly machines, perhaps together with more classical notions of molecular chaperones and/or other scaffold proteins, would have an essential role in directing newly synthesized capsid protein subunits through discrete assembly intermediates culminating in capsid formation (Fig. 1b). The catalytic nature of this reaction was deducted from the absence of co-factors in the final capsid and the process and its energy-dependence (Lingappa et al., 1994). A detailed investigation of this new pathway of viral capsid assembly will be highly relevant to develop novel pharmaceutical targets for antiviral drugs (Gay and Neuman, 2013; Lingappa et al., 2013a) (see below).

2. Protein conformational disorders

A hallmark of neurodegenerative disorders is the accumulation of disease-specific proteins in the brain (Taylor et al., 2002). Remarkably, the same proteins accumulate in sporadic and in inherited forms of neurodegenerative diseases (Prusiner, 2001). These disorders are therefore seen as protein conformational diseases where multimerization of a specific protein is massively out of balance, with the ultimate consequence of fatal neuronal loss.

Over the last thirty years, specific proteins identified as aggregated or insoluble in biochemical purification procedures have been identified in these diseases (Table 1), like Aβ or tau for Alzheimer's disease (AD), α-synuclein for Parkinson's disease (PD), superoxide dismutase 1 in amyotrophic lateral sclerosis, huntingtin in Huntington's disease (for review see, for example (Prusiner, 2001), or Disrupted-in-schizophrenia 1 (DISC1) in subsets of chronic mental illnesses (Korth, 2012; Leliveld et al., 2008; Ottis et al., 2011).

The classical prion diseases like Creutzfeldt-Jakob disease in humans or scrapie in sheep are caused by an alternatively folded, disease-associated protein, termed PrP^{Sc}, that induces conversion of "normally" folded substrate conformers, termed PrP^{C}, into the disease-associated conformer thereby initiating a chain-reaction type of replication of the alternatively, disease-associated conformation which triggers a neurotoxic cascade (Prusiner, 1998). Initially thought to be unique to the specific, extracellular prions, this concept of cell-to-cell transmission is now seen also in other protein aggregates, including yeast prions, Aβ and cytosolic proteins such as α-synuclein, tau, polyglutamine diseases, or DISC1 assemblies (Auli et al., 2014; Bader et al., 2012; Clavaguera et al., 2009; Desplats et al., 2009; Domert et al., 2014; Grad et al., 2011; Korth, 2012; Lee et al., 2010; Li et al., 2008; Munch et al., 2011; Ottis et al., 2011; Ren et al., 2009).

Thus, compelling *in vitro* and *in vivo* evidence demonstrates that prion replication of protein aggregates is a general biological feature. Even though the misfolding pathway of most of these proteins (Table 1) can be modeled in cell-free *in vitro* systems with exclusively synthetic or purified protein present, an efficient replication *in vivo* in the context of a crowded, complex cytosol is likely to involve assembly-assisting molecules or multimolecular complexes. These are potentially energy-dependent as many steps in cellular protein folding from protein biogenesis to protein assembly are such energy-dependent, active processes, perhaps not unlike that described for capsid assembly above.

Spontaneous folding as originally conceived by Anfinsen (1973) seems to be mainly caused by solvophobic interactions of polar water molecules with hydrophobic side chains of proteins. In the

Table 1
Protein confromational diseases associated with protein misfolding and amyloid aggregation.

Disease	Protein involved	Cellular localization of aggregated protein	Possible aggregation caused
Prion diseases	PrP	Extracellular	Mutations in prion protein gene, spontaneous conversion[a]
AD	Aβ	Extracellular	Mutations in APP gene and/or APP cleavage enzymes in prion protein gene, increase in Aβ generation[a]
	Tau protein	Intracellular	Post-translational modifications of tau protein[a]
PD	α-Synuclein	Intraneuronal	Mutations or of α-synuclein or other genes, toxic effects on dopaminergic neurons[a]
Amyotrophic lateral sclerosis	Superoxide dismutase 1	Intracellular	Mutation in Cu/Zn superoxide dismutase[a]
Huntington's disease	Huntingtin	Intracellular	Mutation in huntingtin gene with CAG expansion[a]
Tauopathies, Frontotemporal dementias	Tau, TDP-43	Intracellular	Mutations in Tau[a], TDP-43
Familial amyloidotic polyneuropathy	Transthyretin	Extracellular	Mutations in Transthyretin[a]

[a] Associated with gene mutations, or other alterations, the amyloid can also arise following disruption in the clearance mechanisms of the cell.

resulting dimensional structure of a well folded protein, the majority of hydrophobic side chains are buried in the internal core, while the hydrophilic residues are exposed to polar water molecules (Dyson and P.E., 2005; Uversky et al., 2000). However, even in cell-free *in vitro* systems, evidence against the Anfinsen dogma has been demonstrated: proteins that normally function in globular states can also adopt intermediate conformations (Waudby et al., 2013). Some proteins that have a correct folded structure, can also adopt a subsequently unfolded structure, and as a consequence display dynamic structural fluctuations (Vendruscolo and Dobson, 2013). Upon cellular stress, incorrect protein folding may occur, resulting in aggregation, loss of function or association with other cellular components (gain of function), leading to dramatic changes in the biological functions and homeostasis of the cell (Dobson, 2004; Sgarbossa, 2012).

In order to ensure that cellular integrity is maintained, the chaperone machinery plays a key role in securing correct protein folding. This is executed by reversible binding to unfolded and misfolded proteins, accelerating formation of a correct conformation of a non-native protein in an energy-dependent manner. Proteins that are not correctly folded may also be removed from the cell by the ubiquitin-proteasome system or autophagy, depending on its size (Hartl and Hayer-Hartl, 2002; Lee et al., 2013). Misfolded proteins that escape from the cellular cleaning mechanism tend to aggregate in insoluble clusters, in the extreme cases of neurodegenerative disease packaged into fibrils or amyloid (Knowles et al., 2014; Stefani and Dobson, 2003).

The amyloid fold of a protein is a particular fold because it is one of the tightest ways a protein can be packaged (Greenwald and Riek, 2010). Patterns of amyloid fibrils observed in studies using X-ray diffraction demonstrated that the core of each protofilament adopts a cross-β-structure, in which β-strands form effectively continuous hydrogen-bonded β-sheets run along the length of the fibril (Jimenez et al., 2002; Sunde et al., 1997). *In vivo*, amyloid fibrils can also be characterized by the binding affinity to Congo red dye, showing green birefringence when viewed in polarization microscopy (Glenner et al., 1972; Sipe et al., 2010; Wolman and Bubis, 1965).

The process where proteins are converted from functional, globular and soluble folds to the amyloid fold is a complex phenomenon where multiple precursor species are present (Apetri et al., 2006). In this process, nucleated polymerization is a crucial step for the formation of aggregates from soluble precursor species (Nelson et al., 2005). In the first phase of this process, called lag phase, nucleation occurs through interaction between monomers that expose their amyloid-forming segments at the same time and at sufficient concentration for bonding and templating of the fibril pattern (Eisenberg and Jucker, 2012). Nucleation is considered a rare event that is considered to be a slow process and not frequent for intracellular proteins. Once the aggregate nucleus is formed, a rapid growth phase occurs and the single molecules will end up forming β-sheet rich structures in a thermodynamically favorable process, called elongation phase (Eisenberg and Jucker, 2012; Jarrett and Lansbury, 1993). Subsequently, the amyloid process reaches a plateau, the saturation phase, wherein the total quantity of protein is in equilibrium (Nelson et al., 2005). The susceptibility of proteins to form amyloid structures is correlated to their chemical properties such as net charge, secondary structure, hydrophobicity and aromatic interactions (Chiti et al., 2003).

Remarkably, not all amyloid proteins are toxic, but some even execute physiological functions (for review see Greenwald and Riek, 2010). In bacteria, fungi and yeast, amyloid species can function in formation of biofilms, helping in host invasion, in the modulation of fungal adhesion and promotion of an antiviral innate immune response (Chapman et al., 2002; Fowler et al., 2007; Hou et al., 2011). In mammals, these protein species are involved in skin pigmentation and some hormones adopt the amyloid structure when stored in secretory granules (Maji et al., 2009).

Amyloidogenic HetS protein has a function in fungal self/non-self recognition (Seuring et al., 2012; Wasmer et al., 2008), and in the invertebrate Aplysia, CPEB amyloid plays a role in regulating synaptic strength (Si et al., 2010, 2003).

Even though the presence of amyloid deposits may be the most striking feature in neurodegenerative diseases, the primary pathogenic agents in these conditions seem to be oligomeric species rather than the fibrils that correlate with clinical symptoms (Lue et al., 1999; McLean et al., 1999; Naslund et al., 2000). These oligomers may fulfill physiological functions and, in a disease context, are observed in the transition phase between protein assembly and aggregation with neurotoxic properties (Cremades et al., 2012; Haass and Selkoe, 2007; Koffie et al., 2009). Oligomer toxicity could in part be caused by their inherently misfolded nature, since the oligomer surfaces display chemical groups that are non-accessible under normal physiological conditions in a normal cellular environment (Cheon et al., 2007). Several different types of oligomeric species can be detected during the aggregation process depending on the nature of the cells where they are formed and correlating with a distinct cellular pathology (Campioni et al., 2010) (Table 1). Fibril formation has also been considered to be part of a cellular defense mechanism against oligomer toxicity (Ross and Poirier, 2004). At any stage during the assembly of protein monomeric educts to low-n oligomers and larger multimers or amyloid could assembly machines assist. For replication of mammalian prions (PrP^{Sc}), early on the existence of cellular cofactors assisting in prion conversion was deduced based on genetic experiments (Kaneko et al., 1997; Telling et al., 1995). It is likely that these are specific assembly machines. It is remarkable that the concept of prion replication has now been extended to many other protein mutlimers

characteristic in particular neurodegenerative diseases (Prusiner, 2013). It is clear that a cellular, catalyzed assembly will greatly accelerate cell-to-cell transmission of an otherwise slowly occuring conversion as demonstrated numerous times in cell-free *in vitro* systems.

The following section will review the evidence for a sharing of host factors or assembly machines between viral (capsid) assembly and endogenous multimer assembly, respectively.

3. Evidence for the use of similar cellular factors for virus assembly and protein assembly

Similarities between viral factories and the cellular localization of protein aggregates in protein conformational diseases support the notion that viruses and endogenous protein assemblies use similar, overlapping or sometimes even same cellular machinery for molecular assembly (Wileman, 2007). Disturbance of the cell by hijacking the cellular machinery for aberrant purposes by either viruses or protein conformational disease creates a proteostasis problem which then results in a specific cellular phenotype of protein inclusions. We now introduce a selection of examples for this.

3.1. Involvement of cellular clearance systems

Cellular structures involved in the removal of protein aggregates localize not only in the cytoplasm but also in the nucleus. These structures are called nuclear domain 10 (ND10) bodies and can contain ubiquitinated proteins and molecular chaperones (Fu et al., 2005). When the degradative capacity of the cell is exceeded or a defect in the mechanisms of clearance of the cell occurs, misfolded proteins are deposited near the microtubule organization center (MTOC) and/or in ND10 bodies and form aggregates (Wileman, 2007). In cells infected with viruses, similar structures are formed by material containing full viruses and virus assembly intermediates designated "viral factories" (Novoa et al., 2005; Wileman, 2006). In both cases, protein aggregates and viral factories are localized near the MTOC, recruiting cellular chaperones, ubiquitin and mitochondria (Wileman, 2006).

Mitochondria are invariably recruited during the viral assembly indicating energy-dependent processes involved in viral replication/assembly. Studies with African swine fever virus (Cobbold et al., 2000) and with Human Immunodeficiency Virus (HIV) Type 1 (Tritel and Resh, 2001) showed that virus assembly is an ATP-dependent process. Similarly, mitochondria are also recruited to the cellular locations of protein aggregation to provide ATP for correcting folding where the chaperone machinery is also of paramount importance (Hartl and Hayer-Hartl, 2002). Expression and colocalization of the chaperone machinery seems to be present during the entire virus assembly process, and, for example, for vaccinia virus, the inhibition of HSP90 chaperone negatively affects virus assembly (Hung et al., 2002). Finally, cell-free systems that reconstitute viral capsid formation *de novo* have revealed its ATP-dependence, suggestive of energy-dependent catalysis (Lingappa et al., 1994, 1997, 2013a) (see below).

The autophagy system is another subcellular structure that is important for the removal of pathogens from the cytoplasm of the cell, in a process termed xenophagy (Gomes and Dikic, 2014; Kirkegaard et al., 2004). Viruses submerged by autophagosomes can be released from cells after fusion of lysosomes with the plasma membrane, just as the clearance of soluble and aggregated forms of protein in protein conformational disorders (Ravikumar and Rubinsztein, 2006; Wileman, 2006). In poliovirus, for example, the suppression of Atg12 and Atg18 genes, both required for autophagy, leads to decreased poliovirus production (Jackson et al., 2005). Similar links exist to other viruses: in HIV type 1, autophagosome formation is a platform for viral assembly (Cheng et al., 2014). During cellular infection with hepatitis B virus, the autophagy machinery from the host is activated and when autophagy is insufficient, production of hepatitis B virus particles is decreased (Li et al., 2011).

Interestingly, it has been observed for a long time that viral infection of cells can induce subcellular, inclusion-like structures that resemble protein aggregates (reviewed in Moshe and Gorovits, 2012). In fact, historically and in the absence of molecular diagnostics, the morphology of inclusions was an important diagnostic phenotype.

For example, Negri bodies (NBs), cytoplasmic inclusions formed during rabies virus infection (Jackson et al., 2001; Kristensson et al., 1996) resemble aggresomes seen in some neurodegenerative disorders. NBs have a functional role in the Rabies virus transcription and replication. The organization of NBs can follow a mechanism similar to cytoplasmic inclusions formed by a mutant form of huntingtin protein in Huntington's disease. These agressomes are composed by a dense core of huntingtin aggregates surrounded by a ring that consists of proteins that are successively recruited from the exterior surface of the dense core (Matsumoto et al., 2006). The NBs can also have a concentric organization due to the association of Toll-like receptors and viral proteins, forming a ring into which proteins can be inserted. Although the complete composition of NBs is still unknown, these structures also accumulate HSP70 and ubiquitinated proteins similar to aggresomes from protein conformational diseases (Menager et al., 2009). However, NBs are not localized at the MTOC where the "viral factories" are preferentially localized, likely because of the lack of involvement of microtubule network in the formation of these structures (Lahaye et al., 2009). Possibly, NBs are a consequence of a cytoplasmic sequestration within a cellular defense mechanism against viral infection involving components of aggresome pathway such as some host factors involved in stress response (Lahaye et al., 2009).

In protein conformational disorders, higher order oligomers and aggregates that are inaccessible to the narrow proteasome opening have a higher dependency of autophagy for the degradation process. Previous studies using knockout mice for *Atg* genes, essential gene for autophagy, revealed that autophagy is a critical process for neruonal health. It was demonstrated contingent with loss of *Atg5* and *Atg7* genes, an age dependent accumulation of intraneuronal aggregates with polyubiquitination, inclusion formation and neurodegeneration occurred (Hara et al., 2006; Komatsu et al., 2006). A change in this process can be one of the key factors involved in the increase of cell aggregates evident in misfolding diseases.

3.2. Direct or indirect interactions of viral proteins with hallmark proteins of protein conformational disease

The similarity of the cellular localization of viral factories and that of endogenous protein aggregates has led to the hypothesis that viral infections increase the risk of protein conformational diseases (De Chiara et al., 2012; Zhou et al., 2013). Likewise, alterations in the CNS related to aging, the increase in oxidative stress and the impairment in energy production can lead to an increased susceptibility of the CNS to infections agents (Mattson, 2004). Taking this into account, external insults, including the toxicity of viral proteins or proteins aggregates, can lead to a vicious circle of mutually increasing the vulnerability of aged neurons.

So far, direct evidence for a mechanistic involvement of such a mutual increase in vulnerability of viral infections and protein conformational diseases is rather sporadic or anecdotal. Chronic exposition to Herpes simplex virus type-1 (HSV-1) has been associated to an increase in the risk of AD by herpes viruses particles specifically recruiting cell membranes from the host containing

amyloid precursor protein (APP) (Bearer, 2004). This process can affect the location and proteolysis of APP, and consequently leads to an increase in toxic Aβ formation, resulting in a neuronal dysfunction associated with the progression of AD (Satpute-Krishnan et al., 2003).

The presence of viral DNA in post-mortem brains of AD patients, mainly in patients that carry the allele of the gene encoding apolipoprotein E, a risk factor for this disease, is one of the facts that supports this hypothesis (Itzhaki et al., 1997). Another study identified an increased phosphorylation of several residues of tau protein due to a HSV-1 infection (Wozniak et al., 2009). Wozniak et al. also demonstrated a higher association between HSV-1 and Aβ plaques in temporal and frontal cortices of AD patient's brains, compared with normal aged brains. Some genome wide association studies have also correlated the brain susceptibility to HSV-1 infection with a genetic risk of AD (Porcellini et al., 2010).

Infection by HIV seems also to be correlated with an increased deposition of Aβ plaques in the brains (Andras and Toborek, 2013). However, the mechanism that triggers this is not fully understood and could be due to the increase of Aβ synthesis (Aksenov et al., 2010), decreased Aβ degradation by the inhibition of neprilysin, an enzyme responsible for Aβ degradation (Rempel & Pulliam, 2005), changing the transport mechanisms across the blood brain barrier (Andras et al., 2010), or a combination of all. The improvement and general well-being of AD patients after antiviral treatment remains to be established (Zhou et al., 2013).

Influenza virus has been implicated in PD when typical symptoms developed in the aftermath of the acute infection. This disease was coincident with encephalitis lethargica causing postencephalitic Parkinsonism, apparently occurring at the same time of influenza A pandemic (1916–1926) (Maurizi, 1985; Poskanzer and Robert, 1963). In addition, it was subsequently shown that individuals born during the influenza pandemic had a two or three-fold increased risk of developing PD compared to individuals born before or after the pandemic (De Chiara et al., 2012). Immunohistochemical and biochemical analyses were performed in different brain regions of patients with postencephalitic parkinsonism and neurofibrillary tangles with hyperphosphorylation of 3R and 4R variant of tau protein were detected. Interestingly, Lewy bodies or other α-synuclein deposits, characteristic features of idiopathic PD, however, were not detected, thus presenting a possibly atypical pathological variant of parkinsonism (Buee-Scherrer et al., 1997; Jellinger, 2009).

Jang et al. demonstrated that in mice infected with A/Vietnam/123/04 influenza virus, viruses can be detected in the CNS. A loss of dopaminergic neurons in substantia nigra, the region most affected in PD, a persistent activation of microglia, an increase in phosphorylation, and aggregation of α-synuclein was detectable—all features of pathological alterations observable in PD patients (Jang et al., 2009). Rohn et al. demonstrated the presence of influenza A virus in macrophages of the substantia nigra of PD patients (Rohn and Catlin, 2011). There is however no direct correlation between presence of the virus and PD symptoms or typical pathology which leaves a mechanistic understanding difficult.

These scattered findings but not systematical investigations show that viral infections of CNS could be causative agents or at least co-factors of some of brain protein conformational diseases.

4. Targeting assembly host factors for pharmacotherapy

Thus, in summary, it is conceivable that not only virus capsids are formed aided by redirected host factors to serve as enzymes of capsid assembly, but that protein aggregation in neurodegenerative diseases is ultimately the result of aberrant catalysis by dyregulated/misdirected assembly machinery. These cellular factors may be transiently assembled and biochemically labile multimeric complexes themselves which is why they may be difficult to detect.

These ideas led us to hypothesize that compounds acting to block the aberrant virally modified assembly machines might prove to be valuable starting points for drug discovery relevant to degenerative diseases not related to viral infections. Thus, for example, the promising compounds or their chemical analogues acting against neurotropic rabies capsid assembly (Lingappa et al., 2013a,b) might also exhibit activity in protein conformational disease, like AD. The assumption would be that the lead drugs would target allosteric sites on similar assembly machines (Tsai et al., 2009).

According to the amyloid cascade hypothesis (Hardy and Selkoe, 2002), AD is triggered by increased production or reduced clearance of the aggregation prone Aβ peptide, in particular $A\beta_{42}$. Especially the formation of synaptotoxic low-n oligomers (dimers and trimers) of Aβ has been correlated with disease progression (Mc Donald et al., 2010). Synaptotoxicity of these oligomers has been demonstrated for naturally-derived, secreted, as well as for synthetic oligomers, with cell-derived Aβ dimers and trimers being invariably up to 100× more toxic than their fully synthetic counterparts (Jin et al., 2011; Reed et al., 2011). Bulk preparation of synthetic Aβ oligomers is generally carried out in non-physiological buffer systems without any cellular co-factors and using high micromolar concentrations of the peptide which leads to a highly heterogenous assembly of unfolded Aβ monomers. Within the cell, the processing of APP as well as N- and C-terminal modifications of the resulting Aβ peptide is tightly controlled by cellular factors (Muller-Schiffmann et al., 2011). Oligomerization of Aβ supported by cellular assembly machines may yield superior biological activity since there is evidence that very low picomolar concentrations of Aβ oligomers positively modulate synaptic plasticity (Puzzo et al., 2008).

If mechanisms of protein assembly between capsids and proteins in neurodegenerative diseases were shared, drugs identified for interfering with viral capsid assembly (Lingappa et al., 2013a,b) should also interfere with assembly of proteins aggregating in neurodegenerative diseases.

In order to test this hypothesis we used the 7PA2 cell line that secretes high amounts of synaptotoxic low-n oligomeric Aβ species (Podlisny et al., 1995). These cells express full length APP including the familial Indiana mutation that increases the amount of cleaved, aggregation-prone $A\beta_{42}$ peptide. These cells have frequently been used to screen drugs with anti-oligomerization potential (Muller-Schiffmann et al., 2010; Walsh et al., 2002, 2005; Yamin et al., 2009). We analyzed a subset of structurally related antiviral compounds that had been demonstrated to interfere with the cellular assembly machine of rabies virus (Lingappa et al., 2013a,b).

Here, 1 μM of the compounds was used to treat 7PA2 cells as described before (Muller-Schiffmann et al., 2010). After immunoprecipitation, the secreted Aβ species were visualized on Western Blot using the 4G8 antibody (Covance) (Fig. 2). In the control lane, SDS-stable dimeric and trimeric Aβ species are clearly visible. The monomeric Aβ is absent due to the lack of monomer stabilizing serum (Podlisny et al., 1995). Non-toxic concentrations of the antiviral compounds used in this assay had different effects on oligomer formation. Compound C strongly reduced the overall formation of low-n Aβ oligomers without changing APP expression levels indicating an effect on a very early step of Aβ oligomer assembly, whereas compound B led to a conversion of oligomers back into monomers. In contrast, compound A was without effect. Thus, all of these compounds may interfere with Aβ oligomerization but at different assembly steps and with qualitatively different

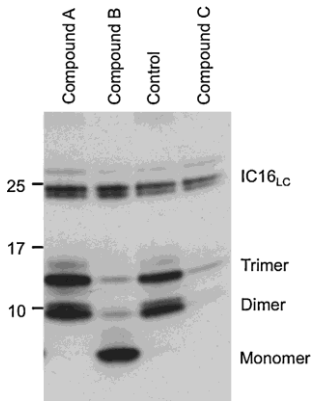

Fig. 2. Assembly-inhibiting antiviral compounds have distinct effects on oligomerization of Aβ peptides. Western Blot of Aβ species (monomers to trimers) derived from supernatants of 7PA2 cells that were treated for 7 days with 1 μM of different antiviral compounds derived from a capsid assembly assay (Lingappa et al., 2013a). Aβ was immunoprecipitated by IC16 that recognizes an epitope in the N-terminus of Aβ (aa 2-8) and visualized by the 4G8 antibody (epitope 17–24 of Aβ). Signals in the range of 25 kDa belong to the light chain of the IC16 antibody that was used for the IP. Compared to the mock treated control, the compounds differentially affected oligomer formation.

activity, indicating that different components and allosteric sites of the assembly machine were targeted.

In summary, surprising similarities in the cellular biology of virus capsid assembly and endogenous protein assembly suggest that cellular host factors, i.e. assembly machines, assist in and accelerate protein multimerization. Through their rapid generation cycles compared to their host cells, viruses have identified and exploited cell-resident macromolecules provided by host proteins used them to their advantage, i.e. fast and stable virus replication including capsid assembly. Similarly, same assembly machines may also accelerate endogenous protein multimerization, either aberrant in protein conformational diseases, or beneficial as in the case of functional protein multimers. The catalytic nature of these assembly machines makes them ideal targets for drug discovery since blocking assembly machinery will slow down assembly and the ensuing functional or toxic effects at substoichiometric concentrations. As proof-of-principle, we present candidate compounds, identified by virtue of their activity against a host assembly machine subverted by a neurotrophic virus (rabies), that inhibit various assembly steps of Aβ, the key molecule in AD.

Acknowledgements

We acknowledge funding support by the Brain Behavior and Research Foundation (NARSAD Independent Investigator Award #20350), NEURON-ERANET ("DISCover", BMBF 01EW1003), BMBF KNDD rpAD (BMBF 01GI1010A), and EU-FP7 (PRIORITY and MC-ITN "IN-SENS" #607616) to C.K, a grant from the Forschungskommission of the Medical Faculty Heinrich-Heine University Düsseldorf to A.M.S., and grant AI101276 from the NIH to VRL.

References

Aksenov, M.Y., Aksenova, M.V., Mactutus, C.F., Booze, R.M., 2010. HIV-1 protein-mediated amyloidogenesis in rat hippocampal cell cultures. Neurosci. Lett. 475 (3), 174–178, http://dx.doi.org/10.1016/j.neulet.2010.03.073.

Alberts, B., 1998. The cell as a collection of protein machines: preparing the next generation of molecular biologists. Cell 92, 291–296, http://dx.doi.org/10.1016/S0092-8674(00)80922-8.

Amos, L.A., Finch, J.T., 2004. Aaron Klug and the revolution in biomolecular structure determination. Trends Cell Biol. 14 (3), 148–152, http://dx.doi.org/10.1016/j.tcb.2004.01.002.

Andras, I.E., Eum, S.Y., Huang, W., Zhong, Y., Hennig, B., Toborek, M., 2010. HIV-1-induced amyloid beta accumulation in brain endothelial cells is attenuated by simvastatin. Mol. Cell Neurosci. 43 (2), 232–243, http://dx.doi.org/10.1016/j.mcn.2009.11.004.

Andras, I.E., Toborek, M., 2013. Amyloid beta accumulation in HIV-1-infected brain: the role of the blood brain barrier. IUBMB Life 65 (1), 43–49, http://dx.doi.org/10.1002/iub.1106.

Anfinsen, C.B., 1973. Principles that govern the folding of protein chains. Science 181, 223–230, http://dx.doi.org/10.1126/science.181.4096.223.

Apetri, M.M., Maiti, N.C., Zagorski, M.G., Carey, P.R., Anderson, V.E., 2006. Secondary structure of alpha-synuclein oligomers: characterization by raman and atomic force microscopy. J. Mol. Biol. 355 (1), 63–71, http://dx.doi.org/10.1016/j.jmb.2005.10.071.

Auli, S., Le, T.T., Moda, F., Abounit, S., Corvaglia, S., Casalis, L., Legname, G., 2014. Defined alpha-synuclein prion-like molecular assemblies spreading in cell culture. BMC Neurosci. 15 (1), 69, http://dx.doi.org/10.1186/1471-2202-15-69.

Bader, V., Ottis, P., Pum, M., Huston, J.P., Korth, C., 2012. Generation, purification, and characterization of cell-invasive DISC1 protein species. J. Visualized Exp. (66), e4132, http://dx.doi.org/10.3791/413.

Bearer, E.L., 2004. Perspectives on herpes-APP interactions. Aging Cell 3 (2), 81–84, http://dx.doi.org/10.1111/j.1474-9728.2004.00089.x.

Buee-Scherrer, V., Buee, L., Leveugle, B., Perl, D.P., Vermersch, P., Hof, P.R., Delacourte, A., 1997. Pathological tau proteins in postencephalitic parkinsonism: comparison with Alzheimer's disease and other neurodegenerative disorders. Ann. Neurol. 42 (3), 356–359, http://dx.doi.org/10.1002/ana.410420312.

Campioni, S., Mannini, B., Zampagni, M., Pensalfini, A., Parrini, C., Evangelisti, E., Chiti, F., 2010. A causative link between the structure of aberrant protein oligomers and their toxicity. Nat. Chem. Biol. 6, 140–147, http://dx.doi.org/10.1038/nchembio.283.

Carter, J.C., Saunders, V., 2007. VIROLOGY-Principles and Application. John Wiley & Sons Ltd.

Chapman, M.R., Robinson, L.S., Pinkner, J.S., Roth, R., Heuser, J., Hammar, M., Hultgren, S.J., 2002. Role of Escherichia coli curli operons in directing amyloid fiber formation. Science 295 (5556), 851–855, http://dx.doi.org/10.1126/science.1067484.

Cheng, C.Y., Chi, P.I., Liu, H.J., 2014. Commentary on the regulation of viral proteins in autophagy process. Biomed. Res. Int. 2014, 962915, http://dx.doi.org/10.1155/2014/962915.

Cheon, M., Chang, I., Mohanty, S., Luheshi, L.M., Dobson, C.M., Vendruscolo, M., Favrin, G., 2007. Structural reorganisation and potential toxicity of oligomeric species formed during the assembly of amyloid fibrils. PLoS Comput. Biol. 3 (9), 1727–1738, http://dx.doi.org/10.1371/journal.pcbi.0030173.

Chiti, F., Stefani, M., Taddei, N., Ramponi, G., Dobson, C.M., 2003. Rationalization of the effects of mutations on peptide and protein aggregation rates. Nature 424 (6950), 805–808, http://dx.doi.org/10.1038/nature01891.

Clavaguera, F., Bolmont, T., Crowther, R.A., Abramowski, D., Frank, S., Probst, A., Tolnay, M., 2009. Transmission and spreading of tauopathy in transgenic mouse brain. Nat. Cell Biol. 11 (7), 909–913, http://dx.doi.org/10.1038/ncb1901.

Cobbold, C., Brookes, S.M., Wileman, T., 2000. Biochemical requirements of virus wrapping by the endoplasmic reticulum: involvement of ATP and endoplasmic reticulum calcium store during envelopment of African swine fever virus. J. Virol. 74 (5), 2151–2160, http://dx.doi.org/10.1128/JVI.74.5.2151-2160.2000.

Cremades, N., Cohen, S.I., Deas, E., Abramov, A.Y., Chen, A.Y., Orte, A., Klenerman, D., 2012. Direct observation of the interconversion of normal and toxic forms of alpha-synuclein. Cell 149 (5), 1048–1059, http://dx.doi.org/10.1016/j.cell.2012.03.037.

De Chiara, G., Marcocci, M.E., Sgarbanti, R., Civitelli, L., Ripoli, C., Piacentini, R., Palamara, A.T., 2012. Infectious agents and neurodegeneration. Mol. Neurobiol. 46 (3), 614–638, http://dx.doi.org/10.1007/s12035-012-8320-7.

Dennis, J.W., Granovsky, M., Warren, C.E., 1999. Protein glycosylation in development and disease. Bioessays 21 (5), 412–421, http://dx.doi.org/10.1002/(SICI)1521-1878(199905)21:5<412::AID-BIES8>3.0.CO;2-5.

Desplats, P., Lee, H.J., Bae, E.J., Patrick, C., Rockenstein, E., Crews, L., Lee, S.J., 2009. Inclusion formation and neuronal cell death through neuron-to-neuron transmission of alpha-synuclein. Proc Natl Acad Sci U S A 106 (31), 13010–13015, http://dx.doi.org/10.1073/pnas.0903691106.

Dimmock, N.J., Easton, A.J., Leppard, K.N., 2007. Introduction to Modern Virology, 6th ed. Blackwell Publishing Ltd.

Dobson, C.M., 2004. Principles of protein folding, misfolding and aggregation. Semin. Cell Dev. Biol. 15 (1), 3–16, http://dx.doi.org/10.1016/j.semcdb.2003.12.008.

Domert, J., Rao, S.B., Agholme, L., Brorsson, A.C., Marcusson, J., Hallbeck, M., Nath, S., 2014. Spreading of amyloid-beta peptides via neuritic cell-to-cell transfer is dependent on insufficient cellular clearance. Neurobiol. Dis. 65, 82–92, http://dx.doi.org/10.1016/j.nbd.2013.12.019.

Dyson, J., P.E., W., 2005. Elucidation of the protein folding landscape by NMR. Methods Enzymol. 394, 299–321, http://dx.doi.org/10.1016/S0076-6879(05)94011-1.

Eisenberg, D., Jucker, M., 2012. The amyloid state of proteins in human diseases. Cell 148 (6), 1188–1203, http://dx.doi.org/10.1016/j.cell.2012.02.022.

Endres, D., Zlotnick, A., 2002. Model-based analysis of assembly kinetics for virus capsids or other spherical polymers. Biophys. J. 83 (2), 1217–1230, http://dx.doi.org/10.1016/S0006-3495(02)75245-4.

Fink, A.L., 1999. Chaperone-mediated protein folding. Physiol. Rev. 79, 425–449, http://dx.doi.org/0031-9333/99.
Fowler, D.M., Koulov, A.V., Balch, W.E., Kelly, J.W., 2007. Functional amyloid—from bacteria to humans. Trends Biochem. Sci. 32 (5), 217–224, http://dx.doi.org/10.1016/j.tibs.2007.03.003.
Fulton, A.B., 1982. How crowded is the cytoplasm? Cell 30 (2), 345–347, http://dx.doi.org/10.1016/0092-8674(82)90231-8.
Gay, L., Neuman, N., 2013. Antiviral strategies: building a better defense. Cell 153, 728–729, http://dx.doi.org/10.1016/j.cell.2013.04.039.
Glenner, G.G., Eanes, E.D., Page, D.L., 1972. The relation of the properties of Congo red-stained amyloid fibrils to the ß-conformation. J. Histochem. Cytochem. 20 (10), 821–826, http://dx.doi.org/10.1177/20.10.821.
Gomes, L.C., Dikic, I., 2014. Autophagy in antimicrobial immunity. Mol. Cell 54 (2), 224–233, http://dx.doi.org/10.1016/j.molcel.2014.03.009.
Grad, L.I., Guest, W.C., Yanai, A., Pokrishevsky, E., O'Neill, M.A., Gibbs, E., Cashman, N.R., 2011. Intermolecular transmission of superoxide dismutase 1 misfolding in living cells. Proc. Natl. Acad. Sci. U. S. A. 108 (39), 16398–16403, http://dx.doi.org/10.1073/pnas.1102645108.
Greenwald, J., Riek, R., 2010. Biology of amyloid: structure, function, and regulation. Structure 18 (10), 1244–1260, http://dx.doi.org/10.1016/j.str.2010.08.009.
Haass, C., Selkoe, D.J., 2007. Soluble protein oligomers in neurodegeneration: lessons from the Alzheimer's amyloid beta-peptide. Nat. Rev. Mol. Cell Biol. 8 (2), 101–112, http://dx.doi.org/10.1038/nrm2101.
Hara, T., Nakamura, K., Matsui, M., Yamamoto, A., Nakahara, Y., Suzuki-Migishima, R., Mizushima, N., 2006. Suppression of basal autophagy in neural cells causes neurodegenerative disease in mice. Nature 441 (7095), 885–889, http://dx.doi.org/10.1038/nature04724.
Hardy, J., Selkoe, D.J., 2002. The amyloid hypothesis of Alzheimer's disease: progress and problems on the road to therapeutics. Science 297 (5580), 353–356, http://dx.doi.org/10.1126/science.1072994.
Hartl, F.U., Bracher, A., Hayer-Hartl, M., 2011. Molecular chaperones in protein folding and proteostasis. Nature 475 (7356), 324–332, http://dx.doi.org/10.1038/nature10317.
Hartl, F.U., Hayer-Hartl, M., 2002. Molecular chaperones in the cytosol: from nascent chain to folded protein. Science 295 (5561), 1852–1858, http://dx.doi.org/10.1126/science.1068408.
Hou, F., Sun, L., Zheng, H., Skaug, B., Jiang, Q.X., Chen, Z.J., 2011. MAVS forms functional prion-like aggregates to activate and propagate antiviral innate immune response. Cell 146 (3), 448–461, http://dx.doi.org/10.1016/j.cell.2011.06.041.
Hung, J.J., Chung, C.S., Chang, W., 2002. Molecular chaperone Hsp90 is important for vaccinia virus growth in cells. J. Virol. 76, 1379–1390, http://dx.doi.org/10.1128/JVI.76.3.1379-1390.2002.
Itzhaki, R.F., Lin, W.R., Shang, D., Wilcock, G.K., Faragher, B., Jamieson, G.A., 1997. Herpes simplex virus type 1 in brain and risk of Alzheimer's disease. Lancet 349, 241–244, http://dx.doi.org/10.1016/S0140-6736(96)10149-5.
Jackson, A.C., Ye, H., Ridaura-Sanz, C., Lopez-Corella, E., 2001. Quantitative study of the infection in brain neurons in human rabies. J. Med. Virol. 65 (3), 614–618, http://dx.doi.org/10.1002/jmv.2080.
Jackson, W.T., Giddings Jr., T.H., Taylor, M.P., Mulinyawe, S., Rabinovitch, M., Kopito, R.R., Kirkegaard, K., 2005. Subversion of cellular autophagosomal machinery by RNA viruses. PLoS Biol. 3 (5), e156, http://dx.doi.org/10.1371/journal.pbio.0030156.
Jang, H., Boltz, D., Sturm-Ramirez, K., Shepherd, K.R., Jiao, Y., Webster, R., Smeyne, R.J., 2009. Highly pathogenic H5N1 influenza virus can enter the central nervous system and induce neuroinflammation and neurodegeneration. Proc Natl Acad Sci U S A 106 (33), 14063–14068, http://dx.doi.org/10.1073/pnas.0900096106.
Jarrett, J.T., Lansbury, P.T., 1993. Seeding one-dimensional crystallization of amyloid: a pathogenic mechanism in Alzheimer's disease and scrapie? Cell 73, 1055–1058, http://dx.doi.org/10.1016/0092-8674(93)90635-4.
Jellinger, K.A., 2009. Absence of a-synuclein pathology in postencephalitic parkinsonism. Acta Neuropathol. 118, 371–379, http://dx.doi.org/10.1007/s00401-009-0537-9.
Jimenez, J.L., Nettleton, E.J., Bouchard, M., Robinson, C.V., Dobson, C.M., Saibil, H.R., 2002. The protofilament structure of insulin amyloid fibrils. Proc. Natl. Acad. Sci. U. S. A. 99 (14), 9196–9201, http://dx.doi.org/10.1073/pnas.142459399.
Jin, M., Shepardson, N., Yang, T., Chen, G., Walsh, D., Selkoe, D.J., 2011. Soluble amyloid beta-protein dimers isolated from Alzheimer cortex directly induce Tau hyperphosphorylation and neuritic degeneration. Proc. Natl. Acad. Sci. U. S. A. 108 (14), 5819–5824, http://dx.doi.org/10.1073/pnas.1017033108.
Johnson, J.M., Tang, J., Nyame, Y., Willits, D., Young, M.J., Zlotnick, A., 2005. Regulating self-assembly of spherical oligomers. Nano Lett. 5 (4), 765–770, http://dx.doi.org/10.1021/nl050274q.
Kaneko, K., Zulianello, L., Scott, M., Cooper, C.M., Wallace, A.C., James, T.L., Prusiner, S.B., 1997. Evidence for protein X binding to a discontinuous epitope on the cellular prion protein during scrapie prion propagation. Proc. Natl. Acad. Sci. U.S.A. 94, 10069–10074, http://dx.doi.org/10.1073/pnas.94.19.10069.
Kirkegaard, K., Taylor, M.P., Jackson, W.T., 2004. Cellular autophagy: surrender, avoidance and subversion by microorganisms. Nat. Rev. Microbiol. 2 (4), 301–314, http://dx.doi.org/10.1038/nrmicro865.
Kirschner, M., Gerhart, J., 1998. Evolvability. Proc. Natl. Acad. Sci. U. S. A. 95 (15), 8420–8427, http://dx.doi.org/10.1073/pnas.0404656101.
Klein, K.C., Polyak, S.J., Lingappa, J.R., 2004. Unique features of hepatitis C virus capsid formation revealed by de novo cell-free assembly. J. Virol. 78 (17), 9257–9269, http://dx.doi.org/10.1128/JVI.78.17.9257-9269.2004.
Klein, K.C., Reed, J.C., Tanaka, M., Nguyen, V.T., Giri, S., Lingappa, J.R., 2011. HIV Gag-leucine zipper chimeras form ABCE1-containing intermediates and RNase-resistant immature capsids similar to those formed by wild-type HIV-1 Gag. J. Virol. 85 (14), 7419–7435, http://dx.doi.org/10.1128/JVI. 00288-11.
Klug, A., 1999. The tobacco mosaic virus particle: structure and assembly. Philos. Trans. R. Soc. Lond. B. Biol. Sci. 354 (1383), 531–535, http://dx.doi.org/10.1098/rstb.1999.0404.
Knowles, T.P., Vendruscolo, M., Dobson, C.M., 2014. The amyloid state and its association with protein misfolding diseases. Nat. Rev. Mol. Cell Biol. 15 (6), 384–396, http://dx.doi.org/10.1038/nrm3810.
Koffie, R.M., Meyer-Luehmann, M., Hashimoto, T., Adams, K.W., Mielke, M.L., Garcia-Alloza, M., Spires-Jones, T.L., 2009. Oligomeric amyloid beta associates with postsynaptic densities and correlates with excitatory synapse loss near senile plaques. Proc. Natl. Acad. Sci. U. S. A. 106 (10), 4012–4017, http://dx.doi.org/10.1073/pnas.0811698106.
Komatsu, M., Waguri, S., Chiba, T., Murata, S., Iwata, J., Tanida, I., Tanaka, K., 2006. Loss of autophagy in the central nervous system causes neurodegeneration in mice. Nature 441 (7095), 880–884, http://dx.doi.org/10.1038/nature04723.
Korth, C., 2012. Aggregated proteins in schizophrenia and other chronic mental diseases: DISC1opathies. Prion 6 (2), 134–141, http://dx.doi.org/10.4161/pri.18989.
Kristensson, K., Dastur, D.K., Manghani, D.K., Tsiang, H., Bentivoglio, M., 1996. Rabies: interactions between neurons and viruses. A review of the history of Negri inclusion bodies. Neuropathol. Appl. Neurobiol. 3, 179–187, http://dx.doi.org/10.1111/j. 1365-2990.1996.tb00893.x.
Lahaye, X., Vidy, A., Pomier, C., Obiang, L., Harper, F., Gaudin, Y., Blondel, D., 2009. Functional characterization of Negri bodies (NBs) in rabies virus-infected cells: evidence that NBs are sites of viral transcription and replication. J. Virol. 83 (16), 7948–7958, http://dx.doi.org/10.1128/JVI. 00554-09.
Lee, S., Desplats, P., Sigurdson, C., Tsigelny, I., Masliah, E., 2010. Cell-to-cell transmission of non-prion protein aggregates. Nat. Rev. Neurol. 6, 702–706, http://dx.doi.org/10.1038/nrneurol.2010.145.
Lee, M.J., Lee, J.H., Rubinsztein, D.C., 2013. Tau degradation: the ubiquitin-proteasome system versus the autophagy-lysosome system. Prog Neurobiol 105, 49–59, http://dx.doi.org/10.1016/j.pneurobio.2013.03.001.
Leliveld, S.R., Bader, V., Hendriks, P., Prikulis, I., Sajnani, G., Requena, J.R., Korth, C., 2008. Insolubility of disrupted-in-schizophrenia 1 disrupts oligomer-dependent interactions with nuclear distribution element 1 and is associated with sporadic mental disease. J. Neurosci. 28 (15), 3839–3845, doi: 28/15/3839[pii]10.1523/JNEUROSCI.5389-07.2008.
Li, J., Liu, Y., Wang, Z., Liu, K., Wang, Y., Liu, J., Yuan, Z., 2011. Subversion of cellular autophagy machinery by hepatitis B virus for viral envelopment. J. Virol. 85 (13), 6319–6333, http://dx.doi.org/10.1128/JVI.02627-10.
Li, J.Y., Englund, E., Holton, J.L., Soulet, D., Hagell, P., Lees, A.J., Brundin, P., 2008. Lewy bodies in grafted neurons in subjects with Parkinson's disease suggest host-to-graft disease propagation. Nat. Med. 14 (5), 501–503, http://dx.doi.org/10.1038/nm1746.
Lingappa, J.R., Martin, R.L., Wong, M.L., Ganem, D., Welch, W.J., Lingappa, V.R., 1994. A Eukaryotic Cytosolic Chaperonin Is Associated with a High Molecular Weight Intermediate in the Assembly of Hepatitis B Virus Capsid, a Multimeric. J Cell Biol 125, 99–111, doi:0021-9525/94/04/99/13.
Lingappa, J.R., Hill, R.L., Wong, M.L., Hegde, R.S., 1997. A multistep, ATP-dependent pathway for assembly of human immunodeficiency virus capsids in a cell-free system. J Cell Biol 136, 567–581, http://dx.doi.org/10.1083/jcb.136.3.567.
Lingappa, J.R., Dooher, J.E., Newman, M.A., Kiser, P.K., Klein, K.C., 2006. Basic residues in the nucleocapsid domain of Gag are required for interaction of HIV-1 gag with ABCE1 (HP68), a cellular protein important for HIV-1 capsid assembly. J. Biol. Chem. 281 (7), 3773–3784, http://dx.doi.org/10.1074/jbc.M507255200.
Lingappa, V.R., Rutkowsi, D.T., Hegde, R.S., Andersen, O.S., 2002. Conformational control through translocational regulation: a new view of secretory and membrane protein folding. BioEssays 24 (8), 741–748, http://dx.doi.org/10.1002/bies.10130.
Lingappa, U.F., Wu, X., Macieik, A., Yu, S.F., Atuegbu, A., Corpuz, M., Ruprecht, C.E., 2013a. Host-rabies virus protein-protein interactions as druggable antiviral targets. Proc. Natl. Acad. Sci. U. S. A. 110 (10), E861–E868, http://dx.doi.org/10.1073/pnas.1210198110.
Lingappa, V.R., Hurt, C.R., Garvey, E., 2013b. Capsid assembly as a point of intervention for novel anti-viral therapeutics. Curr. Pharm. Biotechnol. 14 (5), 513–523, http://dx.doi.org/10.2174/1389201013149990201.
Lue, L.F., Kuo, Y.M., Roher, A.E., Brachova, L., Shen, Y., Sue, L., Rogers, J., 1999. Soluble amyloid beta peptide concentration as a predictor of synaptic change in Alzheimer's disease. Am. J. Pathol. 155 (3), 853–862, http://dx.doi.org/10.1016/S0002-9440(10)65184-X.
Maji, S.K., Perrin, M.H., Sawaya, M.R., Jessberger, S., Vadodaria, K., Rissman, R.A., R., R. (2009). Functional amyloids as natural storage of peptide hormones in pituitary secretory granules. Science, 325, 328–332. http://dx.doi.org/10.1126/science.1173155
Maurizi, C.P., 1985. Why was the 1918 influenza pandemic so lethal? The possible role of a neurovirulent neuraminidase. Med Hypothesis 16 (1), 1–5, http://dx.doi.org/10.1016/0306-9877(85)90034-9.
Mateu, M.G., 2013a. Assembly, stability and dynamics of virus capsids. Arch Biochem Biophys 531 (1–2), 65–79, http://dx.doi.org/10.1016/j.abb.2012.10.015.
Mateu, M.G., 2013b. Structure and physics of viruses. Subcell Biochem 68, 3–51, http://dx.doi.org/10.1007/978-94-007-6552-8_1.

Matsumoto, G., Kim, S., Morimoto, R.I., 2006. Huntingtin and mutant SOD1 form aggregate structures with distinct molecular properties in human cells. J. Biol. Chem. 281 (7), 4477–4485, http://dx.doi.org/10.1074/jbc.M509201200.
Mattson, M.P., 2004. Infectious agents and age-related neurodegenerative disorders. Ageing Res. Rev. 3 (1), 105–120, http://dx.doi.org/10.1016/j.arr.2003.08.005.
Mc Donald, J.M., Savva, G.M., Brayne, C., Welzel, A.T., Forster, G., Shankar, G.M., Walsh, D.M., 2010. The presence of sodium dodecyl sulphate-stable Abeta dimers is strongly associated with Alzheimer-type dementia. Brain 133 (Pt 5), 1328–1341, http://dx.doi.org/10.1093/brain/awq065.
McLean, C.A., Cherny, R.A., Fraser, F.W., Fuller, S.J., Smith, M.J., Beyreuther, K., Masters, C.L., 1999. Soluble pool of Abeta amyloid as a determinant of severity of neurodegeneration in Alzheimer's disease. Ann. Neurol. 46 (6), 860–866, http://dx.doi.org/10.1002/1531-8249(199912)46:6<860::AID-ANA8>3.0.CO;2-M.
Menager, P., Roux, P., Megret, F., Bourgeois, J.P., Le Sourd, A.M., Danckaert, A., Lafon, M., 2009. Toll-like receptor 3 (TLR3) plays a major role in the formation of rabies virus Negri Bodies. PLoS Pathog. 5 (2), e1000315, http://dx.doi.org/10.1371/journal.ppat.1000315.
Moshe, A., Gorovits, R., 2012. Virus-induced aggregates in infected cells. Viruses 4 (10), 2218–2232, http://dx.doi.org/10.3390/v4102218.
Muller-Schiffmann, A., Andreyeva, A., Horn, A.H., Gottmann, K., Korth, C., Sticht, H., 2011. Molecular engineering of a secreted, highly homogenous, and neurotoxic Abeta dimer. ACS Chem. Neurosci. 2 (5), 242–248, http://dx.doi.org/10.1021/cn200011h.
Muller-Schiffmann, A., Marz-Berberich, J., Andreyeva, A., Ronicke, R., Bartnik, D., Brener, O., Korth, C., 2010. Combining independent drug classes into superior, synergistically acting hybrid molecules. Angew. Chem. Int. Ed. Engl. 49 (46), 8743–8746, http://dx.doi.org/10.1002/anie.201004437.
Munch, C., O'Brien, J., Bertolotti, A., 2011. Prion-like propagation of mutant superoxide dismutase-1 misfolding in neuronal cells. Proc. Natl. Acad. Sci. U. S. A. 108 (9), 3548–3553, http://dx.doi.org/10.1073/pnas.1017275108.
Naslund, J., Haroutunian, V., Mohs, R., Davis, K.L., Davies, P., Greengard, P., Buxbaum, J.D., 2000. Correlation between elevated levels of amyloid beta-peptide in the brain and cognitive decline. Jama 283 (12), 1571–1577, http://dx.doi.org/10.1001/jama.283.12.1571.
Nelson, R., Sawaya, M.R., Balbirnie, M., Madsen, A.O., Riekel, C., Grothe, R., Eisenberg, D., 2005. Structure of the cross-beta spine of amyloid-like fibrils. Nature 435 (7043), 773–778, http://dx.doi.org/10.1038/nature03680.
Novoa, R.R., Calderita, G., Arranz, R., Fontana, J., Granzow, H., Risco, C., 2005. Virus factories: associations of cell organelles for viral replication and morphogenesis. Biol. Cell 97 (2), 147–172, http://dx.doi.org/10.1042/BC20040058.
Ottis, P., Bader, V., Trossbach, S., Kretzschmar, H., Michel, M., Leliveld, S.R., Korth, C., 2011. Convergence of two independent mental disease genes on the protein level: recruitment of dysbindin to cell invasive DISC1 aggresomes. Biol. Psychiatry 70, 604–610, http://dx.doi.org/10.1016/j.biopsych.2011.03.027.
Podlisny, M.B., Ostaszewski, B.L., Squazzo, S.L., Koo, E.H., Rydell, R.E., Teplow, D.B., Selkoe, D.J., 1995. Aggregation of secreted amyloid beta-protein into sodium dodecyl sulfate-stable oligomers in cell culture. J. Biol. Chem. 270 (16), 9564–9570, http://dx.doi.org/10.1074/jbc.270.16.9564.
Porcellini, E., Carbone, I., Ianni, M., Licastro, F., 2010. Alzheimer's disease gene signature says: beware of brain viral infections. Immun. Ageing 7, 16, http://dx.doi.org/10.1186/1742-4933-7-16.
Poskanzer, D.C., Robert, S.S., 1963. Cohort analysis of Parkinson's syndrome: evidence for a single etiology related to subclinical infection about 1920. J. Chron. Dis. 16 (9), 961–973, http://dx.doi.org/10.1016/0021-9681(63)90098-5.
Prasad, B.V., Schmid, M.F., 2012. Principles of virus structural organization. Adv Exp Med Biol 726, 17–47, http://dx.doi.org/10.1007/978-1-4614-0980-9_3.
Prevelige Jr., P.E., 1998. Inhibiting virus-capsid assembly by altering the polymerisation pathway. Trends Biotechnol. 16 (2), 61–65, http://dx.doi.org/10.1016/S0167-7799(97)01154-2.
Prusiner, S.B., 1998. Prions. Proc. Natl. Acad. Sci. U.S.A. 95, 13363–13383, http://dx.doi.org/10.1073/pnas.95.23.13363.
Prusiner, S.B., 2001. Shattuck lecture—neurodegenerative diseases and prions. N. Engl. J. Med. 344, 1516–1526, http://dx.doi.org/10.1056/NEJM200105173442006.
Prusiner, S.B., 2013. Biology and genetics of prions causing neurodegeneration. Ann. Rev. Genet. 47, 601–623, http://dx.doi.org/10.1146/annurev-genet-110711-155524.
Puzzo, D., Privitera, L., Leznik, E., Fa, M., Staniszewski, A., Palmeri, A., Arancio, O., 2008. Picomolar amyloid-beta positively modulates synaptic plasticity and memory in hippocampus. J. Neurosci. 28 (53), 14537–14545, http://dx.doi.org/10.1523/JNEUROSCI.2692-08.2008.
Ravikumar, B., Rubinsztein, D.C., 2006. Role of autophagy in the clearance of mutant huntingtin: a step towards therapy? Mol. Aspects Med. 27 (5–6), 520–527, http://dx.doi.org/10.1016/j.mam.2006.08.008.
Reed, M.N., Hofmeister, J.J., Jungbauer, L., Welzel, A.T., Yu, C., Sherman, M.A., Cleary, J.P., 2011. Cognitive effects of cell-derived and synthetically derived Abeta oligomers. Neurobiol Aging 32 (10), 1784–1794, http://dx.doi.org/10.1016/j.neurobiolaging.2009.11.007.
Rempel, H.C., Pulliam, L., 2005. HIV-1 Tat inhibits neprilysin and elevates amyloid beta. AIDS 19, 127–135, http://dx.doi.org/10.1097/00002030-200501280-00004.
Ren, P.H., Lauckner, J.E., Kachirskaia, I., Heuser, J.E., Melki, R., Kopito, R.R., 2009. Cytoplasmic penetration and persistent infection of mammalian cells by polyglutamine aggregates. Nat. Cell Biol. 11 (2), 219–225, http://dx.doi.org/10.1038/ncb1830.
Rohn, T.T., Catlin, L.W., 2011. Immunolocalization of influenza A virus and markers of inflammation in the human Parkinson's disease brain. PLoS One 6 (5), e20495, http://dx.doi.org/10.1371/journal.pone.0020495.
Ross, C.A., Poirier, M.A., 2004. Protein aggregation and neurodegenerative disease. Nat. Med. 10 (Suppl), S10–S17, http://dx.doi.org/10.1038/nm1066.
Satpute-Krishnan, P., DeGiorgis, J.A., Bearer, E.L., 2003. Fast anterograde transport of Herpes Simplex Virus: role for the amyloid precursor protein of Alzheimer's disease. Aging Cell 2, 305–318, http://dx.doi.org/10.1046/j.1474-9728.2003.00069.
Seuring, C., Greenwald, J., Wasmer, C., Wepf, R., Saupe, S.J., Meier, B.H., Riek, R., 2012. The mechanism of toxicity in HET-S/HET-s prion incompatibility. PLoS Biol. 10 (12), e1001451, http://dx.doi.org/10.1371/journal.pbio.1001451.
Sgarbossa, A., 2012. Natural biomolecules and protein aggregation: emerging strategies against amyloidogenesis. Int. J. Mol. Sci. 13 (12), 17121–17137, http://dx.doi.org/10.3390/ijms131217121.
Si, K., Choi, Y.B., White-Grindley, E., Majumdar, A., Kandel, E.R., 2010. Aplysia CPEB can form prion-like multimers in sensory neurons that contribute to long-term facilitation. Cell 140 (3), 421–435, http://dx.doi.org/10.1016/j.cell.2010.01.008.
Si, K., Lindquist, S., Kandel, E.R., 2003. A neuronal isoform of the aplysia CPEB has prion-like properties. Cell 115 (7), 879–891, http://dx.doi.org/10.1016/S0092-8674(03)01020-1.
Sipe, J.D., Benson, M.D., Buxbaum, J.N., Ikeda, S., Merlini, G., Saraiva, M.J., Westermark, P., 2010. Amyloid fibril protein nomenclature: 2010 recommendations from the nomenclature committee of the International Society of Amyloidosis. Amyloid 17 (3-4), 101–104, http://dx.doi.org/10.3109/13506129.2010.526812.
Stefani, M., Dobson, C.M., 2003. Protein aggregation and aggregate toxicity: new insights into protein folding, misfolding diseases and biological evolution. J. Mol. Med. (Berl.) 81 (11), 678–699, http://dx.doi.org/10.1007/s00109-003-0464-5.
Sunde, M., Serpell, L.C., Bartlam, M., Fraser, P.E., Pepys, M.B., Blake, C.C., 1997. Common core structure of amyloid fibrils by synchrotron X-ray diffraction. J. Mol. Biol. 273 (3), 729–739, http://dx.doi.org/10.1006/jmbi.1997.1348.
Taylor, J.P., Hardy, J., Fischbeck, K.H., 2002. Toxic proteins in neurodegenerative disease. Science 296 (5575), 1991–1995, http://dx.doi.org/10.1126/science.1067122.
Telling, G.C., Scott, M., Mastrianni, J., Gabizon, R., Torchia, M., Cohen, F.E., Prusiner, S.B., 1995. Prion propagation in mice expressing human and chimeric PrP transgenes implicates the interaction of cellular PrP with another protein. Cell 83, 79–90.
Tritel, M., Resh, M.D., 2001. The late stage of human immunodeficiency virus type 1 assembly is an energy-dependent process. J Virol 75 (12), 5473–5481, http://dx.doi.org/10.1128/JVI.75.12.5473-5481.2001.
Tsai, C.-J., del Sol, A., Nussinov, R., 2009. Protein allostery, signal transmission and dynamics: a classification scheme of allosteric mechanisms. Mol. BioSyst. 5, 207–216, http://dx.doi.org/10.1039/b819720b.
Uversky, V.N., Gillespie, J.R., Fink, A.L., 2000. Why are natively unfolded proteins unstructured under physiologic conditions? Proteins: Struct., Funct. Genet. 41 (3), http://dx.doi.org/10.1002/1097-0134.
Vendruscolo, M., Dobson, C.M., 2013. Structural biology: protein self-assembly intermediates. Nat. Chem. Biol. 9 (4), 216–217, http://dx.doi.org/10.1038/nchembio.1210.
Walsh, D.M., Klyubin, I., Fadeeva, J.V., Cullen, W.K., Anwyl, R., Wolfe, M.S., Selkoe, D.J., 2002. Naturally secreted oligomers of amyloid beta protein potently inhibit hippocampal long-term potentiation in vivo. Nature 416 (6880), 535–539, http://dx.doi.org/10.1038/416535a.
Walsh, D.M., Townsend, M., Podlisny, M.B., Shankar, G.M., Fadeeva, J.V., El Agnaf, O., Selkoe, D.J., 2005. Certain inhibitors of synthetic amyloid beta-peptide (Abeta) fibrillogenesis block oligomerization of natural Abeta and thereby rescue long-term potentiation. J. Neurosci. 25 (10), 2455–2462, http://dx.doi.org/10.1523/JNEUROSCI.4391-04.2005.
Wasmer, C., Lange, A., Van Melckebeke, H., Siemer, A.B., Riek, R., Meier, B.H., 2008. Amyloid fibrils of the HET-s(218–289) prion form a beta solenoid with a triangular hydrophobic core. Science (New York, N.Y.) 319 (5869), 1523–1526, http://dx.doi.org/10.1126/science.1151839.
Waudby, C.A., Launay, H., Cabrita, L.D., Christodoulou, J., 2013. Protein folding on the ribosome studied using NMR spectroscopy. Prog. Nucl. Magn. Reson. Spectrosc. 74, 57–75, http://dx.doi.org/10.1016/j.pnmrs.2013.07.003.
Wileman, T., 2006. Aggresomes and autophagy generate sites for virus replication. Science 312 (5775), 875–878, http://dx.doi.org/10.1126/science.1126766.
Wileman, T., 2007. Aggresomes and pericentriolar sites of virus assembly: cellular defense or viral design? Annu. Rev. Microbiol. 61, 149–167, http://dx.doi.org/10.1146/annurev.micro.57.030502.090836.
Wolman, M., Bubis, J.J., 1965. The cause of the green polarization color of amyloid sgay tained with Congo red. Histochemie 4, 351–356, http://dx.doi.org/10.1007/BF00306246.
Wozniak, M.A., Frost, A.L., RF, I., 2009. Alzheimer's disease-specific tau phosphorylation is induced by herpes simplex virus type 1. J. Alzheimers Dis. 16, 341–350, http://dx.doi.org/10.3233/JAD-2009-0963.
Xue, S., Barna, M., 2012. Specialized ribosomes: a new frontier in gene regulation and organismal biology. Nat. Rev. Mol. Cell Biol. 13 (6), 355–369, http://dx.doi.org/10.1038/nrm3359.
Yamin, R., Zhao, C., O'Connor, P.B., McKee, A.C., Abraham, C.R., 2009. Acyl peptide hydrolase degrades monomeric and oligomeric amyloid-beta peptide. Mol. Neurodegener. 4, 33, http://dx.doi.org/10.1186/1750-1326-4-33.

Zhou, L., Miranda-Saksena, M., Saksena, N.K., 2013. Viruses and neurodegeneration. Virol. J. 1, 0, http://dx.doi.org/10.1186/1743-422X-10-172.
Zimmerman, C., Klein, K.C., Kiser, P.K., Singh, A.R., Firestein, B.L., Riba, S.C., Lingappa, J.R., 2002. Identification of a host protein essential for assembly of immature HIV-1 capsids. Nature 415 (6867), 88–92, http://dx.doi.org/10.1038/415088a.
Zlotnick, A., 2003. Are weak protein-protein interactions the general rule in capsid assembly? Virology 315 (2), 269–274, http://dx.doi.org/10.1016/S0042-6822(03)00586-5.
Zlotnick, A., 2005. Theoretical aspects of virus capsid assembly. J. Mol. Recognit. 18 (6), 479–490, http://dx.doi.org/10.1002/jmr.754.

Chapter 2

Viral infections: a real threat to protein misfolding disorders?

Disruption of cellular proteostasis by H1N1 influenza A virus causes alpha-synuclein aggregation

Rita Marreiros, Andreas Müller-Schiffmann, Ingrid Prikulis, Ana Raquel Moreira, Shriya Sahu, Irina Soloviev, Suganya Selvarajah,, Vishwanath R. Lingappa, Carsten Korth

Proc Natl Acad Sci U S A, under review

Author's contribution (80 %):

- Design of experimental setup
- Cell culture maintenance
- Influenza A/WS/33 viral maintenance and replication
- Influenza A/WS/33 viral infection of cellular models
- Immunocytochemistry
- Complete microscopy analysis
- Complete data and statistics analysis
- Manuscript co- writing

In the present study, we investigated the effect of a mouse-neuroadapted influenza A virus (H1N1) strain in protein homeostasis disruption, associated with protein misfolding disorders. It is still not clear what are the factors that might trigger the initial events involved in proteostasis disruption leading to protein aggregation. In line with this, after acute influenza infection, human-dopamine-like neurons (LUHMES) showed α-syn and DISC1 aggregates. Interestingly, for tau and TDP-43 proteins, hallmarks of AD and ALS, aggregated inclusions were not observed after infection.

Furthermore, in an *in vivo* mice model (Rag KO) instilled intranasally with influenza virus, a dramatic increase in α-syn expression associated exclusively to the virally infected brain regions was observed. We also observed an increase in DISC1 expression in the virally infected brain areas. Surprisingly, the expression levels of tau and TDP-43 proteins were independent of viral infection. Together, the *in vitro* and *in vivo* data indicates a selective influenza effect in the homeostasis disruption of specific proteins.

Following treatment of infected cells with oseltamivir phosphate, an anti-influenza drug used as a prophylactic treatment in clinical practice, we could prevent influenza-induced α-syn aggregation. A reduction of > 50% in α-syn aggregates was observed with two distinct drug concentrations. The possible cellular mechanism involved in protein homeostasis disruption of α-syn and DISC1 upon influenza infection was also explored. We observed disturbances in the macroautophagy pathway, with a decrease in autophagosomes and autolysosomes formation as a consequence of the infection. Notably, influenza virus leads to an increase in lysosomal number, although with a decrease in α-syn aggregates present in the lysosomes.

These findings contribute significantly to understanding the causes that could trigger the cascade of events leading to protein misfolding disorders. Various expositions to influenza virus across lifespan might induce/accumulate/accelerate protein homeostasis disruption, and potentially trigger a critical mass of protein inclusions, such as the α-syn and DISC1 aggregates, subsequently enabling seeding. We suggest that influenza infection might be an environmental risk factor for synuclein - and DISC1 – pathies.

Disruption of cellular proteostasis by H1N1 influenza A virus causes □-synuclein aggregation

Rita Marreiros[a]., Andreas Müller-Schiffmann[a], Ingrid Prikulis[a], , Ana Raquel Moreira[b], Shriya Sahu[b], Irina Soloviev[b], Suganya Selvarajah[b], Vishwanath R. Lingappa[b], Carsten Korth[a,1]

[a]Department Neuropathology, Heinrich Heine University Düsseldorf Medical School, Moorenstrasse 5, 40225 Düsseldorf, Germany; [b]Prosetta Biosciences, Inc, San Francisco, CA 94107, USA

Corresponding Author

[1]Carsten Korth, MD PhD, Department Neuropathology, Heinrich Heine University Düsseldorf Medical School, Moorenstrasse 5, 40225 Düsseldorf, Germany

Email: ckorth@hhu.de

Keywords

Influenza A virus, protein misassembly, alpha-synuclein, influenza-induced aggregates, DISC1

Abstract

Neurodegenerative diseases feature specific, misfolded or misassembled proteins associated with neurotoxicity. The precise mechanisms by which the progressive increase in protein aggregates is triggered in the majority of sporadic cases has remained unclear. Likely, a first critical mass of misfolded proteins starts a vicious cycle of a prion-like expansion. We hypothesize that viruses, having evolved to hijack the host cellular machinery for catalyzing their replication, lead to profound disturbances of cellular proteostasis resulting in such a critical mass of protein aggregates.

Here, we investigated the effect of influenza virus (H1N1) strains on proteostasis of proteins associated with neurodegenerative diseases in Lund human mesencephalic dopaminergic (LUHMES) cells *in vitro* and infection of RAG knockout mice *in vivo*. We demonstrate that acute H1N1 infection leads to the formation of α-synuclein and Disrupted-in schizophrenia 1 (DISC1) aggregates, but not of tau or TDP-43 aggregates indicating a selective effect on proteostasis. Oseltamivir phosphate, an anti-influenza drug, prevented H1N1-induced α- synuclein aggregation. As a cell pathobiological mechanism, we identified H1N1-induced blocking of autophagosome formation and inhibition of autophagic flux. In addition, α- synuclein aggregates appeared in infected cell populations connected to the olfactory bulbs following intranasal instillation of the influenza virus in mice.

We propose that H1N1 virus replication in neuronal cells can induce seeds of aggregated α-synuclein that may be able to initiate further detrimental downstream events and should thus be considered a risk factor in the pathogenesis of synuleinopathies. More generally, aberrant proteostasis induced by viruses may be an underappreciated factor in initiating protein misfolding.

Significance Statement

Synucleinopathies like Parkinson's disease feature deposition of misfolded α-synuclein. A critical concentration of misfolded α-synuclein is necessary to exhaust cellular control mechanisms and favor a prion-like spread in the brain. Here, we demonstrate that in a cellular model of human dopaminergic-like neurons and in the mouse brain, H1N1 influenza A virus induces aggregation of α-synuclein by blocking protein degradation pathways. Following intranasal instillation, H1N1 spreading along the olfactory route into brain areas mimics synuclein deposits in synucleinopathies. H1N1 may therefore be considered a risk factor for synuleinopathies that could potentially be minimized by regular, lifelong vaccination. On the other hand, tropism for olfactory epithelium of intranasal, live attenuated virus vaccines should be investigated for possible long-term effects on protein misfolding.

Introduction

A hallmark of neurodegenerative diseases is the occurrence of misfolded proteins (1), each specific for a clinical disease: α-synuclein-containing Lewy bodies in synuleinopathies such as Parkinson's disease (PD), PD with dementia (PDD), multiple systems atrophy (MSA) and dementia with Lewy bodies (DLB), extracellular beta-amyloid plaques and intraneuronal tangles of hyperphosphorylated tau in Alzheimer's disease (AD), or TAR-DNA-binding protein 43 (TDP-43) aggregates in amyotrophic lateral sclerosis (ALS). The fact that the same proteins form aggregates in familial cases of neurodegenerative disease where a mutant protein is involved, and in sporadic cases where aggregates are caused independent of a mutation (2) has led to the notion that aggregates are a manifestation of a step common to both familial and sporadic disease that is critical for the disease process leading to neuronal death.

The synucleinopathies are characterized by cytosolic Lewy bodies, consisting of fibrillar α-synuclein associated with neuronal degeneration. In PD degeneration is most prominent dopaminergic neurons in the *substantia nigra* (SN), which leads to a loss of dopaminergic innervation of basal ganglia and the characteristic motor symptoms of PD (3), In PDD limbic structures are also involved, while in DLB the changes do not extend widely out of the olfactory system connectome as described and reviewed in several papers (4-6).

Aggregate formation may also occur in at least a subset of chronic mental illnesses (CMI) like schizophrenia or the recurrent affective disorders (7). Insoluble Disrupted-in- schizophrenia 1 (DISC1) protein has been identified in 15% of *post mortem* brains from patients with schizophrenia, bipolar disease or major depression (8), and a transgenic rat model modestly overexpressing the DISC1 protein modeling this CMI subset features aberrant dopaminergic homeostasis, as seen in behavioral, neurochemical and biochemical changes, including the induction of perinuclear DISC1 aggregates mainly in dopamine-rich regions (9).

An increasing set of data suggests that misfolded proteins, including α-synuclein and DISC1, amplify their pathogenetic signaling similar to prion replication, i.e. misfolded conformers accelerate conversion of correctly folded physiological conformers (10-14). In this case, once a critical threshold of aggregated proteins is present, a cascade of events is triggered that ends with neuronal death in affected anatomical areas (14). Similar to prions, misfolded synucleins can also propagate transneuronally following anatomical connections (5).

We currently lack an understanding for the initial phases of the formation of the critical mass of misfolded proteins ("first prions") that can initiate prion replication and trigger signaling events leading to acceleration of the process and neuronal death. One hypothesis is that a disturbance in protein homeostasis (proteostasis), i.e. a cellular imbalance between genesis of misfolded proteins and their degradation, can contribute to the steady accumulation of aggregated proteins (15, 16). Reasons for disturbed proteostasis can be manifold and involve toxins, inflammation, oxidative stress and infections with viruses (17).

Viruses have much shorter replication cycles then their host cells (18, 19) and thus they have evolved to take advantage of a host cell's machinery for an efficient viral replication. We have previously demonstrated that this catalysis is not limited to the viral genome but also comprises its capsid assembly that is catalyzed by host multiprotein complexes (20). During viral replication, host cell proteostasis is disturbed by affecting quality control mechanisms (21) and depleting energy resources (reviewed in refs. (22-24). Viral infections could thus lead to aberrant proteostasis and misassembly or aggregation of susceptible proteins instrumental in fatal signaling cascades in neurodegenerative diseases (25).

In this study we used H1N1 influenza A/WS/33 strain for infections *in vitro* (26) and the mouse-neuroadapted H1N1 influenza A/WSN/33 *in vivo* (27). This strain has been used for studies on molecular and neurophysiological interactions with neurons (28). Although influenza is not considered neuropathogenic in humans, certain strains, such as H5N1, have been found to be highly neuroinvasive and spread along olfactory and trigeminal nerve routes following intranasal instillation in mice and ferrets (29, 30). Suggestions for a pathogenetic role for influenza in nervous system diseases such as post-encephalitic parkinsonism appeared following the lethargic encephalitis epidemic 1916-1926 or "Spanish flu", as well as certain neuropsychiatric are controversial (31-33). Although there is no clear evidence for this, influenza can still not be fully excluded to trigger such diseases (34).

Here, we demonstrate that the H1N1 influenza A/WS/33 strain (26) leads to aggregation of endogenous α-synuclein and DISC1 in differentiated human dopaminergic neuron-like Lund mesencephalic (LUHMES) cells, as well as in the brain of infected-mice. In addition, α- synuclein aggregates are seen in populations of infected neurons connected to the olfactory bulb following intranasal viral instillation of the neuroadapted WSN/33 strain in mice. We also show mechanistically that the proteostatic disturbance of the autophagic flux in LUHMES cells caused by H1N1 infection, which impairs protein degradation, could initiate a critical mass of aggregated proteins.

Results

Influenza A infection disturbs protein homeostasis in human-dopamine-like neurons. In order to understand whether influenza A (H1N1) viral infection leads to a specific impairment in protein homeostasis relevant for PD, LUHMES cells were differentiated into human-dopamine-like neurons (35). At post-differentiation day 5, the morphology (Fig. S1A) as well as the expression of dopaminergic cellular markers (dopamine transporter and tyrosine hydroxylase; Fig. S1B, C) indicated neuronal maturity. In a candidate protein approach, several endogenously expressed proteins related to protein misfolding diseases where investigated in differentiated LUHMES cells. In undifferentiated, proliferating LUHMES cells, human DISC1 and α-synuclein protein expression was not detected (Fig. S1D). A small amount of TDP-43 and a noticeable expression of total tau was already detected in undifferentiated cells (Fig. S1D). At differentiation day 5, a significant increase in the expression of all proteins was observed ($p = 0.05$; Fig. S1D). All subsequent experiments were therefore all done in 5-day differentiated LUHMES cells.

LUHMES cells were infected with a low multiplicity of infection (MOI) of H1N1 influenza A virus strain A/WS/33 (36), MOI = 1 which resulted in an infection rate of 30% - 40% in LUHMES cells 24 h after viral infection (% of infected cells 33.3 ± 3.92; Fig. S2A). The replication kinetics of H1N1 influenza A virus from 0h - 24h p.i. were analyzed. The viral concentration in the medium increased substantially 12 h p.i. (log_{10} pfu/ml, $0.6 \times 10^4 \pm 0.46 \times 10^4$) being stable at 24 h p.i. (log_{10} pfu/ml, $1.7 \times 10^4 \pm 1.32 \times 10^4$; Fig. S2B). Since no morphological changes in the cells 24 h p.i. were observed, all following analyses in the present study were done at 24 h p.i.

Immunofluorescence analysis revealed dotted α-synuclein aggregates similar to what has been described as “Lewy dots” (37) in LUHMES cells infected with H1N1 influenza A virus (Fig. 1A and B). Quantification of aggregated α-synuclein showed a significant increase after viral infection (59% ± 19.20%, $p = 0.002$) in comparison with non-infected condition where α-synuclein aggregates were rare detectable (Fig. 1C). An immunoblot analysis indicates that total protein levels of α-synuclein were not affected by H1N1 influenza A infection (Fig. 1D). To demonstrate the effect of H1N1 influenza A viral infection on α-synuclein in an independent cell line, human NLF (non-dopaminergic) neuroblastoma cells (38) transiently transfected with human α-synuclein were also infected with H1N1 (for 24 h, MOI 1), and likewise led to the induction of α-synuclein aggregates (Fig. S3A, B).

We were also interested to understand whether H1N1 influenza A replication leads to misassembly of other disease-specific proteins, such as DISC1, which we had previously identified to aggregate *in vitro* (39) and *in vivo* in a subpopulation of CMI patients (8, 9), tau protein (40) or TDP-43 (41). Like for α-synuclein, H1N1 influenza A viral infection induced DISC1 aggregates from endogenously expressed DISC1 cells as observed by immunofluorescence in LUHMES cells (Fig. S4A-B). DISC1 aggregates were quantified and a significant increase in the percentage of aggregates per cell was observed after viral infection (93% ± 29.20%, p = 0.01) compared to the non-infected condition (Fig. S4C). We thus clearly demonstrate that endogenous human DISC1 protein aggregates if stressed, in this case through by H1N1 infection. Induction of aggregated DISC1 by H1N1 infection was corroborated in human NLF neuroblastoma cells transiently transfected with human mRFP- DISC1 (Fig. S4D). Of note, α-synuclein and DISC1 did not co-aggregate excluding cross- seeding mechanisms (Figure S4E).

H1N1 influenza A infection in LUHMES cells did not lead to abnormal accumulation of cytoplasmic TDP-43 aggregates (Fig. S5A). Neither tau protein changes like aggregation or hyperphosphorylation were seen after H1N1 infection (Fig. S5B).

These data demonstrate that influenza A infection induces aggregation of α-synuclein and DISC1, but not in tau or TDP-43, and suggest a selective effect of the Influenza A H1N1 replication on molecular circuitry of proteostasis.

Influenza A infection causes dramatically increases in α-synuclein expression *in vivo.* Next, we wanted to understand the direct effect of H1N1 influenza A virus infection on neuronal proteostasis of α-synuclein *in vivo.* In order to prevent any interference of an influenza infection with the adaptive immune system, genetically modified mice lacking B and T cells due to a deletion of the recombinant activating gene 1 (Rag-/-), necessary for an MHC-dependent adaptive immune response were used (27). 3-5 month old female knockout mice were intranasally instilled with 3.6 x 10^5 PFU/µl of A/WSN/33 (H1N1) strain (27) or with 0.01 M of PBS, and sacrificed 28 days later. Notably, in this animal H1N1 viral antigens were mainly detected in brain areas connected to the olfactory and trigeminal pathway projections (27). Sections of the lateral hypothalamus from the study by Tesoriero and coworkers (27), taken at 28 days p.i., showed cells with densely dotted and cytoplasmic immunolabelling for α-synuclein only in those also immunolabelled for viral antigens. In the neighboring non- infected areas, α-synuclein was not detected, neither in the infected nor in the PBS- inoculated mice (Fig. 2). To assess whether the different α-synuclein protein expression levels observed in the H1N1 -infected brain area were due to an effect in the promoter

activity of α-synuclein gene (SNCA), a luciferase reporter assay was performed. A pGL3 luciferase reporter vector with the canonical transcriptional start site 5' of exon 1 of the SNCA gene was transiently transfected to NLF neuroblastoma cells and the cells were infected with H1N1 influenza A. Changes in the expression of SNCA 5′-promoter construct upon influenza infection were not detected (Fig. S6) suggesting that the increase in α-synuclein levels was not due to increased transcription or translation but, therefore, rather due to decreased degradation (see below).

Next, we investigated whether H1N1 influenza A infection in mouse brain affected DISC1 as well as tau and TDP-43 proteins. For DISC1, an increase in expression levels was observed in brain areas infected with H1N1 influenza A (Fig. S7A), compared to PBS – inoculated mice where a low background DISC1 expression level was observed (Fig. S7A). In a control experiment *in vitro*, promoter activity of DISC1 gene after H1N1 infection was probed using a luciferase reporter assay. NLF neuroblastoma cells transiently transfected with a construct comprising the DISC1 promoter, from – 2300 - + 45 bp relative to the transcription start site (42), in front of the luciferase gene were infected with H1N1. No change in DISC1 promoter activity in infected vs. non-infected controls was observed (Fig. S7B), likewise suggesting that the increase in DISC1 expression levels was not due to an effect of increased transcription or translation but likely decreased degradation. For tau and TDP-43, we observed protein expression pattern independent of H1N1 influenza A infection and without signs of aggregation (Fig. S8A-D) as for α-synuclein and DISC1. These data suggest that H1N1 influenza A infection increased aggregation of α-synuclein and DISC1 proteins but not tau and TDP43 protein levels in mouse brains and thus was an effect on a particular proteostatic molecular circuitry.

Complete influenza A replication is required to disrupt α-synuclein protein homeostasis. Influenza virus is an RNA coding virus with a helical nucleocapsid that comprises the viral genome and four viral proteins with the nucleocapsid protein (NP) as the quantitatively major component. During the viral replication cycle, NP plays a central role in transcription, replication and packaging (43). Each viral RNA segment is associated with NP molecules in order to protect the viral genome from nuclease degradation by the host cell (44).

To understand whether a complete influenza A virus replication with assembly of all polypeptides was required for proteostasis disruption or whether NP assembly alone was enough to induce α-synuclein proteostatic changes, NLF neuroblastoma cells were transiently co-transfected with influenza A virus (A/WS/33) segment 5 NP and human α- synuclein. 48 hours after transfection, changes in the α-synuclein proteostasis were analyzed

by immunocytochemistry (Fig. 3A). In NLF neuroblastoma cells, expression of the viral NP alone was not able to trigger α-synuclein aggregates to the same extent as a complete H1N1 influenza A infection (147% increase ± 50.40%, p = 0.04) (Fig. 3B). Viral antigen detection in the immunolabelling confirmed that the helical capsid protein was expressed by the host cell (Fig. 3A).

NLF neuroblastoma cells were also co-transfected with H1N1 NP and mRFP-DISC1. 48 hours after transfection, immunocytochemistry was performed (Fig. S9A). A slight, but no significant increase in DISC1 aggregate number was detected in the co-transfected cells with NP (14% increase ± 21.70%) in comparison with non-infected condition (Fig. S9B). As expected, the number of DISC1 aggregates with H1N1 influenza A infection (63% increase ± 31.30%, p = 0.05) was observed. We conclude that replication of a complete viral genome of H1N1 influenza virus is required to trigger aberrant proteostasis of α-synuclein and DISC1.

An antiviral compound can prevent the alterations in α-synuclein protein homeostasis caused by the influenza A infection. Next, we wanted to understand whether a pharmacological compound that interferes with H1N1 viral life cycle, would inhibit α-synuclein aggregation. Oseltamivir phosphate inhibits the neuraminidase enzyme of influenza A and B preventing the efficient release of newly replicated influenza virus (45, 46). LUHMES cells were used to assess the effect of the anti- viral compound on H1N1-induced α-synuclein aggregates. Cells were treated with two different concentrations of oseltamivir phosphate, 0.5 or 50 μM. PBS was used as a control. The oseltamivir phosphate concentrations were selected according to a correspondent range tested in different cell types, of EC_{50} against influenza virus ($EC_{50,}$ 0.0008 – 35 μM) (47). After the first 8 hours of compound treatment, cells were infected with H1N1 influenza A virus (MOI 1 for 24h). The antiviral activity of oseltamivir phosphate was assessed by $TCID_{50}$ assay, and a reduction in influenza infectivity was observed in a compound concentration manner. In the supernatant of LUHMES cells treated with oseltamivir phosphate, the viral infectivity decreased 57% for 0.5 μM and 99.9% for 50 μM (Fig. 4A).

The compound concentrations used were non-toxic to the cells, not demonstrating any effect in the cell viability in comparison with the PBS condition. (cell number/mm^2: PBS - 12.8 ± 1.14; 50 μM - 13.6 ± 1.26; 0.5 μM - 13.18 ± 0.56; Fig. 4B). The effect of oseltamivir phosphate on H1N1-induced α-synuclein aggregates was measured 30 h after compound treatment by immunofluorescence (Fig. 4C). We observed a significant decrease in the percentage of α-synuclein aggregates with both concentrations used (0.5 μM: 63 % ± 10.00% reduction, p = 0.007; 50 μM: 65% ± 14.90% reduction, p = 0.006) relative to

untreated PBS conditions (Fig. 4D). These data suggest that pharmacological modulation of H1N1 replication also affects α-synuclein aggregation levels.

Influenza A infection affects the autophagic machinery leading to changes of α- synuclein protein homeostasis. A disturbance in the later macro-autophagy stage (hereafter autophagy) in GFP-LC3- expressing epithelial cells due to the inhibition of autophagosome fusion with lysosome was previously described (48). Through modulation of c-Jun N-terminal protein kinase 1 and PI3K-Akt-mTOR pathways, an inhibition in the autophagosome formation was also reported. (49). Early autophagy disruption was assumed to affect the clearance of presynaptic α-synuclein. In 20-month old mice with a deletion in an essential gene involved in autophagosome formation *(Atg7),* α-synuclein aggregates in striatal neuritic swellings were detected. The same inclusions were also seen in cerebellar Purkinje axons from younger age animals (1.5-month old) (50). Therefore, we hypothesized that the disturbance of autophagy by an external stressor, such as an influenza infection, could lead to the accumulation of α-synuclein influenza-induced aggregates.

In order to investigate the specific consequences of H1N1 influenza A infection for cellular autophagy in a model as close to primary human dopaminergic neurons as possible, LUHMES cells were again used. Cells were infected with H1N1 influenza A (MOI 1 for 24 h), and by immunolabelling a decrease in cytoplasmic LC3 punctate structures, a specific protein involved in the autophagosome formation was observed (Fig. 5A - B). Quantifiation of LC3 punctate structures showed a significant reduction of autophagosomes after H1N1 influenza A infection (62% ± 22.70% reduction, $p = 0.05$) in comparison with non- infected cells (Fig. 5C). A tendency in reduction of total LC3 levels was observed by immunoblot (Fig. 5D). Immunolabelling of infected LUHMES cells did not show an overlap between α-synuclein aggregates and LC3 punctate structures indicating an inefficient packing of these aggregates in autophagosomes, or an interruption in the maturation of autophagosomes into autolysosomes, due to impairment of the fusion with lysosomes.

Next, we wanted to analyze whether H1N1 infection leads to impairment of the lysosomal turnover of the autophagosomes. For that, NLF neuroblastoma cells were transiently transfected with a tandem-reporter-construct, mRFP-GFP-LC3 (51) and infected for 24 h with H1N1 influenza A virus (MOI 1). The emission spectrum of the GFP component is pH sensitive, thus not emitting light in the acidic conditions of the lysosome. However, this pH sensitivity does not apply to mRFP. Therefore, the green (-GFP) and red (-mRFP) moieties of this construct are both active when LC3 is localized in autophagosomes (neutral pH) being

visible as yellow color in the images when merged. When autophagosomes fuse with lysosomes forming acidic autolysosomes, LC3 is visible majority in the red channel (Fig. 5E). These changes in fluorescent signal from yellow to red were used to analyze the effect of H1N1 influenza A virus in the autophagic flux,and to determine LC3 location (Fig. 5F). In the infected cells a non-significant decrease in mRFP-LC3 punctate structures (number of autolysosomes/cell, 1.5 ± 0.56) was seen in comparison with non-infected condition (number of autolysosomes/cell, 3.0 ± 0.94) (Fig. 5G). Concomitantly, influenza A infection led to a significant increase in yellow-LC3 punctate structures (number of autophagosomes/cell, 3.6 ± 0.50; $p = 0.05$) in comparison to the non-infected controls (number of autophagosomes/cell, 2.0 ± 0.17) (Fig. 5G). H1N1 influenza A infection led to a 73% ± 7.8% reduction ($p = 0.05$) in the autolysosomes formed compared to non-infected cells, suggesting an impairment in the autophagosome fusion with lysosome (Fig. 5H). The effects of influenza infection on colocalization of LC3 with lysosome-associated membrane protein 1 (LAMP1) were also investigated in LUHMES cells. While in non-infected cells a considerable colocalization was detected, 24h after influenza A infection, a reduction in the colocalization of autophagosomes with the lysosomal marker - LAMP1 was observed (Fig. S10), indicating impaired autophagosome-lysosome fusion.

Next, we wanted to understand the effect of H1N1 influenza A infection in the number of lysosomal structures. LUHMES cells were infected with H1N1 influenza A for 24 h (MOI 1) and immunolabelling of LAMP1 was performed (Fig. 6A-B). A significant increase in number of lysosomes was observed in infected cells (51% ± 8.60% increase, $p = 0.05$) in comparison with non-infected cells (Fig. 6C). Immunoblot analysis of total lysates of infected LUHMES cells did not show a significant effect of H1N1 influenza A in LAMP1 protein levels (Fig. 6D). We then investigated the presence of α-synuclein aggregates in the acidified proteolytic lysosomes. Immunolabeling of infected LUHMES cells showed a decrease in overlaps between α-synuclein aggregates and LAMP1, 24 h of viral infection (Fig. 6E). Quantification of α-synuclein aggregates colocalizing with LAMP1 structures confirmed the significant reduction in the aggregate number present in the lysosomes in the influenza infected condition (24% ± 12.70% reduction, $p = 0.05$) in comparison with non-infected cells (Fig. 6F). These data suggest that, H1N1 influenza A virus disrupts 1. the number of autophagosomes and 2. also the autophagic flux in neurons, leading to an impairment in autophagy that might explain the accumulation of α-synuclein aggregates observed after viral infection.

Discussion

In this study we demonstrated that H1N1 influenza A viral infection and replication can be a significant initiating event in the genesis of a critical mass of misfolded α-synuclein and DISC1 that could trigger disease. We also showed that in human dopaminergic neuron-like cells the H1N1 infection disrupts proteostasis at the level of protein degradation through inhibiting autophagosome-lysosome fusion that could explain the observed increase in endogenous α-synuclein and DISC1 aggregation levels. These findings are mirrored in Rag knockout mice *in vivo* where four weeks after intranasal H1N1 infection, increased expression levels of α-synuclein and DISC1 in neurons can be detected, which was likely to due to decreased degradation rather than upregulated expression. These findings are important for our understanding of the causes of protein misfolding diseases where information is sparse on how a critical, initiating concentration of α-synuclein is built up to trigger the ensuing cascades of cellular events.

In our study we provide a mechanistic link of how a direct cellular H1N1 infection leads to α-synuclein and DISC1 aggregates that make a scenario plausible where α-synuclein seeds are initiated by H1N1 infection disturbing proteostasis via inhibiting autophagosomes and autophagic flux. It is noteworthy that α-synuclein aggregates themselves inhibit autophagy (52) thereby leading to a self-reinforcing loop of autophagy inhibition and promoting α-synuclein aggregation (reduction in α-synuclein aggregate clearance). Inhibition of autophagy, in turn, promotes the secretion of α-synuclein containing exosomes (53) thereby promoting α-synuclein prion spread in the CNS (54) .

A similar effect of H1N1 infection was seen on the DISC1 protein, which is a product of a gene linked to familial cases of CMI (8), and has been identified to be insoluble in a subset of cases with CMI but not controls (8, 39). In continuation to our findings of insoluble DISC1 in the brains of CMI patients (8), we demonstrate for the first time conditions under which endogenous DISC1 protein aggregates after aberrant proteostasis (Fig. S4A-C). This could mean that in addition to the suggested effects of influenza infections on prenatal immune activation (55, 56), influenza virus might affect DISC1 protein functions directly during neurodevelopment (57). Furthermore, our data suggest that DISC1 aggregation induced by H1N1 infection may also affect the adult brain and influence homeostatic processes related to CMI. Interestingly, the induction of protein aggregation is dramatically stronger for α-synuclein and DISC1 than for tau and TDP43, two other proteins misfolded in different neurodegenerative diseases, such as tau protein found in hyperphosphorylated and aggregated form in AD brain patients (58) and TDP-43 protein found in cytoplasmic

aggregates in ALS patients (41). This suggests that the effects of H1N1 on proteostasis are selective.

One of the control mechanisms that cell uses to maintain cellular homeostasis, in order to avoid accumulation of protein aggregates is autophagy (59). Indeed, many pathogens have been found to interfere with this catabolic process in order to reduce host cell death during the infection process (60-62). Previous publications described a disruption in the autophagy process in epithelial cells and in human lung samples by influenza A virus (48, 49, 63, 64) . In line with this, our findings showed that a 24 h acute infection with H1N1 influenza virus (A/WS/33) led to a decrease in autophagosome formation (Fig. 5A-C) and an increase in lysosomes (Fig. 6A-C) in human dopaminergic neurons. Interestingly, we observed a reduction in the number of α-synuclein aggregates in the acidified proteolytic lysosomes (Fig. 6E-F). This might be the effect of a decreased degradation of the cargo that is imported to the autolysosomes by the reduced fusion with autophagosomes. This finding could be a consequence of the impairment in the autophagic flux in neuronal cells, seen after influenza infection (Fig. 5F-H; Fig. S10). A similar effect was previously reported by Gannagé et al. in epithelial cells (48).

Tanik and coworkers reported that seeded α-synuclein aggregates *per se*, in an *in vitro* cellular model, were able to impair autophagy, due to a reduction in autophagosome clearance (52). However, since we showed already a low background of existing α-synuclein aggregates in non-infected cells (Fig. 1A-C), the dramatic increase in α-synuclein aggregates must have been the consequence of H1N1 infection and cannot have resulted of an interaction of α-synuclein with autophagosomes. Taking this into account, we propose a possible explanation for the increase in α-synuclein aggregates. First, influenza A infection suppresses the autophagy process at an early stage, leading to less available autophagosomes to transport the misfolded proteins for lysosomal degradation. Second, infection also affects autophagy at a later stage, with a blockage of autophagosome fusion with lysosomes. These effects will consequently lead to a vicious circle of increase in misfolded α-synuclein in dopaminergic neurons, protein homeostasis impairment and a concomitantly dopamine neuronal loss, one of the neuropathological characteristics of PD brains (Fig. 7). This scenario is corroborated by reports that impairments in autophagy system result in α-synuclein accumulation (50, 65, 66).

Considering the fact that misassembled DISC1 protein located in aggresomes has been shown to be degraded by autophagy (67), it is straightforward to attribute the accumulation of DISC1 aggregates seen here (Fig. S4) also relates to impairments in autophagy. It is still not

clear what the main degradation pathways are for clearing misfolded tau (68-70) and TDP-43 protein (71, 72). An equal involvement of ubiquitin – proteasome system (UPS) and the autophagy system has been proposed. Links between UPS and autophagy have being extensively demonstrated (73-76). Previous work from Korolchuk and coworkers, showed that autophagy inhibition compromises the UPS, due to accumulation of p62, that inhibits the clearance of soluble ubiquitinated proteins leading to an increase in the levels of UPS clients. However, they also showed that aggregation levels of a mutant polyglutamine (polyQ)-expanded huntingtin fragment, a disease-associated protein like, proved to be cleared by UPS and autophagy systems (77), did not increase with autophagy or UPS inhibition (78). Thus, if we take into account that for different proteins, the clearance mechanisms used by the cell for degradation of misfolded forms are different, we cannot exclude an UPS compensatory mechanism as the reason for the absence of influenza A infection effect in tau and TDP-43 protein homeostasis.

We observed a reduction in >50% of α-synuclein aggregates in H1N1 infected human dopaminergic neurons treated with oseltamivir phosphate (Fig. 4C-D). This compound is commonly used in the prophylaxis of influenza A and B and inhibits neuraminidase, thus exosomal release of the virus from the host cell. Indirectly, this affects the re-infection rate of the same cell and neighboring cells through the decrease in viral titers (79) and, eventually, a higher rate of defective viral assembly (80) such that proteostasis would be less affected in the overall cell population, The effect of oseltamivir phosphate on α-synuclein aggregates was concentration dependent, and our data also confirmed a parallel antiviral activity with a decrease in the viral titer for both concentrations tested (0.5 and 50 μM) (Fig. 4A). These data demonstrate that pharmacological treatment of H1N1-infected dopaminergic neurons can prevent α-synuclein aggregation.

In our *in vivo* study the changes in α-synuclein were detected strictly in conjunction with the presence of viral antigens after viral replication. Our data therefore suggest that influenza A replication was able to disturb protein homeostasis directly and not only as a consequence of the activation of the adaptive immune system. The infection was restricted to areas connected to the olfactory and trigeminal systems and there was no further spread into the neocortex or hippocampus, except in rare instances. From the infection in the olfactory bulbs we could follow the retrograde axonal spread of the virus to nerve cell groups that send projections to the olfactory bulbs (81). These included the diagonal bands, piriform cortex, cortical amygdaloid area, lateral hypothalamic areas and locus coeruleus, but not, or only the most medial aspect, of the *substantia nigra* (27). The lack of involvement of the substantia nigra does not reflect a default neurotropism for the virus, since this nucleus is heavily

infected following intracerebral viral injections (82), probably through retrograde spread in axonal projections tothe striatum. Following injections of fibrillary α-synuclein into the olfactory bulbs thread-like aggregates were initially seen only in areas that send or receive projections from olfactory regions with a later slow (months) and secondary spread to limbic structures (5). This distribution of Lewy body in neurons tallies well with that described in DLB disease (review see ref (6)) and has been proposed as trajectories for spreading α- synuclein aggregates (83).

Notably, various strains of the highly pathogenic H5N1 influenza can, without prior adaptation, distribute within the olfactory pathway only, or in combination with the brainstem in ferrets following intranasal infection (30). A systemic infection of H5N1 strain, which spread widely in the brain including *substantia nigra*, was followed by appearance of α- synuclein granules which were localized to the nuclei of the cells (29). Whether our present findings of cytoplasmic α-synuclein aggregates could link influenza infections to the postencephalitic parkinsonism following *encephalitis lethargica* is not clear, since neither Lewy bodies nor α-synuclein aggregates have been found in the brainstem of patients deceased from postencephalitic parkinsonism. This disease is instead characterized by neurofibrillary degeneration and tau aggregates (for review, see Jellinger (84)).

In summary, we show that direct effects of H1N1 replication may lead to a critical mass of α-synuclein aggregates that subsequently have the potential to trigger a synucleinopathy. In light of the efficient pharmacotherapy presented, our findings may inspire further research,
e.g. on the effects of anti-influenza vaccines on synucleinopathy incidence. It should also be carefully evaluated whether live vaccines taken intranasally could cause aggregates in the olfactory epithelium – and if so, whether they will be cleared by the turnover of neurons in the epithelia or olfactory bulbs or slowly propagates over months or years as α-synuclein injected into the bulb do. Since the olfactory epithelium is the only site where neurons are in direct contact with the environment, effects of vaccine on the recruitment of resident memory T (T_{REM}) cells to (85) prevent viral-induced misfolding in the olfactory domain, burdened by DLB and PDD, is an urgent research topic.

Methods

Influenza A/WS/33 viral stock preparation and viral replication. The WS/33 viral strain H1N1 influenza, with 1 x 10^8 PFU/µl, purchased from ATCC® (ATCC® VR-1520™), was used to prepare the viral stocks (26). Viral propagation was performed in MDCK.2 canine cells for 5 days, in a serum free medium. After the incubation time cells were harvested and centrifuged at 1000g for 5 min and the supernatant was collected and snap-frozen. Viral infectious titers were determined using the $TCID_{50}$ method (86). Briefly, MDCK.2 cells were seeded in a 96 well plate with a density of 3 x 10^4 cells per well and incubated in a serum free medium with serial $\log_{10}$ viral dilutions. 72h later, the number of infected wells was counted and the tissue culture infective dose was calculated. For animal inoculations a mouse-neuroadapted influenza A virus (A/WSN/33) (1.4 x 10^5 PFU/ml) (kindly provided by Dr. S. Nakajima, The Institute of Public Health, Tokyo, Japan) was used.

Culture and differentiation of LUHMES cells. Lund human mesencephalic (LUHMES) cells were purchased from ATCC® company. LUHMES cells were maintained in an proliferative state in DMEM:F12 medium supplemented with 1% N2 (ThermoFisher Scientific), 1% (v / v) penicillin/streptomycin (PenStrep) (Invitrogen) and 40 ng/ml b-FGF (basic recombinant human Fibroblast Growth Factor) (Sigma) in a pre-coated flask with 50 µg/mL poly-L- ornithine (Sigma) and then with 1 µg/mL of laminin (Sigma). Proliferating LUHMES cells were converted into uniformly post-mitotic neurons by using a differentiation procedure, triggered by suppression of v-myc expression, as previously described (87). The differentiation procedure in dopamine-like neurons involves the cell maintenance in DMEM:F12 medium supplemented with 1 µg/ml tetracycline (Sigma), 2 ng/ml GDNF (glial cell line-derived neurotrophic factor) (Sigma), and 1mM db-cAMP (Sigma) for 5 days. Dopaminergic neuronal phenotype of differentiated LUHMES cells was described previously (35, 87)

Human neuroblastoma and MDCK.2 cells. The Human neuroblastoma NLF cells were obtained mycoplasma-free from the DSMZ (German Collection of Microorganisms and Cell Cultures, Braunschweig, Germany) and regularly checked for mycoplasma. 2,5 x 10^4 NLF cells were seeded onto 30 mm glass coverslips. 24h later, cells were incubated with the DNA/metafectene complexes (METAFECTENE® PRO) in Opti-MEM without serum (Invitrogen) for 4h, and then the transfection medium was replaced with RPMI medium (Invitrogen) supplemented with 10% (v/v) FBS (Invitrogen), 1% (v/v) L-glutamine (Invitrogen), and 1% (v/v) PenStrep (Invitrogen) for 48h. In order to assess the promoter activity of □-

synuclein and DISC1we used a pGL3 luciferase reporter vector with the canonical transcriptional start site of SNCA gene, and pGL4.10 with a medium DISC1 promoter sequence. These constructs were a kindly gift by Professor Leonidas Stefanis (88) ,and Professor Kathryn L. Evans (42), respectively. Briefly, for the luciferase assays, all transfections were performed in a 96-well plate with 0,2 µg/well of target vector DNA 24h after $4x10^4$ cells have been seeded. Cells were Influenza A/WS/33 infected with a MOI of 1, and 24h later the luciferase activity was measured. MOI was defined as the number of virions added per cell during infection time (89). For all experiments, at least 10 technical replicates were measured per each condition. The assay was performed according to the manufacturers´ recommendations (Dual-Glo®Luciferase Assay System from Promega).

MDCK.2 canine cells were maintained in MEM medium supplemented with 10% (v/v) FBS (Invitrogen), 1% (v/v) non essential amino acids (Sigma), 1% (v/v) sodium pyruvate (ThermoFisher Scientific), 1% (v/v) L-glutamine (Invitrogen), and 1% (v/v) PenStrep (Invitrogen) upon viral infection.

Influenza A/WS/33 virus infection. LUHMES and human NLF neuroblastoma cells were infected with the influenza A/WS/33 virus strain, in serum free medium, with a moi of 1. One hour later, medium was replaced to normal supplemented medium, cell type required medium, and the cells were incubated for 24h until the respectively analysis was performed. As described in the study by Tesoriero and coworkers (27) mice were instilled with 4-5 µL of the virus suspension or with 0.01 M phosphate-buffered saline, pH 7.4 (PBS) into one nostril for immunohistochemistry. Previously we have found that intranasal instillation of WSN/33 in small volumes causes a spread to the brain in RAG-/- mice that is not accompanied by virus spread to the lung as determined by PCR (90). For the infection, the mice were briefly anaesthetized with isoflurane (Baxter, Deerfield, Illinois, USA). They were then followed daily and sacrificed, together with matched controls, before or when they showed signs of body weight loss, following the institutional guidelines and ethical protocols.

Antiviral compound administration. LUHMES cells were kept for four days in differentiation medium. Cells received 0,5 µM or 50 µM of oseltamivir phosphate (Sigma) dissolved in PBS. For the negative control conditions, cells were treated with a PBS solution with an equivalent concentration used to dilute the compounds. The compound was applied to the cells 8 hours before A/WS/33 influenza infection. The dose was renewed when the new differentiation medium was added to LUHMES cells after the viral infection or not. All the analyses were performed 30h after the first compound dose administration.

Immunocytochemistry. For immunocytochemistry analysis, cells were washed three times with PBS (Invitrogen) and fixed with 4% (v/v) PFA in PBS for 15 min, followed by three washing steps with PBS. Fixed cells were permeabilized and blocked with PBS including 0.5% (v/v) Saponin (Sigma), 5% (v/v) nonfat milk (Oxoid), 1% BSA (Sigma) to PBS for 1h at room temperature (RT). Primary antibodies (described in Table 1) were applied overnight at 4°C in blocking solution without milk. At the day after, coverslips were washed three times with PBS and incubated with Alexa-Fluor antibodies (anti-mouse IgG AlexaFluor 594; anti- rabbit IgG AlexaFluor 594; anti-mouse IgG AlexaFluor 488; anti-rabbit IgG AlexaFluor 488; Invitrogen) for 1h at RT. After washing three times with PBS and two times with water, cells were mounted with ProLong Gold with DAPI (Invitrogen), and images collected with a Zeiss Axiovision Apotome.2 confocal microscope (Zeiss).

Immunoblot. In brief, LUHMES cells were manually lysed with buffer A, containing 10 mM Tris-HCL (Sigma), pH8; 150 mM NaCl (Sigma); 2 mM EDTA (Sigma); 0,5% Sodium Deoxycholate (Sigma); 2% Nonidet P40 (Sigma) dissolved in water (for Western blots showed in Fig. S1B; D) or lysed with buffer B, containing 1% Nonidet P40 (Sigma) dissolved in PBS (for Western blots showed in Fig. 1D; 5D; 6D). Protein concentration was determined using the Dc Protein Assay Kit (Bio-Rad), and 10 µg/ml of each sample dissolved in NuPAGE LDS Sample Buffer (including 2% β-mercaptoethanol) were applied to the gel. Novex NuPAGE SDS-PAGE Gel System (Thermo Fisher Scientific) with the corresponding NuPAGE Novex 4–12% Bis-Tris Midi Protein Gels, NuPAGE MES SDS Running buffer was used. Proteins were transferred to a nitrocellulose or PVDF membrane, and then blocked with 5% nonfat milk in PBS containing 0.05% Tween-20, for 1h at RT. Western blot analysis was performed with the correspondent antibodies described in table 1 followed by a secondary species specific antibody (IR Dye 680 or 800; LI-COR Corp.). VDAC was used as a loading control for all immunoblots performed. The membranes were scanned using the LI- COR Odyssey CLX. Band intensities were calculated from fluorescent signal using the Image Studio Version 2.1 software (LI-COR Biosciences).

Immunohistochemistry. For the immunohistochemical process, mice were deeply anesthetized with sodium pentobarbital (50 mg/kg, i.p., APL, Stockholm, Sweden), and perfused transcardially with 4% paraformaldehyde (wt/vol) with picric acid as previously described (91). Brains, trigeminal ganglia and lungs were dissected out and post-fixed in the same fixative for 90 min at 4°C, followed by rinsing in 10% sucrose (wt/vol) in 0.1M phosphate buffer, pH 7.4, containing 0.01% sodium azide (Merck) and 0.02% bacitracin (Sigma). The tissues were kept in 10% sucrose solution for 2 days at 4°C, and then frozen with liquid carbon dioxide and sectioned on a cryostat (Microm, Heidelberg, Germany). Serial

coronal sections were collected at 12 µm thickness for trigeminal ganglia, and 20 µm for brains and lung. The sections were mounted onto superfrost plus microscope slides (Thermo Scientific) and stored at -20°C (27)

The slides were then pretreated with a Dako target retrieval solution (Agilent) prior to blocking solution, and incubated with respective primary antibodies listed in table 1. Conjugated Alexa Fluor antibodies, anti-mouse IgG AlexaFluor 594; anti-rabbit IgG AlexaFluor 594; anti-rabbit IgG AlexaFluor 488, (Invitrogen) were used as secondary antibodies and the slides were mounted with ProLong Gold with DAPI (Invitrogen). Images were taken with a Zeiss Axiovision Apotome.2 confocal microscope (Zeiss).

Table 1. Primary antibodies used for western blot (WB)/ immunocytochemistry (ICC) and immunohistochemistry (IHC) analysis

Antibody	Dilution	Source
DAT (rabbit)	1:500 (WB)	MerckMilipore (#AB1591P)
TH (mouse)	1:600 (ICC)	MerckMilipore (#AB152)
MAP2 (rabbit)	1:400 (ICC)	Synaptic Systems (#188002)
14F2 (mouse)	1:1000 (WB; ICC)	In-house
DISC1 (rat)	1:200 (IHC)	In house
Syn211 (mouse)	1:400 (IC)	Santa Cruz biotechnology (#sc-12767)
Syn MJFR1 (rabbit)	1:200 (IC)/1:500(WB)	Abcam (#ab138501)
α-synuclein (Sheep)	1:500(IHC)	Abcam (#ab6162)
HT7 (mouse)	1:1000 (WB;ICC)	Invitrogen (# MN1000)
Tau 5 (mouse)	1:200 (IHC)	Invitrogen (#AHB0042)
AT180 (mouse)	1:400 (ICC)	Invitrogen (#MN1040)
TDP-43 (rabbit)	1:1000 (WB;ICC)	Proteintech (#10782-2-AP)
TDP43 [3H8] (mouse)	1:500 (IHC)	Abcam (#ab104223)
Influenza A NP (rabbit)	1:1000 (WB;ICC)	Invitrogen (# PA5-32242)
Influenza A/WSN/33 (rabbit)	1:100,000 (IHC)	Gift kindly provided by Dr. S. Nakajima, The Institute of Public Health, Tokyo, Japan)
LC3B (mouse)	1:1000 (WB;ICC)	Abcam (#ab48394)
LAMP1 (rabbit)	1:1000 (WB;ICC)	DSHB
HuR [3A2] (mouse)	1:500 (ICC)	Santa Cruz biotechnology (#sc-5261)
VDAC (rabbit)	1:500 (WB)	Enzo (#ALX-210-785/1)

Statistical analysis. For quantification of protein aggregates in LUHMES and NLF neuroblastoma cell line, a systematic manually counting procedure was used. For all immunocytochemistry data, randomized confocal images were taken in an average of 30 images from 2 independent wells per biological replicate, in a total number of, at least 3 independent biological experiments. All data were normalized against the number of cells present in the counted image. All data presented in the histograms were obtained by normalization to the correspondent non-infected condition considered 100%. Autophagosomal and lysosomal structures were quantified using 3D object counter plugin from the imageJ software Fiji. LC3 punctate dots quantified were in the range of 50-200 nm, and LAMP1 positive structures counted were in the range of 100-500 nm. GraphPad Prism (Version 5; GraphPad Software Inc., San Diego, CA, USA) was used to perform the statistical analysis. All data sets were tested for normal distribution based on the expected experimental results and appropriate non-parametric tests were chosen. Appropriate statistical tests and p-values are stated in the respective figure legends. P-values of *P **<**0.05, **P **<** 0.01 were used as significance levels.

References

1. Taylor JP, Hardy J, & Fischbeck KH (2002) Toxic proteins in neurodegenerative disease. *Science* 296(5575):1991-1995.
2. Prusiner SB (2001) Shattuck Lecture -- Neurodegenerative diseases and prions. *N. Engl. J. Med.* 344:1516-1526.
3. Spillantini MG, Crowther RA, Jakes R, Hasegawa M, & Goedert M (1998) alpha- Synuclein in filamentous inclusions of Lewy bodies from Parkinson's disease and dementia with lewy bodies. *Proceedings of the National Academy of Sciences of the United States of America* 95:6469-6473.
4. Rey NL*, et al.* (2018) Spread of aggregates after olfactory bulb injection of alpha- synuclein fibrils is associated with early neuronal loss and is reduced long term. *Acta Neuropathol* 135(1):65-83.
5. Rey NL*, et al.* (2016) Widespread transneuronal propagation of alpha- synucleinopathy triggered in olfactory bulb mimics prodromal Parkinson's disease. *J Exp Med* 213(9):1759-1778.
6. Cersosimo MG (2018) Propagation of alpha-synuclein pathology from the olfactory bulb: possible role in the pathogenesis of dementia with Lewy bodies. *Cell Tissue Res* 373(1):233-243.
7. Bradshaw NJ & Korth C (2018) Protein misassembly and aggregation as potential convergence points for non-genetic causes of chronic mental illness. *Molecular psychiatry*.
8. Leliveld SR*, et al.* (2008) Insolubility of Disrupted-in-Schizophrenia 1 Disrupts Oligomer-Dependent Interactions with Nuclear Distribution Element 1 and Is Associated with Sporadic Mental Disease. *Journal of Neuroscience* 28:3839-3845.
9. Trossbach SV*, et al.* (2016) Misassembly of full-length Disrupted-in-Schizophrenia 1 protein is linked to altered dopamine homeostasis and behavioral deficits. *Mol Psychiatry* 21:1561-1572.
10. Desplats P*, et al.* (2009) Inclusion formation and neuronal cell death through neuron- to-neuron transmission of alpha-synuclein. *Proceedings of the National Academy of Sciences of the United States of America* 106(31):13010-13015.
11. Woerman AL*, et al.* (2018) alpha-Synuclein: Multiple System Atrophy Prions. *Cold Spring Harb Perspect Med* 8(7).
12. Zhu S, Abounit S, Korth C, & Zurzolo C (2017) Transfer of disrupted-in-schizophrenia 1 aggregates between neuronal-like cells occurs in tunnelling nanotubes and is promoted by dopamine. *Open Biol* 7(3).
13. Goedert M (2015) NEURODEGENERATION. Alzheimer's and Parkinson's diseases: The prion concept in relation to assembled Abeta, tau, and alpha-synuclein. *Science* 349(6248):1255555.
14. Luk KC*, et al.* (2012) Intracerebral inoculation of pathological alpha-synuclein initiates a rapidly progressive neurodegenerative alpha-synucleinopathy in mice. *J Exp Med* 209(5):975-986.
15. Taylor RC & Dillin A (2011) Aging as an event of proteostasis collapse. *Cold Spring Harbor perspectives in biology* 3:a004440-a004440.
16. Balchin D, Hayer-Hartl M, & Hartl FU (2016) In vivo aspects of protein folding and quality control. *Science* 353(6294):aac4354.
17. Aviner R & Frydman J (2019) Proteostasis in Viral Infection: Unfolding the Complex Virus-Chaperone Interplay. *Cold Spring Harb Perspect Biol*.
18. Baccam P, Beauchemin C, Macken CA, Hayden FG, & Perelson AS (2006) Kinetics of influenza A virus infection in humans. *J Virol* 80(15):7590-7599.
19. Regoes RR, Hamblin S, & Tanaka MM (2013) Viral mutation rates: modelling the roles of within-host viral dynamics and the trade-off between replication fidelity and speed. *Proc Biol Sci* 280(1750):20122047.

20. Lingappa UF*, et al.* (2013) Host-rabies virus protein-protein interactions as druggable antiviral targets. *Proceedings of the National Academy of Sciences of the United States of America* 110:E861-868.
21. Phillips AM*, et al.* (2017) Host proteostasis modulates influenza evolution. *Elife* 6.
22. Goodwin CM, Xu S, & Munger J (2015) Stealing the Keys to the Kitchen: Viral Manipulation of the Host Cell Metabolic Network. *Trends Microbiol* 23(12):789-798.
23. Watanabe T, Watanabe S, & Kawaoka Y (2010) Cellular networks involved in the influenza virus life cycle. *Cell Host Microbe* 7(6):427-439.
24. Ravindran MS, Bagchi P, Cunningham CN, & Tsai B (2016) Opportunistic intruders: how viruses orchestrate ER functions to infect cells. *Nat Rev Microbiol* 14(7):407-420.
25. Marreiros R*, et al.* (2015) Viral capsid assembly as a model for protein aggregation diseases: Active processes catalyzed by cellular assembly machines comprising novel drug targets. *Virus research* 207:155-164.
26. Smith W, Manch MD, Andrewas CH, & Lond MD (1933) A virus obtained from influenza patients. *Lancet* 225:66-68.
27. Tesoriero C*, et al.* (2016) H1N1 influenza virus induces narcolepsy-like sleep disruption and targets sleep-wake regulatory neurons in mice. *Proceedings of the National Academy of Sciences of the United States of America* 113:E368-377.
28. Kristensson K (2006) Avian influenza and the brain--comments on the occasion of resurrection of the Spanish flu virus. *Brain Res Bull* 68(6):406-413.
29. Jang H*, et al.* (2009) Highly pathogenic H5N1 influenza virus can enter the central nervous system and induce neuroinflammation and neurodegeneration. *Proceedings of the National Academy of Sciences of the United States of America* 106:14063- 14068.
30. Shinya K*, et al.* (2011) Subclinical brain injury caused by H5N1 influenza virus infection. *J Virol* 85(10):5202-5207.
31. McCall S, Henry JM, Reid AH, & Taubenberger JK (2001) Influenza RNA not detected in archival brain tissues from acute encephalitis lethargica cases or in postencephalitic Parkinson cases. *J Neuropathol Exp Neurol* 60(7):696-704.
32. Sheng ZM*, et al.* (2011) Autopsy series of 68 cases dying before and during the 1918 influenza pandemic peak. *Proc Natl Acad Sci U S A* 108(39):16416-16421.
33. Vilensky JA, Gilman S, & McCall S (2010) A historical analysis of the relationship between encephalitis lethargica and postencephalitic parkinsonism: a complex rather than a direct relationship. *Movement disorders : official journal of the Movement Disorder Society* 25:1116-1123.
34. Tappe D & Alquezar-Planas DE (2014) Medical and molecular perspectives into a forgotten epidemic: encephalitis lethargica, viruses, and high-throughput sequencing. *J Clin Virol* 61(2):189-195.
35. Lotharius J*, et al.* (2002) Effect of mutant alpha-synuclein on dopamine homeostasis in a new human mesencephalic cell line. *The Journal of biological chemistry* 277:38884-38894.
36. Burnet FM (1951) A genetic approach to variation in influenza viruses; the characters of three substrains of influenza virus A (WS). *J Gen Microbiol* 5(1):46-53.
37. Outeiro TF*, et al.* (2019) Dementia with Lewy bodies: an update and outlook. *Mol Neurodegener* 14(1):5.
38. Schwab M*, et al.* (1983) Amplified DNA with limited homology to myc cellular oncogene is shared by human neuroblastoma cell lines and a neuroblastoma tumour. *Nature* 305(5931):245-248.

39. Ottis P*, et al.* (2011) Convergence of two independent mental disease genes on the protein level: recruitment of dysbindin to cell invasive DISC1 aggresomes. *Biological Psychiatry* 70:604-610.
40. Grundke-Iqbal I*, et al.* (1986) Abnormal phosphorylation of the microtubule- associated protein tau (tau) in Alzheimer cytoskeletal pathology. *Proc Natl Acad Sci U S A* 83(13):4913-4917.
41. Neumann M*, et al.* (2006) Ubiquitinated TDP-43 in frontotemporal lobar degeneration and amyotrophic lateral sclerosis. *Science* 314(5796):130-133.
42. Walker RM*, et al.* (2012) The DISC1 promoter: characterization and regulation by FOXP2. *Human molecular genetics* 21:2862-2872.
43. Cheung TK & Poon LL (2007) Biology of influenza a virus. *Ann N Y Acad Sci* 1102:1- 25.
44. Lo C-Y, Tang Y-S, & Shaw P-C (2018) Structure and Function of Influenza Virus Ribonucleoprotein. *Sub-cellular biochemistry* 88:95-128.
45. Kim CU*, et al.* (1997) Influenza neuraminidase inhibitors possessing a novel hydrophobic interaction in the enzyme active site: design, synthesis, and structural analysis of carbocyclic sialic acid analogues with potent anti-influenza activity. *J Am Chem Soc* 119(4):681-690.
46. Mendel DB*, et al.* (1998) Oral administration of a prodrug of the influenza virus neuraminidase inhibitor GS 4071 protects mice and ferrets against influenza infection. *Antimicrob Agents Chemother* 42(3):640-646.
47. Anonymous (Oseltamivir phosphate information. https://www.accessdata.fda.gov/drugsatfda_docs/label/2006/021087s033lbl.pdf.
48. Gannagé M*, et al.* (2009) Matrix protein 2 of influenza A virus blocks autophagosome fusion with lysosomes. *Cell host & microbe* 6:367-380.
49. Kuroki T, Osari S, Nagata K, & Kawaguchi A (2018) Influenza A Virus NS1 Protein Suppresses JNK1-Dependent Autophagosome Formation Mediated by Rab11a Recycling Endosomes. *Frontiers in microbiology* 9:3120.
50. Friedman LG*, et al.* (2012) Disrupted Autophagy Leads to Dopaminergic Axon and Dendrite Degeneration and Promotes Presynaptic Accumulation of -Synuclein and LRRK2 in the Brain. *Journal of Neuroscience* 32:7585-7593.
51. Kimura S, Noda T, & Yoshimori T (Dissection of the autophagosome maturation process by a novel reporter protein, tandem fluorescent-tagged LC3. *Autophagy* 3:452-460.
52. Tanik SA, Schultheiss CE, Volpicelli-Daley LA, Brunden KR, & Lee VM (2013) Lewy body-like alpha-synuclein aggregates resist degradation and impair macroautophagy. *J Biol Chem* 288(21):15194-15210.
53. Lee HJ*, et al.* (2013) Autophagic failure promotes the exocytosis and intercellular transfer of alpha-synuclein. *Exp Mol Med* 45:e22.
54. Karpowicz RJ, Jr., Trojanowski JQ, & Lee VM (2019) Transmission of alpha-synuclein seeds in neurodegenerative disease: recent developments. *Lab Invest*.
55. Garbett KA, Hsiao EY, Kalman S, Patterson PH, & Mirnics K (2012) Effects of maternal immune activation on gene expression patterns in the fetal brain. *Transl Psychiatry* 2:e98
56. Shi L, Fatemi SH, Sidwell RW, & Patterson PH (2003) Maternal influenza infection causes marked behavioral and pharmacological changes in the offspring. *J Neurosci* 23(1):297-302.
57. Kamiya A*, et al.* (2005) A schizophrenia-associated mutation of DISC1 perturbs cerebral cortex development. *Nat Cell Biol* 7(12):1167-1178.
58. Arriagada PV, Growdon JH, Hedley-Whyte ET, & Hyman BT (1992) Neurofibrillary tangles but not senile plaques parallel duration and severity of Alzheimer's disease. *Neurology* 42:631-639.

59. Lamark T & Johansen T (2012) Aggrephagy: selective disposal of protein aggregates by macroautophagy. *International journal of cell biology* 2012:736905.
60. Jackson WT*, et al.* (2005) Subversion of cellular autophagosomal machinery by RNA viruses. *PLoS biology* 3:e156.
61. Kirkegaard K, Taylor MP, & Jackson WT (2004) Cellular autophagy: surrender, avoidance and subversion by microorganisms. *Nature reviews. Microbiology* 2:301- 314.
62. Schmid D & Münz C (2007) Innate and adaptive immunity through autophagy. *Immunity* 27:11-21.
63. Zhou Z*, et al.* (2009) Autophagy is involved in influenza A virus replication. *Autophagy* 5:321-328.
64. Sun Y*, et al.* (2012) Inhibition of autophagy ameliorates acute lung injury caused by avian influenza A H5N1 infection. *Science signaling* 5:ra16.
65. Xilouri M, Vogiatzi T, Vekrellis K, & Stefanis L (2008) alpha-synuclein degradation by autophagic pathways: a potential key to Parkinson's disease pathogenesis. *Autophagy* 4:917-919.
66. Höllerhage M*, et al.* (2014) Trifluoperazine rescues human dopaminergic cells from wild-type α-synuclein-induced toxicity. *Neurobiology of aging* 35:1700-1711.
67. Atkin TA, Brandon NJ, & Kittler JT (2012) Disrupted in Schizophrenia 1 forms pathological aggresomes that disrupt its function in intracellular transport. *Human molecular genetics* 21:2017-2028.
68. Wang Y & Mandelkow E (2012) Degradation of tau protein by autophagy and proteasomal pathways. *Biochemical Society transactions* 40:644-652.
69. Tai H-C*, et al.* (2012) The synaptic accumulation of hyperphosphorylated tau oligomers in Alzheimer disease is associated with dysfunction of the ubiquitin- proteasome system. *The American journal of pathology* 181:1426-1435.
70. Guo JL*, et al.* (2016) The Dynamics and Turnover of Tau Aggregates in Cultured Cells: INSIGHTS INTO THERAPIES FOR TAUOPATHIES. *The Journal of biological chemistry* 291:13175-13193.
71. Scotter EL*, et al.* (2014) Differential roles of the ubiquitin proteasome system and autophagy in the clearance of soluble and aggregated TDP-43 species. *Journal of cell science* 127:1263-1278.
72. Wang X*, et al.* (2010) Degradation of TDP-43 and its pathogenic form by autophagy and the ubiquitin-proteasome system. *Neuroscience letters* 469:112-116.
73. Ding WX*, et al.* (2007) Linking of autophagy to ubiquitin-proteasome system is important for the regulation of endoplasmic reticulum stress and cell viability. *Am J Pathol* 171(2):513-524.
74. Zhu K, Dunner K, Jr., & McConkey DJ (2010) Proteasome inhibitors activate autophagy as a cytoprotective response in human prostate cancer cells. *Oncogene* 29(3):451-462.
75. Pandey UB*, et al.* (2007) HDAC6 rescues neurodegeneration and provides an essential link between autophagy and the UPS. *Nature* 447(7146):859-863.
76. Demishtein A*, et al.* (2017) SQSTM1/p62-mediated autophagy compensates for loss of proteasome polyubiquitin recruiting capacity. *Autophagy* 13(10):1697-1708.
77. Ravikumar B, Duden R, & Rubinsztein DC (2002) Aggregate-prone proteins with polyglutamine and polyalanine expansions are degraded by autophagy. *Hum Mol Genet* 11(9):1107-1117.
78. Korolchuk VI, Mansilla A, Menzies FM, & Rubinsztein DC (2009) Autophagy inhibition compromises degradation of ubiquitin-proteasome pathway substrates. *Mol Cell* 33(4):517-527.
79. Dou D*, et al.* (2017) Analysis of IAV Replication and Co-infection Dynamics by a Versatile RNA Viral Genome Labeling Method. *Cell Rep* 20(1):251-263.

80. Heldt FS, Kupke SY, Dorl S, Reichl U, & Frensing T (2015) Single-cell analysis and stochastic modelling unveil large cell-to-cell variability in influenza A virus infection. *Nat Commun* 6:8938.
81. Shipley MT & Adamek GD (1984) The connections of the mouse olfactory bulb: a study using orthograde and retrograde transport of wheat germ agglutinin conjugated to horseradish peroxidase. *Brain Res Bull* 12(6):669-688.
82. Takahashi M*, et al.* (1995) The substantia nigra is a major target for neurovirulent influenza A virus. *J Exp Med* 181(6):2161-2169.
83. Braak H*, et al.* (2003) Staging of brain pathology related to sporadic Parkinson's disease. *Neurobiology of aging* 24(2):197-211.
84. Jellinger KA (2009) Absence of alpha-synuclein pathology in postencephalitic parkinsonism. *Acta Neuropathol* 118(3):371-379.
85. Scholler AS, Fonnes M, Nazerai L, Christensen JP, & Thomsen AR (2019) Local Antigen Encounter Is Essential for Establishing Persistent CD8(+) T-Cell Memory in the CNS. *Front Immunol* 10:351.
86. LaBarre DD & Lowy RJ (2001) Improvements in methods for calculating virus titer estimates from TCID50 and plaque assays. *Journal of virological methods* 96:107- 126.
87. Scholz D*, et al.* (2011) Rapid, complete and large-scale generation of post-mitotic neurons from the human LUHMES cell line. *Journal of neurochemistry* 119:957-971.
88. Clough RL, Dermentzaki G, & Stefanis L (2009) Functional dissection of the alpha- synuclein promoter: transcriptional regulation by ZSCAN21 and ZNF219. *Journal of neurochemistry* 110:1479-1490.
89. Sanjuan R (2017) Collective Infectious Units in Viruses. *Trends Microbiol* 25(5):402- 412.
90. Aronsson F, Robertson B, Ljunggren H-G, & Kristensson K (2003) Invasion and persistence of the neuroadapted influenza virus A/WSN/33 in the mouse olfactory system. *Viral immunology* 16:415-423.
91. Shi TJ*, et al.* (2012) Secretagogin is expressed in sensory CGRP neurons and in spinal cord of mouse and complements other calcium-binding proteins, with a note on rat and human. *Mol Pain* 8:80.

Acknowledgements

The authors thank Krister Kristensson from the Karolinska Institute, Sweden, for providing sections of influenza H1N1 WSN/33-infected $Rag^{-/-}$ mice, for critical discussion of results and the manuscript. This research was funded by grants from EU-FP7 MC-ITN IN-SENS (#.60671), a grant from the Forschungskommission of the Medical Faculty of the Heinrich Heine University Düsseldorf (#9772651), and a grant from the BMBF (01GQ1422A; REMOVAGE).

Figure legends

Fig 1. A/WS/33 (H1N1) infection induces aggregated α-Syn in human dopamine like neurons. (A) Non-infected LUHMES cells show only a low number of α-synuclein aggregates (green - α-Syn, blue –DAPI, nuclear staining). (B) Aggregated α-synuclein was detected in the cytoplasm of LUHMES cells 24h after influenza infection (MOI 1) (green: α-Syn, blue: DAPI,; Red: influenza A). Scale bars 10 or 3μm. (C) Quantification of percentage of influenza induced α-synuclein aggregates per cell in infected condition (black bar) relative to the non-infected condition (grey bar). Data presented as mean of replicates from six independent experiments ± SEM. Mann-Whitney U with one-tailed Dunn's *post hoc* test was use as a statistical test (**p <0.01). (D) Immunoblot of total protein levels of α-synuclein in lysates of infected and non-infected LUHMES cells. One of the three experiments is shown. Quantification of the Western blot band intensity, shown in percentage relative to the non- infected condition, normalized to VDAC used as a loading control. Grey bar represents the non-infected condition and black bar represents the infected condition (n=3 ± SEM).

Fig 2. 28 days of A/WSN/33 (H1N1) influenza virus infection affects mouse α-Syn expression *in vivo.* Mouse α-synuclein expression was exclusively detected co-localizing with influenza A (hemagglutinin protein) in Rag1 knock-out mice (green-α-Syn, red – influenza A, blue –DAPI, nuclear staining). In non-viral infected area and in non-infected mice (PBS control) there was no detectable α-synuclein signal (green-α-Syn, red – influenza A, blue –DAPI, nuclear staining). Scale bars 50 or 10μm.

Fig 3. Influenza A virus (A/WS/33) segment 5 nucleocapsid protein is not sufficient to induce α-Syn aggregates. (A) Influenza induced aggregated α-synuclein was only detected in influenza infected condition in NLF neuroblastoma cells, transiently transfected with human α-synuclein. In double transfected cells with α-synuclein and influenza virus segment 5 nucleocapsid, α-synuclein aggregates were not visible. Non-infected cells did not show aggregated α-synuclein (green- α-syn, Red – influenza A, blue – DAPI, nuclear staining). Scale bars 10 μm. (B) Quantification of percentage of aggregated α-synuclein per cell infected for 24h with A/WS/33 virus (MOI 1) and transfected with A/WS/33 nucleocapsid, relative to the non-infected condition. Dark grey bar represents the non-infected condition, black bar represents A/WS/33 infected cells, and light grey bar represents A/WS/33 nucleocapsid transfected condition. Data presented as mean of replicates from three independent experiments ± SEM. Two-way ANOVA test was use as a statistical test (*P < 0.05; n.s. not significant).

Fig 4. Oseltamivir phosphate prevents α-syn aggregate formation in human dopamine-like neurons. The effect of the antiviral drug oseltamivir phosphate in α-synuclein aggregate formation in infected LUHMES cells (MOI 1 24h) was tested. Histograms in the panels A, B, D have an identical color code. Black bar represents PBS treated condition, red bar represents 0.5 μM and blue bar 50 μM (A) Compound antiviral activity measured by reduction in the percentage of pfu/ml of A/WS/33 virus. $TCID_{50}$ assay performed in MDCK.2 cells (n=2 ± SEM). (B) Quantification of cell number per square millimeter in LUHMES preparation did not show a compound dependent effect in cell viability. (C) Representative image of immunocytochemistry of LUHMES cells virally infected and treated with 50 μM oseltamivir phosphate or the respective PBS control (green- α-Syn, red- Influenza NP, blue – DAPI, nuclear staining). Scale bars 10 or 3μm. (D) Ratio of aggregated α-synuclein per cell in infected LUHMES treated with low- and high- compound concentrations. Oseltimivir phosphate treatment showed a reduction in α-synuclein aggregate formation. Data shown in percentage of aggregated α-synuclein in infected condition normalized for non-infected condition. Data presented as mean of replicates from three independent experiments ± SEM. Two-way ANOVA test was used as a statistical test (** $p < 0.01$).

Fig 5. 24h of influenza A (A/WS/33) infection decreases autophagosome number and impairs autophagic flux in human dopamine-like neuros. (A-B) Visualization of the decrease in LC3 structures in influenza infected LUHMES cells (MOI 1 for 24h) in comparison with non-infected condition (green - LC3, blue – DAPI, nuclear staining). Scale bar 10 or 3 μm. (C) Quantification of percentage of LC3 punctate structures in infected condition (black bar) relative to the non-infected condition (grey bar). Data presented as mean of replicates from three independent experiments ± SEM. Mann-Whitney U with two- tailed Dunn's *post hoc* test was use as a statistical test (* $p < 0.05$). (D) Immunoblot for LC3B in lysates of infected and non-infected LUHMES cells. One of four experiments is shown. Quantification of the Western blot band intensity in percentage relative to the non-infected condition, normalized with VDAC protein levels used as loading control. Grey bar represents the non-infected condition and black bar represents the infected condition (n=4 ± SEM). Mann-Whitney U with one-tailed Dunn's *post hoc* test was used as a statistical test (*$p < 0.05$). (E) Schematic representation of the tandem report construct mRFP-GFP-LC3 used to accesses the changes in autophagic flux under influenza infection. (F) NLF neuroblastoma cells transiently transfected with mRFP-GFP-LC3 construct and, subsequently infected with influenza or non-infected (MOI 1 for 24h). GFP – and RFP – fluorescence was analyzed by fluorescence microscopy. DAPI was use as nuclear staining. Scale bar 10 μm. (G) Quantification of yellow LC3 structures (merged mRFP – and GFP signals) labeling

autophagosomes and the red LC3 (mRFP) structures labeling autolysosomes. Yellow bars represent autophagosomes, and red bars represent autolysosomes. Under viral infection an increased number of autophagosomes was detected. Data presented as mean of replicates from three independent experiments ± SEM. Mann-Whitney U with one-tailed Dunn's *post hoc* test was used as a statistical test (* p <0.05; n.s. non-statistical significance). (H) A decrease in the percentage of autolysosomes formed per cell was visible in infected condition (represented by black bar) relative to the non-infected control (represented by grey bar). Data presented as mean of replicates from three independent experiments ± SEM. Mann-Whitney U with one-tailed Dunn's *post hoc* test was used as a statistical test (* <0.05; n.s. not significant).

Fig 6. 24h of influenza A (A/WS/33) infection leads to an accumulation of lysosomal structures and a reduction in α-syn aggregate clearance by autolysosomes in human dopamine like neuros. (A-B) Immunostaining of LAMP-1 showed an accumulation of lysosomes in influenza viral infected LUHMES cells (MOI 1 for 24 h) in comparison with non-infected cells (green- LAMP-1, blue –DAPI, nuclear staining). Scale bar 10 μm. (C) Quantification of the percentage of acidified lysosomes in infected LUHMES cells (represented by black bar) relative to the non-infected condition (represented by grey bar). Data presented as mean of replicates from three independent experiments ± SEM. Mann- Whitney U with one-tailed Dunn's *post hoc* test was used as a statistical test (* P <0.05). (D) Immunoblot for LAMP-1 in lysates of infected and non-infected LUHMES cells. One of three experiments is shown. Quantification of the Western blot band intensity in percentage relative to the non-infected condition, normalized with VDAC used as a loading control. Grey bar represents the non-infected condition and black bar represents the infected condition (n=3 ± SEM). (E) Orthogonal projections demonstrated a decrease in the co-localization of aggregated α-synuclein with lysosomal structures in infected LUHMES cells in comparison with non-infected cells (green- α-syn, red –LAMP-1). Scale bar 10 μm. (F) Quantification of percentage of aggregated α-synuclein associated with LAMP-1 per cell in infected condition (represented by black bar) relative to the non-infected condition (represented by grey bar). Data presented as mean of replicates from three independent experiments ± SEM. Mann- Whitney U with one-tailed Dunn's *post hoc* test was used as a statistical test (* p <0.05).

Fig 7. Potential mechanism of protein homeostasis disruption in neuronal cells due to H1N1 influenza A infection. Schematic representation of influenza A infection effect in autophagy. Autophagy is one of the clearance mechanisms in the cell responsible for removing misfolded proteins and dysfunctional organelles, in order to prevent accumulation

of toxic species. Under normal conditions cell components selected for autophagy degradation are engulfed into a phagophore to form the autophagosome. Then the autolysosome is created by the fusion of autophagosome with lysosome where the cargo is delivered for degradation. Regular autophagy allows a proper cellular protein homeostasis and a normal cell function. Influenza A infection impairs autophagy at two stages. In an early stage, autophagosome formation and in a late stage autolysosome formation.

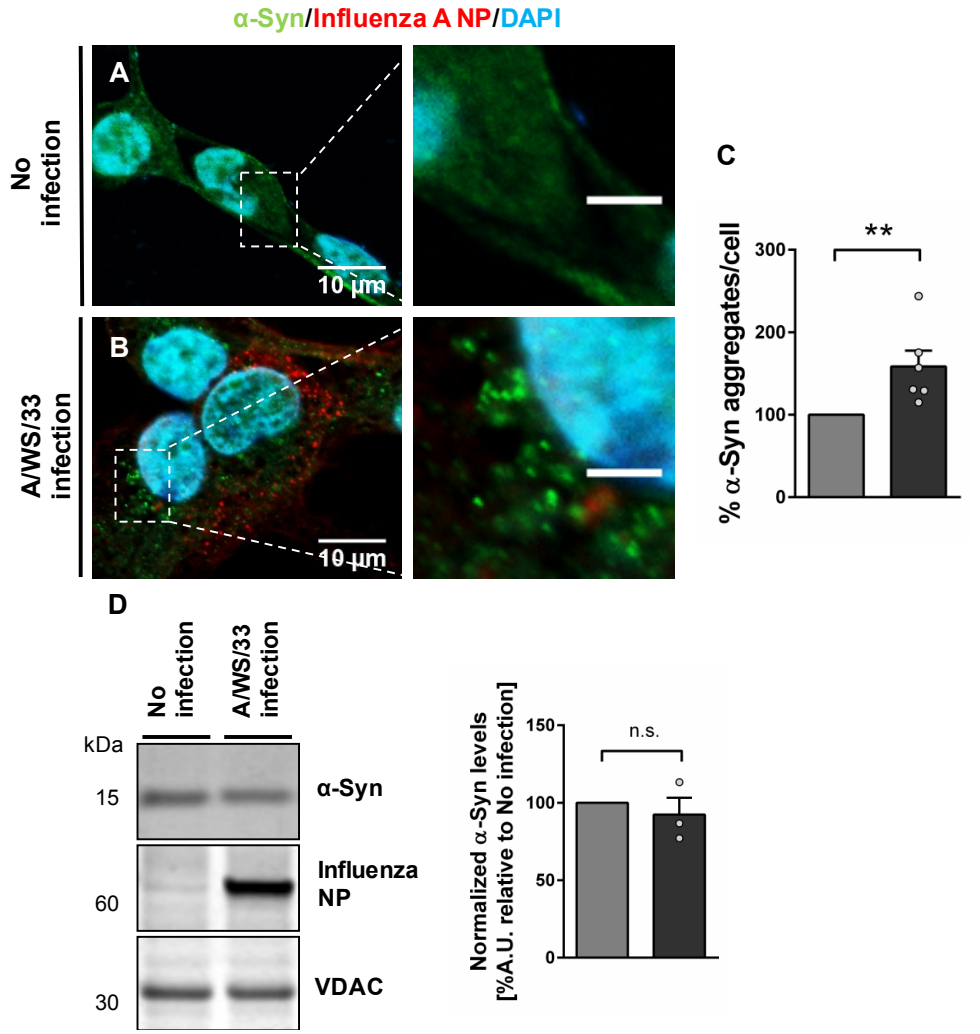
α-Syn/Influenza A NP/DAPI
No infection
A/WS/33 infection
A
B
10 µm
10 µm
C
% α-Syn aggregates/cell
**
300
200
100
0
D
No infection
A/WS/33 infection
kDa
15
60
30
α-Syn
Influenza NP
VDAC
Normalized α-Syn levels [%A.U. relative to No infection]
n.s.
150
100
50
0

Fig. 1

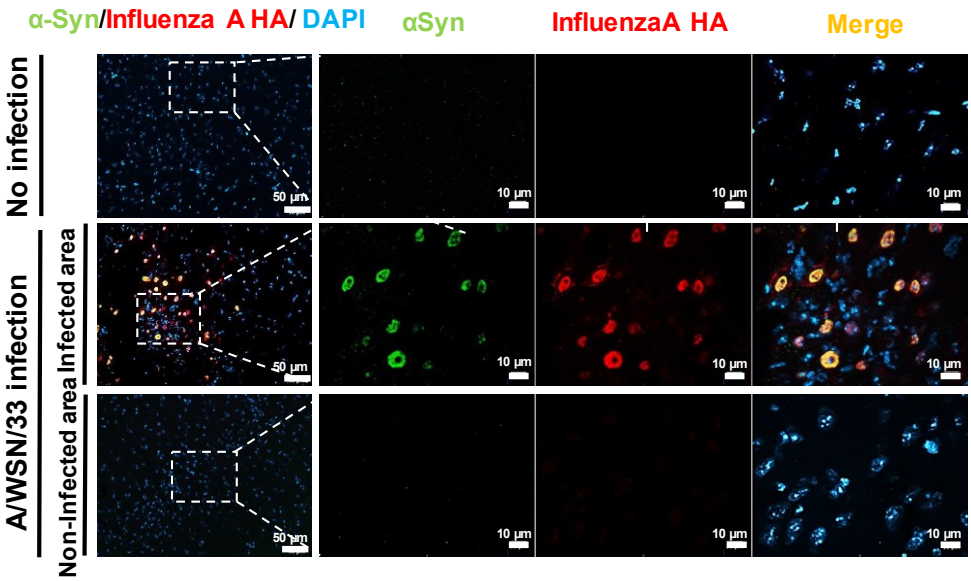
α-Syn/Influenza A HA/ DAPI
αSyn
InfluenzaA HA
Merge
No infection
A/WSN/33 infection
Infected area
Non-Infected area
50 µm
10 µm

Fig. 2

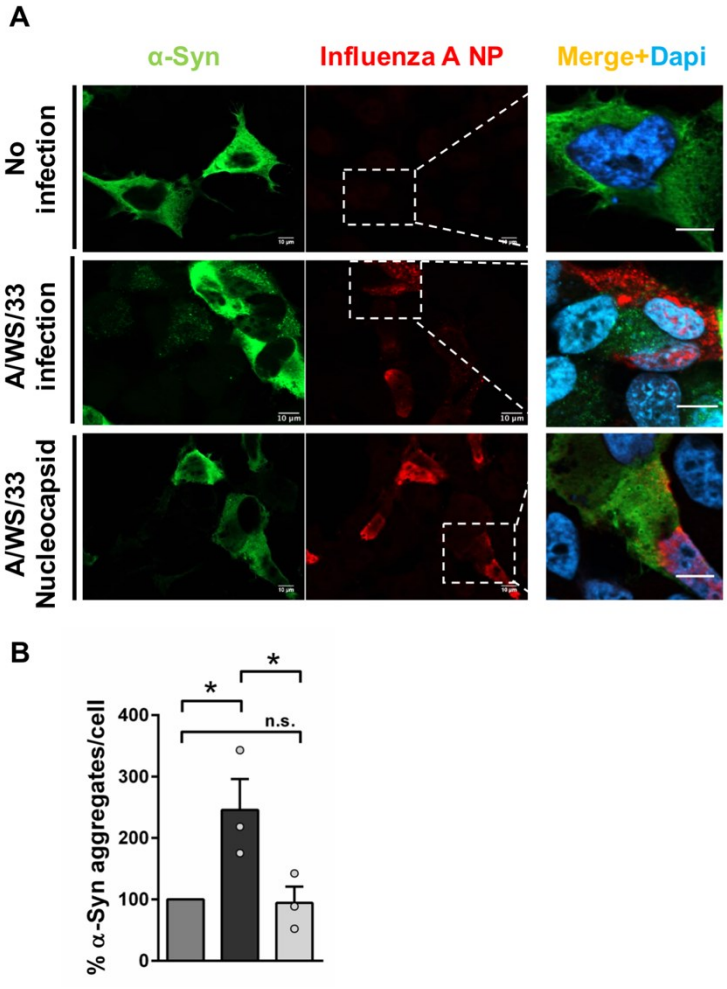
A
α-Syn
Influenza A NP
Merge+Dapi
No infection
A/WS/33 infection
A/WS/33 Nucleocapsid
B
% α-Syn aggregates/cell
400
300
200
100
0
*
*
n.s.

Fig. 3

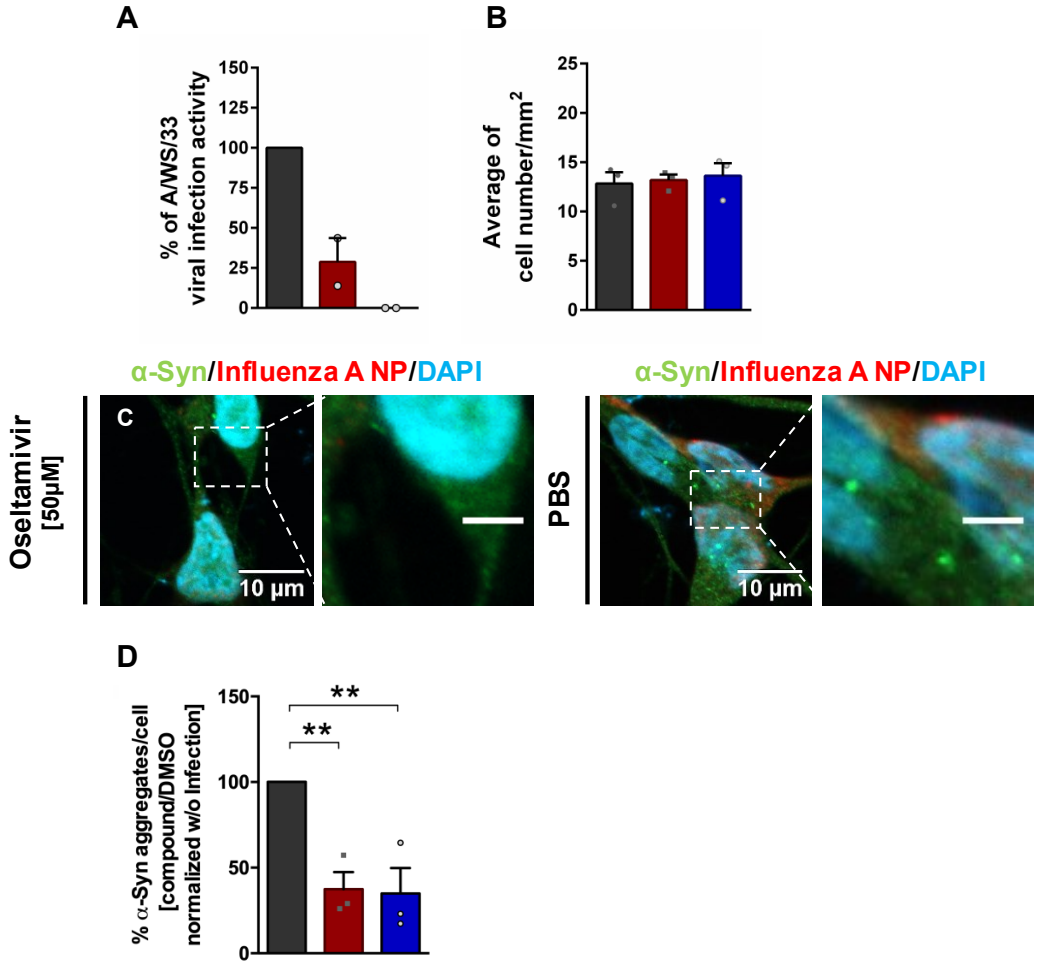
A
% of A/WS/33 viral infection activity
150
125
100
75
50
25
0
B
Average of cell number/mm2
25
20
15
10
5
0
α-Syn/Influenza A NP/DAPI
α-Syn/Influenza A NP/DAPI
Oseltamivir [50μM]
PBS
C
10 μm
10 μm
D
% α-Syn aggregates/cell [compound/DMSO normalized w/o Infection]
150
100
50
0
**
**

Fig. 4

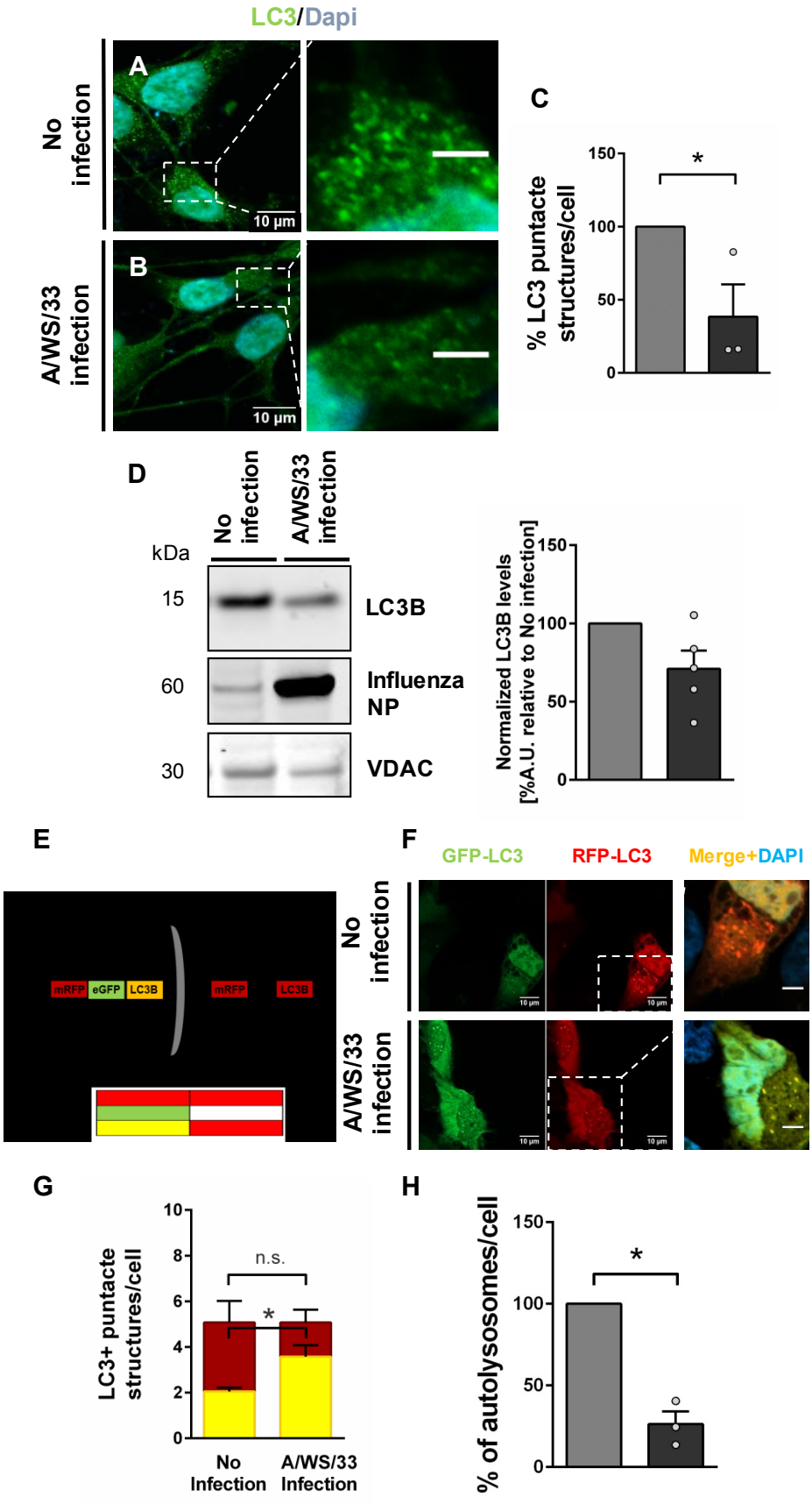
LC3/Dapi
No infection
A/WS/33 infection
A
B
10 µm
C
% LC3 puntacte structures/cell
150
100
50
0
*
D
No infection
A/WS/33 infection
kDa
15
60
30
LC3B
Influenza NP
VDAC
Normalized LC3B levels [%A.U. relative to No infection]
E
mRFP
eGFP
LC3B
F
GFP-LC3
RFP-LC3
Merge+DAPI
G
LC3+ puntacte structures/cell
n.s.
No Infection
A/WS/33 Infection
H
% of autolysosomes/cell

Fig. 5

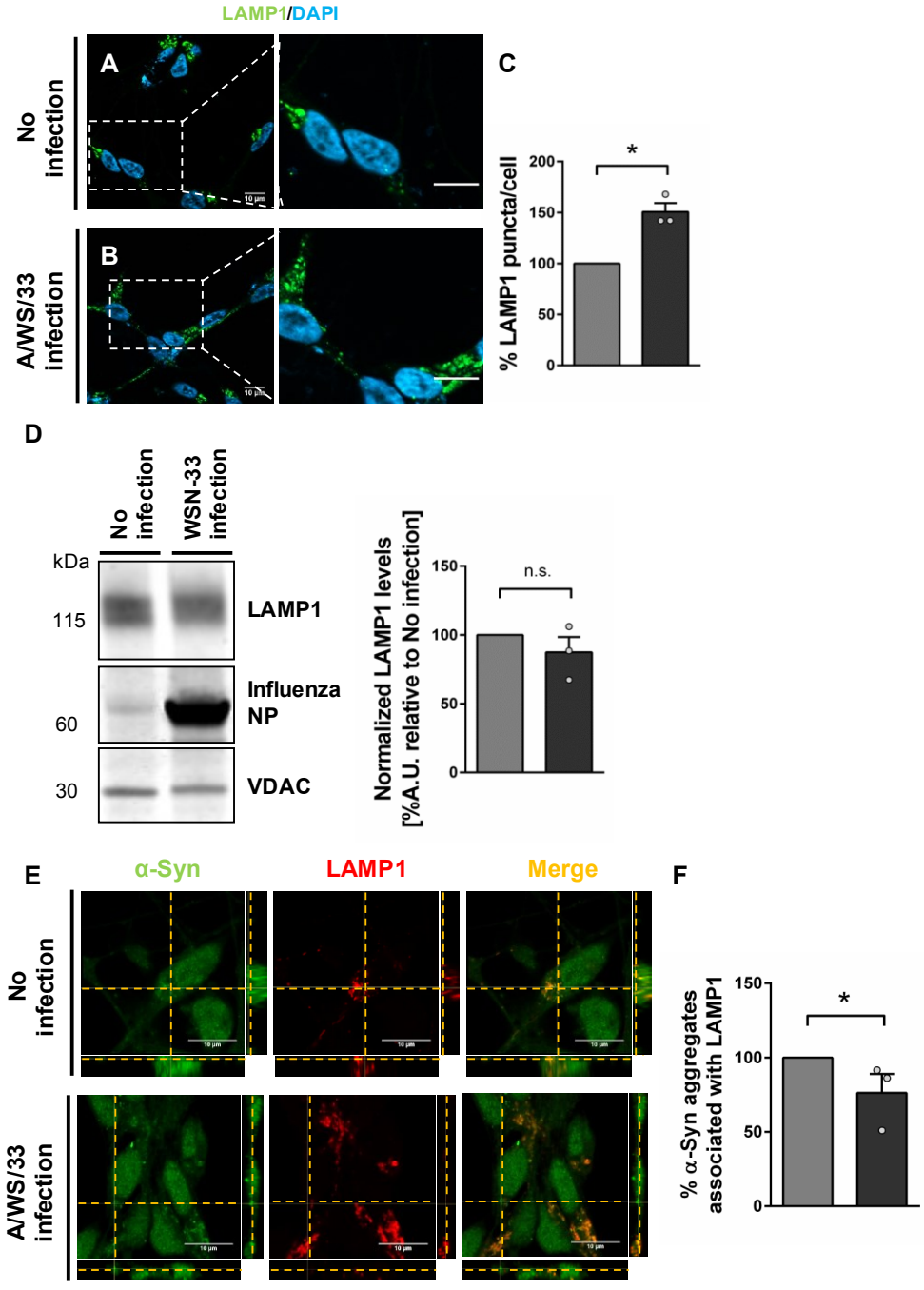
LAMP1/DAPI
No infection
A/WS/33 infection
A
B
C
% LAMP1 puncta/cell
200
150
100
50
0
*
D
No infection
WSN-33 infection
kDa
115
60
30
LAMP1
Influenza NP
VDAC
Normalized LAMP1 levels [%A.U. relative to No infection]
150
100
50
0
n.s.
E
α-Syn
LAMP1
Merge
No infection
A/WS/33 infection
F
% α-Syn aggregates associated with LAMP1
150
100
50
0
*

Fig. 6

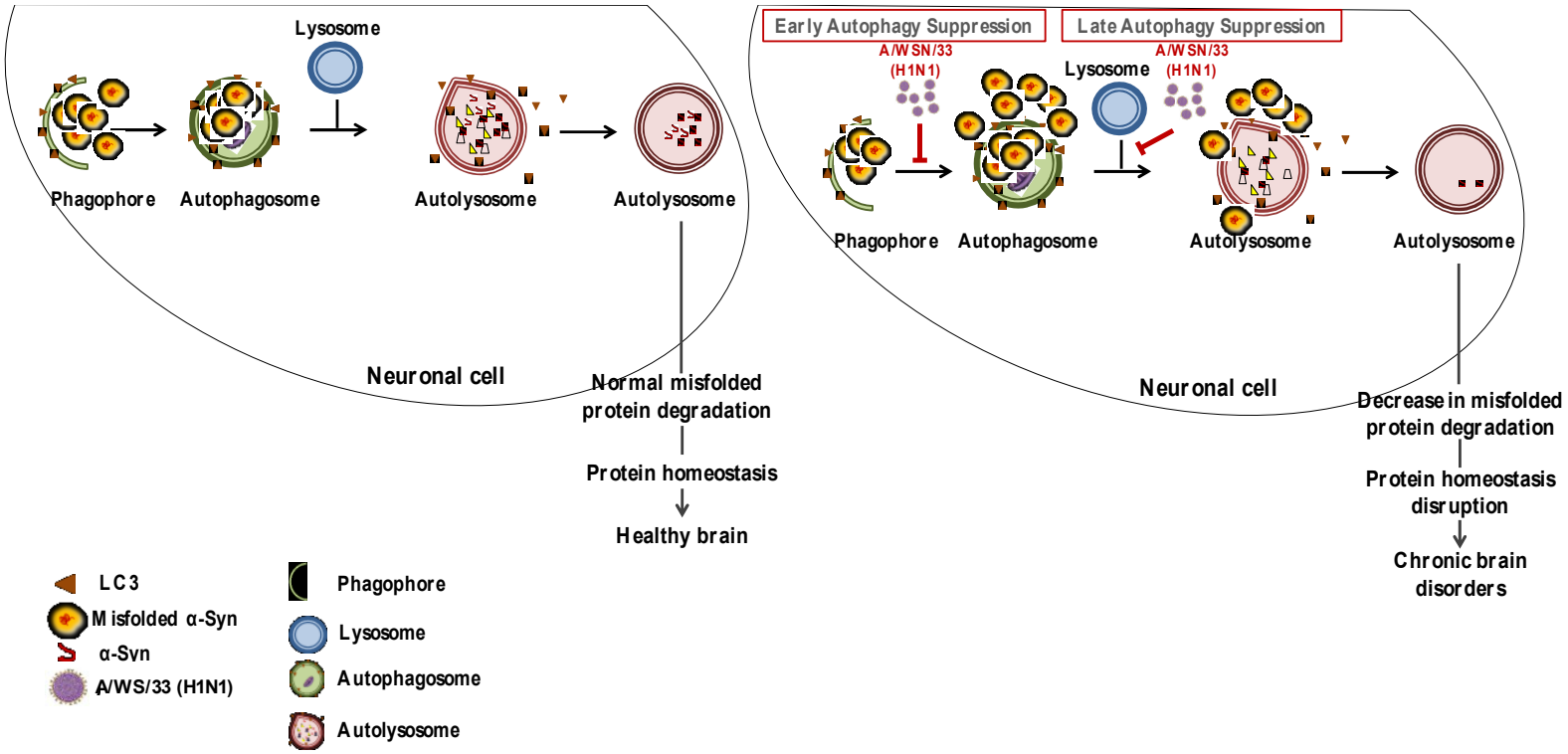
Lysosome
Phagophore
Autophagosome
Autolysosome
Autolysosome
Neuronal cell
Normal misfolded protein degradation
Protein homeostasis
Healthy brain
Early Autophagy Suppression
Late Autophagy Suppression
A/WSN/33 (H1N1)
A/WSN/33 (H1N1)
Lysosome
Phagophore
Autophagosome
Autolysosome
Autolysosome
Neuronal cell
Decrease in misfolded protein degradation
Protein homeostasis disruption
Chronic brain disorders
LC3
Misfolded α-Syn
α-Syn
A/WS/33 (H1N1)
Phagophore
Lysosome
Autophagosome
Autolysosome

Fig. 7

Supplementary figure legends

Fig S1. Characterization of Human-dopamine-like neurons (LUHMES). (A) Phase contrast microscope images of undifferentiated LUHMES (0 day) and at day 5 of differentiation. Scale bars 100µm (B) Representative immunoblot of dopamine transporter –DAT expression in LUHMES cells at differentiated day 0, 5. VDAC was used as a loading control. One of the three experiments is shown. (C) Immunostainings representing the dopaminergic phenotype of LUHMES cells at day 5 day of differentiation (green -TH, Red – MAP2). (D) Immunoblot analysis of endogenous total protein levels of alpha synuclein, DISC1, Tau and TDP-43 at differentiation days 0, 5. One of the three experiments is shown. Histograms showing the respective quantification of the protein levels normalized to VDAC, the loading control used. Data presented as mean of replicates from three independent experiments ± SEM. Mann-Whitney U with one-tailed Dunn's *post hoc* test was use as a statistical test (* P <0.05).

Fig S2. Determination of A/WS/33 (H1N1) viral activity in LUHMES cells. (A) Percentage of infected LUHMES cells in a culture preparation 24 h after A/WS/33 (H1N1) infection with MOI 1. Data presented as mean of replicates from five independent experiments ± SEM. (B) Viral infection titer at different time points (0; 12; 24 h) showed an increase in viral replication activity across time. Measurements done in MDCK cells infected with the culture medium from infected LUHMES cells with MOI 1 (n=2 ± SEM) .

Fig S3. A/WS/33 (H1N1) infection induces changes in α-syn protein homeostasis in human neuroblastoma cells. (A) Aggregated alpha synuclein was detected in the cytoplasma of NLF neuroblastoma cells transiently transfected with human alpha synuclein after 24 h of influenza infection (MOI 1). Aggregated alpha synuclein was not detected in non-infected cells (Red – Influenza A, hSyn - green, blue –DAPI, Nuclear staining) Scale bars 10µm. (B) Viral infection titer (in log10 pfu/ml) measured at different time points- during 48 h, showed a stable viral replication activity 24 h after infection. Measurements done in MDCK cells infected with the culture medium from infected NLF neuroblastoma cells (± SEM) .

Fig S4. A/WS/33 (H1N1) infection induces DISC1 aggregation in human cells. (A) Non-infected LUHMES cells did not show DISC1 aggregates (green -DISC1, blue –DAPI, nuclear staining) (B) DISC1 aggregates were detected in the cytoplasma of LUHMES cells 24 h after Influenza infection (MOI 1) (green -DISC1, blue –DAPI, nuclear staining, red – Influenza A). Scale bars 10µm. (C) Quantification of percentage of aggregated DISC1 per cell in infected LUHMES (represented by black bar) relative to the non-infected cells (represented by grey bar). Data presented as mean of replicates from four independent experiments ± SEM. Mann-Whitney U with one-tailed Dunn's *post hoc* test was use as a statistical test (*P <0.05). (D) 24h of Influenza infection (MOI 1) induces DISC1 aggregation in NLF neuroblatoma cells transiently transfected with human DISC1. In non-infected cells influenza

induced aggregates were not visible (blue –DAPI, Nuclear staining; red – Influenza A , mRFP-hDISC1 -green). Scale bars 10µm. (E) LUHMES cells did not show alpha synuclein and DISC1 co-aggregation 24 h after Influenza infection (MOI 1) (green - α-Syn, red - DISC1, blue –DAPI, nuclear staining). Scale bars 10; 3µm.

Fig S5. A/WS/33 (H1N1) infection does not induce cytoplasmic TDP-43 aggregates, neither tau protein changes in human dopamine like neurons. (A) Cytoplasmic inclusions of TDP-43 were not detected in LUHMES cells 24 h after Influenza infection (MOI 1). Viral infection did not affect TDP-43 presence in stress granules - HuR signal (TDP-43 -green, red – Influenza A or HuR). Scale bars 10µm. (B) 24 h of infection did not induce changes in phosphorylation pattern of tau neither in the total tau in LUHMES cells (phospho-tau (AT180) and total- tau (HT7) -green, blue –DAPI, nuclear staining, red – Influenza A). Scale bars 10µm. (C) LUHMES cells stained only with fluorescent secondary antibodies (blue –DAPI, nuclear staining; green-Alexa 488, Red – Alexa 594). Scale bars 10µm.

Fig S6. A/WS/33 (H1N1) infection does not affect the SNCA promotor activity. 24 h of influenza infection (MOI 1) did not induce changes in the activity of SNCA 5'promotor gene. A luciferase reporter assay was performed in NLF neuroblatoma cells transiently transfected with pLG3- SNCA 5'-promoter and influenza infected for 24 h (MOI 1). Data presented as mean of replicates from three independent experiments ± SEM. Mann-Whitney U with one-tailed Dunn's *post hoc* test was used as a statistical test.

Fig S7. 28 days of A/WSN/1933 (H1N1) infection changes mouse DISC1 expression *in vivo.* (A) Increase mouse DISC1 expression was detected in A/WSN/33 (H1N1) infected brain region of a Rag1 knock-out mice in comparison with the non-infected animal (PBS control) (green-mDISC1, blue – DAPI,nuclear staining; red – Influenza A). Scale bars 10µm. (B) Luciferase reporter assay did not reveal an effect of influenza infection in the activity of DISC1 promotor region. NLF neuroblatoma cells were transiently transfected with pLG4.10- DISC1 promoter and 24 h after influenza infection a luciferase reporter assay was performed. Data presented as mean of replicates from three independent experiments ± SEM. Mann-Whitney U with one-tailed Dunn's *post hoc* test was used as a statistical test.

Fig S8. A/WS/33 (H1N1) infection does not affect the protein homeostasis of Tau neither TDP-43 *in vivo.* (A; C) Changes in tau expression were not visible in the Rag1 knock-out mice infected for 28 days with A/WSN/33 (H1N1) in comparison with non-infected PBS mice (blue –DAPI, nuclear staining, green -mTau, red – Influenza A). Scale bars 50, 10µm. (B; D) Similar levels of mouse TDP-43 was detected in A/WS/33 (H1N1) infected Rag1 knock-out mice and in the non-infected PBS animal (blue – DAPI, nuclear staining, green-mTDP-43, red – Influenza A. (E) A/WS/33 (H1N1) infected Rag1 knock-out mice co-stained for hemagglutinin Influenza A protein and secondary antibody only (blue –DAPI,

nuclear staining, green-Alexa 594, red – Influenza A). Scale bars 10μm. (F) Co-stained cells of A/WSN/33 (H1N1) infected Rag1 knock-out mice only with the secondary antibodies used in the immunostaining analysis (blue –DAPI, nuclear staining, green -Alexa 594, red – Alexa 488). Scale bars 10μm.

Fig S9. Influenza A virus (A/WS/33) segment 5 nucleocapsid protein induces lower DISC1 aggregation levels (A) NLF neuroblastoma cells were double transfected with human DISC1 and influenza virus segment 5 nucleocapsid, and a low number of DISC1 aggregates was visible in comparison with influenza infected condition (24 h, MOI 1). Non-infected cells did not show influenza induced aggregates. (green - mRFP-DISC1, Red – Influenza A; blue –DAPI, nuclear staining;). Scale bars 10μm. (B) Quantification of percentage of aggregated DISC1 per cell infected with A/WS/33 virus (MOI 1) and transfected with A/WS/33 nucleocapsid relative to the non-infected condition. Dark grey bar represents the non-infected condition, black bar represents A/WS/33 infected cells, and light grey represents A/WS/33 nucleocapsid transfected condition. Data presented as mean of replicates from three independent experiments ± SEM. Two-away ANOVA test was used as a statistical test (*P <0.05; n.s. non-statistical significance).

Fig S10. 24H of Influenza A virus (A/WS/33) infection lead to a decrease in the fusion of autophagosomes with the acidified proteolytic lysosomes. Immunostainings of autophagosome marker-LC3, and lysosomal marker -LAMP-1 showed a decrease in co-localization of LC3-LAMP1 in influenza infected LUHMES cells (24 h, MOI 1) in comparison with non-infected condition (blue –DAPI, nuclear staining, green – LC3, red -LAMP1). Scale bars 10μm.

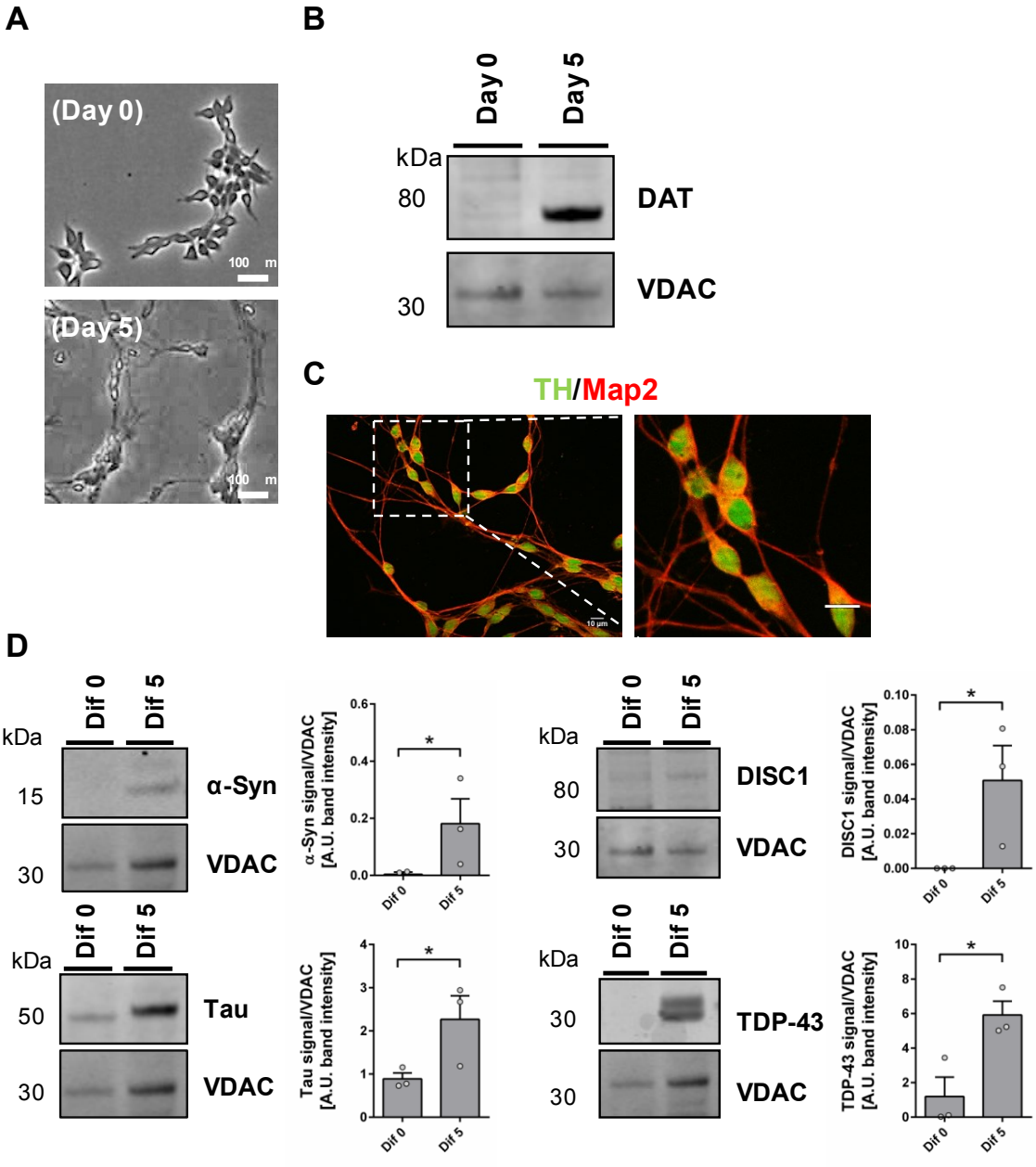
A
(Day 0)
100 m
(Day 5)
100 m
B
Day 0
Day 5
kDa
80
DAT
30
VDAC
C
TH/Map2
10 µm
D
Dif 0
Dif 5
kDa
15
α-Syn
30
VDAC
α-Syn signal/VDAC [A.U. band intensity]
0.6
0.4
0.2
0.0
*
Dif 0
Dif 5
kDa
80
DISC1
30
VDAC
DISC1 signal/VDAC [A.U. band intensity]
0.10
0.08
0.06
0.04
0.02
0.00
*
Dif 0
Dif 5
kDa
50
Tau
30
VDAC
Tau signal/VDAC [A.U. band intensity]
4
3
2
1
0
*
Dif 0
Dif 5
kDa
30
TDP-43
30
VDAC
TDP-43 signal/VDAC [A.U. band intensity]
10
8
6
4
2
0
*
Dif 0
Dif 5

Fig. S1

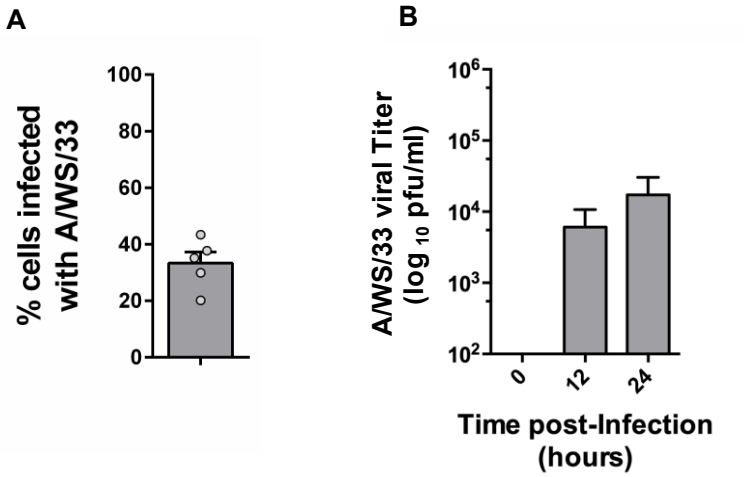
A
% cells infected with A/WS/33
100
80
60
40
20
0
B
A/WS/33 viral Titer (log 10 pfu/ml)
10^6
10^5
10^4
10^3
10^2
0
12
24
Time post-Infection (hours)

Fig. S2

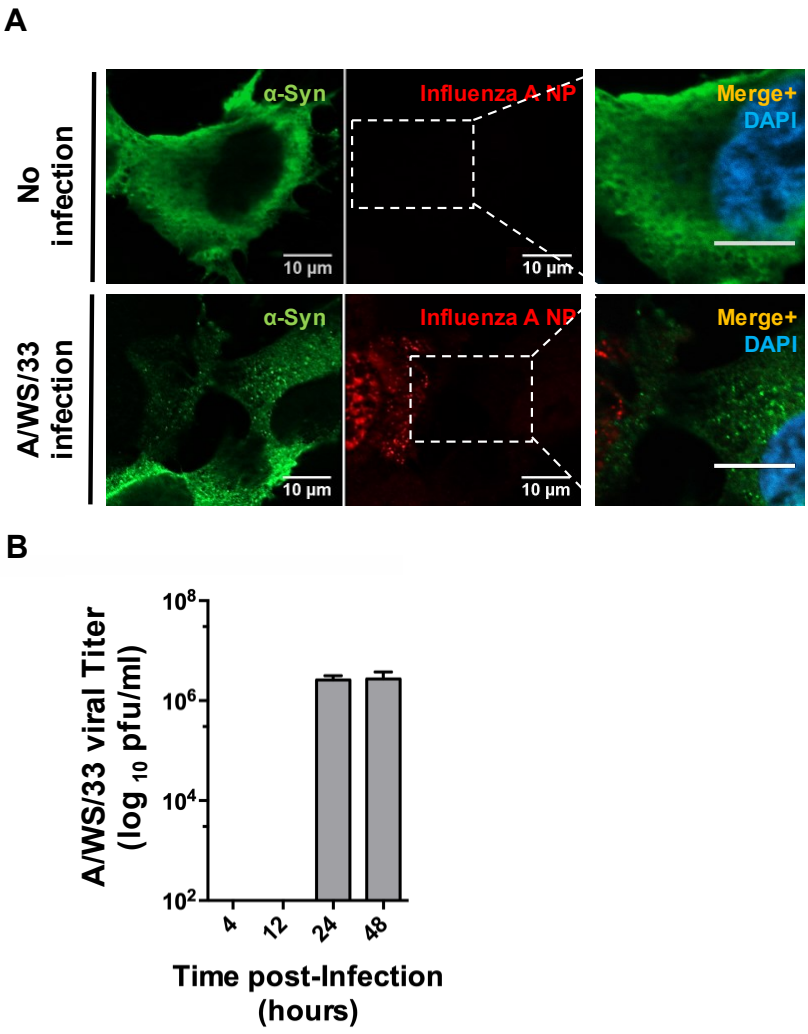
A
No infection
A/WS/33 infection
α-Syn
Influenza A NP
Merge+ DAPI
10 µm
B
A/WS/33 viral Titer (log 10 pfu/ml)
10^8
10^6
10^4
10^2
4
12
24
48
Time post-Infection (hours)

Fig. S3

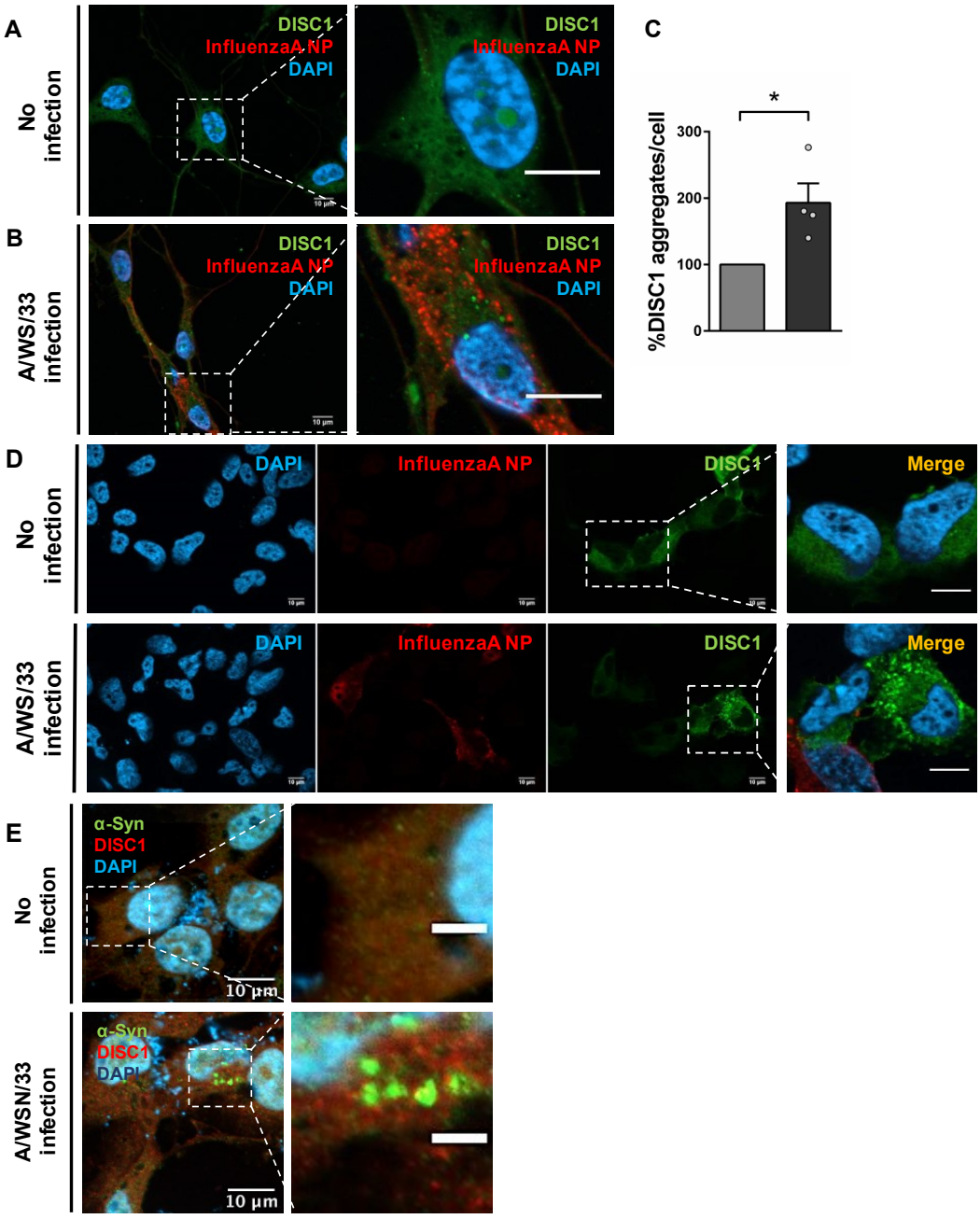
A
No infection
DISC1
InfluenzaA NP
DAPI
B
A/WS/33 infection
C
%DISC1 aggregates/cell
300
200
100
0
*
D
DAPI
InfluenzaA NP
DISC1
Merge
E
α-Syn
DISC1
DAPI
A/WSN/33 infection
10 µm

Fig. S4

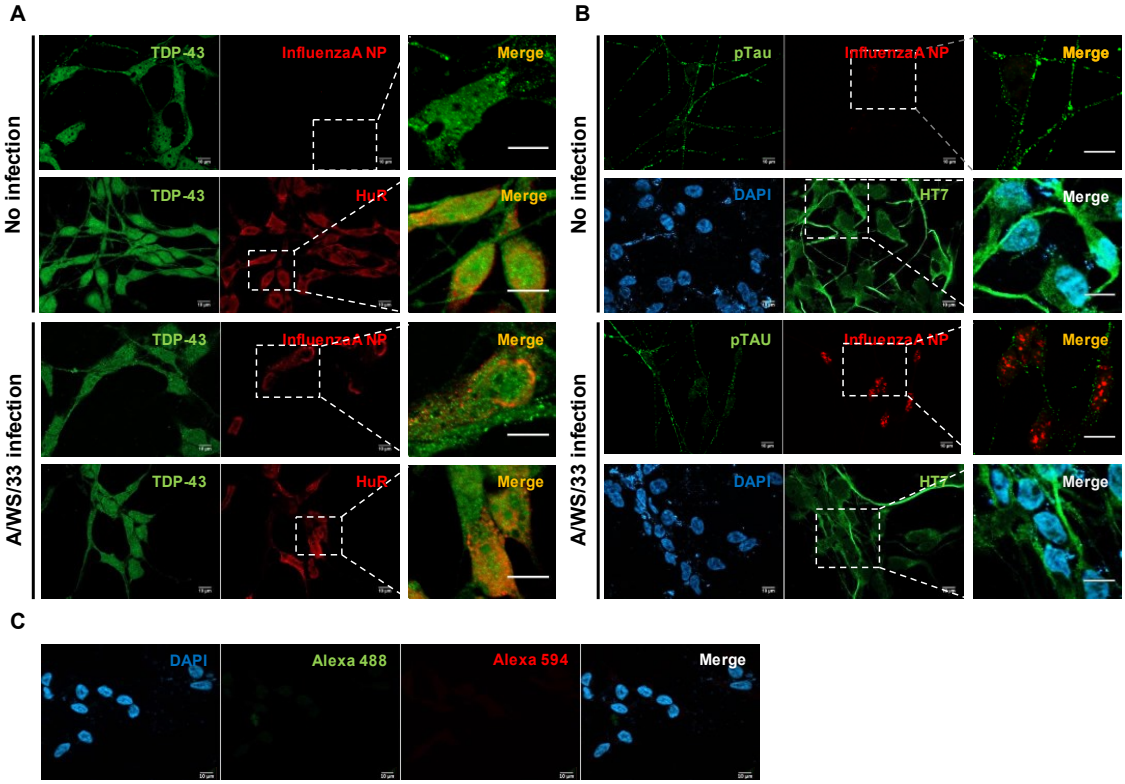
A
TDP-43
Influenza A NP
Merge
No infection
TDP-43
HuR
Merge
A/WS/33 infection
TDP-43
Influenza A NP
Merge
TDP-43
HuR
Merge
B
pTau
Influenza A NP
Merge
No infection
DAPI
HT7
Merge
A/WS/33 infection
pTAU
Influenza A NP
Merge
DAPI
HT7
Merge
C
DAPI
Alexa 488
Alexa 594
Merge

Fig. S5

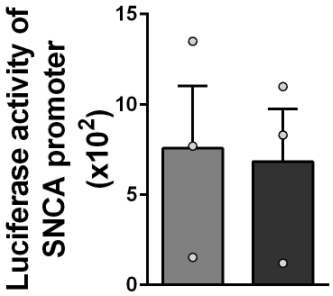
Luciferase activity of SNCA promoter (x10²)
15
10
5
0

Fig. S6

A

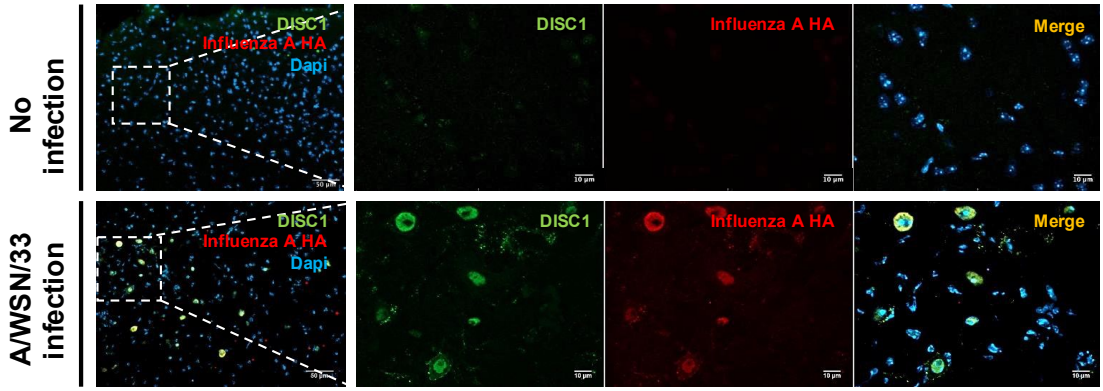
No infection
A/WSN/33 infection
DISC1
Influenza A HA
Dapi
DISC1
Influenza A HA
Merge

B

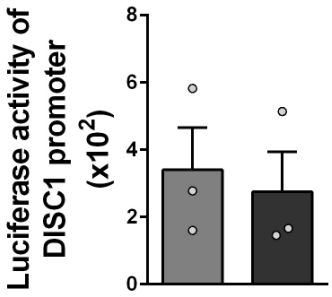
Luciferase activity of DISC1 promoter (x10²)
0
2
4
6
8

Fig. S7

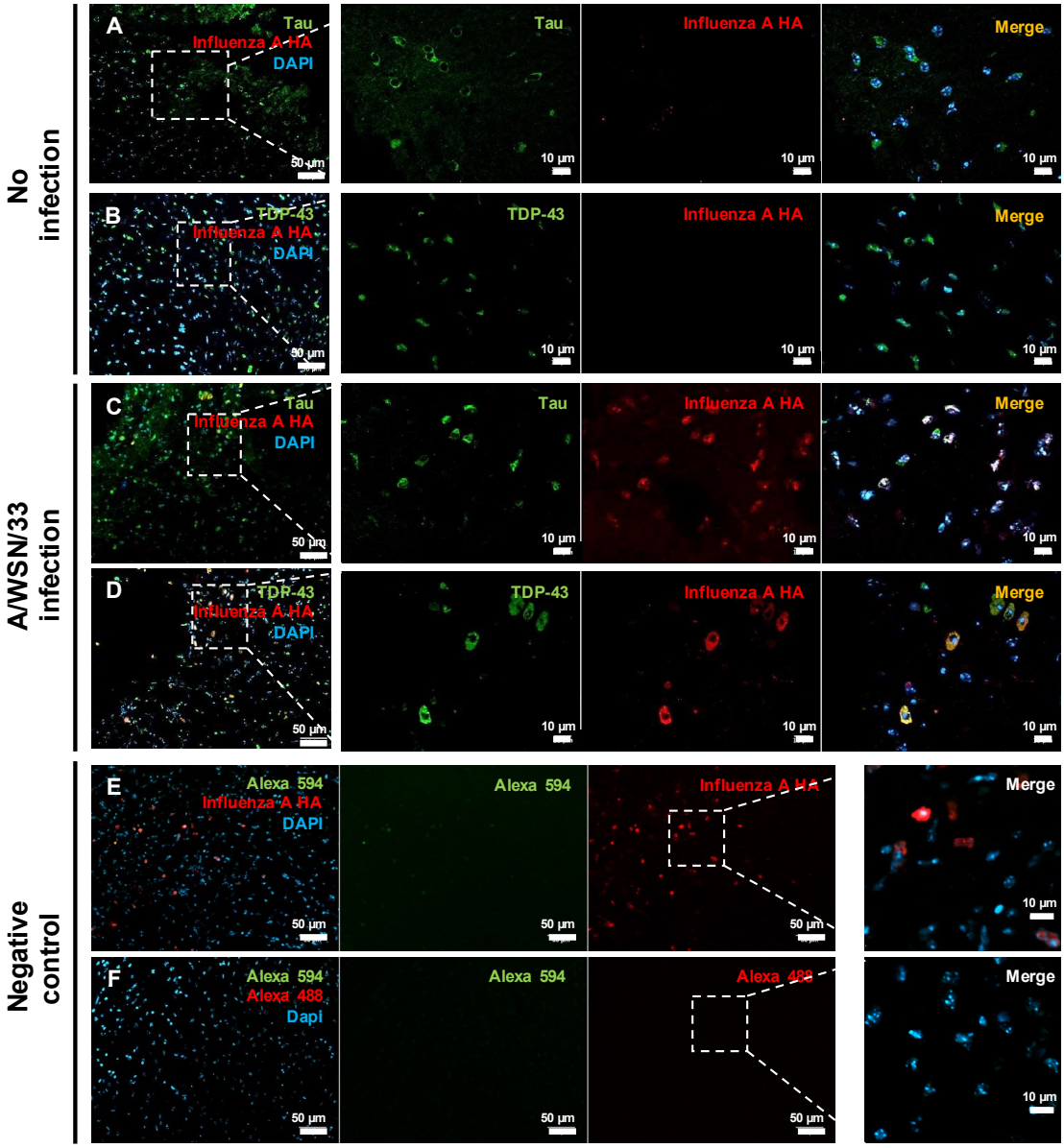
No infection
A/WSN/33 infection
Negative control
A
Tau
Influenza A HA
DAPI
50 µm
Tau
10 µm
Influenza A HA
10 µm
Merge
10 µm
B
TDP-43
Influenza A HA
DAPI
50 µm
TDP-43
10 µm
Influenza A HA
10 µm
Merge
10 µm
C
Tau
Influenza A HA
DAPI
50 µm
Tau
10 µm
Influenza A HA
10 µm
Merge
10 µm
D
TDP-43
Influenza A HA
DAPI
50 µm
TDP-43
10 µm
Influenza A HA
10 µm
Merge
10 µm
E
Alexa 594
Influenza A HA
DAPI
50 µm
Alexa 594
50 µm
Influenza A HA
50 µm
Merge
10 µm
F
Alexa 594
Alexa 488
Dapi
50 µm
Alexa 594
50 µm
Alexa 488
50 µm
Merge
10 µm

Fig. S8

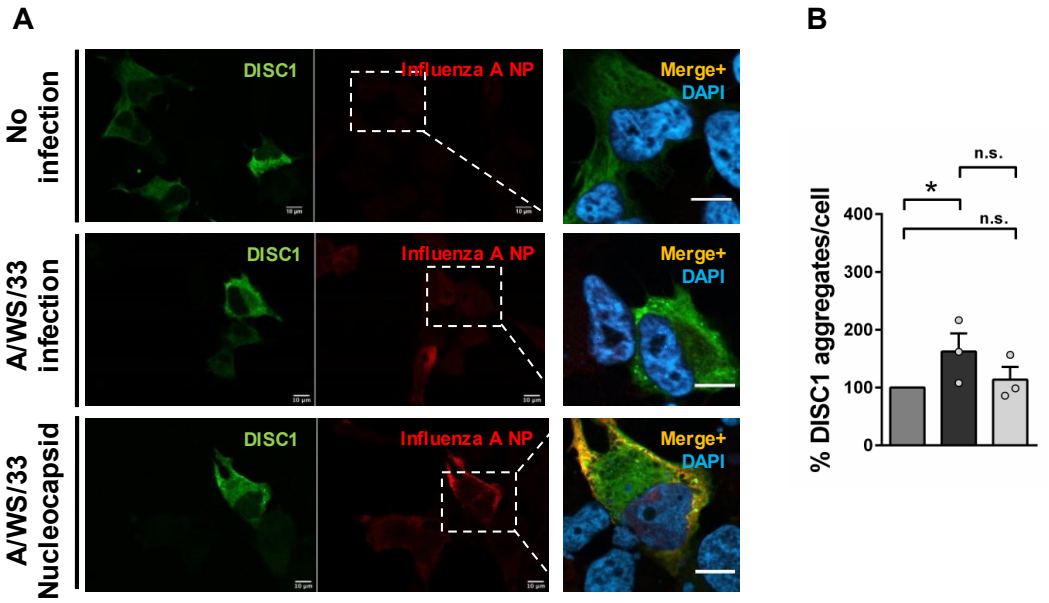

Fig. S9

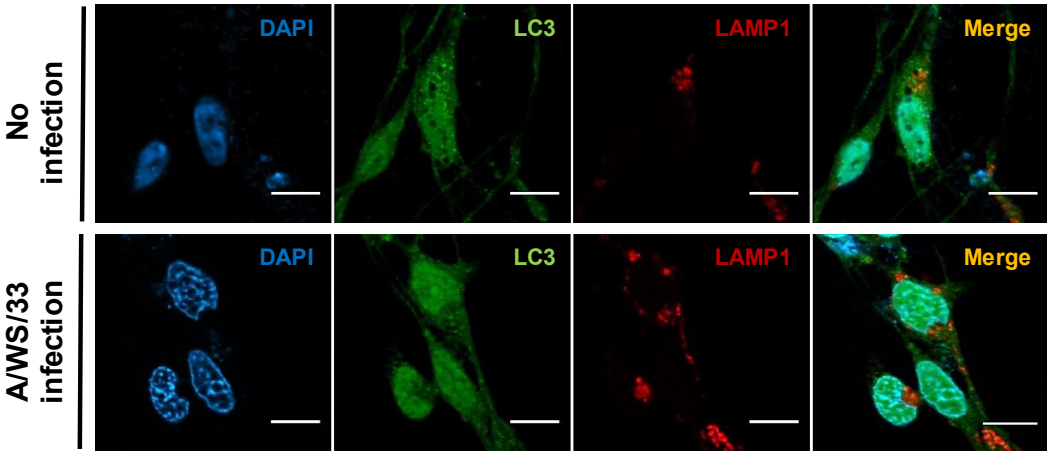

Fig. S10

Chapter 3

Accumulation of insoluble aggregates: a biological marker in sporadic mental illness patients

Functional proteomic analysis identifies insoluble GAD2 in a subset of sporadic mental illness patients

Rita Marreiros, Svenja V Trossbach, Ingrid Prikulis, Miguel Lozano, K.W. Li, Philip Ottis, David Just, Peter Nilsson, Vishal Sinha, William Hennah, Thomas M. Hyde, Joel E. Kleinman, August B. Smit, Carsten Korth

Manuscript in submission

Author's contribution (50%):

- Design of experimental setup
- Optimization of insoluble protein purification protocols in rodent models, including insoluble protein purification and immunoblot
- Purification of insoluble proteome from *post mortem* human brains
- Mass spectrometry data analysis
- Data analysis and validation
- Manuscript co- writing

In this study, we attempted to identify novel misfolded candidate proteins present in the insoluble proteome in *post mortem* brains of CMIs patients in a hypothesis-free manner in order to better define the pathophysiology of mental disorders. Following up on the efforts conducted in our laboratory to identify subsets of sporadic CMIs patients characterized by misassembled proteins, (186-189), but this time by using a hypothesis-free proteomic approach, we identified novel, insoluble proteins linked to CMIs.

The insoluble proteome of *post mortem* brains from two independent human cohorts (termed sMRI and LIBD), diagnosed with SCZ, recurrent affective disorders, and matched healthy controls was purified. We identified in the performed MS/MS analysis > 300 candidate proteins in sMRI, and > 180 candidate proteins in LIBD cohorts, associated with the pathology.

The singularity of this study was the identification of insoluble proteins exclusively present in disease conditions, and present in both human cohorts. Furthermore, selected candidate proteins could be validated by immunoblot in the insoluble proteome of individual patient samples. We subsequently focused on the identified GAD2, an enzyme involved in GABA synthesis by decarboxylation of glutamate to GABA and carbon dioxide, where insolubility

was strongly associated with a subset of CMIs patients. We further investigated the GAD2 tendency to aggregate using cellular models of overexpression. In a neuroblastoma cell line *in vitro* model, GAD2 showed an clear aggregation pattern, visualized by immunofluorescence without any external trigger factor. The insoluble GAD2 inclusions were also detected by biochemical purification.

This study which is currently prepared for submission for publication describes the insoluble proteome of CMIs patients, presenting specific biological signatures associated with psychiatric conditions that cross the clinical diagnostic boundaries. Ultimately, in the long term, the identification of the insoluble proteins associated with psychiatry conditions might lead to novel diagnostic procedures and generate novel therapeutic targets.

Functional proteomic analysis identifies insoluble GAD2 in a subset of sporadic mental illness patients

Rita Marreiros[a], Svenja V. Trossbach[a], Ingrid Prikulis[a], Miguel Lozano[b], K.W. Li[b], Philip Ottis[C], David Just[D], Peter Nilsson[D], Vishal Sinha[E], William Hennah[E], Thomas M. Hyde[F,G], Joel E. Kleinman [F], August B. Smit[b], Carsten Korth[a,1]

[a]Department Neuropathology, Heinrich Heine University Düsseldorf Medical School, Moorenstrasse 5, 40225 Düsseldorf, Germany; [b]Department of Molecular and Cellular Neurobiology, Center for Neurogenomics and Cognitive Research, Neuroscience Campus Amsterdam, VU University, The Netherlands; [c]Roche pharma research and early development, Basel, Switzerland; [D]Science for Life Laboratory, Division of Affinity Proteomics, Department of Protein Science, KTH - Royal Institute of Technology, Stockholm, Sweden; [E]Institute for Molecular Medicine Finland FIMM, University of Helsinki, Finland; Mental Health Unit, Department of Public Health Solutions, National Institute for Health and Welfare, Helsinki, Finland; [F]The Lieber Institute for Brain Development, Johns Hopkins University School of Medicine, Baltimore, United States of America; [G]Department of Psychiatry and Behavior Sciences, and Neurology, Johns Hopkins University School of Medicine, Johns Hopkins University Medical Campus, Baltimore, United States of America

Corresponding Author

[1]Carsten Korth, Department Neuropathology, Heinrich Heine University Düsseldorf Medical School, Moorenstrasse 5, 40225 Düsseldorf, Germany

Email: ckorth@hhu.de

Keywords

Chronic mental illness, protein aggregation, glutamate decarboxylase 2 (GAD2), GAD65

Abstract

Chronic mental illnesses (CMIs) are complex and devastating brain conditions without a clear biological origin or molecular pathway characterization. Disturbance in protein homeostasis, so-called proteostasis, resulting in protein misfolding and subsequent aggregation recently came into focus as one putative biochemical hallmark of chronic brain disorders. An aberrant proteostasis signature of candidate proteins has been shown to define biological subsets of CMI patients.

Here, we attempted to identify novel misfolded proteins present in the insoluble proteome of CMI patients, in order to identify such biological subsets associated. We could show that *post mortem* brain samples from two large independent cohorts of human brains, the Stanley Medical Research Institute (sMRI) and Lieber institute brain collection (LIBD), including patients with affective disorders and schizophrenia, exhibited a similar protein insolubility phenotype. By using a functional proteomics approach, we identified more than 300 proteins in sMRI and 180 in LIBD exclusively in the insoluble proteome of CMI patients. Sarcosyl-insoluble aggregates of glutamate decarboxylase 2 (GAD2) protein were found in a subset of CMI patients. By applying immunofluorescent and biochemical assays, GAD2 aggregation was reproduced in a cellular neuroblastoma model.

Our data shows that there is a specific biological signature of insoluble proteins in mental illness with misassembled GAD2 as a novel candidate protein associated with sporadic CMI, crossing the clinical diagnostic boundaries.

Introduction

Chronic mental illnesses (CMIs), such as schizophrenia, major depression, and bipolar disorder, are complex heterogeneous disorders with a strong genetic (familiar) and non-genetic (sporadic) component association. So far, the etiology of these diseases is still unknown with the diagnosis relying almost exclusively on subjective psychiatric interviews [1]. CMIs are polygenic conditions characterized mostly by genome-wide association studies (GWAS). So far, they failed in identifying a hit that explains the disease etiology [2] . As in other chronic brain diseases such as neurodegenerative disorders (NDs), most CMI cases are known not to be hereditable, thus involving non-genetic causes [3, 4]. However, it remains unclear which molecular pathways are responsible for the sporadic forms of the disorders. In analogy to the NDs, we rationalized that also in CMIs due to their chronic course, changes in the protein homeostasis would appear [5]. Misassembly of candidate proteins such as DISC1 [6], dysbindin-1 [7], CRMP1 [8], TRIOBP-1 [9], and NPAS3 [10] were previously considered as signatures for a subset of CMI patients crossing the clinical diagnosis boundaries.

In order to gain further insight into the molecular pathways involved in CMI, a liquid chromatography-tandem mass spectrometry (LC-MS/MS)–based proteomics approach was performed with the insoluble proteome of CMI patients. In the past years, mainly studies at the genomic level are being performed [11-13]. So far, counteracting to other chronic brain disorders such as NDs, there is only a published study performed in the insoluble proteome of *post mortem* schizophrenia brain samples. Nucifora *et al*. characterized a subgroup of schizophrenia patients based in an increased ratio of insoluble and ubiquitinated proteins in comparison with the healthy controls [14]. However, the singularity of our study was the identification of an insoluble proteome pattern containing aberrant proteins in CMIs patient brains from two independent *post mortem* human cohorts, and that crosses the clinical diagnostic.

Glutamate decarboxylase 2 (GAD2 or GAD65) was identified to be detergent-insoluble in a subset of CMI sporadic cases in both brain collections analyzed. Surprisingly, the paralogous GAD2 gene, glutamate decarboxylase 1 (GAD1 or GAD67), was not detected in our analyses.

In the adult brain, two isoforms of glutamate decarboxylase (GAD) enzyme are expressed and encoded by two independent regulated genes. They have a critical role in gamma-aminobutyric acid (GABA) synthesis by decarboxylation of glutamate to GABA and carbon dioxide [15]. However, they have distinct brain distributions and play a different functional role in the central nervous system [16, 17]. GAD2 is mainly present in the GABAergic synapses and associated with vesicles, being transiently activated in response to the high demanding of GABA during intense synaptic activity [17]. GAD1, on the other hand, is constitutively active, being distributed throughout the cytosol and contributing to the majority of GABA production levels [18].

Here, we demonstrated the presence of detergent-insoluble GAD2 in a subset of CMI patients from two large cohorts of independent *post mortem* human brain collections (100 samples from LIBD and 50 from sMRI). Using a neuroblastoma cell model, we could demonstrate that GAD2 but not GAD1 has a natural propensity to aggregate *in vitro*. An insoluble proteome list of chronic psychiatric disease-associated cases was generated and validated, using mass-spectrometry analysis as a tool.

This data might contribute to defining unique biological signatures of subsets of CMI patients, based on specific misassembled proteins.

Materials and Methods

***Post mortem* Human brain material.** *Post mortem* brain tissue of the Consortium Collection referred to as sMRI collection was obtained from the Stanley Medical Research Institute [19]. A total of 60 (Brodmann's area [BA] 6) frozen frontal cortex samples, n=15 healthy controls, n=15 schizophrenia, n=15 major depression, and n=15 bipolar patient samples were provided. In the case of LIBD collection, a total of 100 *post mortem* brain tissue samples were evaluated according to the respective clinical diagnosis: n=50 healthy controls, n=25 schizophrenia, and n=25 major depression patient samples were obtained from BA23 cingulate cortex [20].

Rodent brain samples. Brains from 3 months old male transgenic rats expressing human DISC1 [21] were extracted according to methods approved by the LANUV (State Agency for Nature, Environment and Consumer Protection), North Rhine-Westphalia, Germany. Brains from 6 months old male mice overexpressing the 383 aa form of human tau with a P301S mutation [22] were a gift from Dr. Michel Goedert (University of Cambridge, UK).

Insoluble protein fraction purification. For the insoluble proteome extraction via the high stringency protocol (Method 1), rodent brain samples were homogenized to 10% (w/v) in 50 mM HEPES pH7.5/250 mM sucrose/5 mM magnesium chloride/100 mM potassium acetate/2 mM PMSF containing a protease inhibitor cocktail and were lysed by the addition of Triton X-100 to a final concentration of 0.5% (v/v). The lysate was then centrifuged at 20,000 x *g* for 20 min. The pellet was resuspended in the same buffer (including Triton X-100) and centrifuged a second time. Then, the pellet was resuspended in a high sucrose buffer containing 50 mM HEPES pH 7.5/1.6 M sucrose/100 mM potassium acetate/1 mM PMSF/0.5% Triton X-100 and ultracentrifuged at 130,000 x g for 45 min. This step was repeated a second time. The pellet was

resuspended in a high salt buffer containing 50 mM HEPES pH7.5/1 M sodium chloride/20 mM magnesium chloride/30 mM calcium chloride plus 40 units/ml DNase I and a protease inhibitor cocktail. The solution was then incubated at 4 °C for 16 hours on a rotary wheel and afterwards ultracentrifuged at 130,000 x g for 45 min. The pellet was resuspended again in the high salt buffer (minus the DNaseI) and ultracentrifuged at 130,000 g for 45 min. In the next step, the pellet was resuspended in a sarkosyl buffer with 50 mM HEPES pH7.5/0.5% sarcosyl and ultracentrifuged at 130,000 x g for 45 min. This was repeated and the final pellet subjected to TCA protein precipitation. This entire procedure, including centrifugation steps, was done at 4 °C and is adapted and optimized from one of our previously published protocols [6].

The insoluble proteome of rodent brains and *post mortem* human brain samples extracted with the low stringency protocol (Method 3) were homogenized to 10% or 5% (w/v) in 50 mM HEPES pH7.5/250 mM sucrose/5 mM magnesium chloride/100 mM potassium acetate/2 mM PMSF containing protease inhibitor cocktail. Homogenates were lysed by the addition of sucrose buffer (in a 2:1 homogenate to sucrose buffer ratio): 50 mM HEPES pH 7.5/250mM sucrose/20 mM magnesium chloride/100mM potassium acetate/2mM PMSF/3% NP-40/0.6% sarcosyl/15 mM glutathione/120 units/ml DNase I, containing protease inhibitor cocktail. Lysis was performed for 16h at 4 °C on a rotary wheel. The following high sucrose / sarcosyl buffer was applied in a 5:4 homogenate to buffer ratio: 50 mM HEPES p H7.5/2.3 M sucrose/5 mM glutathione/1 mM PMSF/1% NP-40/0.2% sarcosyl. The homogenate was then ultracentrifuged at 100,000 x *g* for 45 min. The pellet was resuspended in 50 mM HEPES pH 7.5/1.6 M sucrose/5 mM glutathione/1 mM PMSF/1% NP-40/0.2% sarcosyl and ultracentrifuged at 100,000 x *g* for 45 min. Pellet was resuspended with a high salt buffer containing 50 mM HEPES pH 7.5/1.5M NaCl/5 mM glutathione and ultracentrifuged at 100,000 x g for 45 min. Pellet was resuspended with a sarcosyl buffer (50 mM HEPES pH 7.5/250 mM sucrose/5 mM glutathione/1% NP-40/0.2% sarcosyl) and ultracentrifuged at 100,000 x g for 45 min. The final pellets from the rodent brain samples were subjected to TCA protein precipitation. In the case of the extracted *post mortem*

human brain samples, the insoluble fraction was solubilized in a dissolution buffer containing 5 M Triethylaminbicarbonat/ 8 M urea/ 1% SDS/ 10 mM Tris (2-carboxyethyl) phosphine hydrochloride. This entire procedure, including centrifugation steps, was done at 0-4 °C and is adapted and optimized from one of our previously published protocols [23]. Insoluble proteome purification for neuroblastoma cells (NLF) was performed using the previously described low stringency protocol.

TCA protein precipitation. Proteins present in last pellet fraction were precipitated with a 25% solution of 2,2,2-trichloroacetic acid (TCA) and incubated on ice for 30 min. The eluates were centrifuged at 22,000 x *g* for 15 min at 4°C and the resulting pellets were washed 2x with cold acetone. The resulting insoluble pellets were air-dried and solubilized in 2x SDS-loading buffer containing 2% β-mercaptoethanol.

Liquid chromatography-mass spectrometry (LC-MS) analysis. The sample preparation and mass spectrometry analysis were performed as described previously [24]. The proteins were separated on a 10% SDS polyacrylamide gel, fixed overnight (50% ethanol/ 3% phosphoric acid) and stained with colloidal Coomassie Brilliant Blue G (Sigma-Aldrich). Each sample lane was split into two fractions and cut into small fragments. The gel pieces went through two subsequent destaining cycles with 50% acetonitrile in 50 mM ammonium bicarbonate, dehydration in 100% acetonitrile and rehydration with 50 mM ammonium bicarbonate. After the second dehydration, the fragments were digested with Trypsin/Lys-C Mix solution (Promega) in 50 mM ammonium bicarbonate overnight in a humid chamber at 37°C. Peptides were extracted twice with 150µL 50% and 80% acetonitrile in 0.1% TFA and dried in a speedvac.

Peptides were re-dissolved in 2% acetonitrile/ 0.1% formic acid solution and injected into the Ultimate 3000 LC system. A 5 mm C18 PepMap 100 column was used to trap the peptides for 5 min before its separation on a homemade 200 mm C18 Alltima column at a flow rate of 5 µL/min. The acetonitrile concentration was linearly increased from 5 to 22% in 88 min, to 25% at 98 min, to 40% at 108 min and to 95% in 2 min. The peptides were electro-sprayed (at 5500 V) into the TripleTOF 5600 MS (Sciex) operated in data-dependent mode. A single MS full scan was acquired (m/z 350−1250, 200 msec) followed by the top 20 most abundant precursors MS/MS (m/z 200-1800, 100 msec) at high sensitivity mode in LOW resolution (precursor ion > 100 counts/s, charge state from +2 to +5). CID spread energy was set to 15eV and the exclusion time window to 16 sec. The data were analyzed using MaxQuant software (1.5.2.8) with default settings [25]. Label-free quantification (LFQ) was enabled with an LFQ min. ratio count of 1.

Proteins described in the insoluble proteome list were categorized according to LFQ or Intensity Based Absolute Quantification (iBAQ) values (description in the figure legend).

Immunoblot. For total homogenates and TCA precipitated fractions, 10 µg/ml of each sample dissolved in NuPAGE LDS Sample Buffer (4X plus 8% β-mercaptoethanol) were applied to the gel. For the insoluble fractions, 15 µl of solubilized pellet in NuPAGE LDS Sample Buffer (4X, plus 8% β-mercaptoethanol) was applied to the gel. Novex NuPAGE SDS-PAGE Gel System (Thermo Fisher Scientific) with the corresponding NuPAGE Novex 4–12% Bis-Tris Midi Protein Gels, NuPAGE MES SDS Running buffer was used. Proteins were transferred to a nitrocellulose membrane and then blocked with 5% nonfat milk in PBS containing 0.05% Tween-20, for 1h at RT. Western blot analysis was performed with the correspondent antibodies described and followed by a secondary species-specific antibody (IR Dye 680 or 800; LICOR Corp.). The membrane was scanned using the LI-COR Odyssey CLX. Band intensities were calculated from

the fluorescent signal using the Image Studio Version 2.1 software (LI-COR Biosciences). Total protein in acrylamide gels was visualized using InstantBlue (Expedeon, Swavesey, UK).

Cell culture and immunocytochemistry. The human neuroblastoma cells (SH-SY5Y and NLF) were obtained mycoplasma-free from the DSMZ (Leibniz Institute DSMZ-German Collection of Microorganisms and Cell Cultures, Braunschweig, Germany). NLF cells used in sequential biochemical fractionation were seeded in a 6-well plate format with a cell density of 5 x 10^5 cells/well. Twenty-four hours later, cells were transfected with Metafectene (Biontex) according to manufacturer's instructions in Opti-MEM reduced serum media (Invitrogen) for 24h, and then the transfection medium was replaced for RPMI medium (Invitrogen) supplemented with 10% (v/v) FBS (Invitrogen), 1% (v/v) L-glutamine (Invitrogen) and 1% (v/v) PenStrep (Invitrogen) for another 24h. The insoluble protein purification was performed as described in the 'Insoluble protein fraction purification' section. SH-SY5Y cells used in the immunofluorescence analysis were seeded onto 13mm glass coverslips with a density of 5 x 10^4 cells/well. Twenty-four hours later, pLHCX-GAD1 or pLHCX-GAD2 transfection was performed using Lipofectamine (Lipofectamine 2000) according to manufacturer's instructions in Opti-MEM reduced serum media (Invitrogen) for 24h, and then the transfection medium was replaced for DMEM:F12 medium (Invitrogen) supplemented with 10% (v/v) FBS (Invitrogen), 1% (v/v) MEM Non-Essential Amino Acids (Invitrogen) and 1% (v/v) PenStrep (Invitrogen) for 48h. For immunocytochemistry analysis, cells were washed three times with PBS (Invitrogen) and fixed with cold 4% (v/v) PFA in PBS for 10 min, followed for one washing step with PBS. Fixed cells were permeabilized and blocked by adding 0.5% (v/v) Saponin (Sigma), 5% (v/v) nonfat milk, 1% BSA (Sigma) in PBS for 1h at room temperature (RT). Cells were incubated at 4°C for 16h with GAD2 or GAD1 antibody (1:500; both mouse), washed 3x for 5 min with PBS and subsequent AlexaFluor 488 secondary antibody (1:500; Invitrogen) for 1 h in PBS. Cells were

mounted with ProLong Gold with DAPI (Invitrogen), and images collected with the 63x oil objective of a Zeiss Axiovision Apotome.2 confocal microscope (Zeiss).

Quantitative real-time PCR. For the quantitative real-time PCR the mRNA expression levels of human GAD2 were measured in *post mortem* RNA samples, obtained from the sMRI Array Collection, resulting in a final n = 8 healthy control subjects, and n = 13 CMI patients. Fragment Analyzer (Advanced Analytical Technologies, Thermo Fisher, USA) was used to test the RNA integrity and only samples with RNA Quality Number (RQN) > 8 were used for the analysis. The StepOnePlus Real-Time PCR System (Applied Biosystems, Carlsbad, CA, USA), the Platinum SYBR Green qPCR SuperMix-UDG mix (Invitrogen, Carlsbad, CA, USA), and MicroAMP Fast Optical 96-Well plates (Applied Biosystems, Carlsbad, CA, USA) were used for the qPCR: 10 min at 95°C, 40 cycles of 15 s at 95 °C and 60°C for 1 min. The data analysis was performed with the StepOne Software v2.3 (Thermo Fisher Scientific, Waltham, MA, USA) and GAD2 expression was normalized to the expression level of ARF1 gene. The primer sequence used to detect hGAD2 were forward primer: 5'-TGCTCTTCCCAGGCTCATTG-3' and reverse primer: 5'-GGCACTCACGAGGAAAGGAA-3'. For normalization, primers targeting the housekeeping gene ARF1 were designed: forward primer: 5'-GACCACGATCCTCTACAAGC-3' and reverse primer: 5'-TCCCACACAGTGAAGCTGTG-3'.

Antibodies. Commercial antibodies were used against actin (#A2066, Sigma-Aldrich, Munich, Germany), total tau protein (HT7# MN1000, Invitrogen), phosphorylated tau (AT8 # MN1020, Invitrogen), glutamate decarboxylase 2 (GAD65 #26113, abcam) and glutamate decarboxylase 1 (GAD1 #26116, abcam). The following described antibodies were obtained from Human Atlas antibodies (www.proteinatlas.org): ALDH4A1 (HPA006401), CLIC4 (HPA060804), GAD2 (HPA044637), HSP90B1 (HPA049856), MAP2K1 (HPA026430), TRIM23 (HPA039605).

Data Analysis. Data alignment, filtering, and characterization were initially performed in Microsoft Excel by manual filtering. In the second stage, the data were independently analyzed using the FunRich_V3.1.3 software [26].

Results

Low stringency protocol, an effective procedure to isolate the insoluble proteome from brain tissue

In order to generate an insoluble proteome list from clinically diagnosed CMIs patients, two previously published protocols [6, 23] to purify insoluble proteins from brain tissue were tested. The methodology used consists of a sequential biochemical fractionation of brain homogenate, which will be referred to as the high and low stringency protocol and mainly differ in the buffer components and centrifugation speeds (Figure 1A, see Materials and Methods). The protocols were validated using brain material from two distinct transgenic rodent lines, 3 month old DISC1 transgenic rats (tgDISC1) and 6 month old TauP301S mice, previously described as models for aggregate-related disorders [21, 22]. In a biochemical context, they are well-suited models for this approach, since tgDISC1 rats modestly overexpressing non-mutant full-length human DISC1 exhibit insoluble perinuclear aggregates, that mimic the DISC1 protein misassembly found in CMI patients [6]. In the case of TauP301S, the P301S mutation in the human tau gene leads to neurofibrillary tangle-like inclusions with the presence of sarkosyl-insoluble tau and hyperphosphorylated tau, associated with frontotemporal lobar degeneration (FTLD) cases [27].

The high stringency protocol, which was developed to enhance specificity, detects exclusively unfolded insoluble proteins such as DISC1, but not actin that is known to exist as insoluble but still folded fibrous F-actin (Figure 1B). Surprisingly, phosphorylated and insoluble tau was barely detected using this procedure (Figure 1C). Unlike high stringency, in the low stringency protocol that was developed to enhance sensitivity both, insoluble DISC1 and phosphorylated tau proteins were enriched in the sarkosyl-resistant pellet to a comparable extent (Figure 1B-C). Considering that in the high stringency protocol the amount of lost protein during the sequential fractionation was higher (Figure S1A), as well the methodology variability, we pursued with the low-stringency-protocol for the insoluble proteome extraction in *post mortem* human brains.

Next, we determined the amount of starting brain material required. Taken the supply of human brain tissue and the potential procedure variability between fractionations into consideration, 200 μl with 10% (w/v) of brain homogenate was chosen to be used as starting material (Figure S1B).

Functional proteomic analysis generates a unique insoluble proteome profile of CMI patients from two independent post mortem human brain collections

In order to advance our research in defining CMI subsets by insoluble proteome signatures, we investigated pooled insoluble proteins of CMI patients from two distinct human cohorts. Sequential biochemical fractionation using the previously described low stringency protocol (see Figure 1A) was performed individually for each biological sample. The sMRI Consortium collection contained frozen brain tissue from the frontal cortex (BA6) of 60 diagnosed *post mortem* cases (*n* = 15 for schizophrenia, major depression, bipolar disorder, and healthy controls). For LIBD collection, frozen brain pieces from the cingulate cortex (BA23) of 100 diagnosed *post mortem* cases, with (*n* = 25 for schizophrenia and major depression, *n* = 50 healthy controls) were used (see Table 1 for demographic information of both collections). For both analyzed collections, brain samples were matched for age, sex, brain pH, and *post mortem* time (PMI). The gender distribution in healthy control cases is significantly distinct between collections (Table 1). With an exception for the brain pH, that was significant higher in the healthy control and schizophrenic cases in LIBD cohort, there was no significant difference in analyzed parameters between collections (see Table 1). For the LC-MS/MS analysis, the insoluble proteome fractions were pooled according to the respective clinical diagnoses. We assessed the global insoluble proteome of ~ 1,600 proteins of the sMRI collection, with 364 being exclusively present in CMI patient samples (Figure S2A) and ~ 900 proteins of the LIBD collection, with 183 being solely present in CMI samples (Figure S2B). The overlapping proteins found to be aggregated in both collections underwent further analysis.

Glutamate decarboxylase 2 (GAD2) was found as the principal insoluble candidate protein in a subset of CMI patients.

There is considerable overlap in the symptomology and genetic background of psychiatric disorders such as schizophrenia, bipolar disorder, and major depression [28], even though they are considered to be distinct disorders in the clinic. In our approach to biologically define subsets of CMI patients by their insoluble protein signature we chose as the main analysis criterion that proteins must be present in CMI conditions (schizophrenia, bipolar disorder, or major depression) and absent in the healthy controls. A total of 18 proteins were identified in the insoluble proteome of CMI patients in both collections (Table 2). Surprisingly, in our LC-MS/MS analysis GAD2 protein, encoded by the *GAD2* gene and an essential element in the control of GABA synthesis, was identified to be insoluble in the patient samples diagnosed with bipolar disorder and schizophrenia but not in the major depression condition (Table 2). A higher immunoreactivity against GAD2 in the sarkosyl-insoluble fraction of a subset of CMI patients was observed in comparison to healthy controls (Figure 2A). The ratio of insoluble GAD2 with respect to the total GAD2 present in the starting material, also confirmed the high GAD2 insolubility in a subgroup of CMI condition in comparison to the healthy controls (Figure 2B). However, changes in GAD2 total protein levels were not detected (Figure 2A). In order to avoid false positive insoluble protein candidates, samples from 12 patients were excluded from the validation study as they exhibited unspecific immunoreactivity to all antibody tested (see red marks in Figure 2A; Figure S3). Six major depression cases showed GAD2 immunoreactivity signal in the immunoblot but not detected by mass spectrometry (MS) analysis. In those cases, we assume that the insoluble GAD2 levels might be below the detection limit of MS technique. Typically, as a drawback of this approach, highly abundant proteins with similar isoelectric point and molecular weight mask the identification of less abundant proteins. In order to exclude a possible variation in GAD2 mRNA levels, a quantitative real-time PCR (qPCR) was performed on the sMRI Array Collection, a separate collection of CMI brain RNA. No changes were

detected in the expression of GAD2 in CMI patients in comparison to healthy controls (1.0 ± 0.10 vs 1.2 ± 0.08) (Figure S4). Interestingly, the paralogue gene *GAD1,* also involved in the control of GABA synthesis and previously associated with increased risk for schizophrenia [29-31], was not detected in the insoluble proteome of CMI patients in our LC-MS/MS analysis. This data demonstrated the presence of a well-described regulatory target of cell activity - GAD2 - in the insoluble proteome of a subset of CMI patients, independently of a previous clinical diagnosis.

The chaperone protein endoplasmin encoded by the *HSP90B1* gene has a role in stabilization and protein folding. Even though it was detected also in the control samples, CMI cases exhibited higher endoplasmin immunoreactivity in insoluble fraction in comparison to healthy controls (11.0 ± 2.17 vs 7.7 ± 0.66; $p < 0.0001$) (Figure S5).

Our data confirms our assumption of an aberrant protein homeostasis signature in CMIs and furthermore suggests the existence of a biological overlapped between the distinct psychiatric conditions.

Glutamate decarboxylase 2 (GAD2) shows an aggregation pattern in an in vitro cell model

To further elucidate the consequence of GAD2 insolubility for the cell, we investigated whether the full-length form of GAD2 was also insoluble in an *in vitro* context. The human neuroblastoma cell line SH-SY5Y was transiently transfected with GAD2 and after 48 hours changes in GAD2 solubility were analyzed by immunocytochemistry (Figure 3A). GAD2 showed a strong aggregation tendency in the cytoplasm of transfected SH-SY5Y cells (Figure 3A). In order to exclude a false positive result, SH-SY5Y cells were in parallel transiently transfected with the control GAD1 protein and no aggregated GAD1 structures in SH-SY5Y cells were detected (Figure 3B). Insoluble GAD2 species were also analyzed in a biochemical context. GAD2 detergent-insoluble aggregates were purified from transfected SH-SY5Y cells, using the low

stringency protocol, and the total and pellet fractions were immunoblotted (Figure 3C). We observed a GAD2 enrichment in the sarkosyl-insoluble fraction that was relatively higher in comparison with the detected levels for the control protein GAD1 (Figure 3C).

The data presented here suggest a propensity of GAD2 to aggregate *in vitro*, in contrast to GAD1, strengthening our previous observations in *post mortem* human brains.

Quantitative analysis of the insoluble proteome of CMI patients

Next, as a second analysis criterion, we investigated overlapping candidate proteins of both human brain cohorts showing an increased fold change in CMI patients in comparison to healthy controls. Twenty-nine proteins were identified in schizophrenia and major depression conditions (Figure S6A).

Identified candidate proteins were validated by immunoblot analysis of sarkosyl-insoluble pellets and homogenate from each case of the 60 fractionated sMRI brain samples. In an unbiased screening, EHD3 and MAP2K1 proteins were selected to be validated. A subset of *post mortem* major depression cases exhibited EHD3 (Figure S6) and MAP2K1 (Figure S6) immunoreactivity in the insoluble fraction. However, there was no detected increased in the signal intensity, for any of proteins tested, neither for major depression or schizophrenia cases compared to healthy controls (Figure S6B-C). These data suggest that although we identified EHD3 and MAP2K1 by MS analysis, we would need higher patient numbers for confirmation.

Discussion

The in-depth analysis of proteins that are present in the insoluble proteome of *post mortem* human brains of patients with chronic brain disorders is a promising strategy to characterize and identify differential protein aggregation profiles associated with disease conditions. In our study, we provide proof-of-concept by applying this strategy to identify, an insoluble proteome profile of chronic psychiatric disorders, such as schizophrenia, bipolar disorder and depression. When the insoluble proteome of CMI patients was analyzed from a large cohort of two independent *post mortem* human brain collections, we identified insoluble GAD2 in a subset of sporadic cases of the disorders, crossing the clinical diagnoses. The GAD2 aggregation phenotype could be reproduced *in vitro*, demonstrating an intrinsically tendency of this protein to aggregate.

Proteins are essential components for the normal cell function, and highly susceptible to changes in their homeostasis [32]. Neurodegenerative disorders are the best reflection of protein homeostasis disruption forming misfolded proteins that form aggregates of various sizes and in distinct subcellular compartments [33]. More subtle protein misassembly without visible deposits in the brain were found to be associated with CMI conditions [5]. In our study, the insoluble proteome from *post mortem* human brain samples of CMI patients and healthy controls were isolated by sequential biochemical fractionation. Two purification protocols were tested to understand which methodology is the most suitable to efficiently isolate the insoluble proteome (Figure 1A; Figure S1). The defined low stringency protocol detects not only aggregated unfolded proteins, such as DISC1 and tau but also actin which is insoluble due to its formation of high molecular weight but still correctly folded F-actin fibers (Figure 1B-C). This protocol was initially developed as a more sensitive method to identify aging-related insoluble proteins in rodents [23]. In comparison, the described high stringency protocol that was previously developed to isolate sarkosyl-resistant DISC1 [6], did not purify F-actin (Figure 1B-C). Curiously, with this procedure tau protein was barely detected in the sarkosyl-insoluble fraction (Figure 1C). It has been well described in the

literature that insoluble protein isolation efficiency is directly correlated with the biophysical characteristics of the intended protein. An example of that is the optimized variation of a standard sarkosyl-based protocol published recently. They could purify only the pathological insoluble inclusions of TDP-43 from Amyotrophic lateral sclerosis (ALS) and FTLD patient brains [34]. Intracellular aggregates of insoluble tau protein, a hallmark of Alzheimer disease (AD) [35], are frequently purified by formic acid extraction which also detects actin in the insoluble fraction [36]. That data is in concordance with our results for the low stringency protocol purification, where insoluble and phosphorylated tau as well as actin was detected in the insoluble fraction. The use of this procedure allowed us a more sensitive and extensive detection of insoluble protein complexes.

The present study aimed to define a biological signature of the insoluble proteome of CMI patients by using functional proteomic analysis to generate an insoluble proteome profile in CMI. Many decades of research in psychiatry illness mainly based on genetic studies, produced an extensive and conflicting database of candidate gene association. An elucidative example of that are the GWAS studies, arguing that the inadequate statistical power is the primary reason for the failure of moving forward in psychiatry research [37]. Parallel to other chronic brain disorders such as AD, where common variants in genes involved in Aβ processing are not highlighted by GWAS studies [38], also in CMI identification of biological subsets of patients might be beneficial. Based on the analysis of misfolded proteins we might be able to better understand the pathophysiology of these disorders [5] or if biological subsets thereof, possibly crossing the restricted purely clinical categorization of mental disorders. In order to do so and as an uniqueness of our approach, in this study only the overlapping insoluble proteins detected in both human brain cohorts were considered. Twenty-nine candidate proteins were observed to have a fold change increase in their insolubility in schizophrenia and major depression patients combined in comparison to healthy controls (Figure S6). Interestingly, there were no insoluble candidates identified in both collections, when the single clinical diagnoses were considered

individually. It makes us raise the point that disruption of protein homeostasis, leading to misassembled or aggregated proteins might be the overlapped molecular event across psychiatric conditions. It is in concordance with our previous publications, where aggregation of DISC1 [6], dysbidin-1 [7], and CRMP1 [8] was found in a subset of patients across different psychiatric diagnoses. In concordance with our findings, a recent study by Nucifora et al. [14], also using an MS approach to identify aggregated proteins in *post mortem* brain samples of schizophrenia patients, described an association of high protein insolubility and protein ubiquitination in a patient subset. The identified proteins, mainly being associated with nervous system development and axon target recognition, were grouped according to their functionality predicted by bioinformatics tools. However, no single insoluble candidate was further investigated in their study [14].

From the insoluble proteome list generated here, eighteen insoluble proteins were identified to be overlapping in both human brain samples of CMI patients and absent in healthy control samples (Table 2). GAD2 protein, preferentially present in presynaptic terminals and responsible for GABA synthesis for vesicle release [39] was found to be present in the insoluble proteome of schizophrenia and bipolar samples (Table 2; Figure 2). GAD2 also seems to have a natural tendency to form aggregates, as it was seen in our *in vitro* experiments, in contrast to the paralogous protein GAD1 (Figure 3). So far, only genetic variations in GAD1 were consistently associated with CMIs, mainly in schizophrenia [29-42]. Histopathological impairments in the GABAergic system are associated with the cognitive dysfunction observed in schizophrenia patients [43]. An overall reduction in GABAergic activity seems to be the most plausible scenario in the disease: it has been suggested an initial presynaptic reduction of GABA synthesis [44, 45], followed by a compensatory reduction in the reuptake by the presynaptic protein transporter GAT-1 [46, 47] and consequent upregulation of postsynaptic GABA receptors [48]. However, it is still not clear the crucial initial factor in the pathological cascade, which lead to GABAergic neurotransmission changes related to the disease. Previous research in *post mortem* human

brains did not reveal a consistent association of GAD2 [39, 45, 46] with changes in Schizophrenia [49, 50]. A recent study showed a decreased expression of GAD2 full-length transcript in the prefrontal cortex of Schizophrenia and bipolar patients, while a truncated form of this gene was shown to be increased in bipolar and decreased in Schizophrenia patients [51]. Despite the lack of consistency in the literature showing a positive association of GAD2 with CMI, we hypothesize that specific environmental challenges might lead to a protein homeostasis disruption and GAD2 misassembly. One possible explanation could be an intrinsic vulnerability of specific neuronal subpopulations to external stressors [52]. A further investigation into the molecular mechanism underlying GAD2 protein insolubility and the physiological consequence of this phenomenon for brain connectivity is necessary. It was also previously described that the absence of the *GAD2* gene did not lead to a lethal phenotype. GAD2 knock-out (KO) mice appear to be healthy and do not exhibit apparent morphological brain abnormalities [53]. In this mouse, also in concordance with a phenotypic characteristic of SCZ patients, deficits in the prepulse inhibition test were observed [54].

Similarly to other aggregated proteins [55], we hypothesize a gain of toxic function by misfolded GAD2 as a possible explanation of CMI pathology in the identified patient subset. In concordance with this thought, i.e. in tau KO mice models [59, 60] a lack of neurodegenerative phenotype was also observed, supporting the hypothesis that aggregation of tau protein associated with AD and FTLD pathology is a consequence of a gain-of-toxic protein function [58]. A similar mechanism is being proposed for aggregated superoxide dismutase 1 (SOD1), found as a hallmark of SOD1-familial ALS [59, 60] In a mouse model of overexpressed SOD1, a SOD1 aggregation and motor neuronal toxicity as seen in ALS patients [61], whereas SOD1-KO mice presents a lack of ALS-like phenotype [62].

Taken together, our results demonstrated an association of insoluble GAD2 with sporadic cases of CMI, which might be a biological signature for a new subset of patients. By presenting an

insoluble proteome list generated by functional proteomic analysis, a set of novel insoluble candidate proteins was provided that could establish unique biological signatures for CMIs (Table 2; Figure S6A). Notably, as it was shown here, *post mortem* tissue analysis represents a valuable resource to investigate the pathophysiology of psychiatric disorders.

Nonetheless, there are limitations that may affect the outcome of *post mortem* measurements [63, 64]. There are many factors commonly described that affect the tissue quality, since brain tissue integrity is particularly sensitive to the manner of death or the process of obtaining and stabilizing samples [65, 66, 67]. For our study, the brain material was obtained from well characterized human brain collections [19, 20]. The factors that might affect the outcome of *post mortem* measurements were carefully considered without a relevant variability in pH and PMI, between individuals. Despite this, a difference in PMI time was observed in healthy and schizophrenia patients between collections.

In past years, proteomic approaches have also been applied to blood, plasma, or serum from psychiatric patients [68]. In other disorders, such as AD, proteomic approaches using peripheral material are being extensively used, to identify new biomarkers and better monitor the disease progression in patients [69-72]. As a next step, we suggest validating our findings in a different set of biological samples

Here, applying a proteomic approach to two independent human brain cohorts, we identified a proteome profile of misassembled proteins in sporadic cases of psychiatry disorders.

Further exploration of the consequence of certain protein misfolding for the brain might help in understanding the molecular pathways underlying psychiatric disorders to improve the diagnosis and generate novel therapeutic targets.

References

1. Tandon R, Gaebel W, Barch DM, Bustillo J, Gur RE, Heckers S *et al.* Definition and description of schizophrenia in the DSM-5. *Schizophr Res* 2013; **150**(1)**:** 3-10.
2. Sullivan PF, Daly MJ, O'Donovan M. Genetic architectures of psychiatric disorders: the emerging picture and its implications. *Nat Rev Genet* 2012; **13**(8)**:** 537-551.
3. Xu B, Roos JL, Levy S, van Rensburg EJ, Gogos JA, Karayiorgou M. Strong association of de novo copy number mutations with sporadic schizophrenia. *Nat Genet* 2008; **40**(7)**:** 880-885.
4. Pardinas AF, Holmans P, Pocklington AJ, Escott-Price V, Ripke S, Carrera N *et al.* Common schizophrenia alleles are enriched in mutation-intolerant genes and in regions under strong background selection. *Nat Genet* 2018; **50**(3)**:** 381-389.
5. Bradshaw NJ, Korth C. Protein misassembly and aggregation as potential convergence points for non-genetic causes of chronic mental illness. *Mol Psychiatry* 2018.
6. Leliveld SR, Bader V, Hendriks P, Prikulis I, Sajnani G, Requena JR *et al.* Insolubility of disrupted-in-schizophrenia 1 disrupts oligomer-dependent interactions with nuclear distribution element 1 and is associated with sporadic mental disease. *J Neurosci* 2008; **28**(15)**:** 3839-3845.
7. Ottis P, Bader V, Trossbach SV, Kretzschmar H, Michel M, Leliveld SR *et al.* Convergence of two independent mental disease genes on the protein level: recruitment of dysbindin to cell-invasive disrupted-in-schizophrenia 1 aggresomes. *Biol Psychiatry* 2011; **70**(7)**:** 604-610.
8. Bader V, Tomppo L, Trossbach SV, Bradshaw NJ, Prikulis I, Leliveld SR *et al.* Proteomic, genomic and translational approaches identify CRMP1 for a role in schizophrenia and its underlying traits. *Hum Mol Genet* 2012; **21**(20)**:** 4406-4418.
9. Bradshaw NJ, Bader V, Prikulis I, Lueking A, Mullner S, Korth C. Aggregation of the protein TRIOBP-1 and its potential relevance to schizophrenia. *PLoS One* 2014; **9**(10)**:** e111196.
10. Nucifora LG, Wu YC, Lee BJ, Sha L, Margolis RL, Ross CA *et al.* A Mutation in NPAS3 That Segregates with Schizophrenia in a Small Family Leads to Protein Aggregation. *Mol Neuropsychiatry* 2016; **2**(3)**:** 133-144.
11. Ramaker RC, Bowling KM, Lasseigne BN, Hagenauer MH, Hardigan AA, Davis NS *et al.* Post-mortem molecular profiling of three psychiatric disorders. *Genome Med* 2017; **9**(1)**:** 72.
12. Duan J, Goring HHH, Sanders AR, Moy W, Freda J, Drigalenko EI *et al.* Transcriptomic signatures of schizophrenia revealed by dopamine perturbation in an ex vivo model. *Transl Psychiatry* 2018; **8**(1)**:** 158.

13. Sanders AR, Drigalenko EI, Duan J, Moy W, Freda J, Goring HHH *et al.* Transcriptome sequencing study implicates immune-related genes differentially expressed in schizophrenia: new data and a meta-analysis. *Transl Psychiatry* 2017; **7**(4)**:** e1093.

14. Nucifora LG, MacDonald ML, Lee BJ, Peters ME, Norris AL, Orsburn BC *et al.* Increased Protein Insolubility in Brains From a Subset of Patients With Schizophrenia. *Am J Psychiatry* 2019**:** appiajp201918070864.

15. Kaufman DL, McGinnis JF, Krieger NR, Tobin AJ. Brain glutamate decarboxylase cloned in lambda gt-11: fusion protein produces gamma-aminobutyric acid. *Science* 1986; **232**(4754)**:** 1138-1140.

16. Esclapez M, Tillakaratne NJ, Tobin AJ, Houser CR. Comparative localization of mRNAs encoding two forms of glutamic acid decarboxylase with nonradioactive in situ hybridization methods. *J Comp Neurol* 1993; **331**(3)**:** 339-362.

17. Nakamura A, Osonoi T, Terauchi Y. Relationship between urinary sodium excretion and pioglitazone-induced edema. *J Diabetes Investig* 2010; **1**(5)**:** 208-211.

18. Asada H, Kawamura Y, Maruyama K, Kume H, Ding RG, Kanbara N *et al.* Cleft palate and decreased brain gamma-aminobutyric acid in mice lacking the 67-kDa isoform of glutamic acid decarboxylase. *Proc Natl Acad Sci U S A* 1997; **94**(12)**:** 6496-6499.

19. Torrey EF, Webster M, Knable M, Johnston N, Yolken RH. The stanley foundation brain collection and neuropathology consortium. *Schizophr Res* 2000; **44**(2)**:** 151-155.

20. Lipska BK, Deep-Soboslay A, Weickert CS, Hyde TM, Martin CE, Herman MM *et al.* Critical factors in gene expression in postmortem human brain: Focus on studies in schizophrenia. *Biol Psychiatry* 2006; **60**(6)**:** 650-658.

21. Trossbach SV, Bader V, Hecher L, Pum ME, Masoud ST, Prikulis I *et al.* Misassembly of full-length Disrupted-in-Schizophrenia 1 protein is linked to altered dopamine homeostasis and behavioral deficits. *Mol Psychiatry* 2016; **21**(11)**:** 1561-1572.

22. Allen B, Ingram E, Takao M, Smith MJ, Jakes R, Virdee K *et al.* Abundant tau filaments and nonapoptotic neurodegeneration in transgenic mice expressing human P301S tau protein. *J Neurosci* 2002; **22**(21)**:** 9340-9351.

23. Ottis P, Topic B, Loos M, Li KW, de Souza A, Schulz D *et al.* Aging-induced proteostatic changes in the rat hippocampus identify ARP3, NEB2 and BRAG2 as a molecular circuitry for cognitive impairment. *PLoS One* 2013; **8**(9)**:** e75112.

24. Pandya NJ, Koopmans F, Slotman JA, Paliukhovich I, Houtsmuller AB, Smit AB *et al.* Correlation profiling of brain sub-cellular proteomes reveals co-assembly of synaptic proteins and subcellular distribution. *Sci Rep* 2017; **7**(1)**:** 12107.

25. Cox J, Mann M. MaxQuant enables high peptide identification rates, individualized p.p.b.-range mass accuracies and proteome-wide protein quantification. *Nat Biotechnol* 2008; **26**(12)**:** 1367-1372.

26. Pathan M, Keerthikumar S, Chisanga D, Alessandro R, Ang CS, Askenase P *et al.* A novel community driven software for functional enrichment analysis of extracellular vesicles data. *J Extracell Vesicles* 2017; **6**(1)**:** 1321455.

27. Bugiani O, Murrell JR, Giaccone G, Hasegawa M, Ghigo G, Tabaton M *et al.* Frontotemporal dementia and corticobasal degeneration in a family with a P301S mutation in tau. *J Neuropathol Exp Neurol* 1999; **58**(6)**:** 667-677.

28. Cardno AG, Owen MJ. Genetic relationships between schizophrenia, bipolar disorder, and schizoaffective disorder. *Schizophr Bull* 2014; **40**(3)**:** 504-515.

29. Straub RE, Lipska BK, Egan MF, Goldberg TE, Callicott JH, Mayhew MB *et al.* Allelic variation in GAD1 (GAD67) is associated with schizophrenia and influences cortical function and gene expression. *Mol Psychiatry* 2007; **12**(9)**:** 854-869.

30. Magri C, Giacopuzzi E, La Via L, Bonini D, Ravasio V, Elhussiny MEA *et al.* A novel homozygous mutation in GAD1 gene described in a schizophrenic patient impairs activity and dimerization of GAD67 enzyme. *Sci Rep* 2018; **8**(1)**:** 15470.

31. Akbarian S, Huang HS. Molecular and cellular mechanisms of altered GAD1/GAD67 expression in schizophrenia and related disorders. *Brain Res Rev* 2006; **52**(2)**:** 293-304.

32. Balchin D, Hayer-Hartl M, Hartl FU. In vivo aspects of protein folding and quality control. *Science* 2016; **353**(6294)**:** aac4354.

33. Taylor JP, Hardy J, Fischbeck KH. Toxic proteins in neurodegenerative disease. *Science* 2002; **296**(5575)**:** 1991-1995.

34. Laferriere F, Maniecka Z, Perez-Berlanga M, Hruska-Plochan M, Gilhespy L, Hock EM *et al.* TDP-43 extracted from frontotemporal lobar degeneration subject brains displays distinct aggregate assemblies and neurotoxic effects reflecting disease progression rates. *Nat Neurosci* 2019; **22**(1)**:** 65-77.

35. Grundke-Iqbal I, Iqbal K, Tung YC, Quinlan M, Wisniewski HM, Binder LI. Abnormal phosphorylation of the microtubule-associated protein tau (tau) in Alzheimer cytoskeletal pathology. *Proc Natl Acad Sci U S A* 1986; **83**(13)**:** 4913-4917.

36. Scholtzova H, Chianchiano P, Pan J, Sun Y, Goni F, Mehta PD *et al.* Amyloid beta and Tau Alzheimer's disease related pathology is reduced by Toll-like receptor 9 stimulation. *Acta Neuropathol Commun* 2014; **2:** 101.

37. Farrell MS, Werge T, Sklar P, Owen MJ, Ophoff RA, O'Donovan MC *et al.* Evaluating historical candidate genes for schizophrenia. *Mol Psychiatry* 2015; **20**(5)**:** 555-562.

38. Bertram L, Lill CM, Tanzi RE. The genetics of Alzheimer disease: back to the future. *Neuron* 2010; **68**(2)**:** 270-281.

39. Tian N, Petersen C, Kash S, Baekkeskov S, Copenhagen D, Nicoll R. The role of the synthetic enzyme GAD65 in the control of neuronal gamma-aminobutyric acid release. *Proc Natl Acad Sci U S A* 1999; **96**(22)**:** 12911-12916.

40. Addington AM, Gornick M, Duckworth J, Sporn A, Gogtay N, Bobb A *et al.* GAD1 (2q31.1), which encodes glutamic acid decarboxylase (GAD67), is associated with childhood-onset schizophrenia and cortical gray matter volume loss. *Mol Psychiatry* 2005; **10**(6)**:** 581-588.

41. Du J, Duan S, Wang H, Chen W, Zhao X, Zhang A *et al.* Comprehensive analysis of polymorphisms throughout GAD1 gene: a family-based association study in schizophrenia. *J Neural Transm (Vienna)* 2008; **115**(3)**:** 513-519.

42. Tao R, Davis KN, Li C, Shin JH, Gao Y, Jaffe AE *et al.* GAD1 alternative transcripts and DNA methylation in human prefrontal cortex and hippocampus in brain development, schizophrenia. *Mol Psychiatry* 2018; **23**(6)**:** 1496-1505.

43. Menzies L, Ooi C, Kamath S, Suckling J, McKenna P, Fletcher P *et al.* Effects of gamma-aminobutyric acid-modulating drugs on working memory and brain function in patients with schizophrenia. *Arch Gen Psychiatry* 2007; **64**(2)**:** 156-167.

44. Lewis DA, Hashimoto T, Volk DW. Cortical inhibitory neurons and schizophrenia. *Nat Rev Neurosci* 2005; **6**(4)**:** 312-324.

45. Guidotti A, Auta J, Davis JM, Dong E, Grayson DR, Veldic M *et al.* GABAergic dysfunction in schizophrenia: new treatment strategies on the horizon. *Psychopharmacology (Berl)* 2005; **180**(2)**:** 191-205.

46. Woo TU, Whitehead RE, Melchitzky DS, Lewis DA. A subclass of prefrontal gamma-aminobutyric acid axon terminals are selectively altered in schizophrenia. *Proc Natl Acad Sci U S A* 1998; **95**(9)**:** 5341-5346.

47. Woo TU, Kim AM, Viscidi E. Disease-specific alterations in glutamatergic neurotransmission on inhibitory interneurons in the prefrontal cortex in schizophrenia. *Brain Res* 2008; **1218:** 267-277.

48. Ishikawa M, Mizukami K, Iwakiri M, Asada T. Immunohistochemical and immunoblot analysis of gamma-aminobutyric acid B receptor in the prefrontal cortex of subjects with schizophrenia and bipolar disorder. *Neurosci Lett* 2005; **383**(3)**:** 272-277.

49. Dracheva S, Elhakem SL, McGurk SR, Davis KL, Haroutunian V. GAD67 and GAD65 mRNA and protein expression in cerebrocortical regions of elderly patients with schizophrenia. *J Neurosci Res* 2004; **76**(4)**:** 581-592.

50. Hashimoto T, Bazmi HH, Mirnics K, Wu Q, Sampson AR, Lewis DA. Conserved regional patterns of GABA-related transcript expression in the neocortex of subjects with schizophrenia. *Am J Psychiatry* 2008; **165**(4)**:** 479-489.

51. Davis KN, Tao R, Li C, Gao Y, Gondre-Lewis MC, Lipska BK *et al.* GAD2 Alternative Transcripts in the Human Prefrontal Cortex, and in Schizophrenia and Affective Disorders. *PLoS One* 2016; **11**(2)**:** e0148558.

52. Saxena S, Caroni P. Selective neuronal vulnerability in neurodegenerative diseases: from stressor thresholds to degeneration. *Neuron* 2011; **71**(1)**:** 35-48.

53. Asada H, Kawamura Y, Maruyama K, Kume H, Ding R, Ji FY *et al.* Mice lacking the 65 kDa isoform of glutamic acid decarboxylase (GAD65) maintain normal levels of GAD67 and GABA in their brains but are susceptible to seizures. *Biochem Biophys Res Commun* 1996; **229**(3)**:** 891-895.

54. Heldt SA, Green A, Ressler KJ. Prepulse inhibition deficits in GAD65 knockout mice and the effect of antipsychotic treatment. *Neuropsychopharmacology* 2004; **29**(9)**:** 1610-1619.

55. Winklhofer KF, Tatzelt J, Haass C. The two faces of protein misfolding: gain- and loss-of-function in neurodegenerative diseases. *EMBO J* 2008; **27**(2)**:** 336-349.

56. Dawson HN, Ferreira A, Eyster MV, Ghoshal N, Binder LI, Vitek MP. Inhibition of neuronal maturation in primary hippocampal neurons from tau deficient mice. *J Cell Sci* 2001; **114**(Pt 6)**:** 1179-1187.

57. Harada A, Oguchi K, Okabe S, Kuno J, Terada S, Ohshima T *et al.* Altered microtubule organization in small-calibre axons of mice lacking tau protein. *Nature* 1994; **369**(6480)**:** 488-491.

58. Trojanowski JQ, Lee VM. Pathological tau: a loss of normal function or a gain in toxicity? *Nat Neurosci* 2005; **8**(9)**:** 1136-1137.

59. Jonsson PA, Bergemalm D, Andersen PM, Gredal O, Brannstrom T, Marklund SL. Inclusions of amyotrophic lateral sclerosis-linked superoxide dismutase in ventral horns, liver, and kidney. *Ann Neurol* 2008; **63**(5)**:** 671-675.

60. Jonsson PA, Ernhill K, Andersen PM, Bergemalm D, Brannstrom T, Gredal O *et al.* Minute quantities of misfolded mutant superoxide dismutase-1 cause amyotrophic lateral sclerosis. *Brain* 2004; **127**(Pt 1)**:** 73-88.

61. Bruijn LI, Houseweart MK, Kato S, Anderson KL, Anderson SD, Ohama E *et al.* Aggregation and motor neuron toxicity of an ALS-linked SOD1 mutant independent from wild-type SOD1. *Science* 1998; **281**(5384)**:** 1851-1854.

62. Reaume AG, Elliott JL, Hoffman EK, Kowall NW, Ferrante RJ, Siwek DF *et al.* Motor neurons in Cu/Zn superoxide dismutase-deficient mice develop normally but exhibit enhanced cell death after axonal injury. *Nat Genet* 1996; **13**(1)**:** 43-47.

63. Stan AD, Ghose S, Gao XM, Roberts RC, Lewis-Amezcua K, Hatanpaa KJ *et al.* Human postmortem tissue: what quality markers matter? *Brain Res* 2006; **1123**(1)**:** 1-11.

64. Meador-Woodruff JH, Watson SJ. Postmortem studies in schizophrenic brain. *J Psychiatr Res* 1997; **31**(2)**:** 157-158.

65. Lewis DA. The human brain revisited: opportunities and challenges in postmortem studies of psychiatric disorders. *Neuropsychopharmacology* 2002; **26**(2)**:** 143-154.

66. Blair JA, Wang C, Hernandez D, Siedlak SL, Rodgers MS, Achar RK *et al.* Individual Case Analysis of Postmortem Interval Time on Brain Tissue Preservation. *PLoS One* 2016; **11**(3)**:** e0151615.

67. Li J, Gould TD, Yuan P, Manji HK, Chen G. Post-mortem interval effects on the phosphorylation of signaling proteins. *Neuropsychopharmacology* 2003; **28**(6)**:** 1017-1025.

68. Comes AL, Papiol S, Mueller T, Geyer PE, Mann M, Schulze TG. Proteomics for blood biomarker exploration of severe mental illness: pitfalls of the past and potential for the future. *Transl Psychiatry* 2018; **8**(1)**:** 160.

69. Guntert A, Campbell J, Saleem M, O'Brien DP, Thompson AJ, Byers HL *et al.* Plasma gelsolin is decreased and correlates with rate of decline in Alzheimer's disease. *J Alzheimers Dis* 2010; **21**(2)**:** 585-596.

70. Hye A, Lynham S, Thambisetty M, Causevic M, Campbell J, Byers HL *et al.* Proteome-based plasma biomarkers for Alzheimer's disease. *Brain* 2006; **129**(Pt 11)**:** 3042-3050.

71. Kitamura Y, Usami R, Ichihara S, Kida H, Satoh M, Tomimoto H *et al.* Plasma protein profiling for potential biomarkers in the early diagnosis of Alzheimer's disease. *Neurol Res* 2017; **39**(3)**:** 231-238.

72. Ashton NJ, Leuzy A, Lim YM, Troakes C, Hortobagyi T, Hoglund K *et al.* Increased plasma neurofilament light chain concentration correlates with severity of post-mortem neurofibrillary tangle pathology and neurodegeneration. *Acta Neuropathol Commun* 2019; **7**(1)**:** 5

Acknowledgments

This research was funded by grants from EU-FP7 MC-ITN IN-SENS (#.60671), a grant from the Forschungskommission of the Medical Faculty of the Heinrich Heine University Düsseldorf (#9772651), and a grant from the BMBF (01GQ1422A;REMOVAGE).

Conflict of interest statement

All authors declare **no conflict of interest** with the presented research.

Figure Legends

Figure 1. Sequential biochemical fractionation procedure used to purify the insoluble protein fraction of brain tissue. (a) Schematic representation of method 1 and method 3, defined as high and low stringency protocols respectively, were optimized to purify the insoluble protein fraction from brain material. Samples were homogenized and solubilized with specific buffers before a double or a single centrifugation step to separate supernatant and pellet fractions. Full detail information can be found in the material and methods section. (b) Biochemical analysis of homogenate and pellet (insoluble) fractions derived from 3 months old DISC1 transgenic rat brain demonstrated aggregated DISC1 for both purification protocols. F-actin is only detectable using low stringency protocol. (c) Corresponding immunoblot for tau and F-actin purified from brain material of 6 months old TauP301S mice. Phosphorylated tau (pTau - at positions Ser202, Thr205), total-Tau (tTau), and F-actin were only detectable with low stringency protocol. In the results shown in b, c, DISC1 and tau insoluble fractions were enriched relative to the whole homogenate signal (high stringency protocol: 6.67-fold, low stringency: 10-fold). One out of the three independent experiments is shown.

Figure 2. Insoluble GAD2 is detected across distinct chronic mental illness conditions independent of clinical diagnosis. (a) Immunoblots for hGAD2 of sarcosyl-insoluble pellets (top panel) and total homogenate (bottom panel) of 60 individual cases from the sMRI collection with a differential clinical diagnosis of schizophrenia (S), bipolar disorder (B), major depression (D) and healthy controls (C) are shown. Each lane corresponds to an independent biological sample. The marked red samples were excluded from the analysis due to unspecific immunoreactivity signal against different antibodies tested. Asterisks indicate immunoreactivity above threshold (defined as the mean immunoreactivity for healthy controls) in the insoluble pellet fraction. (b) Scatter plot of insoluble GAD2 signal in chronic mental illness (CMI) (n=34)

cases versus healthy controls (n=14) [4.7 ± 0.87 vs 2.8 ± 0.55; p < 0.0787]. The ratio of western blot intensity signal of the insoluble fraction by the total homogenate, normalized to the loading control actin (data not showed) is shown. Unpaired t-test with two-tailed Welch's correction was used as a statistical test (**P < 0.01), means ±SEM.

Figure 3. GAD2 aggregates in an *in vitro* neuroblastoma cell model. Immunocytochemistry of SH SY5Y neuroblastoma cells transiently transfected with (a) full-length form of human GAD2 (pLHCX-hGAD2), showing cytoplasmic aggregates (green- hGAD2; blue –DAPI, nuclear staining) and (b) full-length form of human GAD1 (pLHCX-hGAD1) that did not show aggregated structures (green- hGAD1, blue –DAPI, nuclear staining). Scale bars 10μm. (c) Representative immunoblot of total (Top panel) and insoluble (bottom panel) levels of hGAD2 and hGAD1 transiently transfected into NLF neuroblastoma cells. Quantification of band intensity of insoluble by total levels are shown (n=2 ± SEM).

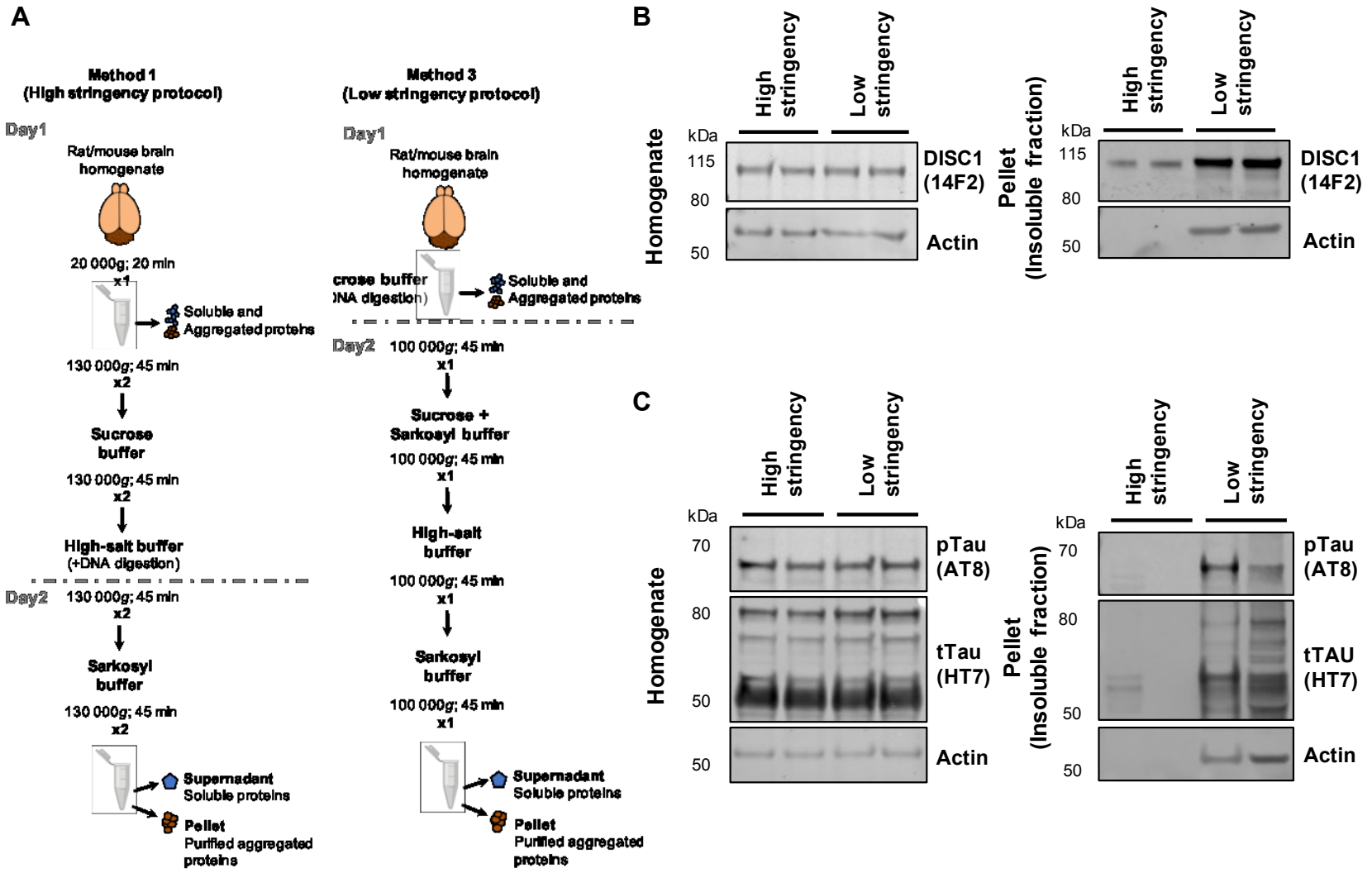
A
Method 1
(High stringency protocol)
Day1
Rat/mouse brain homogenate
20 000g; 20 min
x1
Soluble and Aggregated proteins
130 000g; 45 min
x2
Sucrose buffer
130 000g; 45 min
x2
High-salt buffer
(+DNA digestion)
Day2
130 000g; 45 min
x2
Sarkosyl buffer
130 000g; 45 min
x2
Supernadant
Soluble proteins
Pellet
Purified aggregated proteins
Method 3
(Low stringency protocol)
Day1
Rat/mouse brain homogenate
Soluble and Aggregated proteins
Day2
100 000g; 45 min
x1
Sucrose + Sarkosyl buffer
100 000g; 45 min
x1
High-salt buffer
100 000g; 45 min
x1
Sarkosyl buffer
100 000g; 45 min
x1
Supernadant
Soluble proteins
Pellet
Purified aggregated proteins
B
High stringency
Low stringency
Homogenate
kDa
115
80
50
DISC1 (14F2)
Actin
Pellet (Insoluble fraction)
C
70
pTau (AT8)
tTau (HT7)
tTAU (HT7)

Figure 1

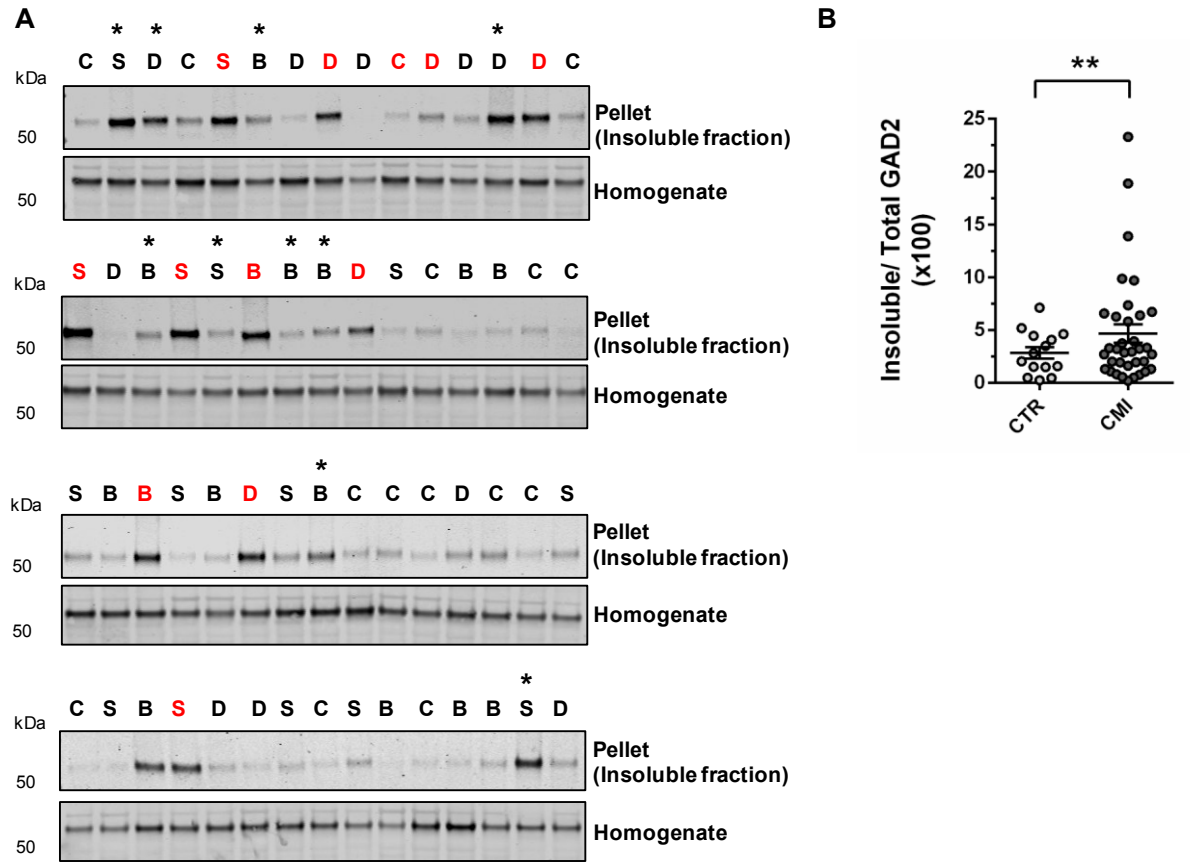

Figure 2

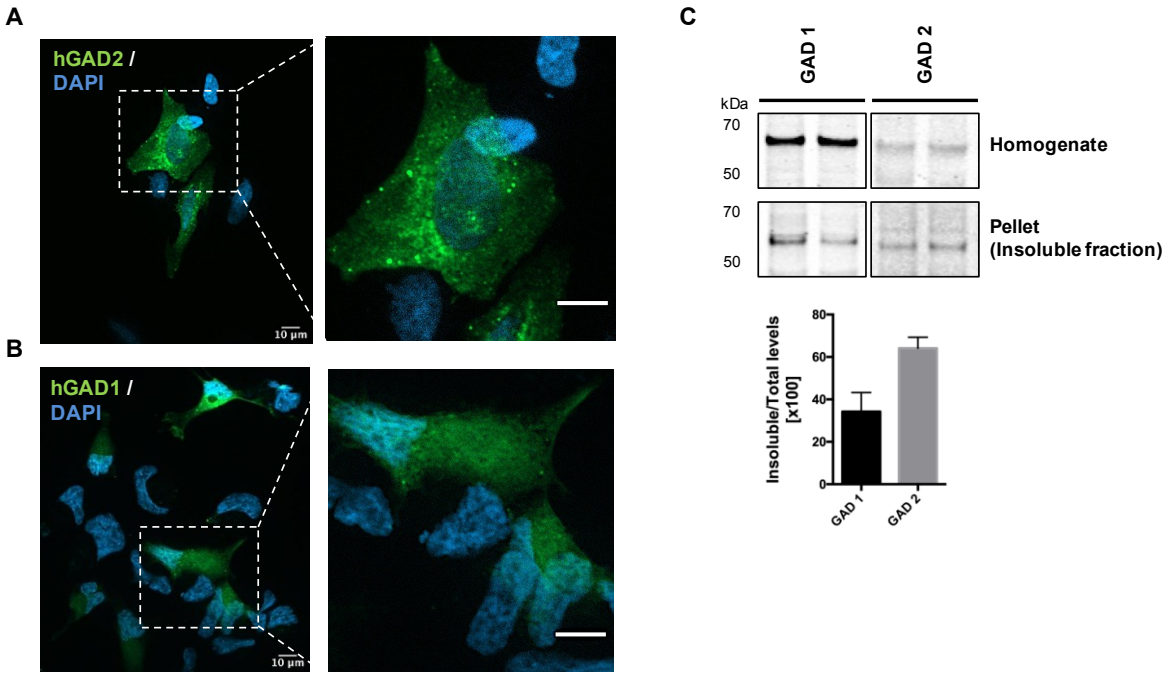

Figure 3

Table 1. Demographic information of *post mortem* human brain samples from two brain collections used for LC-MS/MS analysis. The sMRI collection consists of n=15 cases of schizophrenia (SCZ), n=15 cases of bipolar disorder (B), n=15 cases of major depression (D), and n=15 healthy control cases. The LIBD collection consists in n=25 cases of schizophrenia (SCZ), n=25 cases of major depression (D) and n=50 healthy control cases. The table depicts mean values for age, brain pH, post-mortem interval (PMI) represented by hours, and gender distribution. *p* values correspond to statistical analysis performed to the analyzed variants in between collections. Pearson's chi-squared test was used as a statistical test for gender distribution (**P < 0.0021); Unpaired t-test with two-tailed with Welch's correction was used as a statistical test for age, brain pH and PMI (**P < 0.0021).

		sMRI collection				LIBD collection			*p*		
		Healthy Controls	**SCZ patients**	**D patients**	**B patients**	**Healthy Controls**	**SCZ patients**	**D patients**	**Healthy Controls**	**SCZ patients**	**D patients**
Case Number		15	15	15	15	50	25	25			
Gender (%)	Male	40	40	40	40	66	40	44	0.001**	0.0	0.567
	Female	60	60	60	60	34	60	56			
Age	(mean ± SD)	48.1 ± 2.8	44.5 ± 3.4	46.5 ± 2.4	42.3 ± 3.0	45.4 ± 2.4	53.5 ± 2.8	47.7 ± 2.8	0,526	0,051	0,786
pH	(mean ± SD)	6.3 ± 0.1	6.2 ± 0.1	6.2 ± 0.1	6.2 ± 0.1	6.5 ± 0.0	6.4 ± 0.0	6.2 ± 0.0	0,001**	0,005**	0,752
PMI (h)	(mean ± SD)	23.7 ± 2.6	33.7 ± 3.8	27.5 ± 2.8	32.5 ± 4.2	32.6 ± 2.3	40.4 ± 4.0	41.5 ± 6.4	0,05	0,266	0,108

Table 2. Insoluble proteins identified in chronic mental illnesses patient samples independently of clinical diagnostic Proteins listed were identified by mass spectrometry in the insoluble proteome of CMIs patients independent of clinical diagnosis. Only proteins overlapping to both *post mortem* human brain collections (sMRI and LIBD), as well as being absent in healthy control samples were considered. Color code corresponds to a LFQ signal intensity with dark blue being the lowest and red the highest values. Abbreviations: B = Bipolar; D = Major depression; SCZ = schizophrenia; ID = unique identifier for each protein; Uniprot = Uniprot accession code; gene name = gene name according with Uniprot database; Description = Protein name/description derived from *.fasta database; Σ# Unique Peptides = sum of unique peptides per protein; LFQ = Label-free quantification values for each sample analyzed. LFQ corresponds to the raw intensities and was normalized to accurately reflected the relative protein amount.

Candidate proteins exclusively present in CMI patients [Independently of clinical diagnosis]

					sMRI collection			LIBD collection	
ID	**Uniprot**	**gene name**	**Description**	**Σ# Unique Peptides**	**LFQ B**	**LFQ D**	**LFQ SCZ**	**LFQ D**	**LFQ SCZ**
1	sp|Q05329|	GAD2_HUMAN	Glutamate decarboxylase 2	5	5316	0	1951	0	800
2	sp|P14625|	ENPL_HUMAN	Endoplasmin	17	17376	8901	4235	11247	10741
3	sp|O94826|	TOM70_HUMAN	Mitochondrial import receptor subunit	3	6198	955	0	859	0
4	sp|O95716|	RAB3D_HUMAN	Ras-related protein	3	7155	7744	3659	3612	0
5	sp|P14866|	HNRPL_HUMAN	Heterogeneous nuclear ribonucleoprotein L	17	3698	0	0	0	1135
6	sp|P24534|	EF1B_HUMAN	Elongation factor 1-beta	6	7046	2396	2272	2288	0
7	sp|P28482|	MK01_HUMAN	Mitogen-activated protein kinase 1	7	3729	0	3718	1992	0
8	sp|P31939-2|	PUR9_HUMAN	Bifunctional purine biosynthesis protein PURH	43	11757	0	4788	6282	6818
9	sp|P36406-3|	TRI23_HUMAN	E3 ubiquitin-protein ligase TRIM23	3	0	1589	2729	2006	0
10	sp|P68402|	PA1B2_HUMAN	Platelet-activating factor acetylhydrolase IB subunit beta	6	2729	0	0	0	1985
11	sp|P54750-8|	PDE1B_HUMAN	Phosphodiesterase	21	3905	1121	8295	2757	0
12	sp|Q13153|	PAK1_HUMAN	Serine/threonine-protein kinase PAK 1	53	5611	2356	1824	0	2110
13	sp|Q13424|	SNTA1_HUMAN	Alpha-1-syntrophin	8	10996	3614	3306	1568	0
14	sp|Q15257-3|	PTPA_HUMAN	Serine/threonine-protein phosphatase 2A activator	52	11905	7533	5365	5185	0
15	sp|Q9BY11|	PACN1_HUMAN	Protein kinase C and casein kinase substrate in neurons protein 1	14	11795	3240	2924	0	3892
16	sp|Q9NRX4|	PHP14_HUMAN	14 kDa phosphohistidine phosphatase	5	9658	4518	6977	23082	30074
17	sp|Q9ULC3|	RAB23_HUMAN	Ras-related protein Rab-23	2	3719	0	2343	0	6073
18	sp|Q9Y696|	CLIC4_HUMAN	Chloride intracellular channel protein 4	4	6546	0	0	6672	6891

Intensity
Low High

Supplementary Figure legends

Supplementary Figure S1. Optimization of insoluble proteome purification methodology in brain tissue from DISC1 transgenic rat. (a) The supernatants obtained after the centrifugation steps with method 1 (high -), and method 3 (low- stringency protocols) using DISC1 transgenic rat brain material, were analyzed. Supernatant fractions were subjected to SDS-PAGE followed by Coomassie blue staining of total proteins. By using method 3 (right panel) less material was lost during the fractionation procedure in comparison with method 1 (left panel). (b) An immunoblot against DISC1, showing the relevance of using optimized amounts of brain homogenate starting material in the low stringency protocol. Actin is shown as a loading control, equivalent amounts of insoluble pellet relative to starting material was loaded (a-b) Experiments were independently repeated n>3 times.

Supplementary Figure S2. The total number of insoluble proteins detected in the functional mass spectrometry analysis according to clinical diagnosis. (a) Identified proteins in the insoluble proteome of *post mortem* human brains from the sMRI collection, polled according to the differential clinical diagnostic of schizophrenia (S), bipolar disorder (B), major depression (D). Only proteins absent in healthy control were considered. (b) Corresponding analysis for the LIBD collection. The analysis was done according to the differential clinical phenotype of schizophrenia (S) and major depression (D) and excluding the mass spectrometry hits detected in healthy controls. Represented proteins were selected according to, intensity Based Absolute Quantification (iBAQ) values obtained by the calculation of raw intensities divided by the number of theoretical peptides. iBAQ values are proportional to the molar quantities of the proteins.

Supplementary Figure S3. Immunoblot analysis showing immunoreactivity signal in the 12 samples excluded from the analysis for all tested antibodies. Sarcosyl-insoluble-pellets from 60 sMRI collection patients clinically diagnosed with schizophrenia (S), bipolar disorder (B), major depression (D), and healthy controls (C). Arrows mark immunoblotted samples probed against GAD2, endoplasmin, EHD3, and MAP2K1 that were excluded from the analysis due to immunoreactivity across all antibodies.

Supplementary Figure S4. Expression levels of GAD2 transcript in human brains. Expression of GAD2 transcript in individuals diagnosed with CMI (n=13) versus healthy control individuals (CTR, n=8) from the sMRI Array Collection of brain RNA. The y-axis represents relative expression in the brain normalized to the ARF1 gene.

Supplementary Figure S5. Immunoblot validation of insoluble endoplasmin in chronic mental illnesses patients. Western blot for endoplasmin in sarkosyl-insoluble pellets (top panel) and the total homogenate (bottom panel) of 60 brains from sMRI *post mortem* human brain collection. Each lane corresponds to an independent biological sample, clinically diagnosed with schizophrenia (S), bipolar disorder (B), major depression (D), and healthy controls (C). The marked red samples were excluded from the analysis due to the immunoreactivity signal against different antibodies tested. Quantification of the corresponding levels in insoluble pellet by the total homogenate is presented by scatter plot (left panel) for all subjects considered in this experiment. Every single dot represents an individual subject sorted in two distinct groups, CMI (n=34) and healthy controls (n=14). Unpaired two-tailed t-test with Welch's correction was used as a statistical test (**P < 0.01), with means represented ±SEM.

Supplementary Figure S6. Quantitative proteomic analysis identified 29 proteins with increased insolubility in schizophrenic and depression patients. (a) Heatmap showing the protein fold change for the 29 proteins identified in the insoluble proteome of schizophrenia and major depression patients. Only proteins detected overlapping in the insoluble proteome of both *post mortem* human brain collections were considered. The fold change values correspond to the ratio of peptide intensity in disease versus control. For sMRI collection, only proteins exhibiting > 1.5-fold difference were considered. In the overall analysis, for LIBD collection, the intensity levels of the detected peptides was lower, meaning that proteins with > 1.0-fold difference were taken into account. Protein selection was made according to LFQ signal intensity and the color code corresponds to the fold-increase level for each collection. (b-c) Sarcosyl-insoluble-pellets from the 60 patients in sMRI collection, clinically diagnosed with schizophrenia (S), bipolar disorder (B), major depression (D), and healthy controls (C) were analyzed by SDS-PAGE and immunoblotted against EHD3 and MAP2K1. The marked red samples were excluded from the analysis due to the immunoreactivity signal shown against different antibodies tested. The right panel corresponds to the representative scatter plot for EHD3 and MAPK2. Data obtained by the quantification of the western blot intensity signal in insoluble fraction by the total protein level in the homogenate, normalized to the loading control – actin.

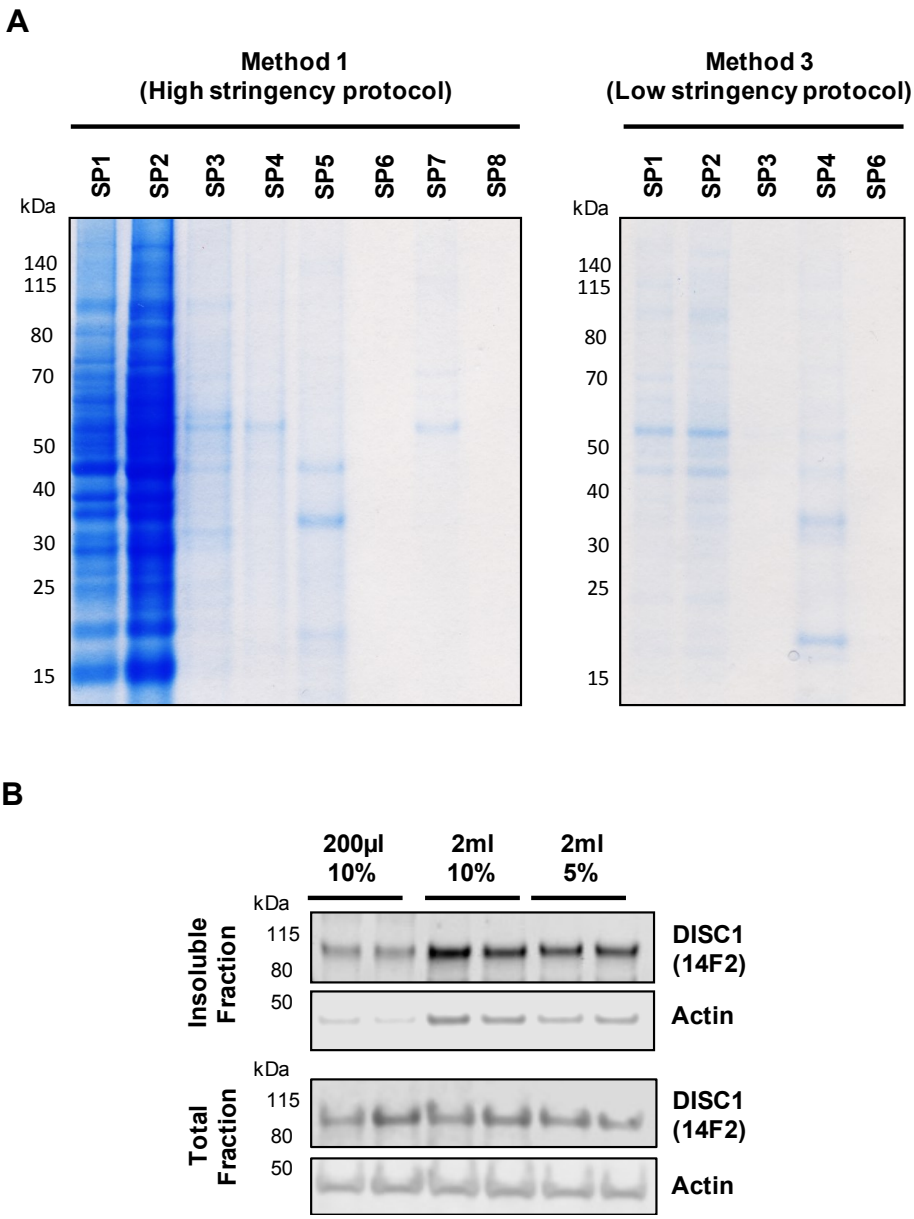

Supplementary Figure S1

A

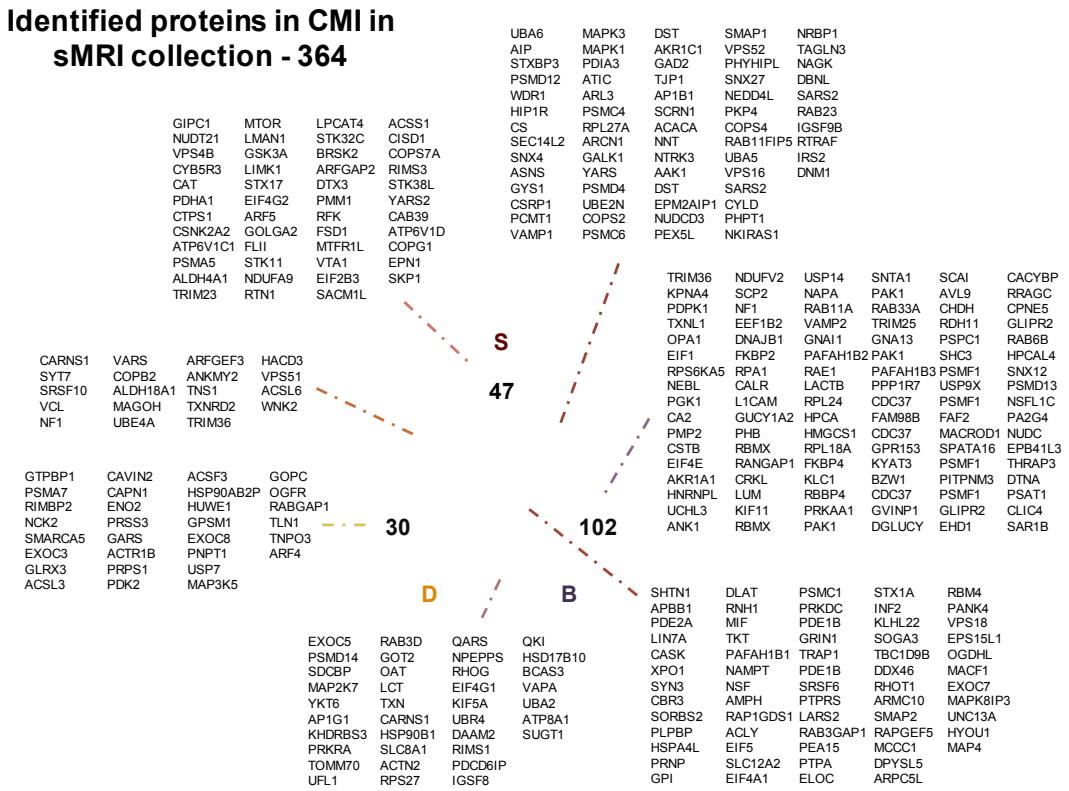

B

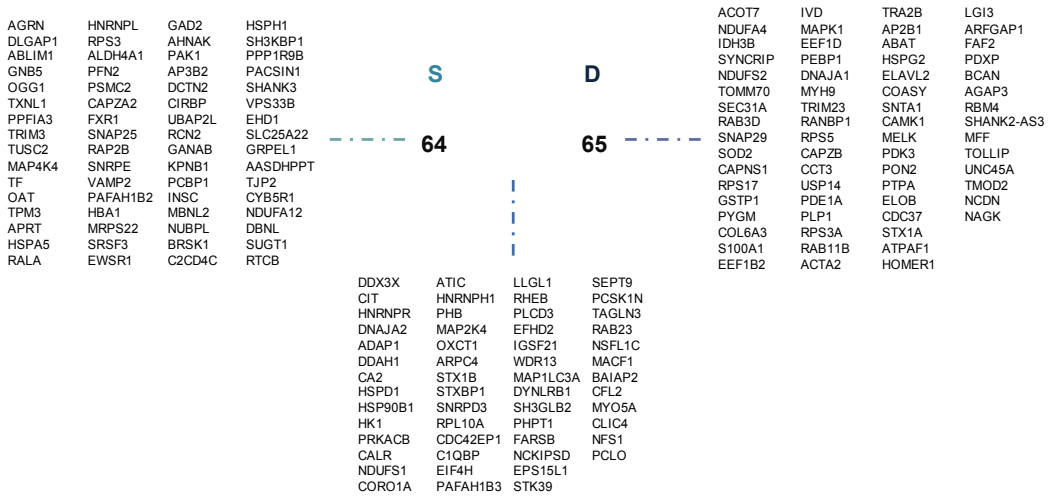

Supplementary Figure S2

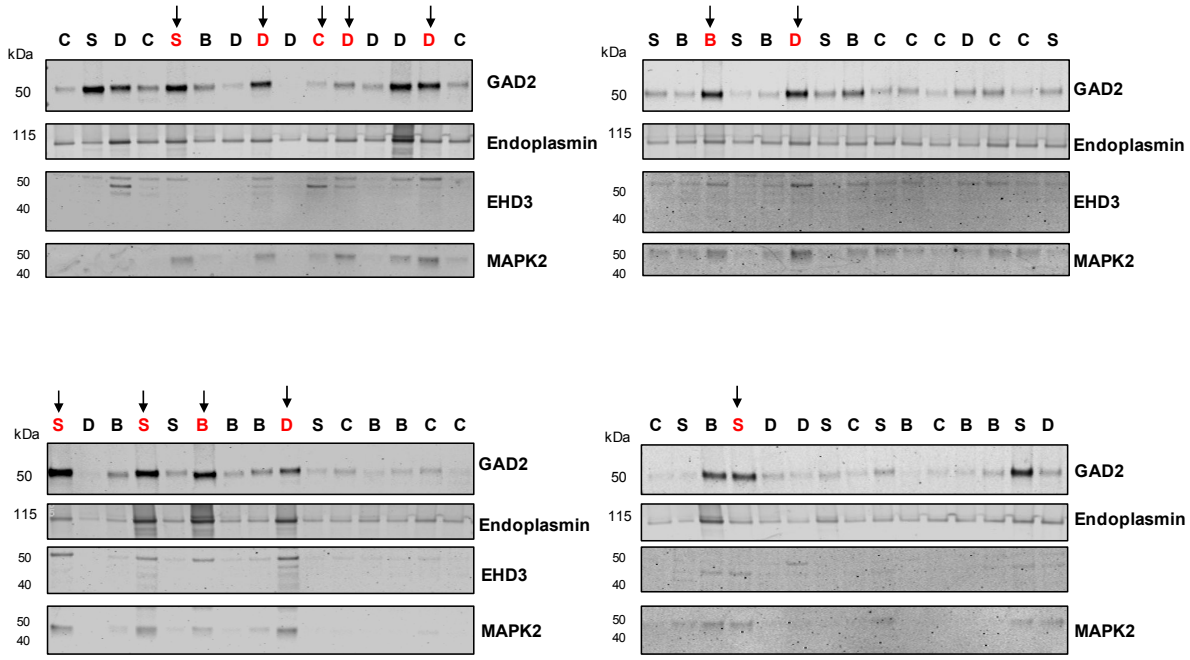

Supplementary Figure S3

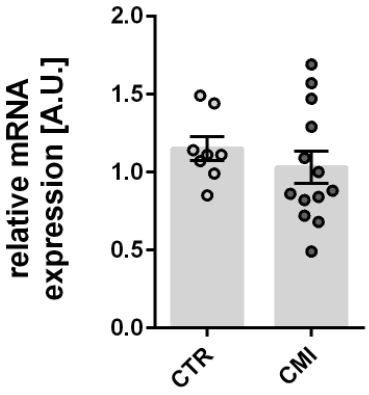

Supplementary Figure S4

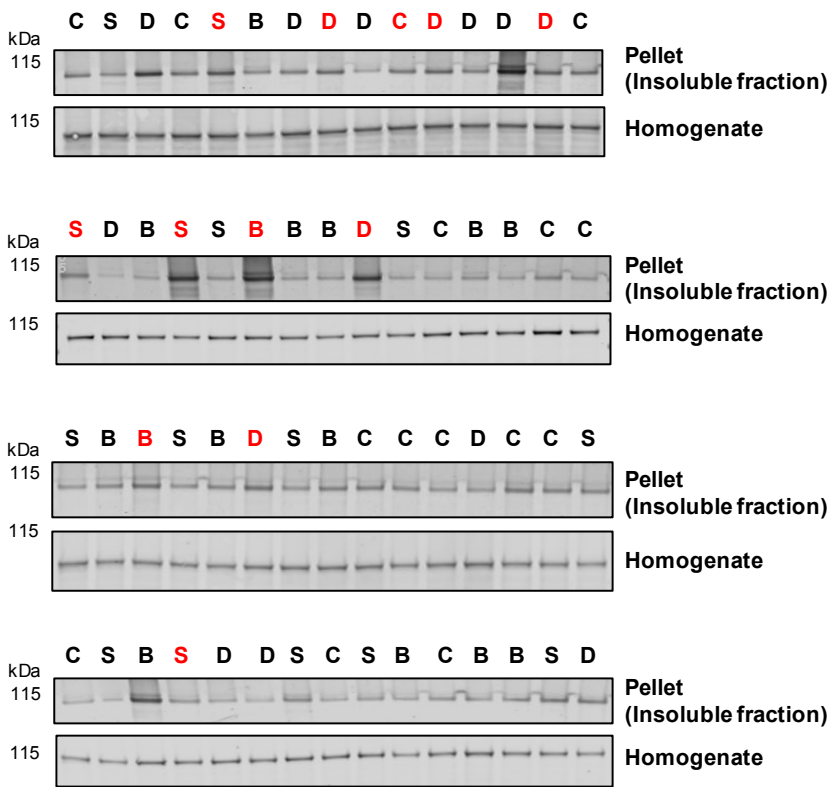

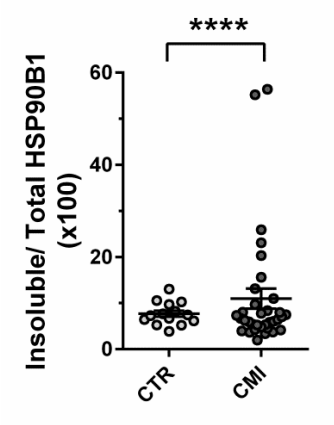

Supplementary Figure S5

Supplementary Figure S6

A

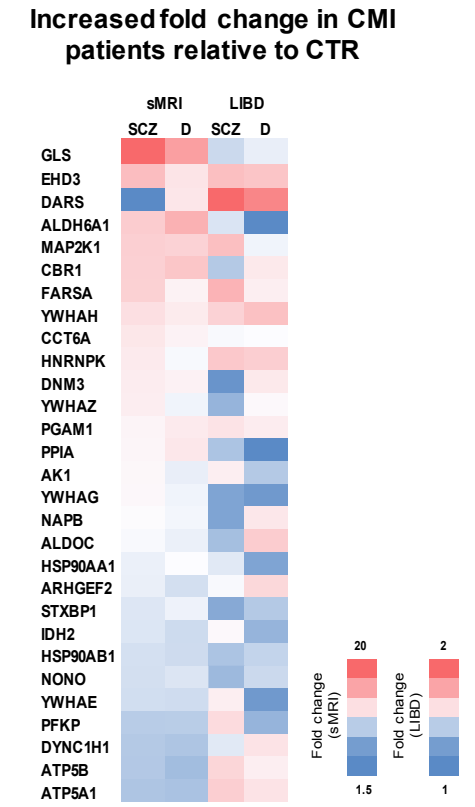

B

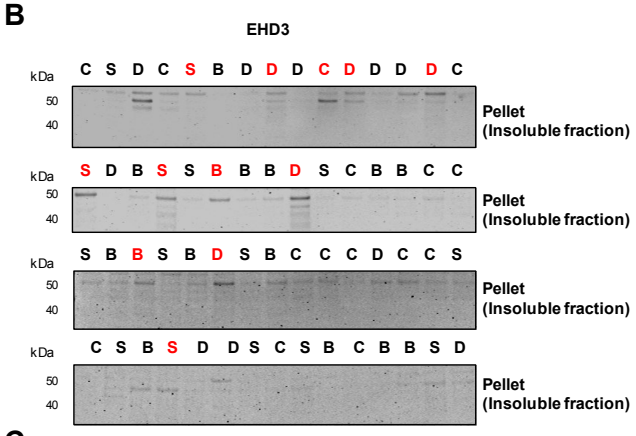

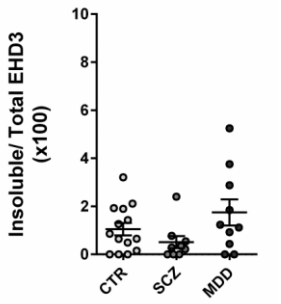

C

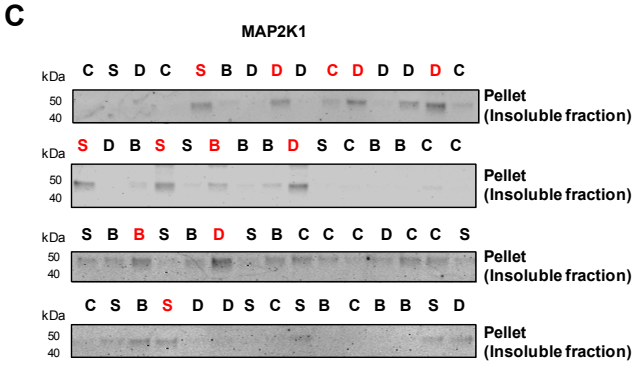

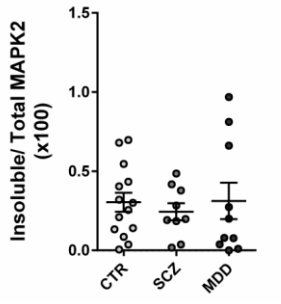

Discussion

Overall, the main aims proposed at the outset of in this dissertation were achieved. **1)** The assembly of toxic protein conformers featured in chronic brain disorders was investigated in the context of proteostasis interference by viral capsid assembly. Acute infection with influenza virus was identified as a possible risk factor for synuclein - and DISC1 – opathies, by triggering the initial events of protein misfolding disorder cascade (Figure 2). **2)** A differential insoluble protein expression profile in the brains of CMI patients was identified and characterized. Specially, insoluble GAD2 was identified as a biological marker of a subset of CMI patients.

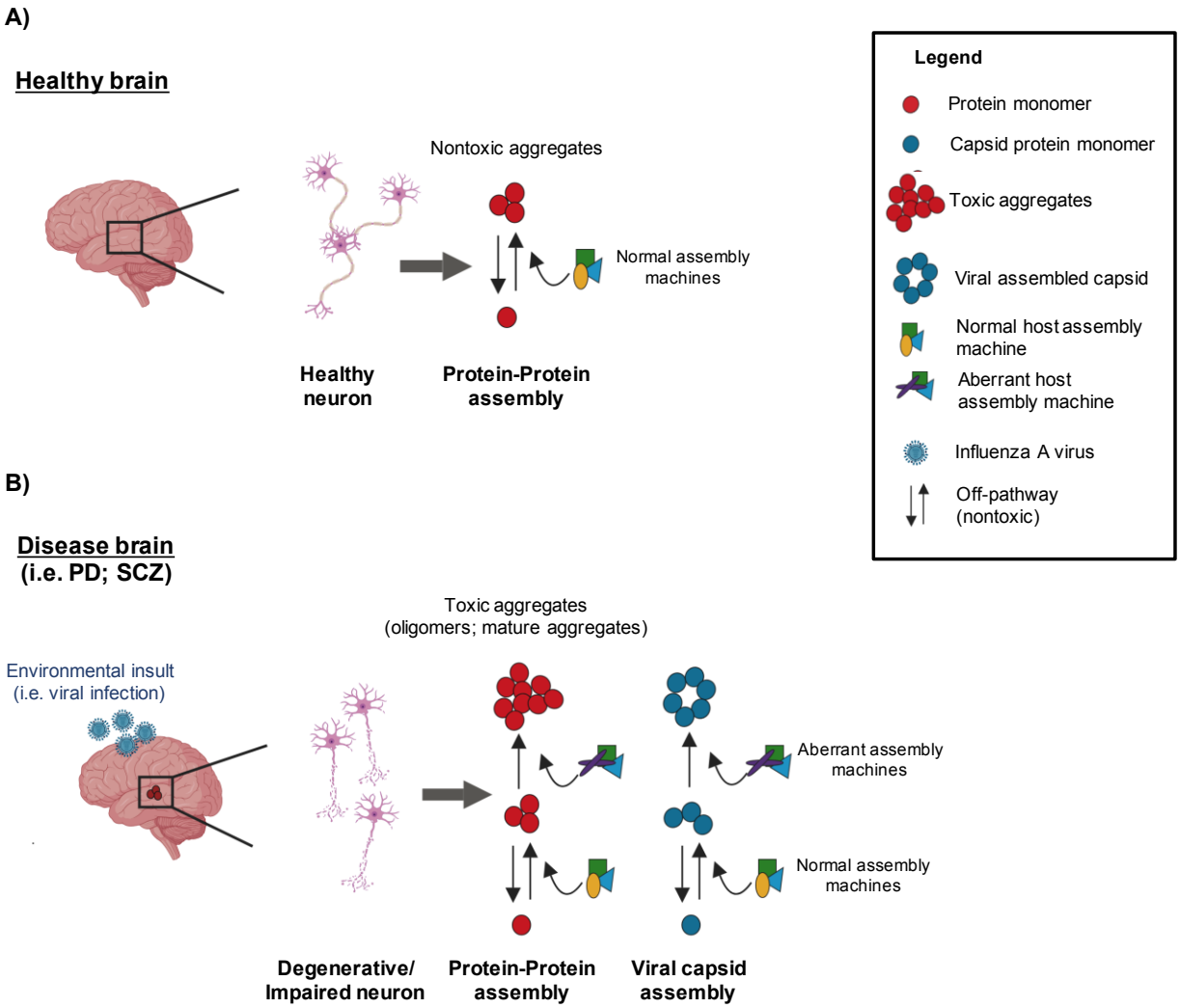

Figure 2. Illustration summary of the findings discussed in the first part of this dissertation (Chapter 1; 2). (A) In healthy brains, monomeric proteins can become misfolded and aggregate. PN components can act in the protein refolding, disaggregation, and clearance avoiding the 'off-pathway' reactions that lead to misfolded and aggregated species. (B) Environmental factors, such as viral infections, could be coadjutants to other factors (i.e., genetics) and inhibit the 'on-pathway' reactions, favoring the formation of toxic aggregates, a hallmark of

protein misfolding disorders – such as NDs and CMIs. The direct consequence is the neuronal degeneration in NDs and the neuronal impairment in CMIs. Aberrant cellular host factors catalyze the assembly of protein aggregates in a similar way to the ones used by the virus, to assembly their capsids.

An alternative view in the aggregation process associated with protein misfolding disorders

Proteins are essential for the normal cellular function, and protein homeostasis maintenance is crucial to avoid their accumulation in toxic species leading to the protein misfolding disorders (206). During the folding process, proteins acquire different conformations until they reach functional proteins. This is an extremely dynamic process that requires precise control of PN to avoid that protein go to the 'off-pathway' and form misfolded toxic species (207). One point that remains questionable is the protein multimerization process, which is still considered as a spontaneous cellular event that occurs mainly by self-assembly (208). The arising question is, how a spontaneous event can occur in a crowded environment as is a cell? Following that idea, here, we suggested that protein aggregation is a catalyzed process that involves the presence of 'assembly machines' (page 25). In parallel to the viral capsid assembly process, where the virus used the host cellular machinery to replicate efficiently, we suggested that similar assembly machines are also involved in the aberrant protein multimerization found in protein misfolding disorders. If we compare the virus lifecycle (hours) and human lifecycle (decades), we immediately perceive that the virus needs to take advantage of the host cell machinery, called 'assembly machines', to efficiently infect a cell (209). These assembly machines are incredibly complex transient cellular components governed by allosteric sites. So far, and despite the impressive advances done in the understanding of misfolding protein disorders (210), they remain incurable (211, 212). One of the explanations for that might be that conventional pharmacologic approaches involve the blockade of enzymes and receptors directly (213). An example is a γ-secretase inhibitor – Semagacestat from Eli Lilly & Co., which was in phase 3 of clinical trials for AD. Preclinical animal studies showed a reduction in soluble Aβ and amyloid plaque burden. In 2011, it was suspended due to ineffectiveness and the increased risk of skin cancer and infections (214). For PD in a similar way to other NDs, a long list of clinical trial failures was described. MK-0657 drug from Merck's company, that is an antagonist of NR2B subunit of the N-methyl-D-aspartate receptor was proved to improve the motor symptoms in a preclinical model of PD. However, an increase in systolic and diastolic blood pressure was the reason given in 2008 to halted the study (215). We suggest that targeting assembly machines might lead to superior therapeutic efficacy since we are modulating a more physiological way of biological regulation. That assumption is based on the results obtained after an antiviral compound treatment developed against viral capsid assembly (203, 204) which a reduction in the Aβ oligomeric species was observed (chapter 1, page 25).

These findings were the proof-of-principle that there is a shared mechanism between viral capsid assembly and aggregate formation in protein misfolding disorders, that might be mediated by cellular host factors, called 'assembly machines'.

Viral infections: a real threat to protein misfolding disorders?

Disturbances in the proteome (imbalance in protein synthesis and degradation and a decline in folding capacity), and metabolome (changes in the local microenvironment) can lead to aberrant protein phase transitions that might be critical drivers for protein misfolding disorders (216). With age, the brain becomes more susceptible to be affected by environmental factors such as viral infections (217). Notwithstanding over the past several years, significant advances have been made in identifying factors that contribute to the pathogenesis of the disorders (218), there are still many critical open questions. A remarkable one is, what the trigger mechanism for the conversion of a normal protein into the misfolded form that leads to their accumulation in pathological cases, is? In concordance with that, we investigated whether an H1N1 influenza A could trigger cellular events that lead to protein aggregation. Following the hypothesis presented in chapter 1 (page 25) we suggested that upon viral infection, the host cellular machinery is used by the virus to catalyze their replication and that might lead to a disruption in protein homeostasis driving aggregate formation (see chapter 2, page 36). Influenza A has demonstrated the ability to infect the CNS without immediately fatal consequences. Across lifetime, multiple expositions to H1N1 influenza A virus might affect the cellular protein homeostasis leading to chronic brain disorders (219). In an H1N1 infected cellular model of human dopamine-like neurons and an *in vivo* viral infected mouse brain, we observed an induction of misfolded α-syn and DISC1. A disruption in the autophagy system was also seen with viral infection, which might explain the observed aberrant protein deposition. Remarkably H1N1 influenza A virus did not disrupt the protein homeostasis of tau either TDP-43 (see chapter 2, fig S5), hallmark insoluble proteins for AD and ALS respectively (see table 1). It is still not clear how aggregates cause toxicity and cellular dysfunction, with variable modes of toxic function be related to specific disease proteins and cell types (220). However, it is undeniable that aberrant toxic depositions interfere with the proper function of PN. In a vicious feedforward cycle a decreased in PN capacity, due to the initial aggregate mass, leads to an increase in misfolded proteins that might end with a protein homeostasis collapse (221). In our study a pharmacological modulation of H1N1 replication was investigated (see chapter 2, Fig. 4). Oseltamivir phosphate, a drug commonly used in the treatment of acute, uncomplicated illness due to influenza A and B infection was seen to prevent α-syn protein misfolding. Taken the data present here (see chapter 2), we can consider H1N1 infection as a risk factor for α-syn and DISC1 related disorders. That might us raise the next question: could be

seasonal influenza vaccination used as a preventive procedure for PD, Dementia with Lew bodies (DLB), or DISC1opathies? Considering the efficient pharmacotherapy, our data suggest that it could be a very effective way to minimize the risk factor of influenza infection for these disorders. Although the type of influenza vaccination administrated should be considered. Currently, there are two main types of approved vaccines available, the trivalent inactivated influenza vaccine (TIV) and the intranasal live attenuated influenza vaccine (LAIV) (222). Since in our research we also described a requirement of an influenza virus with replication ability to induce α-syn aggregation (see chapter 2, Fig. 3), we propose avoiding the administration of LAIV as a prophylactic treatment until a negative interference with proteostasis can be excluded. LAIV is administered intranasal and requires viral replication in the nasal mucosa to trigger host immunization (223). Braak et al initially hypothesized that sporadic PD could trigger by an environmental stressor, as a pathogen, that enters the body via the nasal cavity and trigger the initial event cascade of α-syn misfolding leading to a subsequent α-syn aggregation in the olfactory bulb (224). At that point, no epidemiological studies have been performed investigating the effects of reliable and regular influenza vaccination on the incidence of PD, DLB or CMIs. Since influenza vaccination, however, comes with minimal risk, based on our data and with the appropriated precaution, we would recommend using them for the prevention of critical risk factor for NDs.

Accumulation of insoluble aggregates: a biological marker in sporadic mental illnesses

Analogous to NDs, the accumulation of insoluble proteins has been lately referred as a potential hallmark for CMIs (78). So far visible deposits of toxic species were not found in CMIs patient brains, neither a progressive, and irreversible neuronal death is associated with these conditions (225). Although, it has been hypothesized a subtler protein aggregation phenotype that might lead to neurological impairments, reflecting neuronal dysfunction rather than neuronal loss (226). It is well described in the literature that aberrant misfolded proteins impair the neuronal activity at different levels, inducing synaptic deficits, neural network changes, that precede the ultimate failure of neurological functions (227). That could be a reasonable mechanism behind the psychiatry phenotypes found in the early stages of NDs (228), which forms a continuum with the idea that cellular consequences of insoluble protein deposits might be the overlapped mechanism for CMIs and NDs. Despite decades of research in the field, why is there still a lack of a biological hallmark in the diagnosis of mental illnesses? In the psychiatry field, CMIs are consistently considered as separate clinical entities with distinct pathology and symptoms (229). However, when we have a closer look at the genetic, molecular, and the cellular level is overlapping molecular players and patterns are obvious. In line with this, the present study attempted to define a biological

signature of insoluble proteins for subsets of specimens (5) even though the vast majority of the studies still focusses on the analysis of the proteome of specific brain tissue in disease vs control conditions. In such studies, several candidate proteins differentially expressed and related to specific pathways that might be a tissue-type response associated with nonspecific aspects of the disease, rather than a pathophysiologic effect are identified (230, 231). This concern was well-reviewed in work published by English et al. They combine proteomic studies done in SCZ and NDs patient samples and described a significant overlapped in the identified candidate proteins (232). In the analysis present here, we attempt to counteract the lack of specificity in this approach, and we focus on the subproteome of our interest – the insoluble proteome which represents a functional preselection (see chapter 3, page 84). The common insoluble candidate proteins in two independent *post-mortem* human brain cohorts were used. One of the two proteins involved in GABA synthesis (GAD2), by the decarboxylation of glutamate to GABA, was identified as a biological marker for a subset of CMIs patients (see chapter 3, Table 2, Fig. 2,). To our knowledge, GAD2 insolubility has not been reported in the context of any of the chronic brain disorder. In the study published by Metaxas et al, the analysis of the insoluble proteome of an amyloidosis mice model ($APP_{swe}/PS1_{\Delta E9}$), demonstrated GAD2 downregulation in disease vs wild-type animals at the different time points of disease progression (3 and 24 months) (233).

Therefore, the value of the data generated here is the initial evidence to establish GAD2 as a possible biological hallmark for CMIs. Determination of the functional consequence of GAD2 insolubility for GABA production, as well as, how that modulates the glutamate/GABA-glutamine cycle, and ultimately disrupt the excitatory/inhibitory balance, will be our next attempt.

Conclusion / Final author comments

The last years have been marked by an increase in research leading to remarkable findings in the pathophysiology of chronic brain disorders. Despite the unknown aspects of these disorders, the still critical point is *'What is the relationship between protein homeostasis disruption and the pathologies?'*. So far misfolding protein disorders, such as NDs and CMIs, remains incurable. Translating the basic research to new therapeutic approaches is being the central issue in the field. Although that reality seems not to change soon, due to the lack of new perspectives in the pathological phenomena, that is poisoning further progression. Should protein homeostasis disruption be considered the common mechanism that plays out across the protein misfolding associated pathologies? Or is the aberrant accumulation of toxic species only the consequence of a neuronal impairment that occurs in the pathologies?

In a different perspective, the present work has addressed some central points that might help to give new insights into the field: **1)** A new angle in protein aggregation assembly mechanism was proposed, suggesting a novel and potent therapeutic target for protein misfolding disorders; **2)** A suggested synuclein- and DISC1 - opathy etiological mechanism in which influenza A infection might be a seed for protein aggregation. These findings emphasize the evidence found in the literature that viral and other microbial infections, may play a role in the pathogenesis of misfolded disorders; **3)** Applying the previously published theory of insoluble proteins as a hallmark of CMIs, a new biological marker was described for a subset of CMIs patients. Consider the similarities found in protein misfolding disorders, advances done in NDs research might be used as a mold in the psychiatry field.

List of publications

Marreiros R., Trossbach S.V., Prikulis I., Gonzalez M., Li K.W., Ottis P., Just D., Nilsson P., Sinha V.,Hennah W., Hyde T.M., Kleinman J.E., Smit, A.B., Korth C. Functional proteomic analysis identifies insoluble GAD2 in a subset of sporadic mental illness patients.
Manuscript in submission

Marreiros R., Müller-Schiffmann A.,Prikulis I., Moreira A.R., Sahu S., Soloviev I., Selvarajah S., Lingappa V.R., Korth C. Disruption of cellular proteostasis by H1N1 influenza A virus causes α-synuclein aggregation. *Under review. PNAS*

Yerabham A.S.K., Müller-Schiffmann A., Ziehm T., Arinkin V., Stadler A., Köber S., Indhurkya X., **Marreiros R**., Trossbach S., Bradshaw N.J., Prikulis I., Weiergräber O.H., Korth C. Biophysical insights from a single chain camelid antibody directed against the Disrupted-in-Schizophrenia 1 protein. *PLoS One. 2018 Jan 11* ;13(1):e0191162.

Bradshaw N.J., Yerabham A.S.K., **Marreiros R**., Zhang T., Nagel-Steger L., Korth C. An unpredicted aggregation-critical region of the actin-polymerizing protein TRIOBP-1/Tara, determined by elucidation of its domain structure. The Journal of Biological Chemistry 2017; 292(23):9583-9598.

Steffen J., Krohn M., Paarmann K., Schwitlick C., Brüning T., **Marreiros R**., Müller-Schiffmann A., Korth C., Braun K., Pahnke J. Revisiting rodent models: Octodon degus as Alzheimer's disease model? Acta Neuropathologica Communications 2016; 4(1):91.

Marreiros R., Müller-Schiffmann A., Bader V., Selvarajah S., Dey D., Lingappa V.R., Korth C. Viral capsid assembly as a model for protein aggregation diseases: Active processes catalyzed by cellular assembly machines comprising novel drug targets. Virus Research 2015; 207:155-64.

Acknowledgments

I want to express my sincere gratitude to all the people who supported me in the last years and made this dissertation possible.

Foremost I would like to thank Prof. Carsten Korth for the gave opportunity of doing my Ph.D. under his supervision. He gave me the chance to work in a variety of engaging projects, also in different parts of the world, allowing me to explore and continuously challenge my scientific skills. I appreciated all the enthusiastic (and not so enthusiastic) discussions and advice. Most of all, it was an exciting scientific and personal 'growth path,' which he taught me how to run and reach the end of a marathon.

I would like to specially thank Prof. Dr. Sascha Weggen for courteously officiating as my co-supervisor and Prof. Dr. Dieter Willbold, who consented to be my mentor.

I would like to sincerely express my appreciation to Vishu Lingappa, M.D., Ph.D., for all the support during and after my time at Prosetta Biosciences. It was a tremendous pleasure to have the opportunity to share and discuss my scientific ideas with you. Your enthusiasm and way to look at things in a different perspective was an inspiration for me. To Dr. Suganya Selvarajah, and all Prosetta team, especially Raquel Moreira, Dr. Shriya Sahu, and Irina Soloviev, I would like to express my special thank. You introduced me to the 'viral world' and assisted me throughout the project, making me always feel part of the team.

So...yes…'Korth's Lab family'! The family that I found in Germany which in the end I spent more time with, that with anyone else. Thanks a lot for always be there, to help me to grow as a scientist and most importantly, as a person. Wherever I will go next, I will always remember how did you encouraged me all the time, and made the lab a funny place to work. Mainly I want to thank Ingrid Prikulis (my 'lab/German mama'), and 'my post-docs', Dr. Andreas Müller-Schiffmann and Dr. Svenja Trossbach, as well as 'my former post-doc' Dr. Verian Bader (my microscope 'guru'). To my lab buddy, Dr. Antony Sravan, and to several of my fellow Post-doc and Ph.D. students, Dr. Nicholas Bradshaw, Dr. Sarah Tschirner, Dr. Sandra Vomund, Xela Indurkhya, Hannah Hamburg, Sarah Soellner-Szwed, and Else van Gerresheim, it was a pleasure to share with you such fantastic (and sometimes not really) time.

I want to thank FP7-PEOPLE-2013-ITN – Marie Skłodowska-Curie training IN-SENS program, my graduate school, and Forschungskommission of the Medical Faculty of the

Heinrich Heine University Düsseldorf. They funded the projects and made it possible to participate in inspiring scientific meetings and congresses. Through the IN-SENS program, I was able to do several courses all around Europe, spent a fantastic time sharing enthusiasm and aspirations with other young scientists and perform the secondment at Prosetta Biosciences, Inc. in San Francisco, USA.

My infinitive gratitude goes to my family, and friends that at the end of the day are nothing else than the family that I choose. To my family, that even being a 2000 km of distance never let me fall. I owe the world to them… they encouraged and supported me in every single decision that I made, let me always see life as a magic path (Mama, Papa e Mano um OBRIGADO do tamanho do mundo). I also own my gratitude to Dario (‘my partner in crime’) who supported me in every single day since we meet, never stooped to have faith in me and always make me keep my smile, and look further. You made me believe that the ‘boat would arrive at a safe harbor’… you might be right!
To the family that I chose, the old and the new friends, I have to express my thanks for always be there and having the words and the silence when it was needed. With you, I learned that caress should be beyond distance, time, and the busy life.

I want to express my gratitude towards all the people that were mentioned here, that in such different ways help me to finalize my Ph.D., and move to the next step.

Bibliography

1. D. Balchin, M. Hayer-Hartl, F. U. Hartl, In vivo aspects of protein folding and quality control. *Science* **353**, aac4354 (2016).
2. J. Ellis, Proteins as molecular chaperones. *Nature* **328**, 378-379 (1987).
3. C. L. Klaips, G. G. Jayaraj, F. U. Hartl, Pathways of cellular proteostasis in aging and disease. *J Cell Biol* **217**, 51-63 (2018).
4. B. Bruce Alberts *et al.*, *Molecular Biology of the Cell,* (New York: Garland Science;, 2002), vol. 4th edition.
5. M. R. Wilkins *et al.*, Progress with proteome projects: why all proteins expressed by a genome should be identified and how to do it. *Biotechnol Genet Eng Rev* **13**, 19-50 (1996).
6. N. A. Kulak, P. E. Geyer, M. Mann, Loss-less Nano-fractionator for High Sensitivity, High Coverage Proteomics. *Mol Cell Proteomics* **16**, 694-705 (2017).
7. T. Geiger, A. Wehner, C. Schaab, J. Cox, M. Mann, Comparative proteomic analysis of eleven common cell lines reveals ubiquitous but varying expression of most proteins. *Mol Cell Proteomics* **11**, M111 014050 (2012).
8. A. K. Dunker, Z. Obradovic, The protein trinity--linking function and disorder. *Nat Biotechnol* **19**, 805-806 (2001).
9. M. Levitt, C. Chothia, Structural patterns in globular proteins. *Nature* **261**, 552-558 (1976).
10. J. S. Richardson, The anatomy and taxonomy of protein structure. *Adv Protein Chem* **34**, 167-339 (1981).
11. M. S. Hipp, P. Kasturi, F. U. Hartl, The proteostasis network and its decline in ageing. *Nat Rev Mol Cell Biol* **20**, 421-435 (2019).
12. B. Danielsson, Enzyme thermistor devices. *Bioprocess Technol* **15**, 83-105 (1991).
13. C. B. Anfinsen, Principles that govern the folding of protein chains. *Science* **181**, 223-230 (1973).
14. F. U. Hartl, A. Bracher, M. Hayer-Hartl, Molecular chaperones in protein folding and proteostasis. *Nature* **475**, 324-332 (2011).
15. A. R. Dinner, A. Sali, L. J. Smith, C. M. Dobson, M. Karplus, Understanding protein folding via free-energy surfaces from theory and experiment. *Trends Biochem Sci* **25**, 331-339 (2000).
16. F. Sanger, H. Tuppy, The amino-acid sequence in the phenylalanyl chain of insulin. I. The identification of lower peptides from partial hydrolysates. *Biochem J* **49**, 463-481 (1951).
17. S. Lee, D. Eisenberg, Seeded conversion of recombinant prion protein to a disulfide-bonded oligomer by a reduction-oxidation process. *Nat Struct Biol* **10**, 725-730 (2003).
18. T. L. Blundell, M. S. Johnson, Catching a common fold. *Protein Sci* **2**, 877-883 (1993).
19. D. J. Brockwell, S. E. Radford, Intermediates: ubiquitous species on folding energy landscapes? *Curr Opin Struct Biol* **17**, 30-37 (2007).
20. F. U. Hartl, M. Hayer-Hartl, Molecular chaperones in the cytosol: from nascent chain to folded protein. *Science* **295**, 1852-1858 (2002).
21. J. Zou, Y. Guo, T. Guettouche, D. F. Smith, R. Voellmy, Repression of heat shock transcription factor HSF1 activation by HSP90 (HSP90 complex) that forms a stress-sensitive complex with HSF1. *Cell* **94**, 471-480 (1998).
22. X. Zheng *et al.*, Dynamic control of Hsf1 during heat shock by a chaperone switch and phosphorylation. *Elife* **5** (2016).
23. V. Arndt, C. Rogon, J. Hohfeld, To be, or not to be--molecular chaperones in protein degradation. *Cell Mol Life Sci* **64**, 2525-2541 (2007).

24. A. Ciechanover, The unravelling of the ubiquitin system. *Nat Rev Mol Cell Biol* **16**, 322-324 (2015).
25. A. Hershko, A. Ciechanover, The ubiquitin system. *Annu Rev Biochem* **67**, 425-479 (1998).
26. Y. T. Kwon, A. Ciechanover, The Ubiquitin Code in the Ubiquitin-Proteasome System and Autophagy. *Trends Biochem Sci* **42**, 873-886 (2017).
27. W. Baumeister, J. Walz, F. Zuhl, E. Seemuller, The proteasome: paradigm of a self-compartmentalizing protease. *Cell* **92**, 367-380 (1998).
28. M. F. Rosser, E. Washburn, P. J. Muchowski, C. Patterson, D. M. Cyr, Chaperone functions of the E3 ubiquitin ligase CHIP. *J Biol Chem* **282**, 22267-22277 (2007).
29. W. X. Ding, X. M. Yin, Sorting, recognition and activation of the misfolded protein degradation pathways through macroautophagy and the proteasome. *Autophagy* **4**, 141-150 (2008).
30. C. F. Bento *et al.*, Mammalian Autophagy: How Does It Work? *Annu Rev Biochem* **85**, 685-713 (2016).
31. L. Yu, Y. Chen, S. A. Tooze, Autophagy pathway: Cellular and molecular mechanisms. *Autophagy* **14**, 207-215 (2018).
32. S. Nakamura, T. Yoshimori, New insights into autophagosome-lysosome fusion. *J Cell Sci* **130**, 1209-1216 (2017).
33. T. Lamark, T. Johansen, Aggrephagy: selective disposal of protein aggregates by macroautophagy. *Int J Cell Biol* **2012**, 736905 (2012).
34. J. J. Lemasters, Selective mitochondrial autophagy, or mitophagy, as a targeted defense against oxidative stress, mitochondrial dysfunction, and aging. *Rejuvenation Res* **8**, 3-5 (2005).
35. E. Arias, A. M. Cuervo, Chaperone-mediated autophagy in protein quality control. *Curr Opin Cell Biol* **23**, 184-189 (2011).
36. K. Tekirdag, A. M. Cuervo, Chaperone-mediated autophagy and endosomal microautophagy: Joint by a chaperone. *J Biol Chem* **293**, 5414-5424 (2018).
37. R. Sahu *et al.*, Microautophagy of cytosolic proteins by late endosomes. *Dev Cell* **20**, 131-139 (2011).
38. G. Hewitt, V. I. Korolchuk, Repair, Reuse, Recycle: The Expanding Role of Autophagy in Genome Maintenance. *Trends Cell Biol* **27**, 340-351 (2017).
39. A. Ben-Zvi, E. A. Miller, R. I. Morimoto, Collapse of proteostasis represents an early molecular event in Caenorhabditis elegans aging. *Proc Natl Acad Sci U S A* **106**, 14914-14919 (2009).
40. D. C. David *et al.*, Widespread protein aggregation as an inherent part of aging in C. elegans. *PLoS Biol* **8**, e1000450 (2010).
41. B. Chen, M. Retzlaff, T. Roos, J. Frydman, Cellular strategies of protein quality control. *Cold Spring Harb Perspect Biol* **3**, a004374 (2011).
42. R. C. Taylor, A. Dillin, Aging as an event of proteostasis collapse. *Cold Spring Harb Perspect Biol* **3** (2011).
43. F. W. van Leeuwen *et al.*, Frameshift mutants of beta amyloid precursor protein and ubiquitin-B in Alzheimer's and Down patients. *Science* **279**, 242-247 (1998).
44. N. Gregersen, P. Bross, Protein misfolding and cellular stress: an overview. *Methods Mol Biol* **648**, 3-23 (2010).
45. E. Herczenik, M. F. Gebbink, Molecular and cellular aspects of protein misfolding and disease. *FASEB J* **22**, 2115-2133 (2008).
46. T. Gidalevitz, V. Prahlad, R. I. Morimoto, The stress of protein misfolding: from single cells to multicellular organisms. *Cold Spring Harb Perspect Biol* **3** (2011).
47. M. V. Blagosklonny, Linking calorie restriction to longevity through sirtuins and autophagy: any role for TOR. *Cell Death Dis* **1**, e12 (2010).
48. M. Hansen *et al.*, Lifespan extension by conditions that inhibit translation in Caenorhabditis elegans. *Aging Cell* **6**, 95-110 (2007).

49. A. L. Fink, Protein aggregation: folding aggregates, inclusion bodies and amyloid. *Fold Des* **3**, R9-23 (1998).
50. J. Lee, E. K. Culyba, E. T. Powers, J. W. Kelly, Amyloid-beta forms fibrils by nucleated conformational conversion of oligomers. *Nat Chem Biol* **7**, 602-609 (2011).
51. T. R. Serio *et al.*, Nucleated conformational conversion and the replication of conformational information by a prion determinant. *Science* **289**, 1317-1321 (2000).
52. A. J. Modler, K. Gast, G. Lutsch, G. Damaschun, Assembly of amyloid protofibrils via critical oligomers--a novel pathway of amyloid formation. *J Mol Biol* **325**, 135-148 (2003).
53. G. Plakoutsi *et al.*, Evidence for a mechanism of amyloid formation involving molecular reorganisation within native-like precursor aggregates. *J Mol Biol* **351**, 910-922 (2005).
54. G. Zettlmeissl, R. Rudolph, R. Jaenicke, Reconstitution of lactic dehydrogenase. Noncovalent aggregation vs. reactivation. 1. Physical properties and kinetics of aggregation. *Biochemistry* **18**, 5567-5571 (1979).
55. A. J. Baldwin *et al.*, Metastability of native proteins and the phenomenon of amyloid formation. *J Am Chem Soc* **133**, 14160-14163 (2011).
56. M. J. Bennett, M. R. Sawaya, D. Eisenberg, Deposition diseases and 3D domain swapping. *Structure* **14**, 811-824 (2006).
57. D. Eisenberg *et al.*, The structural biology of protein aggregation diseases: Fundamental questions and some answers. *Acc Chem Res* **39**, 568-575 (2006).
58. M. Sunde, C. Blake, The structure of amyloid fibrils by electron microscopy and X-ray diffraction. *Adv Protein Chem* **50**, 123-159 (1997).
59. A. K. Paravastu, R. D. Leapman, W. M. Yau, R. Tycko, Molecular structural basis for polymorphism in Alzheimer's beta-amyloid fibrils. *Proc Natl Acad Sci U S A* **105**, 18349-18354 (2008).
60. M. R. Nilsson, Techniques to study amyloid fibril formation in vitro. *Methods* **34**, 151-160 (2004).
61. C. A. Ross, M. A. Poirier, Protein aggregation and neurodegenerative disease. *Nat Med* **10 Suppl**, S10-17 (2004).
62. A. M. Morris, M. A. Watzky, R. G. Finke, Protein aggregation kinetics, mechanism, and curve-fitting: a review of the literature. *Biochim Biophys Acta* **1794**, 375-397 (2009).
63. J. Masel, V. A. Jansen, M. A. Nowak, Quantifying the kinetic parameters of prion replication. *Biophys Chem* **77**, 139-152 (1999).
64. J. T. Jarrett, E. P. Berger, P. T. Lansbury, Jr., The carboxy terminus of the beta amyloid protein is critical for the seeding of amyloid formation: implications for the pathogenesis of Alzheimer's disease. *Biochemistry* **32**, 4693-4697 (1993).
65. V. N. Uversky, J. Li, A. L. Fink, Evidence for a partially folded intermediate in alpha-synuclein fibril formation. *J Biol Chem* **276**, 10737-10744 (2001).
66. E. Chatani, N. Yamamoto, Recent progress on understanding the mechanisms of amyloid nucleation. *Biophys Rev* **10**, 527-534 (2018).
67. X. Wang, Y. Zhou, J. J. Ren, N. D. Hammer, M. R. Chapman, Gatekeeper residues in the major curlin subunit modulate bacterial amyloid fiber biogenesis. *Proc Natl Acad Sci U S A* **107**, 163-168 (2010).
68. F. Chiti, C. M. Dobson, Amyloid formation by globular proteins under native conditions. *Nat Chem Biol* **5**, 15-22 (2009).
69. F. Chiti, C. M. Dobson, Protein misfolding, functional amyloid, and human disease. *Annu Rev Biochem* **75**, 333-366 (2006).
70. D. Kaganovich, R. Kopito, J. Frydman, Misfolded proteins partition between two distinct quality control compartments. *Nature* **454**, 1088-1095 (2008).

71. J. A. Johnston, C. L. Ward, R. R. Kopito, Aggresomes: a cellular response to misfolded proteins. *J Cell Biol* **143**, 1883-1898 (1998).
72. R. Garcia-Mata, Z. Bebok, E. J. Sorscher, E. S. Sztul, Characterization and dynamics of aggresome formation by a cytosolic GFP-chimera. *J Cell Biol* **146**, 1239-1254 (1999).
73. R. R. Kopito, Aggresomes, inclusion bodies and protein aggregation. *Trends Cell Biol* **10**, 524-530 (2000).
74. T. A. Atkin, N. J. Brandon, J. T. Kittler, Disrupted in Schizophrenia 1 forms pathological aggresomes that disrupt its function in intracellular transport. *Hum Mol Genet* **21**, 2017-2028 (2012).
75. S. Escusa-Toret, W. I. Vonk, J. Frydman, Spatial sequestration of misfolded proteins by a dynamic chaperone pathway enhances cellular fitness during stress. *Nat Cell Biol* **15**, 1231-1243 (2013).
76. N. E. Farrawell *et al.*, Distinct partitioning of ALS associated TDP-43, FUS and SOD1 mutants into cellular inclusions. *Sci Rep* **5**, 13416 (2015).
77. S. J. Weisberg *et al.*, Compartmentalization of superoxide dismutase 1 (SOD1G93A) aggregates determines their toxicity. *Proc Natl Acad Sci U S A* **109**, 15811-15816 (2012).
78. N. J. Bradshaw, C. Korth, Protein misassembly and aggregation as potential convergence points for non-genetic causes of chronic mental illness. *Mol Psychiatry* 10.1038/s41380-018-0133-2 (2018).
79. A. Aguzzi, T. O'Connor, Protein aggregation diseases: pathogenicity and therapeutic perspectives. *Nat Rev Drug Discov* **9**, 237-248 (2010).
80. J. Xu *et al.*, Gain of function of mutant p53 by coaggregation with multiple tumor suppressors. *Nat Chem Biol* **7**, 285-295 (2011).
81. C. Lopez-Otin, M. A. Blasco, L. Partridge, M. Serrano, G. Kroemer, The hallmarks of aging. *Cell* **153**, 1194-1217 (2013).
82. S. Trautmann, J. Rehm, H. U. Wittchen, The economic costs of mental disorders: Do our societies react appropriately to the burden of mental disorders? *EMBO Rep* **17**, 1245-1249 (2016).
83. L. Bertram, R. E. Tanzi, The genetic epidemiology of neurodegenerative disease. *J Clin Invest* **115**, 1449-1457 (2005).
84. T. E. Golde, D. R. Borchelt, B. I. Giasson, J. Lewis, Thinking laterally about neurodegenerative proteinopathies. *J Clin Invest* **123**, 1847-1855 (2013).
85. E. Bossy-Wetzel, R. Schwarzenbacher, S. A. Lipton, Molecular pathways to neurodegeneration. *Nat Med* **10 Suppl**, S2-9 (2004).
86. K. F. Winklhofer, J. Tatzelt, C. Haass, The two faces of protein misfolding: gain- and loss-of-function in neurodegenerative diseases. *EMBO J* **27**, 336-349 (2008).
87. J. Scekic-Zahirovic *et al.*, Toxic gain of function from mutant FUS protein is crucial to trigger cell autonomous motor neuron loss. *EMBO J* **35**, 1077-1097 (2016).
88. C. Deyts *et al.*, Loss of presenilin function is associated with a selective gain of APP function. *Elife* **5** (2016).
89. M. Jucker, L. C. Walker, Self-propagation of pathogenic protein aggregates in neurodegenerative diseases. *Nature* **501**, 45-51 (2013).
90. J. Brettschneider, K. Del Tredici, V. M. Lee, J. Q. Trojanowski, Spreading of pathology in neurodegenerative diseases: a focus on human studies. *Nat Rev Neurosci* **16**, 109-120 (2015).
91. M. Costanzo, C. Zurzolo, The cell biology of prion-like spread of protein aggregates: mechanisms and implication in neurodegeneration. *Biochem J* **452**, 1-17 (2013).
92. K. M. Danzer *et al.*, Exosomal cell-to-cell transmission of alpha synuclein oligomers. *Mol Neurodegener* **7**, 42 (2012).
93. S. Saman *et al.*, Exosome-associated tau is secreted in tauopathy models and is selectively phosphorylated in cerebrospinal fluid in early Alzheimer disease. *J Biol Chem* **287**, 3842-3849 (2012).

94. Y. Iguchi *et al.*, Exosome secretion is a key pathway for clearance of pathological TDP-43. *Brain* **139**, 3187-3201 (2016).
95. L. Rajendran *et al.*, Alzheimer's disease beta-amyloid peptides are released in association with exosomes. *Proc Natl Acad Sci U S A* **103**, 11172-11177 (2006).
96. Y. I. Yim *et al.*, The multivesicular body is the major internal site of prion conversion. *J Cell Sci* **128**, 1434-1443 (2015).
97. H. J. Lee *et al.*, Assembly-dependent endocytosis and clearance of extracellular alpha-synuclein. *Int J Biochem Cell Biol* **40**, 1835-1849 (2008).
98. J. W. Wu *et al.*, Small misfolded Tau species are internalized via bulk endocytosis and anterogradely and retrogradely transported in neurons. *J Biol Chem* **288**, 1856-1870 (2013).
99. R. S. Omtri, M. W. Davidson, B. Arumugam, J. F. Poduslo, K. K. Kandimalla, Differences in the cellular uptake and intracellular itineraries of amyloid beta proteins 40 and 42: ramifications for the Alzheimer's drug discovery. *Mol Pharm* **9**, 1887-1897 (2012).
100. L. Marzo, K. Gousset, C. Zurzolo, Multifaceted roles of tunneling nanotubes in intercellular communication. *Front Physiol* **3**, 72 (2012).
101. Y. Wang, J. Cui, X. Sun, Y. Zhang, Tunneling-nanotube development in astrocytes depends on p53 activation. *Cell Death Differ* **18**, 732-742 (2011).
102. K. Gousset *et al.*, Prions hijack tunnelling nanotubes for intercellular spread. *Nat Cell Biol* **11**, 328-336 (2009).
103. G. Forloni *et al.*, Preventive study in subjects at risk of fatal familial insomnia: Innovative approach to rare diseases. *Prion* **9**, 75-79 (2015).
104. C. Van Cauwenberghe, C. Van Broeckhoven, K. Sleegers, The genetic landscape of Alzheimer disease: clinical implications and perspectives. *Genet Med* **18**, 421-430 (2016).
105. L. Bertram, C. M. Lill, R. E. Tanzi, The genetics of Alzheimer disease: back to the future. *Neuron* **68**, 270-281 (2010).
106. M. Panpalli Ates, Y. Karaman, S. Guntekin, M. A. Ergun, Analysis of genetics and risk factors of Alzheimer's Disease. *Neuroscience* **325**, 124-131 (2016).
107. M. Hersi *et al.*, Risk factors associated with the onset and progression of Alzheimer's disease: A systematic review of the evidence. *Neurotoxicology* **61**, 143-187 (2017).
108. S. A. Harris, E. A. Harris, Herpes Simplex Virus Type 1 and Other Pathogens are Key Causative Factors in Sporadic Alzheimer's Disease. *J Alzheimers Dis* **48**, 319-353 (2015).
109. B. De Strooper, E. Karran, The Cellular Phase of Alzheimer's Disease. *Cell* **164**, 603-615 (2016).
110. A. Wood-Kaczmar, S. Gandhi, N. W. Wood, Understanding the molecular causes of Parkinson's disease. *Trends Mol Med* **12**, 521-528 (2006).
111. B. Thomas, M. F. Beal, Parkinson's disease. *Hum Mol Genet* **16 Spec No. 2**, R183-194 (2007).
112. J. M. Taylor, B. S. Main, P. J. Crack, Neuroinflammation and oxidative stress: co-conspirators in the pathology of Parkinson's disease. *Neurochem Int* **62**, 803-819 (2013).
113. G. Kouroupi *et al.*, Defective synaptic connectivity and axonal neuropathology in a human iPSC-based model of familial Parkinson's disease. *Proc Natl Acad Sci U S A* **114**, E3679-E3688 (2017).
114. M. Day *et al.*, Selective elimination of glutamatergic synapses on striatopallidal neurons in Parkinson disease models. *Nat Neurosci* **9**, 251-259 (2006).
115. R. J. Marttila, K. O. Kalimo, B. R. Ziola, P. E. Halonen, U. K. Rinne, Herpes simplex virus subunit antibodies in patients with Parkinson's disease. *Arch Neurol* **35**, 668-671 (1978).
116. R. J. Marttila, U. K. Rinne, P. Halonen, D. L. Madden, J. L. Sever, Herpesviruses and parkinsonism. Herpes simplex virus types 1 and 2, and cytomegalovirus antibodies in serum and CSF. *Arch Neurol* **38**, 19-21 (1981).

117. H. Vlajinac *et al.*, Infections as a risk factor for Parkinson's disease: a case-control study. *Int J Neurosci* **123**, 329-332 (2013).
118. L. K. Olsen *et al.*, Viral mimetic priming enhances alpha-synuclein-induced degeneration: Implications for Parkinson's disease. *Brain Behav Immun* 10.1016/j.bbi.2019.04.036 (2019).
119. B. C. Lai, S. A. Marion, K. Teschke, J. K. Tsui, Occupational and environmental risk factors for Parkinson's disease. *Parkinsonism Relat Disord* **8**, 297-309 (2002).
120. F. N. Emamzadeh, A. Surguchov, Parkinson's Disease: Biomarkers, Treatment, and Risk Factors. *Front Neurosci* **12**, 612 (2018).
121. A. Ascherio, M. A. Schwarzschild, The epidemiology of Parkinson's disease: risk factors and prevention. *Lancet Neurol* **15**, 1257-1272 (2016).
122. S. Boillee, C. Vande Velde, D. W. Cleveland, ALS: a disease of motor neurons and their nonneuronal neighbors. *Neuron* **52**, 39-59 (2006).
123. D. Dormann, C. Haass, TDP-43 and FUS: a nuclear affair. *Trends Neurosci* **34**, 339-348 (2011).
124. P. Van Damme, W. Robberecht, L. Van Den Bosch, Modelling amyotrophic lateral sclerosis: progress and possibilities. *Dis Model Mech* **10**, 537-549 (2017).
125. L. Ferraiuolo, J. Kirby, A. J. Grierson, M. Sendtner, P. J. Shaw, Molecular pathways of motor neuron injury in amyotrophic lateral sclerosis. *Nat Rev Neurol* **7**, 616-630 (2011).
126. N. Nowicka, J. Juranek, J. K. Juranek, J. Wojtkiewicz, Risk Factors and Emerging Therapies in Amyotrophic Lateral Sclerosis. *Int J Mol Sci* **20** (2019).
127. I. R. Mackenzie, R. Rademakers, M. Neumann, TDP-43 and FUS in amyotrophic lateral sclerosis and frontotemporal dementia. *Lancet Neurol* **9**, 995-1007 (2010).
128. G. M. McKhann *et al.*, Clinical and pathological diagnosis of frontotemporal dementia: report of the Work Group on Frontotemporal Dementia and Pick's Disease. *Arch Neurol* **58**, 1803-1809 (2001).
129. M. Neumann *et al.*, Ubiquitinated TDP-43 in frontotemporal lobar degeneration and amyotrophic lateral sclerosis. *Science* **314**, 130-133 (2006).
130. B. A. Berning, A. K. Walker, The Pathobiology of TDP-43 C-Terminal Fragments in ALS and FTLD. *Front Neurosci* **13**, 335 (2019).
131. Y. V. Kalkonde *et al.*, Medical and environmental risk factors associated with frontotemporal dementia: a case-control study in a veteran population. *Alzheimers Dement* **8**, 204-210 (2012).
132. A. S. Brown, The environment and susceptibility to schizophrenia. *Prog Neurobiol* **93**, 23-58 (2011).
133. G. W. Roberts, Schizophrenia: the cellular biology of a functional psychosis. *Trends Neurosci* **13**, 207-211 (1990).
134. L. M. Ellman *et al.*, Structural brain alterations in schizophrenia following fetal exposure to the inflammatory cytokine interleukin-8. *Schizophr Res* **121**, 46-54 (2010).
135. A. S. Brown, E. J. Derkits, Prenatal infection and schizophrenia: a review of epidemiologic and translational studies. *Am J Psychiatry* **167**, 261-280 (2010).
136. T. R. Insel, Rethinking schizophrenia. *Nature* **468**, 187-193 (2010).
137. D. A. Lewis, J. A. Lieberman, Catching up on schizophrenia: natural history and neurobiology. *Neuron* **28**, 325-334 (2000).
138. K. Martinowich, R. J. Schloesser, H. K. Manji, Bipolar disorder: from genes to behavior pathways. *J Clin Invest* **119**, 726-736 (2009).
139. N. Craddock, P. Sklar, Genetics of bipolar disorder. *Lancet* **381**, 1654-1662 (2013).
140. T. A. Rowland, S. Marwaha, Epidemiology and risk factors for bipolar disorder. *Ther Adv Psychopharmacol* **8**, 251-269 (2018).
141. I. Grande, M. Berk, B. Birmaher, E. Vieta, Bipolar disorder. *Lancet* **387**, 1561-1572 (2016).

142. D. Brustolim, R. Ribeiro-dos-Santos, R. E. Kast, E. L. Altschuler, M. B. Soares, A new chapter opens in anti-inflammatory treatments: the antidepressant bupropion lowers production of tumor necrosis factor-alpha and interferon-gamma in mice. *Int Immunopharmacol* **6**, 903-907 (2006).
143. S. Sen, R. Duman, G. Sanacora, Serum brain-derived neurotrophic factor, depression, and antidepressant medications: meta-analyses and implications. *Biol Psychiatry* **64**, 527-532 (2008).
144. R. Uher, The role of genetic variation in the causation of mental illness: an evolution-informed framework. *Mol Psychiatry* **14**, 1072-1082 (2009).
145. J. W. Kanter, A. M. Busch, C. E. Weeks, S. J. Landes, The nature of clinical depression: symptoms, syndromes, and behavior analysis. *Behav Anal* **31**, 1-21 (2008).
146. X. Meng *et al.*, Risk factor modifications and depression incidence: a 4-year longitudinal Canadian cohort of the Montreal Catchment Area Study. *BMJ Open* **7**, e015156 (2017).
147. C. Soto, L. Estrada, J. Castilla, Amyloids, prions and the inherent infectious nature of misfolded protein aggregates. *Trends Biochem Sci* **31**, 150-155 (2006).
148. S. B. Prusiner, Novel proteinaceous infectious particles cause scrapie. *Science* **216**, 136-144 (1982).
149. S. B. Prusiner, Molecular biology of prion diseases. *Science* **252**, 1515-1522 (1991).
150. S. B. Prusiner, Prions. *Proc Natl Acad Sci U S A* **95**, 13363-13383 (1998).
151. A. Aguzzi, Cell biology: Beyond the prion principle. *Nature* **459**, 924-925 (2009).
152. P. Brundin, R. Melki, R. Kopito, Prion-like transmission of protein aggregates in neurodegenerative diseases. *Nat Rev Mol Cell Biol* **11**, 301-307 (2010).
153. P. Smethurst, K. C. Sidle, J. Hardy, Review: Prion-like mechanisms of transactive response DNA binding protein of 43 kDa (TDP-43) in amyotrophic lateral sclerosis (ALS). *Neuropathol Appl Neurobiol* **41**, 578-597 (2015).
154. M. Goedert, F. Clavaguera, M. Tolnay, The propagation of prion-like protein inclusions in neurodegenerative diseases. *Trends Neurosci* **33**, 317-325 (2010).
155. A. Aguzzi, A. K. K. Lakkaraju, Cell Biology of Prions and Prionoids: A Status Report. *Trends Cell Biol* **26**, 40-51 (2016).
156. S. B. Prusiner, Scrapie prions, brain amyloid, and senile dementia. *Curr Top Cell Regul* **26**, 79-95 (1985).
157. G. Sajnani, J. R. Requena, Prions, proteinase K and infectivity. *Prion* **6**, 430-432 (2012).
158. S. Simoneau *et al.*, In vitro and in vivo neurotoxicity of prion protein oligomers. *PLoS Pathog* **3**, e125 (2007).
159. R. Morales, Prion strains in mammals: Different conformations leading to disease. *PLoS Pathog* **13**, e1006323 (2017).
160. A. Aguzzi, M. Heikenwalder, M. Polymenidou, Insights into prion strains and neurotoxicity. *Nat Rev Mol Cell Biol* **8**, 552-561 (2007).
161. S. K. Kaufman *et al.*, Tau Prion Strains Dictate Patterns of Cell Pathology, Progression Rate, and Regional Vulnerability In Vivo. *Neuron* **92**, 796-812 (2016).
162. S. Narasimhan *et al.*, Pathological Tau Strains from Human Brains Recapitulate the Diversity of Tauopathies in Nontransgenic Mouse Brain. *J Neurosci* **37**, 11406-11423 (2017).
163. D. W. Sanders *et al.*, Distinct tau prion strains propagate in cells and mice and define different tauopathies. *Neuron* **82**, 1271-1288 (2014).
164. F. Laferriere *et al.*, TDP-43 extracted from frontotemporal lobar degeneration subject brains displays distinct aggregate assemblies and neurotoxic effects reflecting disease progression rates. *Nat Neurosci* **22**, 65-77 (2019).
165. W. Peelaerts *et al.*, alpha-Synuclein strains cause distinct synucleinopathies after local and systemic administration. *Nature* **522**, 340-344 (2015).

166. L. Bousset *et al.*, Structural and functional characterization of two alpha-synuclein strains. *Nat Commun* **4**, 2575 (2013).
167. S. Gribaudo *et al.*, Propagation of alpha-Synuclein Strains within Human Reconstructed Neuronal Network. *Stem Cell Reports* **12**, 230-244 (2019).
168. W. Qiang, W. M. Yau, J. X. Lu, J. Collinge, R. Tycko, Structural variation in amyloid-beta fibrils from Alzheimer's disease clinical subtypes. *Nature* **541**, 217-221 (2017).
169. J. C. Watts *et al.*, Serial propagation of distinct strains of Abeta prions from Alzheimer's disease patients. *Proc Natl Acad Sci U S A* **111**, 10323-10328 (2014).
170. T. L. Spires-Jones, J. Attems, D. R. Thal, Interactions of pathological proteins in neurodegenerative diseases. *Acta Neuropathol* **134**, 187-205 (2017).
171. D. W. Dickson, Neuropathology of Alzheimer's disease and other dementias. *Clin Geriatr Med* **17**, 209-228 (2001).
172. H. Uchikado, W. L. Lin, M. W. DeLucia, D. W. Dickson, Alzheimer disease with amygdala Lewy bodies: a distinct form of alpha-synucleinopathy. *J Neuropathol Exp Neurol* **65**, 685-697 (2006).
173. K. A. Josephs *et al.*, Updated TDP-43 in Alzheimer's disease staging scheme. *Acta Neuropathol* **131**, 571-585 (2016).
174. D. J. Irwin *et al.*, Neuropathological and genetic correlates of survival and dementia onset in synucleinopathies: a retrospective analysis. *Lancet Neurol* **16**, 55-65 (2017).
175. K. E. McAleese *et al.*, TDP-43 pathology in Alzheimer's disease, dementia with Lewy bodies and ageing. *Brain Pathol* **27**, 472-479 (2017).
176. D. L. Castillo-Carranza, M. J. Guerrero-Munoz, U. Sengupta, J. E. Gerson, R. Kayed, alpha-Synuclein Oligomers Induce a Unique Toxic Tau Strain. *Biol Psychiatry* **84**, 499-508 (2018).
177. N. Badiola *et al.*, Tau enhances alpha-synuclein aggregation and toxicity in cellular models of synucleinopathy. *PLoS One* **6**, e26609 (2011).
178. G. M. Pocas, J. Branco-Santos, F. Herrera, T. F. Outeiro, P. M. Domingos, alpha-Synuclein modifies mutant huntingtin aggregation and neurotoxicity in Drosophila. *Hum Mol Genet* **24**, 1898-1907 (2015).
179. A. J. Moszczynski *et al.*, Pathologic Thr(175) tau phosphorylation in CTE and CTE with ALS. *Neurology* **90**, e380-e387 (2018).
180. A. J. Moszczynski, W. Yang, R. Hammond, L. C. Ang, M. J. Strong, Threonine(175), a novel pathological phosphorylation site on tau protein linked to multiple tauopathies. *Acta Neuropathol Commun* **5**, 6 (2017).
181. A. M. Herman, P. J. Khandelwal, B. B. Stanczyk, G. W. Rebeck, C. E. Moussa, beta-amyloid triggers ALS-associated TDP-43 pathology in AD models. *Brain Res* **1386**, 191-199 (2011).
182. L. K. Clinton, M. Blurton-Jones, K. Myczek, J. Q. Trojanowski, F. M. LaFerla, Synergistic Interactions between Abeta, tau, and alpha-synuclein: acceleration of neuropathology and cognitive decline. *J Neurosci* **30**, 7281-7289 (2010).
183. S. Saxena, P. Caroni, Selective neuronal vulnerability in neurodegenerative diseases: from stressor thresholds to degeneration. *Neuron* **71**, 35-48 (2011).
184. A. G. Cardno, M. J. Owen, Genetic relationships between schizophrenia, bipolar disorder, and schizoaffective disorder. *Schizophr Bull* **40**, 504-515 (2014).
185. D. Adam, Mental health: On the spectrum. *Nature* **496**, 416-418 (2013).
186. S. R. Leliveld *et al.*, Insolubility of disrupted-in-schizophrenia 1 disrupts oligomer-dependent interactions with nuclear distribution element 1 and is associated with sporadic mental disease. *J Neurosci* **28**, 3839-3845 (2008).

187. P. Ottis *et al.*, Convergence of two independent mental disease genes on the protein level: recruitment of dysbindin to cell-invasive disrupted-in-schizophrenia 1 aggresomes. *Biol Psychiatry* **70**, 604-610 (2011).
188. V. Bader *et al.*, Proteomic, genomic and translational approaches identify CRMP1 for a role in schizophrenia and its underlying traits. *Hum Mol Genet* **21**, 4406-4418 (2012).
189. N. J. Bradshaw *et al.*, Aggregation of the protein TRIOBP-1 and its potential relevance to schizophrenia. *PLoS One* **9**, e111196 (2014).
190. L. G. Nucifora *et al.*, Increased Protein Insolubility in Brains From a Subset of Patients With Schizophrenia. *Am J Psychiatry* 10.1176/appi.ajp.2019.18070864, appiajp201918070864 (2019).
191. S. B. Prusiner, Shattuck lecture--neurodegenerative diseases and prions. *N Engl J Med* **344**, 1516-1526 (2001).
192. J. K. Millar *et al.*, Disruption of two novel genes by a translocation co-segregating with schizophrenia. *Hum Mol Genet* **9**, 1415-1423 (2000).
193. N. A. Sachs *et al.*, A frameshift mutation in Disrupted in Schizophrenia 1 in an American family with schizophrenia and schizoaffective disorder. *Mol Psychiatry* **10**, 758-764 (2005).
194. S. V. Trossbach *et al.*, Misassembly of full-length Disrupted-in-Schizophrenia 1 protein is linked to altered dopamine homeostasis and behavioral deficits. *Mol Psychiatry* **21**, 1561-1572 (2016).
195. S. R. Leliveld *et al.*, Oligomer assembly of the C-terminal DISC1 domain (640-854) is controlled by self-association motifs and disease-associated polymorphism S704C. *Biochemistry* **48**, 7746-7755 (2009).
196. S. Narayanan, H. Arthanari, M. S. Wolfe, G. Wagner, Molecular characterization of disrupted in schizophrenia-1 risk variant S704C reveals the formation of altered oligomeric assembly. *J Biol Chem* **286**, 44266-44276 (2011).
197. M. Tanaka *et al.*, Aggregation of scaffolding protein DISC1 dysregulates phosphodiesterase 4 in Huntington's disease. *J Clin Invest* **127**, 1438-1450 (2017).
198. R. Endo *et al.*, TAR DNA-Binding Protein 43 and Disrupted in Schizophrenia 1 Coaggregation Disrupts Dendritic Local Translation and Mental Function in Frontotemporal Lobar Degeneration. *Biol Psychiatry* **84**, 509-521 (2018).
199. C. Korth, DISCopathies: brain disorders related to DISC1 dysfunction. *Rev Neurosci* **20**, 321-330 (2009).
200. C. Y. Zhu, Y. Shen, Q. Xu, Propagation of dysbindin-1B aggregates: exosome-mediated transmission of neurotoxic deposits. *Neuroscience* **291**, 301-316 (2015).
201. N. J. Bradshaw *et al.*, An unpredicted aggregation-critical region of the actin-polymerizing protein TRIOBP-1/Tara, determined by elucidation of its domain structure. *J Biol Chem* **292**, 9583-9598 (2017).
202. L. G. Nucifora *et al.*, A Mutation in NPAS3 That Segregates with Schizophrenia in a Small Family Leads to Protein Aggregation. *Mol Neuropsychiatry* **2**, 133-144 (2016).
203. U. F. Lingappa *et al.*, Host-rabies virus protein-protein interactions as druggable antiviral targets. *Proc Natl Acad Sci U S A* **110**, E861-868 (2013).
204. V. R. Lingappa, C. R. Hurt, E. Garvey, Capsid assembly as a point of intervention for novel anti-viral therapeutics. *Curr Pharm Biotechnol* **14**, 513-523 (2013).
205. N. Tian *et al.*, The role of the synthetic enzyme GAD65 in the control of neuronal gamma-aminobutyric acid release. *Proc Natl Acad Sci U S A* **96**, 12911-12916 (1999).
206. A. Kurtishi, B. Rosen, K. S. Patil, G. W. Alves, S. G. Moller, Cellular Proteostasis in Neurodegeneration. *Mol Neurobiol* **56**, 3676-3689 (2019).
207. W. E. Balch, R. I. Morimoto, A. Dillin, J. W. Kelly, Adapting proteostasis for disease intervention. *Science* **319**, 916-919 (2008).
208. Y. Phillip, G. Schreiber, Formation of protein complexes in crowded environments--from in vitro to in vivo. *FEBS Lett* **587**, 1046-1052 (2013).

209. C. M. Goodwin, S. Xu, J. Munger, Stealing the Keys to the Kitchen: Viral Manipulation of the Host Cell Metabolic Network. *Trends Microbiol* **23**, 789-798 (2015).
210. Anonymous, Focus on neurodegenerative disease. *Nat Neurosci* **21**, 1293 (2018).
211. C. W. Olanow, K. Kieburtz, A. H. Schapira, Why have we failed to achieve neuroprotection in Parkinson's disease? *Ann Neurol* **64 Suppl 2**, S101-110 (2008).
212. H. Mitsumoto, B. R. Brooks, V. Silani, Clinical trials in amyotrophic lateral sclerosis: why so many negative trials and how can trials be improved? *Lancet Neurol* **13**, 1127-1138 (2014).
213. D. Mehta, R. Jackson, G. Paul, J. Shi, M. Sabbagh, Why do trials for Alzheimer's disease drugs keep failing? A discontinued drug perspective for 2010-2015. *Expert Opin Investig Drugs* **26**, 735-739 (2017).
214. R. S. Doody *et al.*, A phase 3 trial of semagacestat for treatment of Alzheimer's disease. *N Engl J Med* **369**, 341-350 (2013).
215. C. Addy *et al.*, Single-dose administration of MK-0657, an NR2B-selective NMDA antagonist, does not result in clinically meaningful improvement in motor function in patients with moderate Parkinson's disease. *J Clin Pharmacol* **49**, 856-864 (2009).
216. E. T. Powers, R. I. Morimoto, A. Dillin, J. W. Kelly, W. E. Balch, Biological and chemical approaches to diseases of proteostasis deficiency. *Annu Rev Biochem* **78**, 959-991 (2009).
217. J. Leng, D. R. Goldstein, Impact of aging on viral infections. *Microbes Infect* **12**, 1120-1124 (2010).
218. L. Gan, M. R. Cookson, L. Petrucelli, A. R. La Spada, Converging pathways in neurodegeneration, from genetics to mechanisms. *Nat Neurosci* **21**, 1300-1309 (2018).
219. S. Karim *et al.*, The role of viruses in neurodegenerative and neurobehavioral diseases. *CNS Neurol Disord Drug Targets* **13**, 1213-1223 (2014).
220. Anonymous, State of aggregation. *Nat Neurosci* **14**, 399 (2011).
221. M. S. Hipp, S. H. Park, F. U. Hartl, Proteostasis impairment in protein-misfolding and -aggregation diseases. *Trends Cell Biol* **24**, 506-514 (2014).
222. A. E. Fiore, C. B. Bridges, N. J. Cox, Seasonal influenza vaccines. *Curr Top Microbiol Immunol* **333**, 43-82 (2009).
223. K. G. Mohn, I. Smith, H. Sjursen, R. J. Cox, Immune responses after live attenuated influenza vaccination. *Hum Vaccin Immunother* **14**, 571-578 (2018).
224. H. Braak, U. Rub, W. P. Gai, K. Del Tredici, Idiopathic Parkinson's disease: possible routes by which vulnerable neuronal types may be subject to neuroinvasion by an unknown pathogen. *J Neural Transm (Vienna)* **110**, 517-536 (2003).
225. L. A. Glantz, J. H. Gilmore, J. A. Lieberman, L. F. Jarskog, Apoptotic mechanisms and the synaptic pathology of schizophrenia. *Schizophr Res* **81**, 47-63 (2006).
226. C. Korth, Aggregated proteins in schizophrenia and other chronic mental diseases: DISC1opathies. *Prion* **6**, 134-141 (2012).
227. J. J. Palop, J. Chin, L. Mucke, A network dysfunction perspective on neurodegenerative diseases. *Nature* **443**, 768-773 (2006).
228. J. D. Woolley, B. K. Khan, N. K. Murthy, B. L. Miller, K. P. Rankin, The diagnostic challenge of psychiatric symptoms in neurodegenerative disease: rates of and risk factors for prior psychiatric diagnosis in patients with early neurodegenerative disease. *J Clin Psychiatry* **72**, 126-133 (2011).
229. R. S. Lee *et al.*, Neuropsychological and functional outcomes in recent-onset major depression, bipolar disorder and schizophrenia-spectrum disorders: a longitudinal cohort study. *Transl Psychiatry* **5**, e555 (2015).
230. J. Petrak *et al.*, Deja vu in proteomics. A hit parade of repeatedly identified differentially expressed proteins. *Proteomics* **8**, 1744-1749 (2008).

231. K. Chandramouli, P. Y. Qian, Proteomics: challenges, techniques and possibilities to overcome biological sample complexity. *Hum Genomics Proteomics* **2009** (2009).

232. J. A. English, K. Pennington, M. J. Dunn, D. R. Cotter, The neuroproteomics of schizophrenia. *Biol Psychiatry* **69**, 163-172 (2011).

233. A. Metaxas *et al.*, Tauopathy in the APPswe/PS1ΔE9 mouse model of familial Alzheimer's disease. *bioRxiv* https://doi.org/10.1101/405647 (2018).